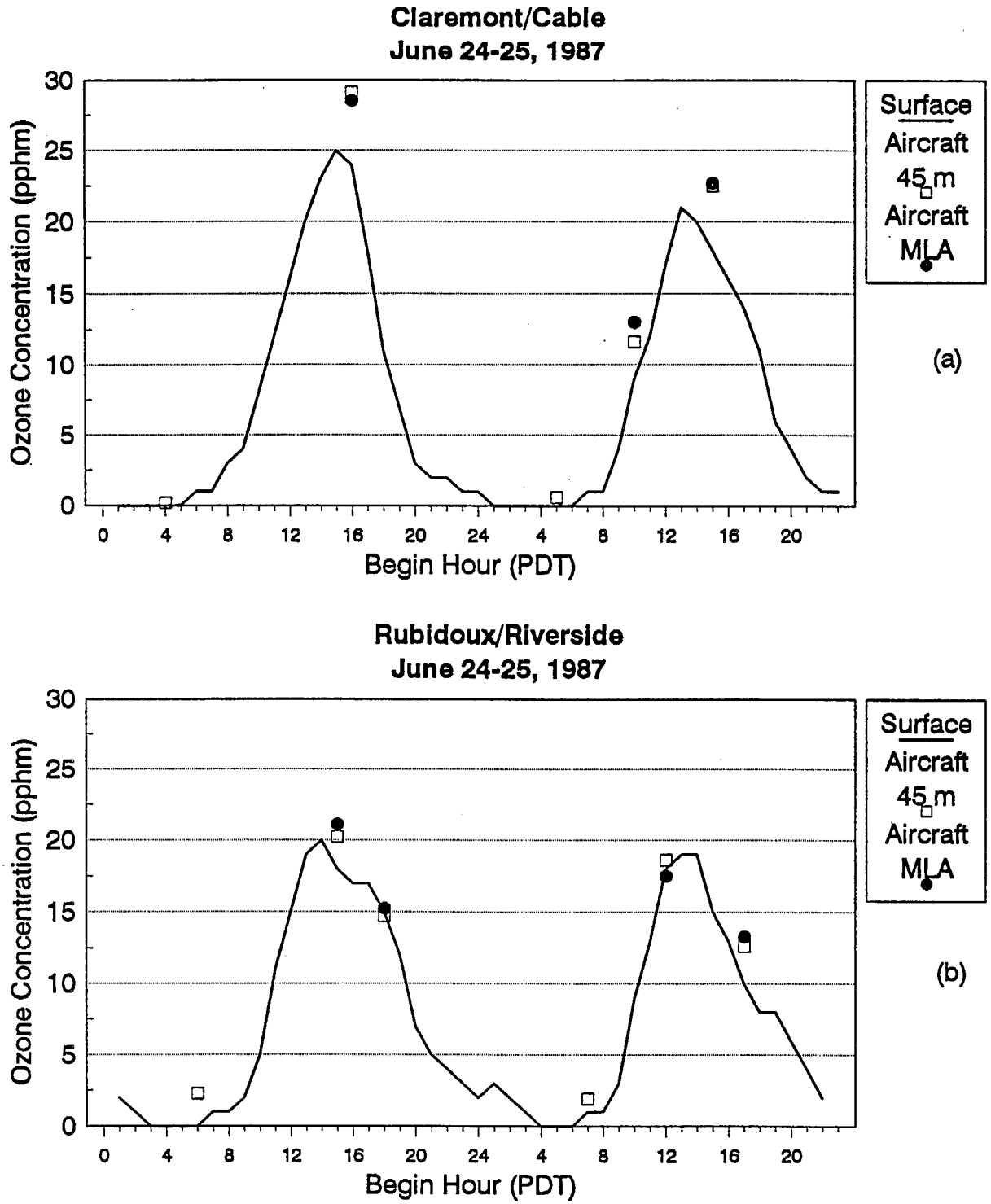

Figure 3-44. Comparison of Surface Ozone Concentrations With Mixed-Layer-Average (MLA) and the Lowest 45-Meter Average (45 m) Ozone at (a) Cable and (b) Riverside on June 24-25, 1987. The data compared to the Cable and Riverside spirals are from the Claremont and Rubidoux surface monitors, respectively.

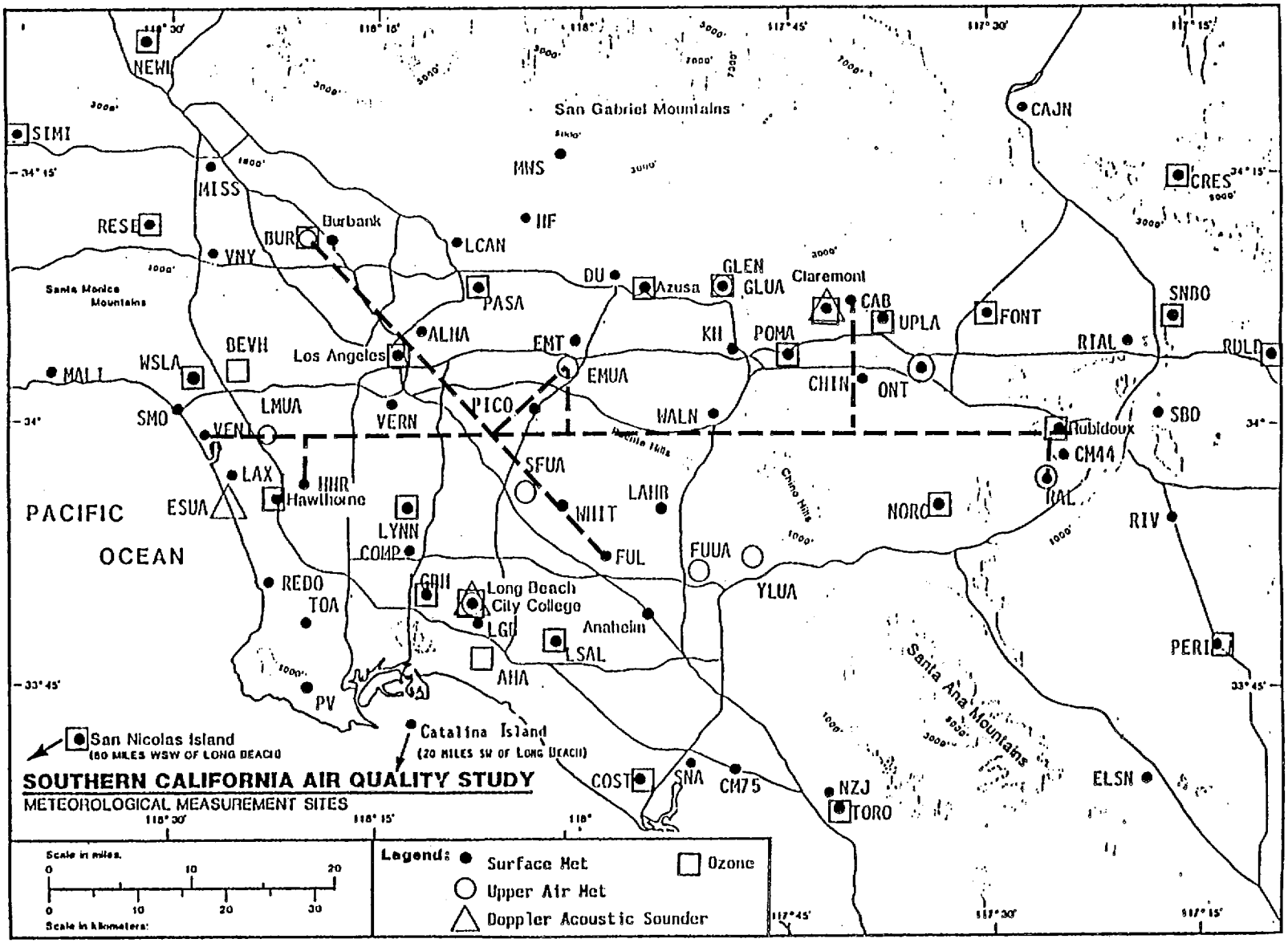

Figure 3-45. Location of Aircraft Spiral Locations on West-East Line and North-South Line Used in Ozone Contour Plots. All sites are listed in Appendix A. (Base map from Hering and Blumenthal, 1989.)

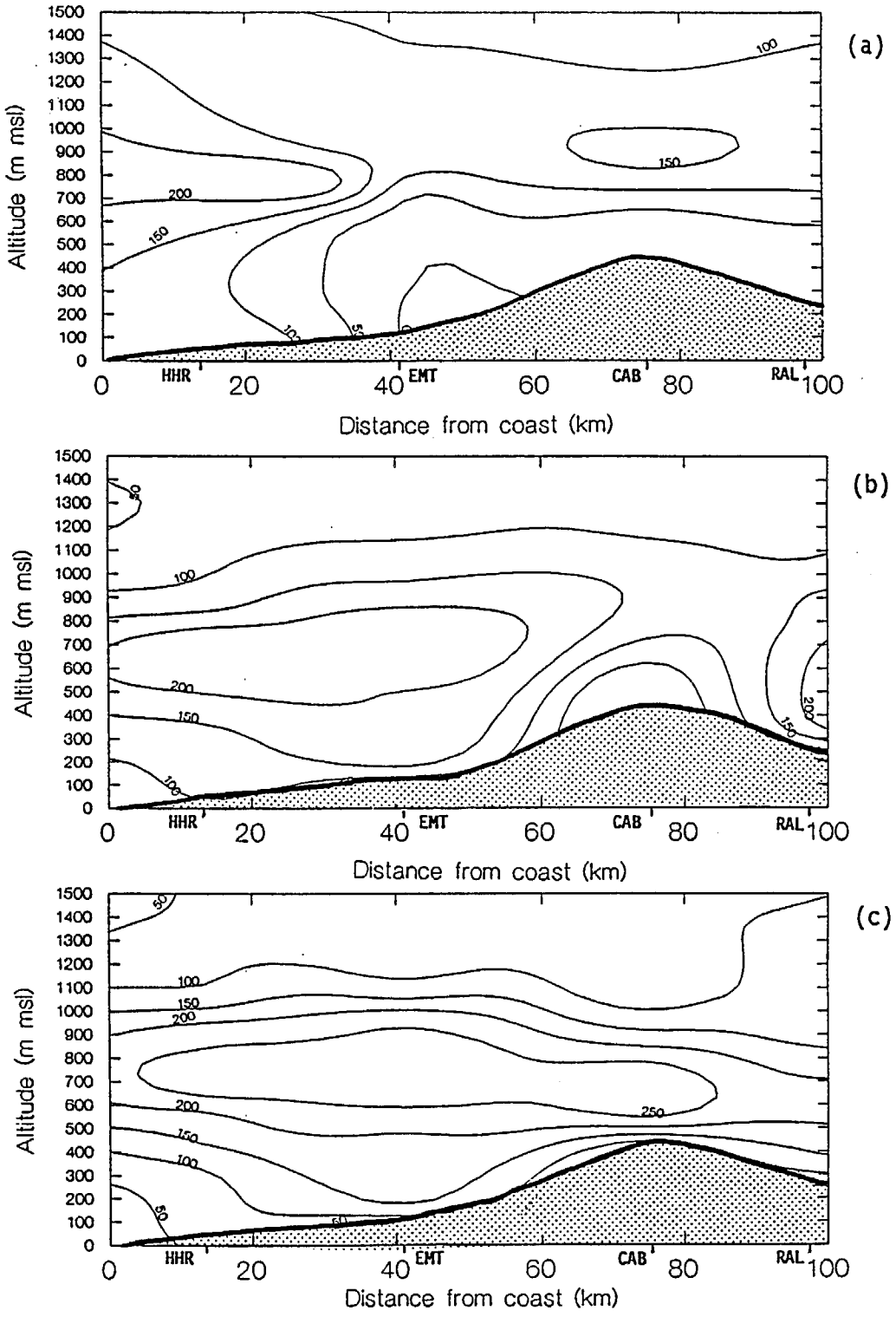

Figure 3-46. Ozone Concentrations (ppb) Aloft During the (a) Morning, (b) Midday, and (c) Afternoon of June 24, 1987. Ozone contours were generated along a west-to-east plane from the coast near Hawthorne to Riverside using data from aircraft spirals. The shaded area approximately represents the ground.

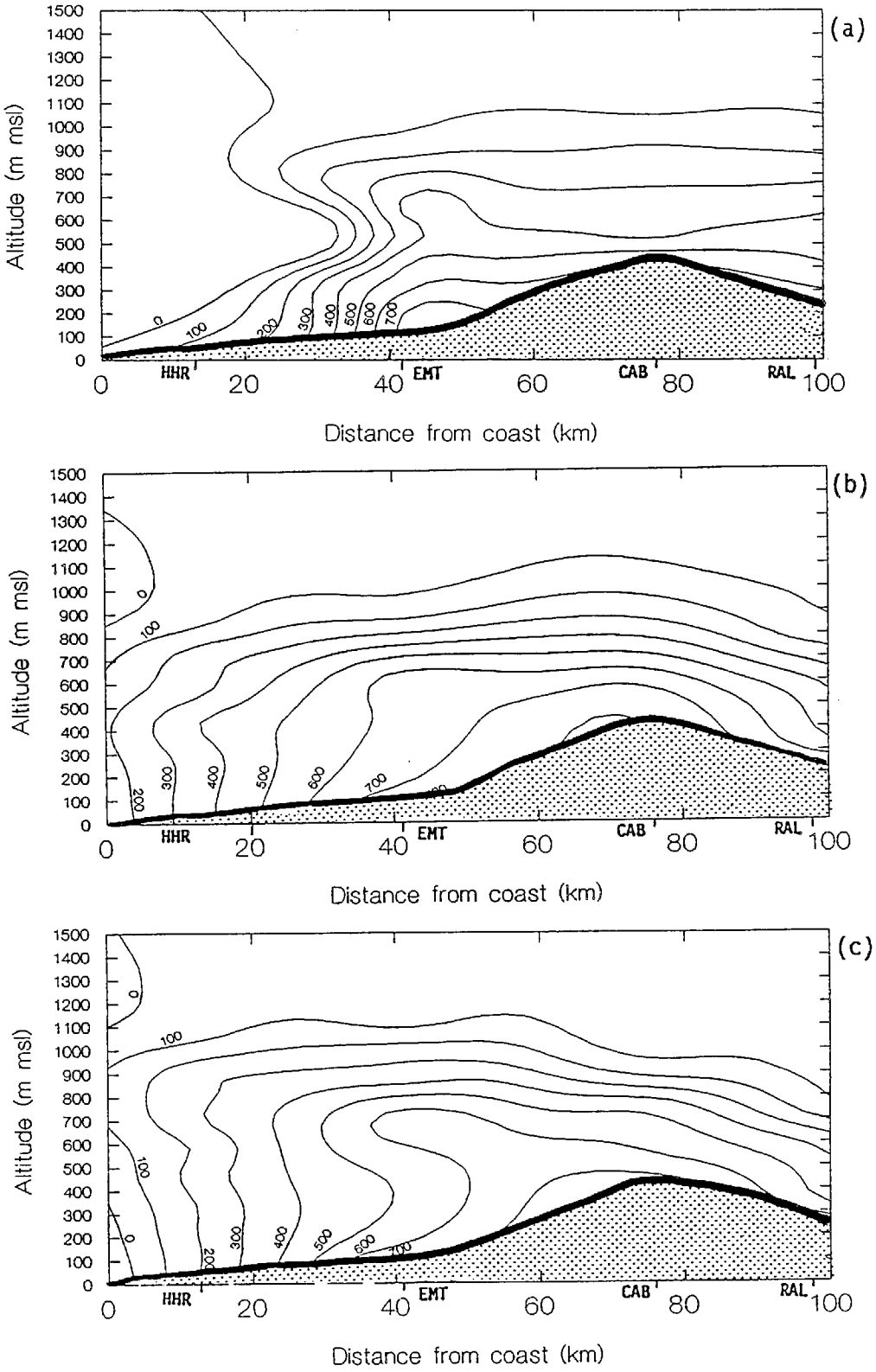

Figure 3-47. Light Scattering (b_{scat} - Mm^{-1}) Aloft During the (a) Morning, (b) Midday, and (c) Afternoon of June 24, 1987. Contours were generated along a west-to-east plane from the coast near Hawthorne to Riverside using data from aircraft spirals. The shaded area approximately represents the ground.

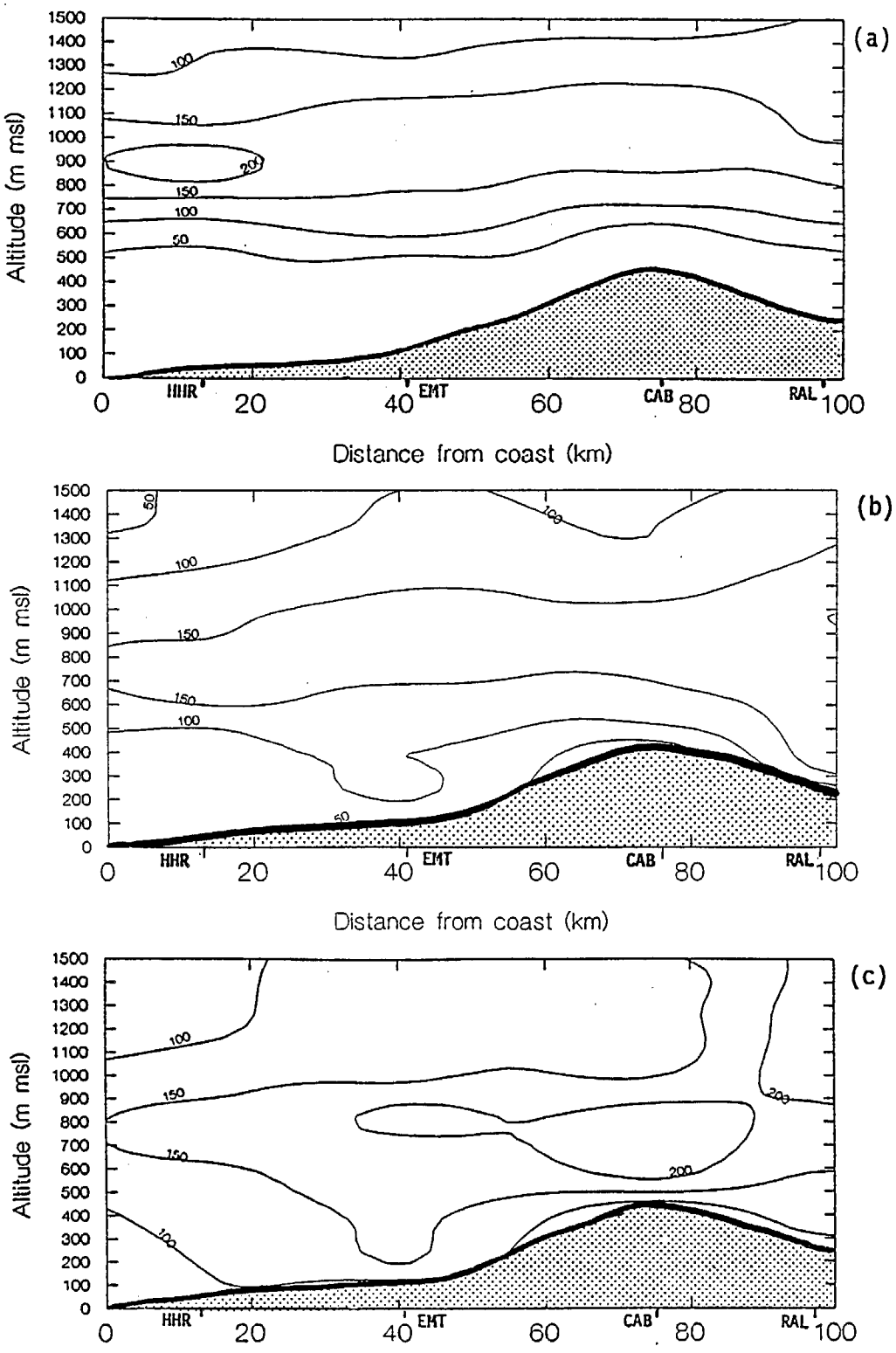

Figure 3-48. Ozone Concentrations (ppb) Aloft During the (a) Morning, (b) Midday, and (c) Afternoon of June 25, 1987. Ozone contours were generated along a west-to-east plane from the coast near Hawthorne to Riverside using data from aircraft spirals. The shaded area approximately represents the ground.

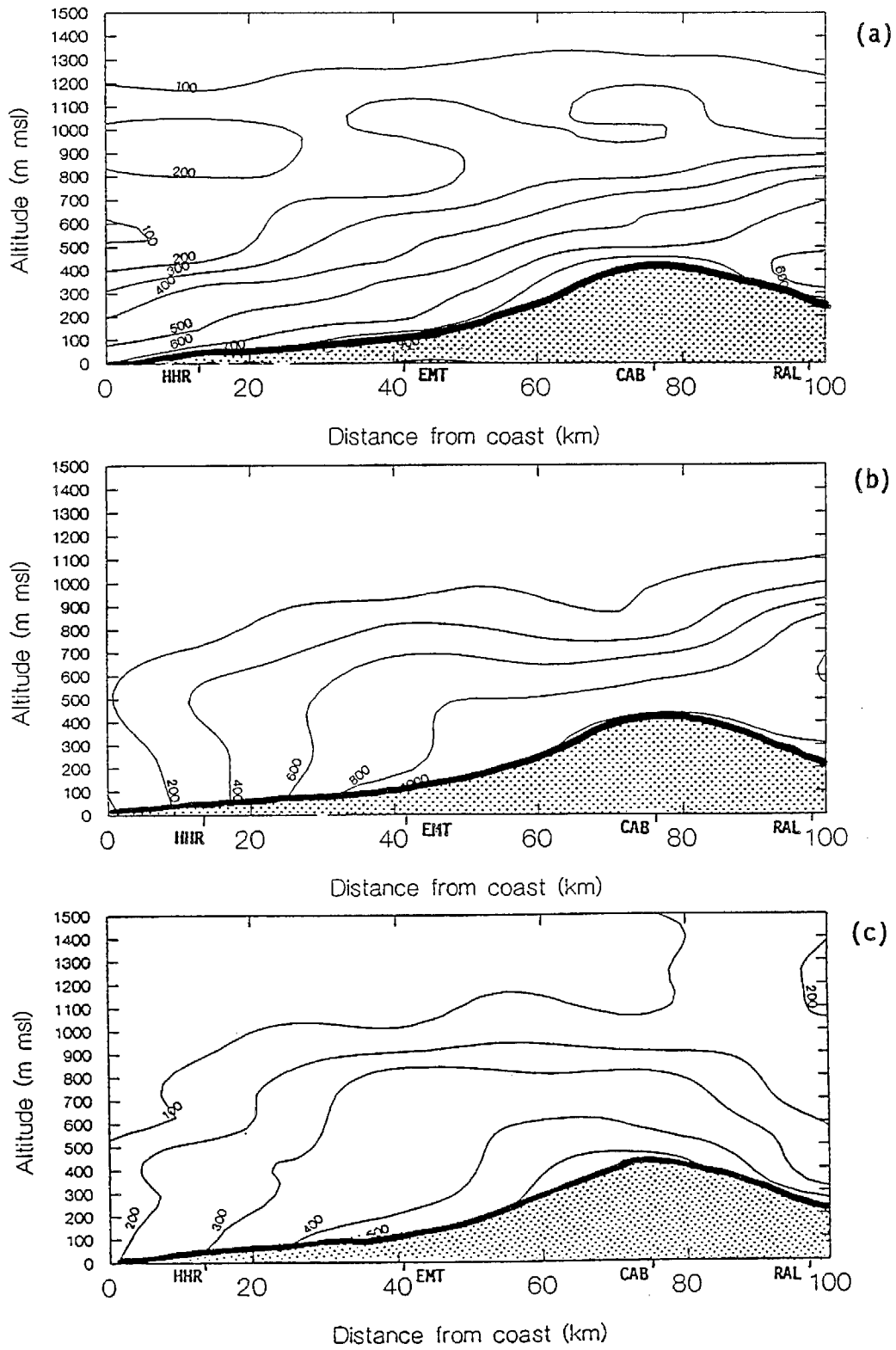

Figure 3-49. Light Scattering (b_{scat} - Mm^{-1}) Aloft During the (a) Morning, (b) Midday, and (c) Afternoon of June 24, 1987. Contours were generated along a west-to-east plane from the coast near Hawthorne to Riverside using data from aircraft spirals. The shaded area approximately represents the ground.

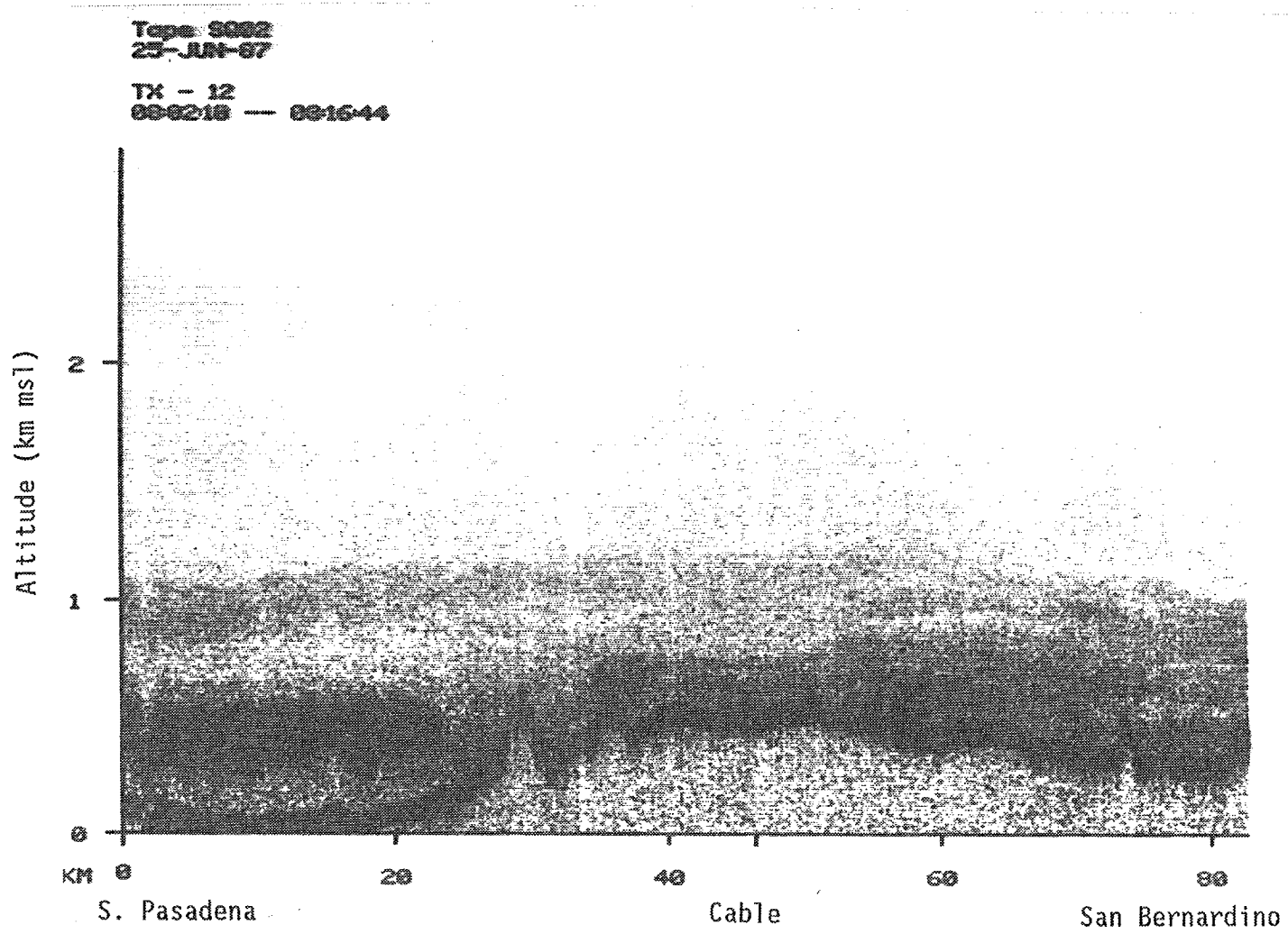

Figure 3-50. Aircraft Lidar Gray-Scale Plot of Particle Backscatter on the Morning of June 25, 1987 From South Pasadena to San Bernardino, Looking From the South. The thin layer of particle backscatter at about 800 to 1000 m msl indicates a polluted layer at about the same altitude across the plot.

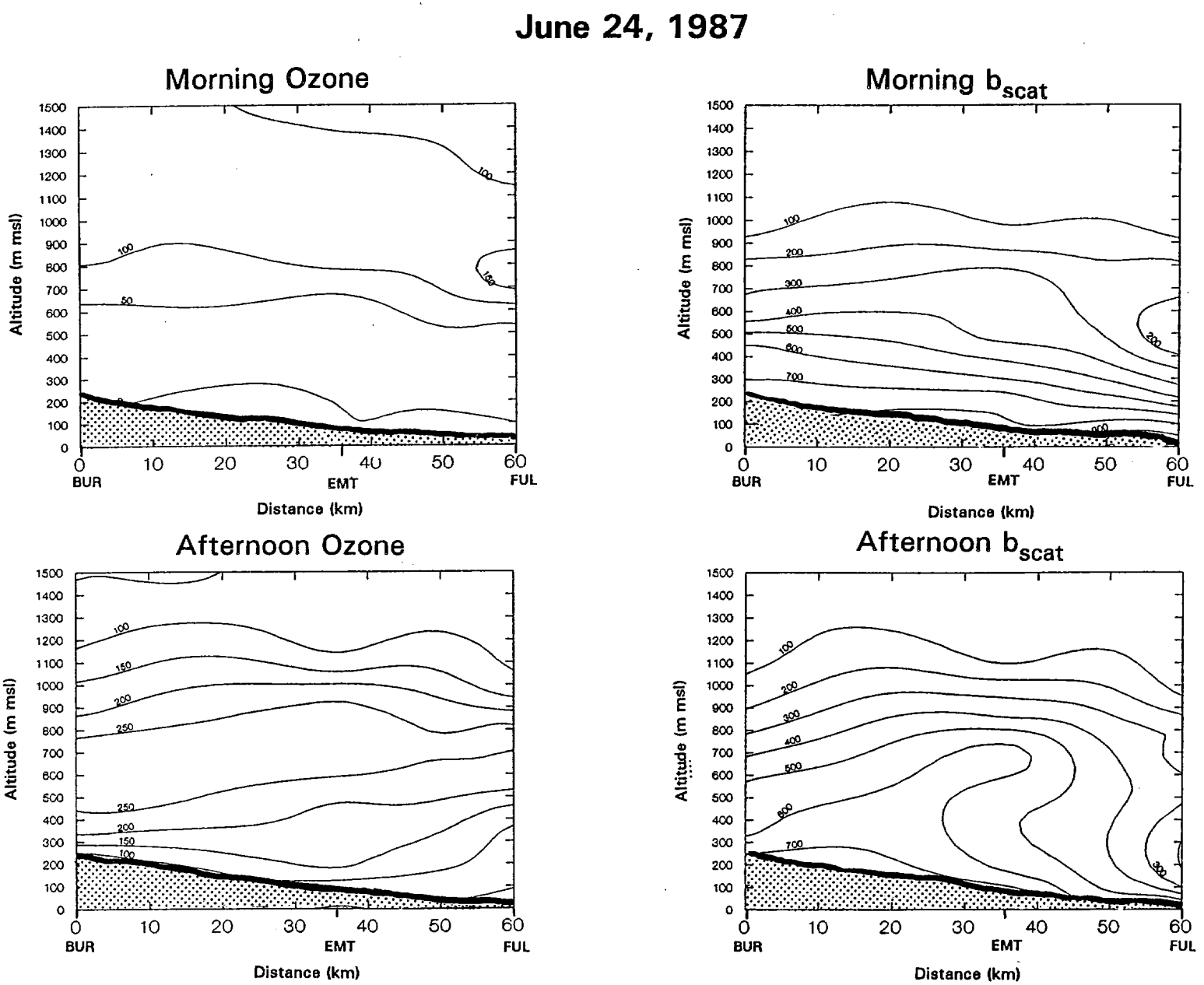

Figure 3-51. Ozone Concentrations (ppb) and Light Scattering (b_{scat} - Mm^{-1}) Aloft on the Morning and Afternoon of June 24, 1987 Along a North-to-South Plane From Burbank to Fullerton Using Data From Aircraft Spirals. The shaded area approximately represents the ground.

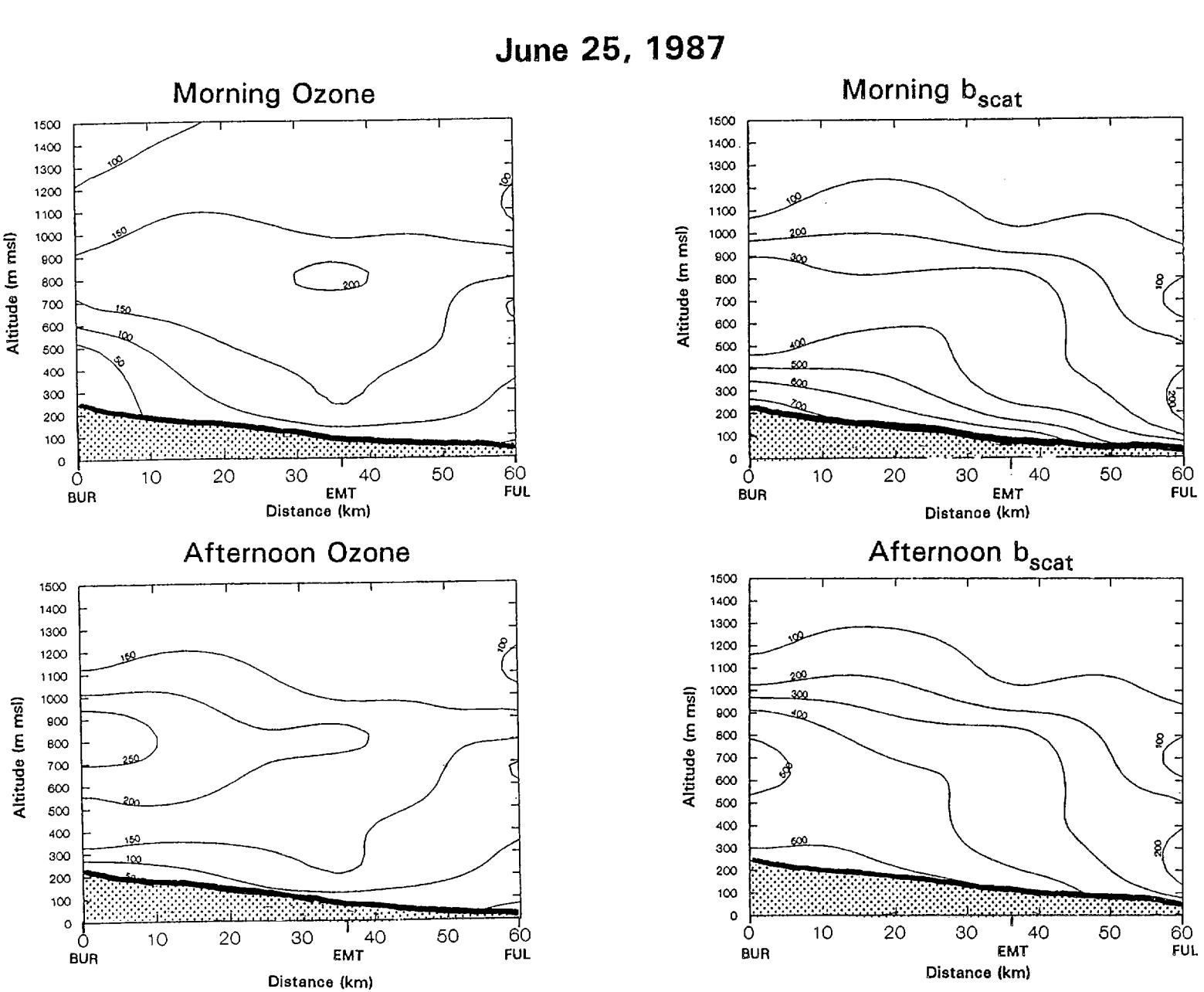

Figure 3-52. Ozone Concentrations (ppb) and Light Scattering (b_{scat} - Mm^{-1}) Aloft on the Morning and Afternoon June 25, 1987 Along a North-to-South Plane From Burbank to Fullerton Using Data From Aircraft Spirals. The shaded area approximately represents the ground.

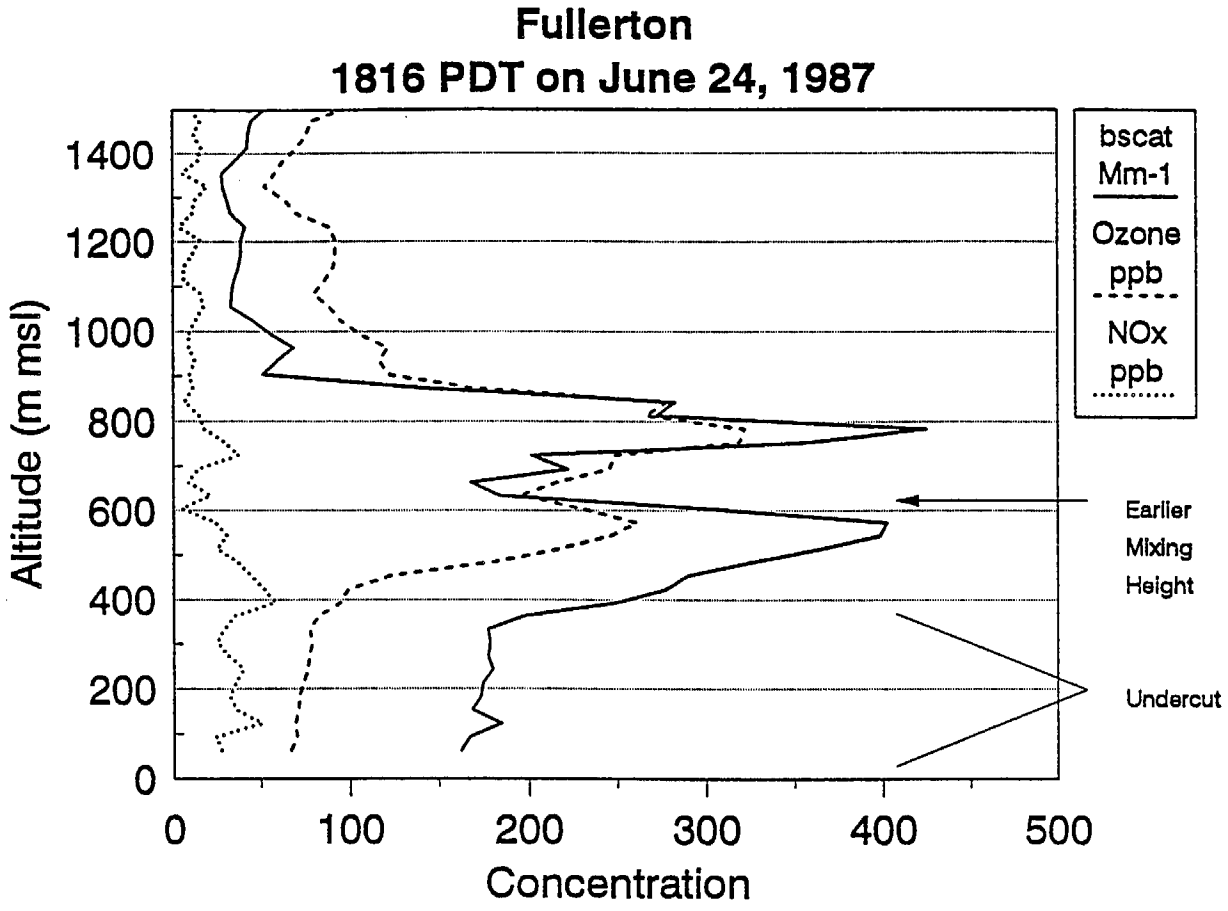

Figure 3-53. NO_x, b_{scat}, and Ozone Profiles at Fullerton on June 24, 1987 at 1816 PDT (b_{scat} units are Mm^{-1}). The mixing height earlier in the day reached about 650 m msl. The relatively-clean marine layer (surface to about 400 m msl) can be seen undercutting the mixed layer.

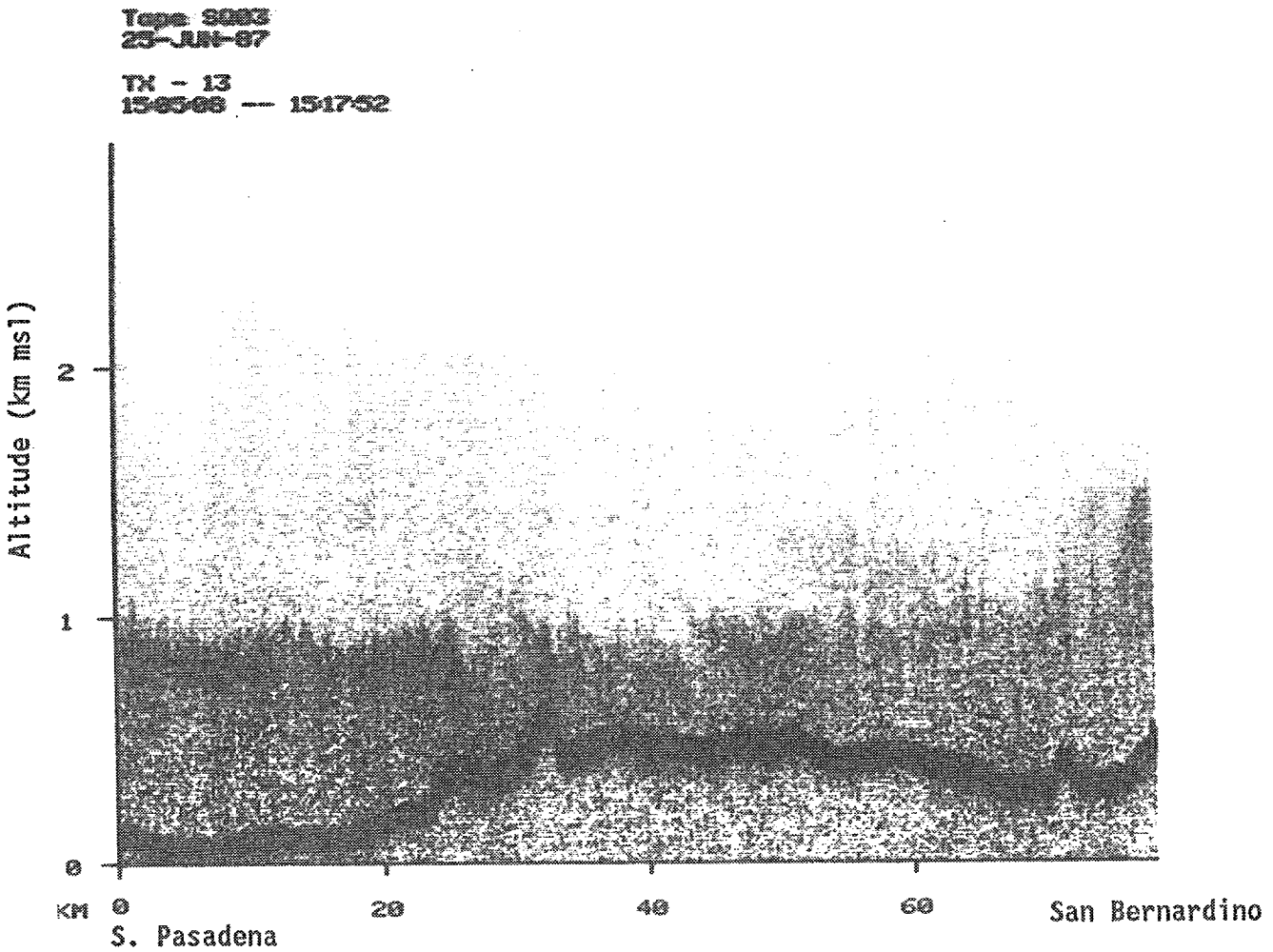

Figure 3-54. Aircraft Lidar Gray-Scale Plot of Particle Backscatter on the Afternoon of June 25, 1987 From South Pasadena to San Bernardino, Looking From the South. The sea breeze has penetrated to about El Monte as shown by the lighter backscatter signal from the ground to about 500 m msl.

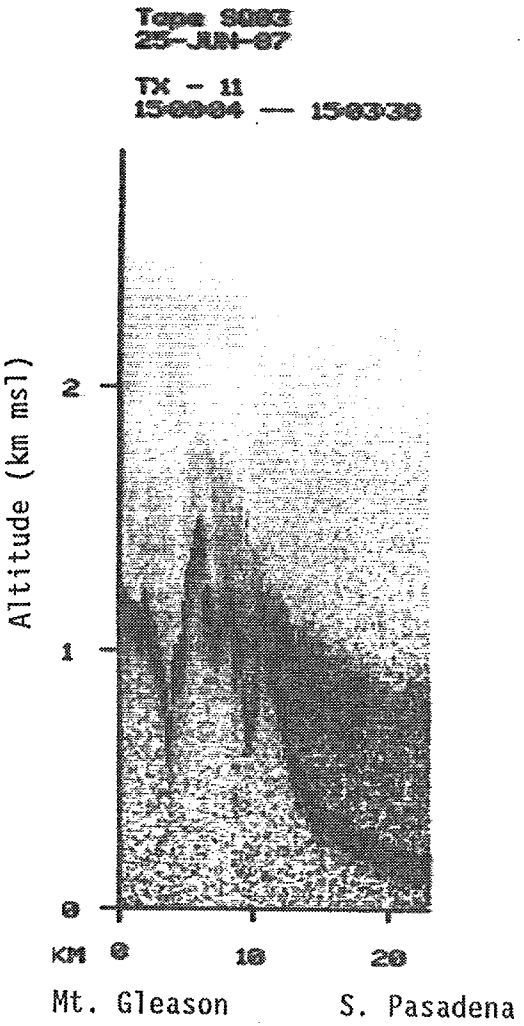

Figure 3-55. Aircraft Lidar Gray-Scale Plot of Particle Backscatter on the Afternoon of June 25, 1987 From Mt. Gleason to South Pasadena, Looking From the West. The upslope flow of the mixed layer is clearly seen in this plot.

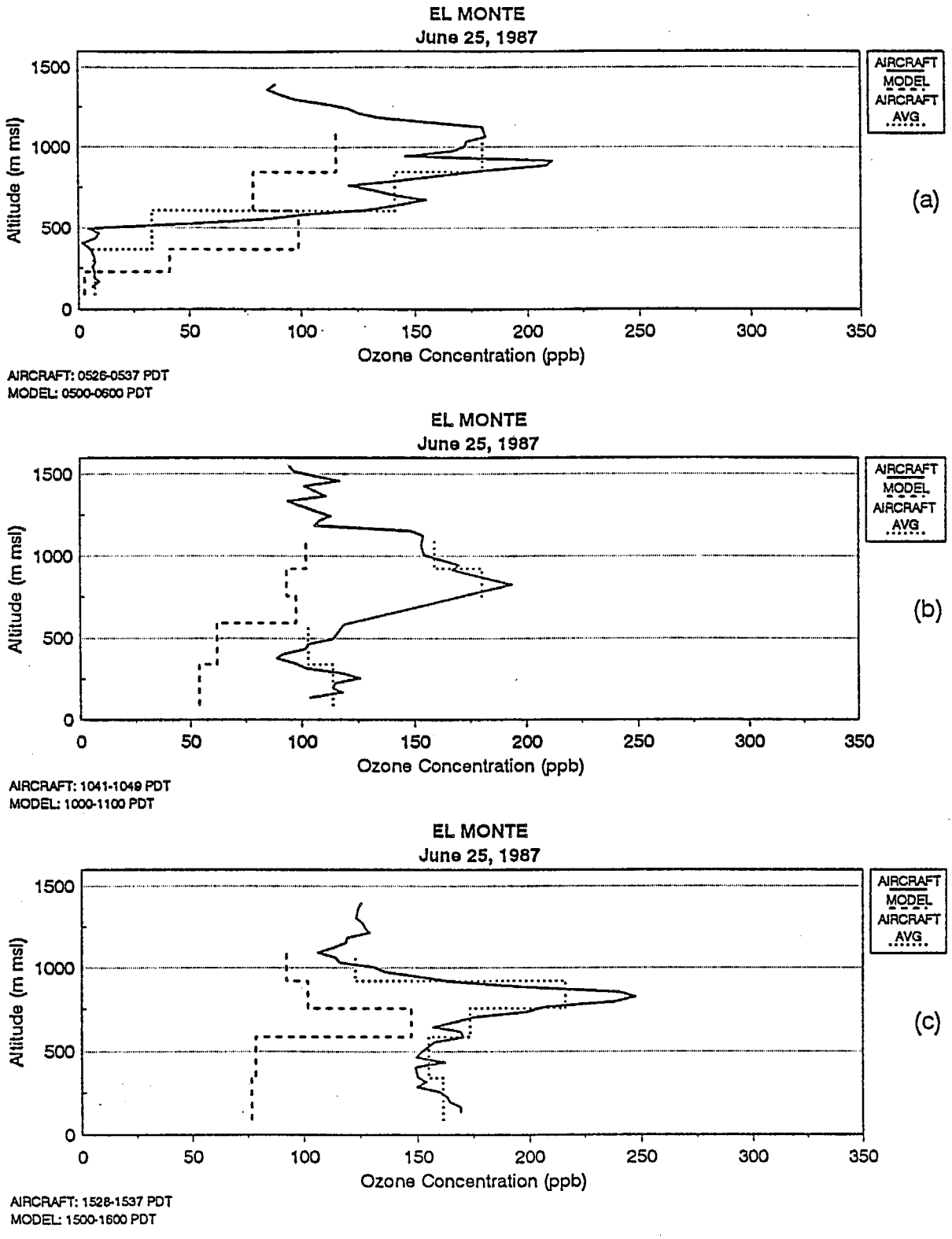

Figure 3-56. Vertical Profiles of Ozone Concentration Measured by Aircraft Spiral Compared to the UAM Average for the (a) Morning, (b) Midday, and (c) Afternoon at El Monte on June 25, 1987.

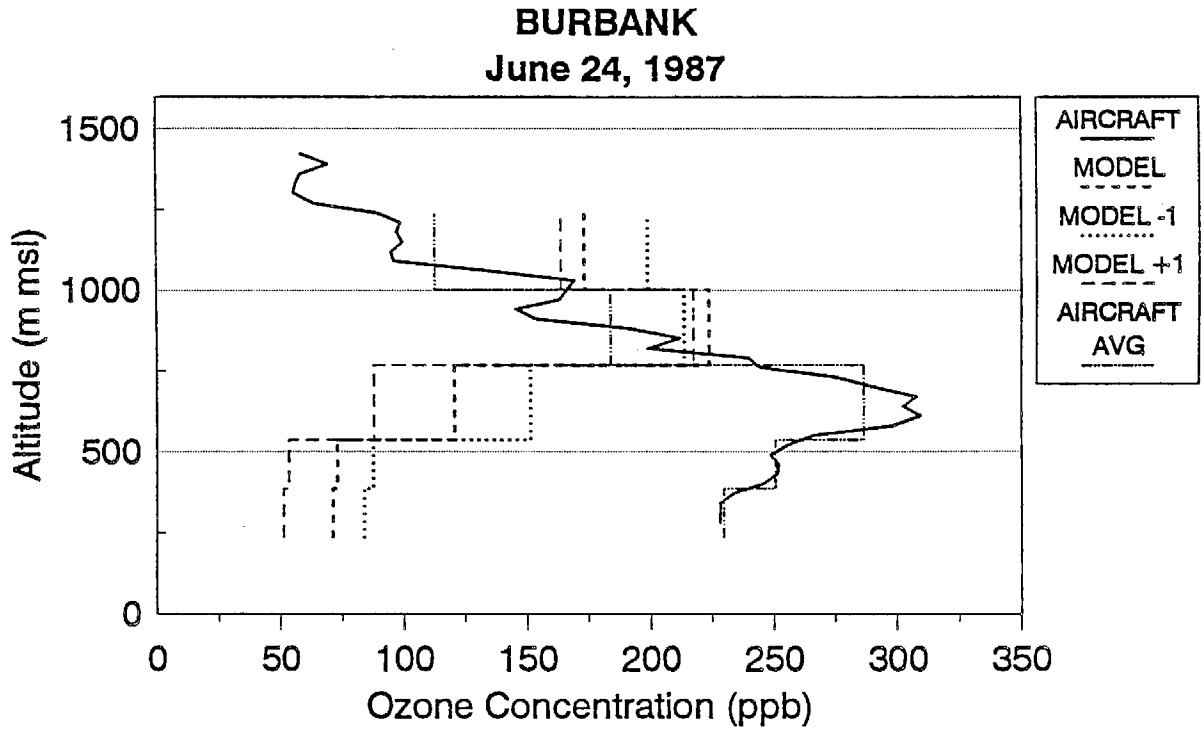

Figure 3-57. Vertical Profile of Ozone Concentration Measured by Aircraft Spiral Compared to the UAM Averages for the Afternoon of June 24, 1987. The UAM average data for the hour before and the hour after the aircraft flight are provided to illustrate temporal variation in the model output.

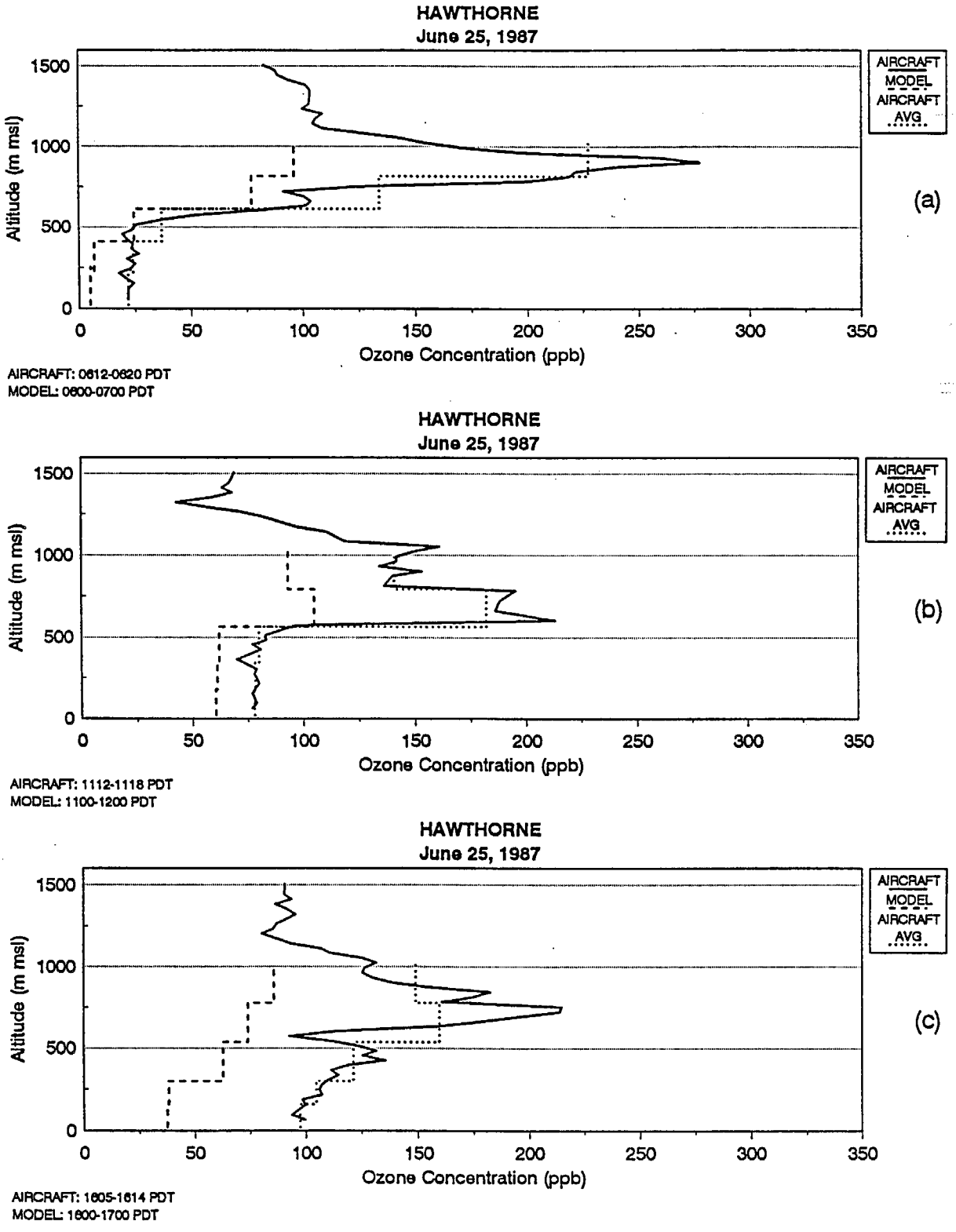

Figure 3-58. Vertical Profiles of Ozone Concentration Measured by Aircraft Spiral Compared to the UAM Average for the (a) Morning, (b) Midday, and (c) Afternoon at Hawthorne on June 25, 1987.

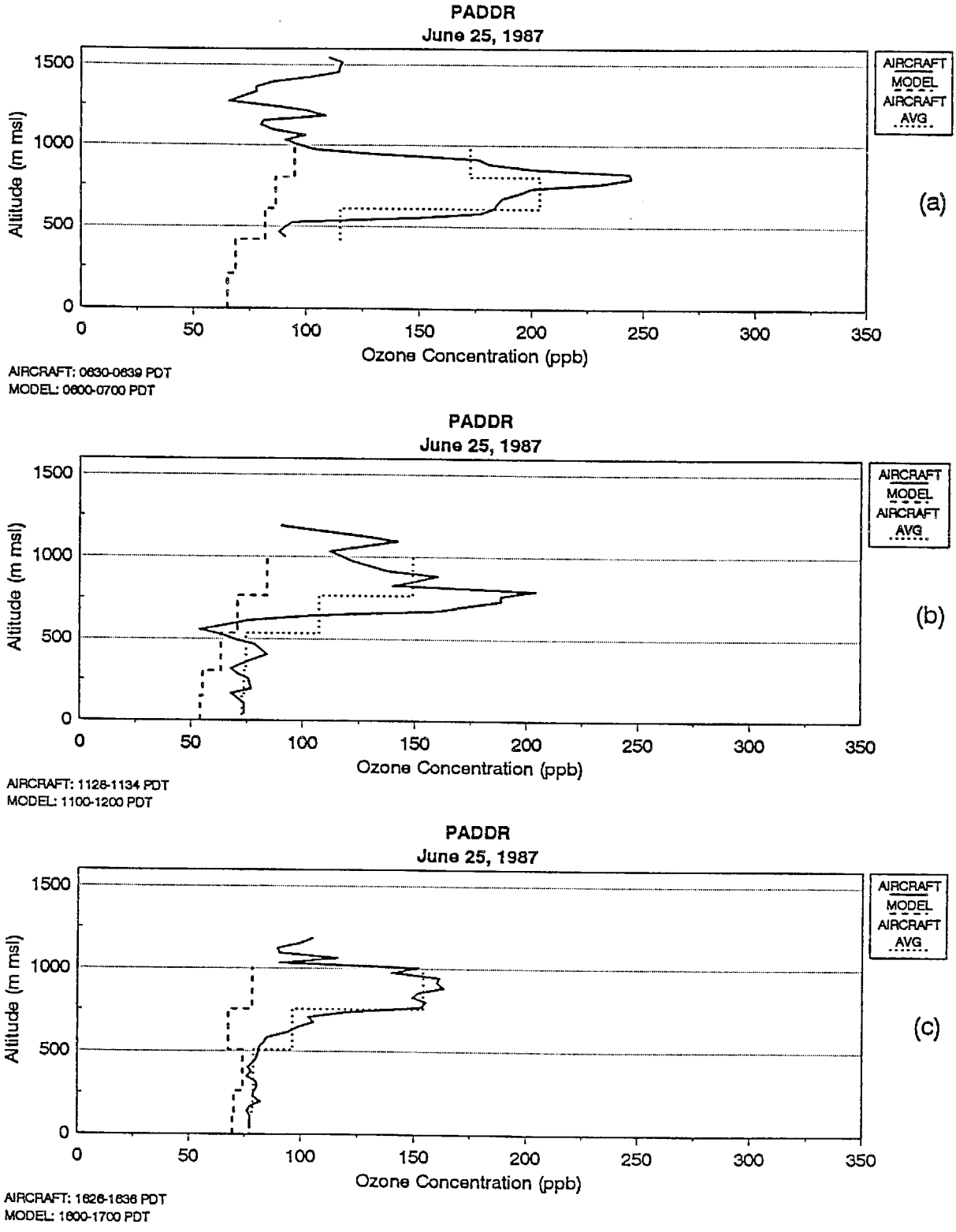

Figure 3-59. Vertical Profiles of Ozone Concentration Measured by Aircraft Spiral Compared to the UAM Average for the (a) Morning, (b) Midday, and (c) Afternoon at PADDR on June 25, 1987.

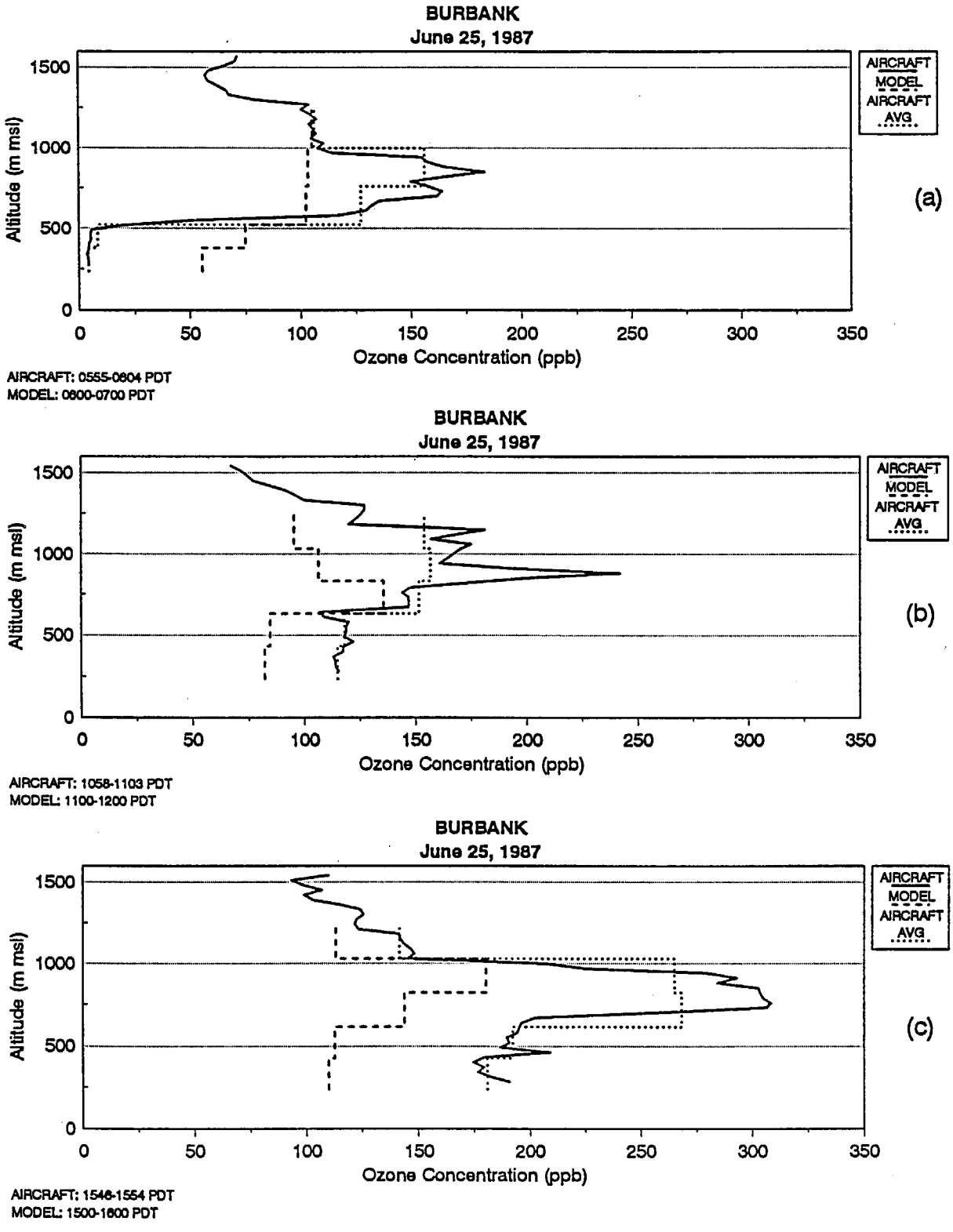

Figure 3-60. Vertical Profiles of Ozone Concentration Measured by Aircraft Spiral Compared to the UAM Average for the (a) Morning, (b) Midday, and (c) Afternoon at Burbank on June 25, 1987.

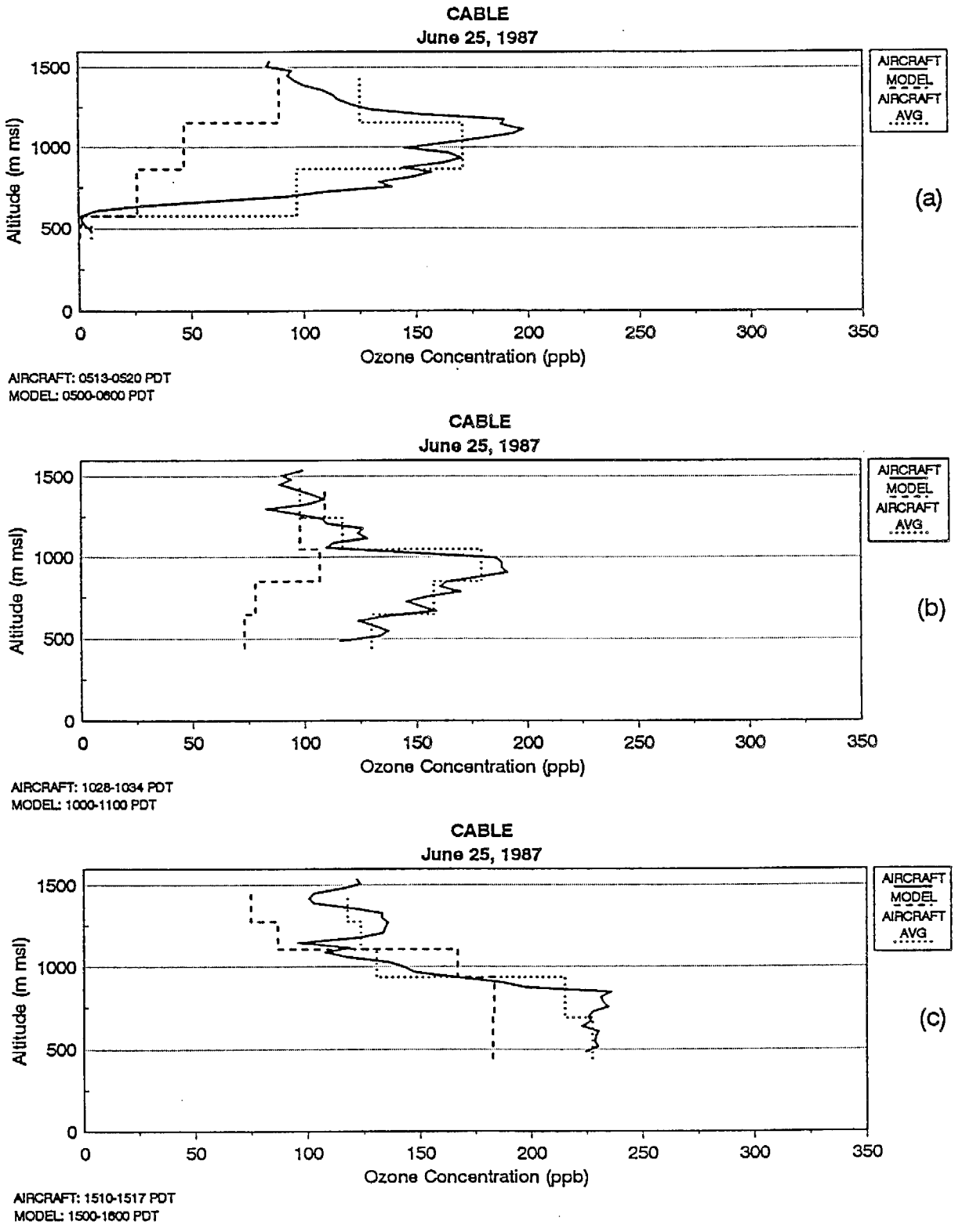

Figure 3-61. Vertical Profiles of Ozone Concentration Measured by Aircraft Spiral Compared to the UAM Average for the (a) Morning, (b) Midday, and (c) Afternoon at Cable on June 25, 1987.

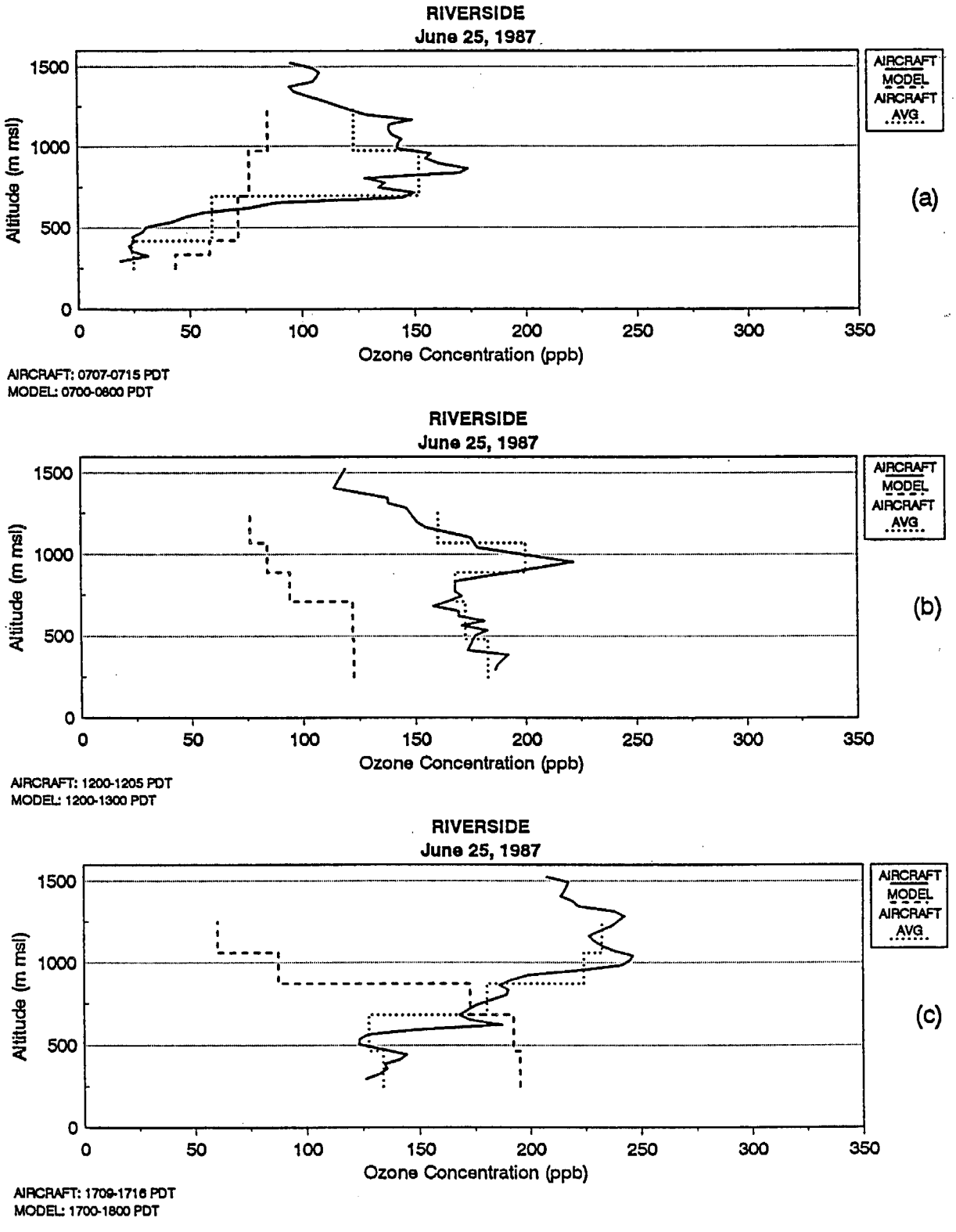

Figure 3-62. Vertical Profiles of Ozone Concentration Measured by Aircraft Spiral Compared to the UAM Average for the (a) Morning, (b) Midday, and (c) Afternoon at Riverside on June 25, 1987.

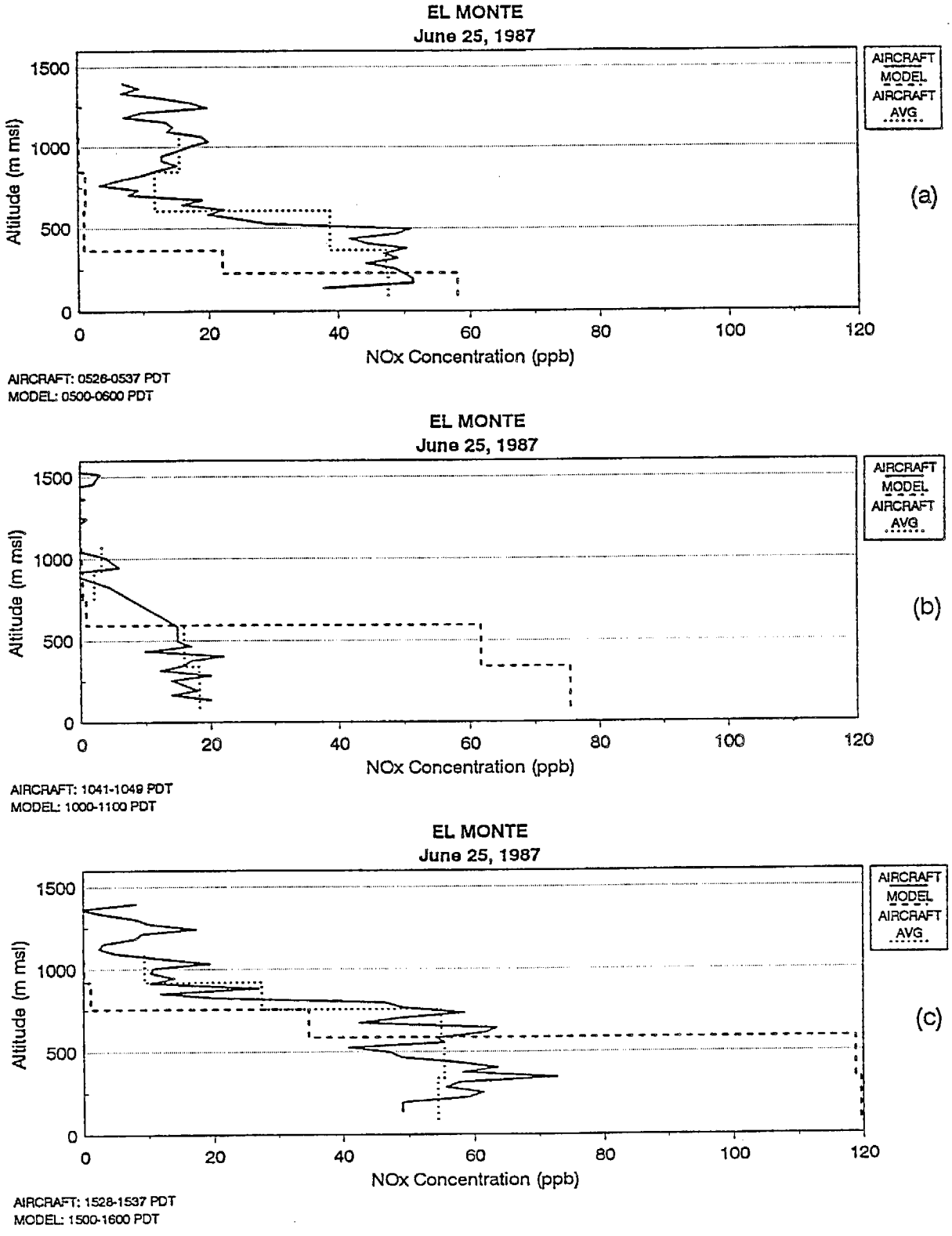

Figure 3-63. Vertical Profiles of NO_x Concentration Measured by Aircraft Spiral Compared to the UAM Average for the (a) Morning, (b) Midday, and (c) Afternoon at El Monte on June 25, 1987.

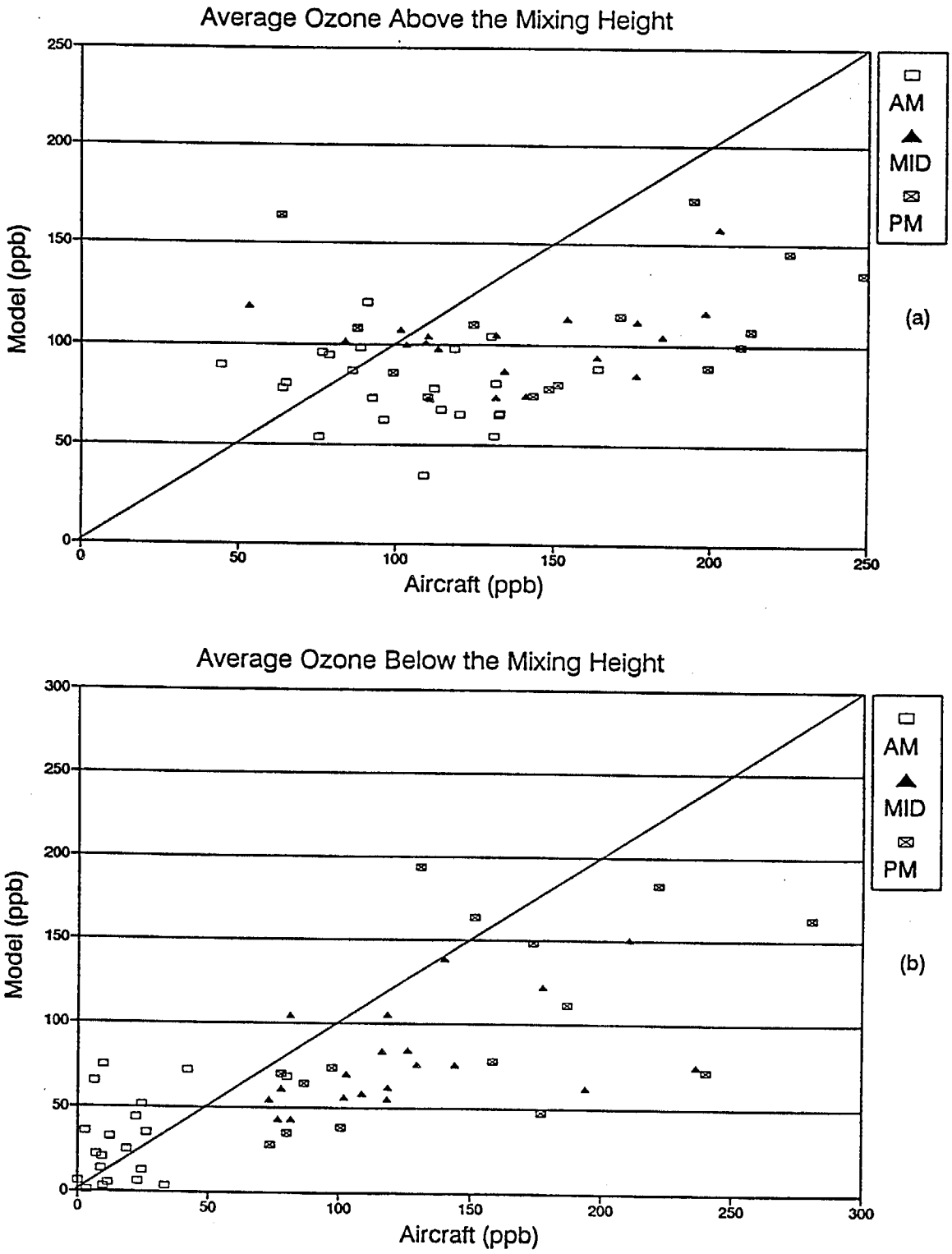

Figure 3-64. Comparison of Measured and Model-Generated Average Ozone Concentrations a) Above and (b) Below the Model-Predicted Mixing Height.

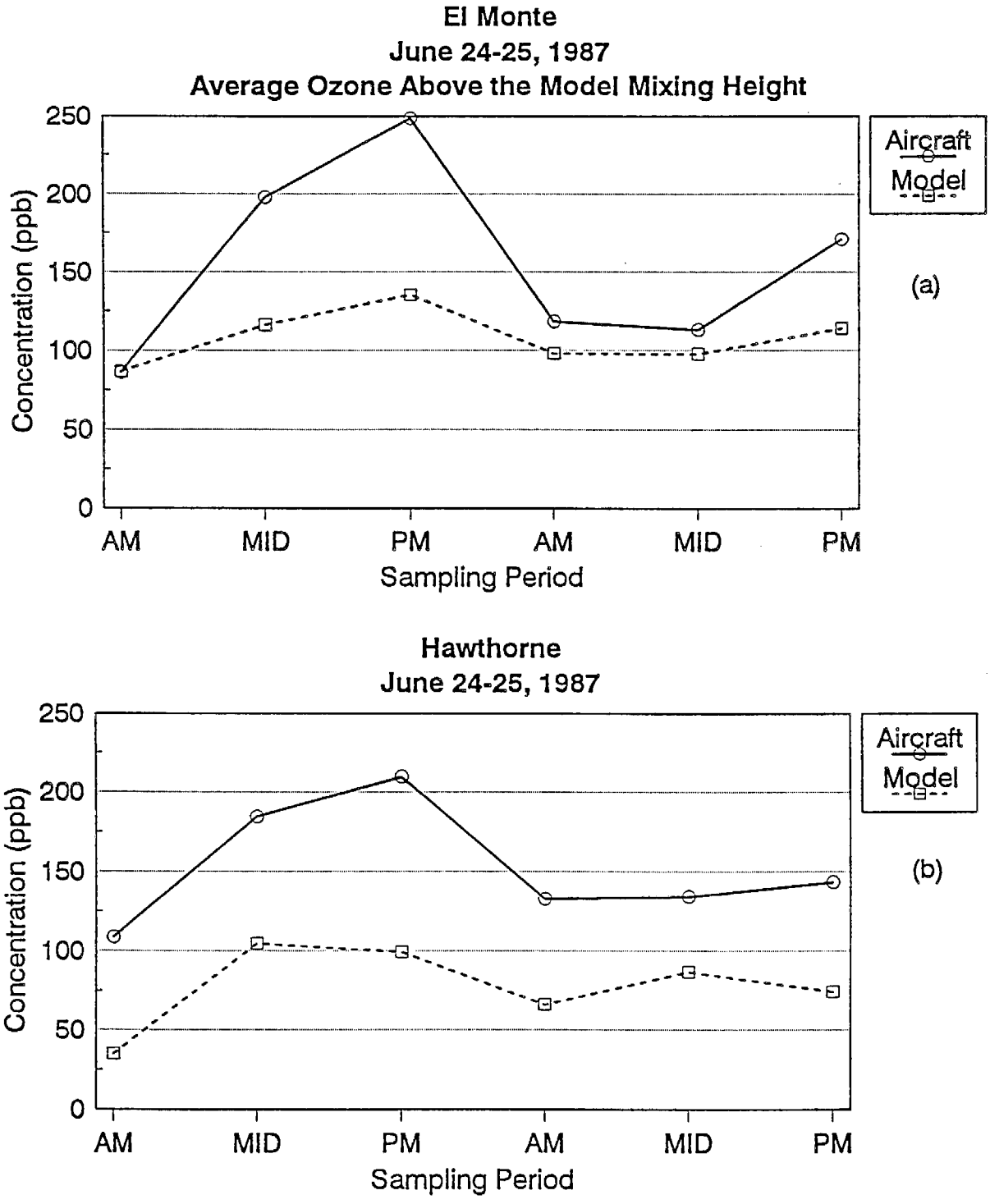

Figure 3-65. Average Ozone Concentrations Above the Model-Predicted Mixing Height for June 24-25, 1987 at a) El Monte and (b) Hawthorne.

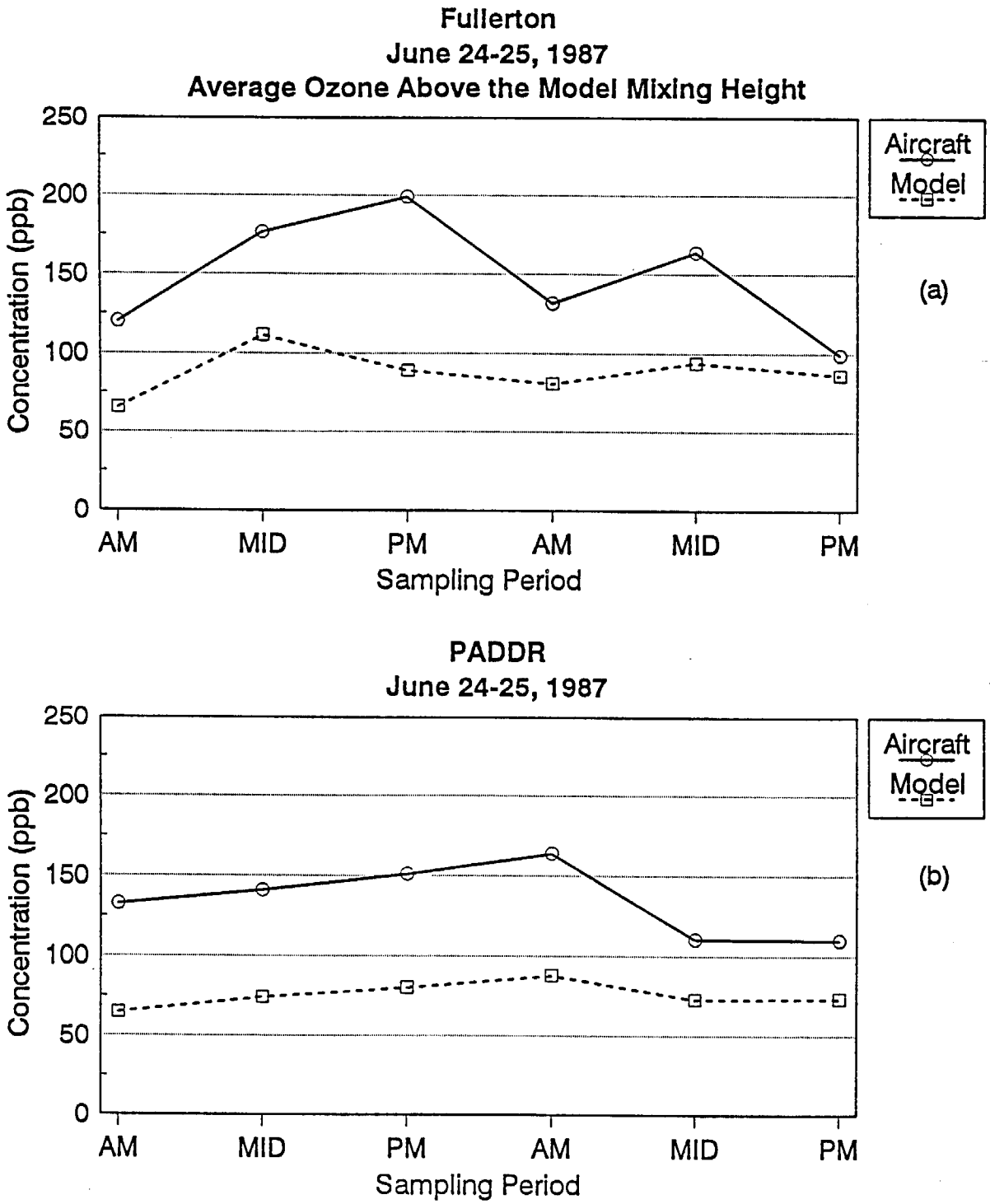

Figure 3-66. Average Ozone Concentrations Above the Model-Predicted Mixing Height for June 24-25, 1987 at (a) Fullerton and (b) PADDR.

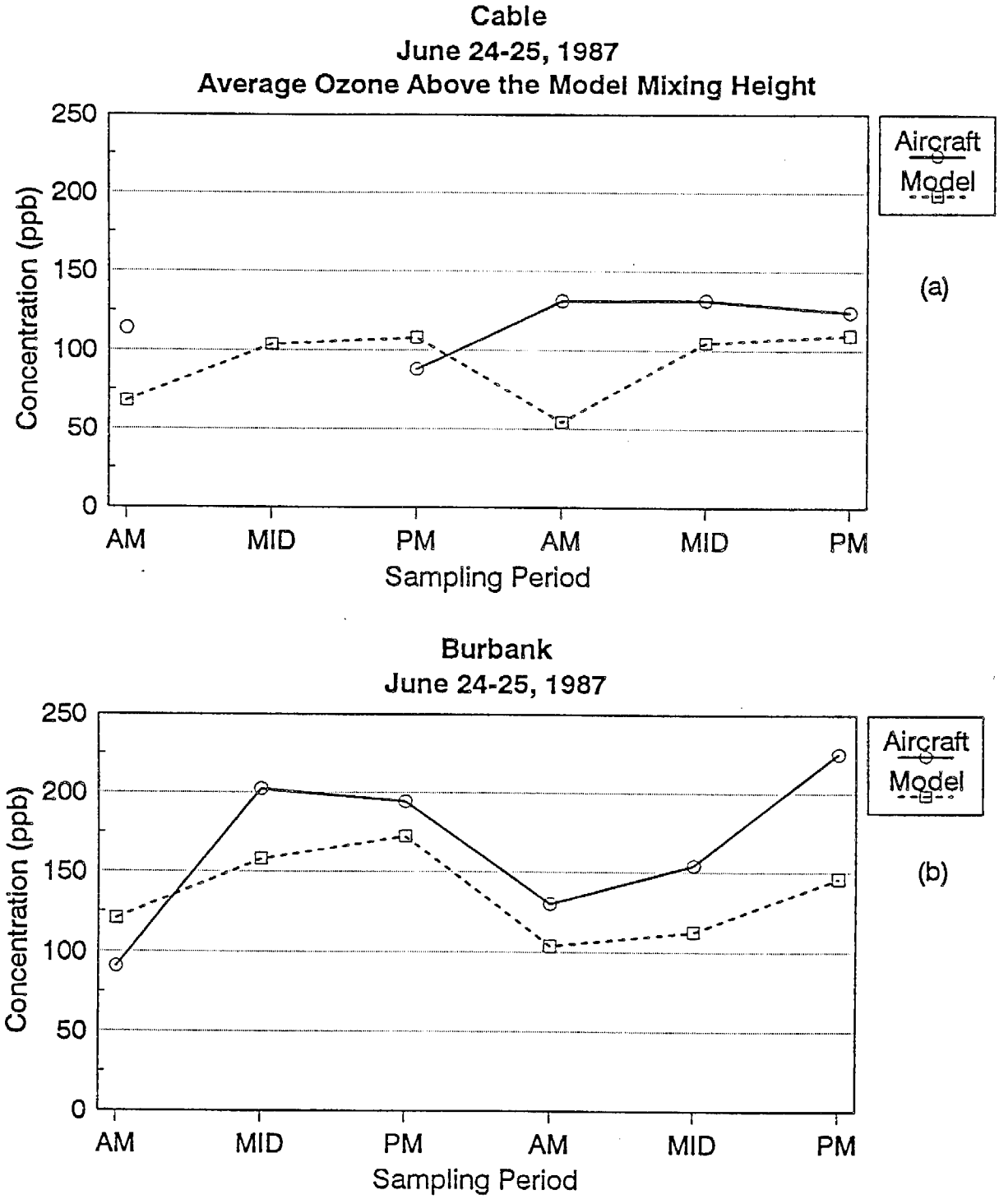

Figure 3-67. Average Ozone Concentrations Above the Model-Predicted Mixing Height for June 24-25, 1987 at (a) Cable and (b) Burbank.

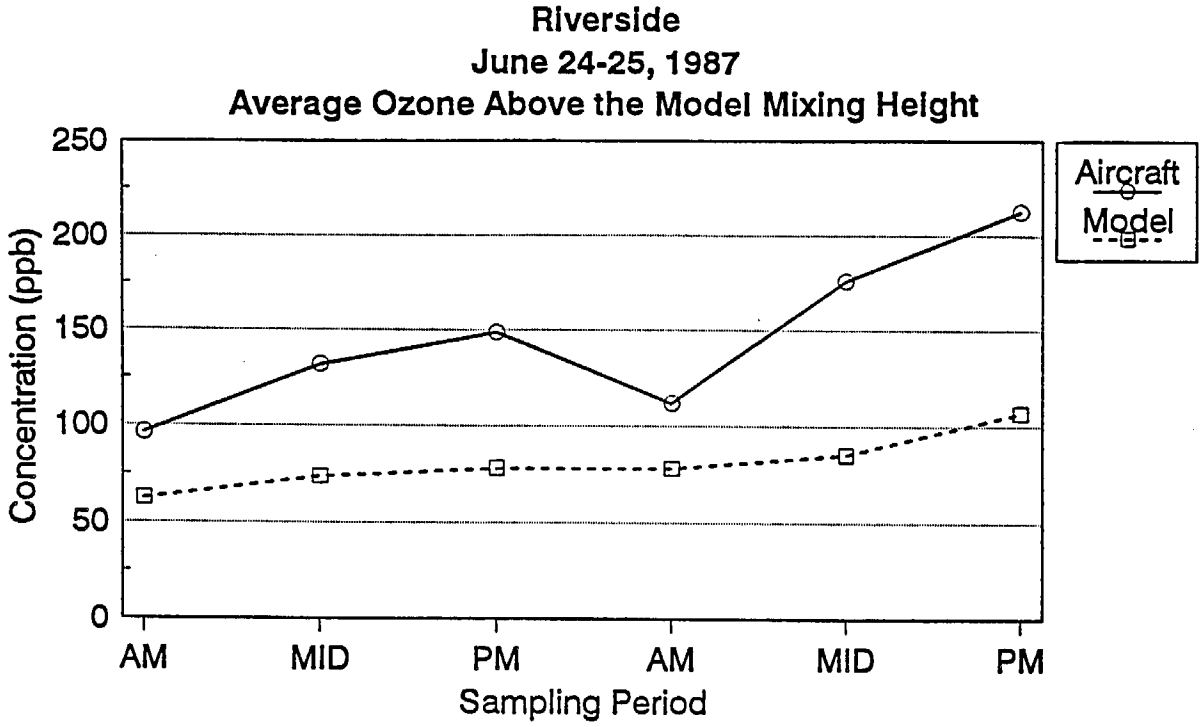

Figure 3-68. Average Ozone Concentrations Above the Model-Predicted Mixing Height for June 24-25, 1987 at Riverside.

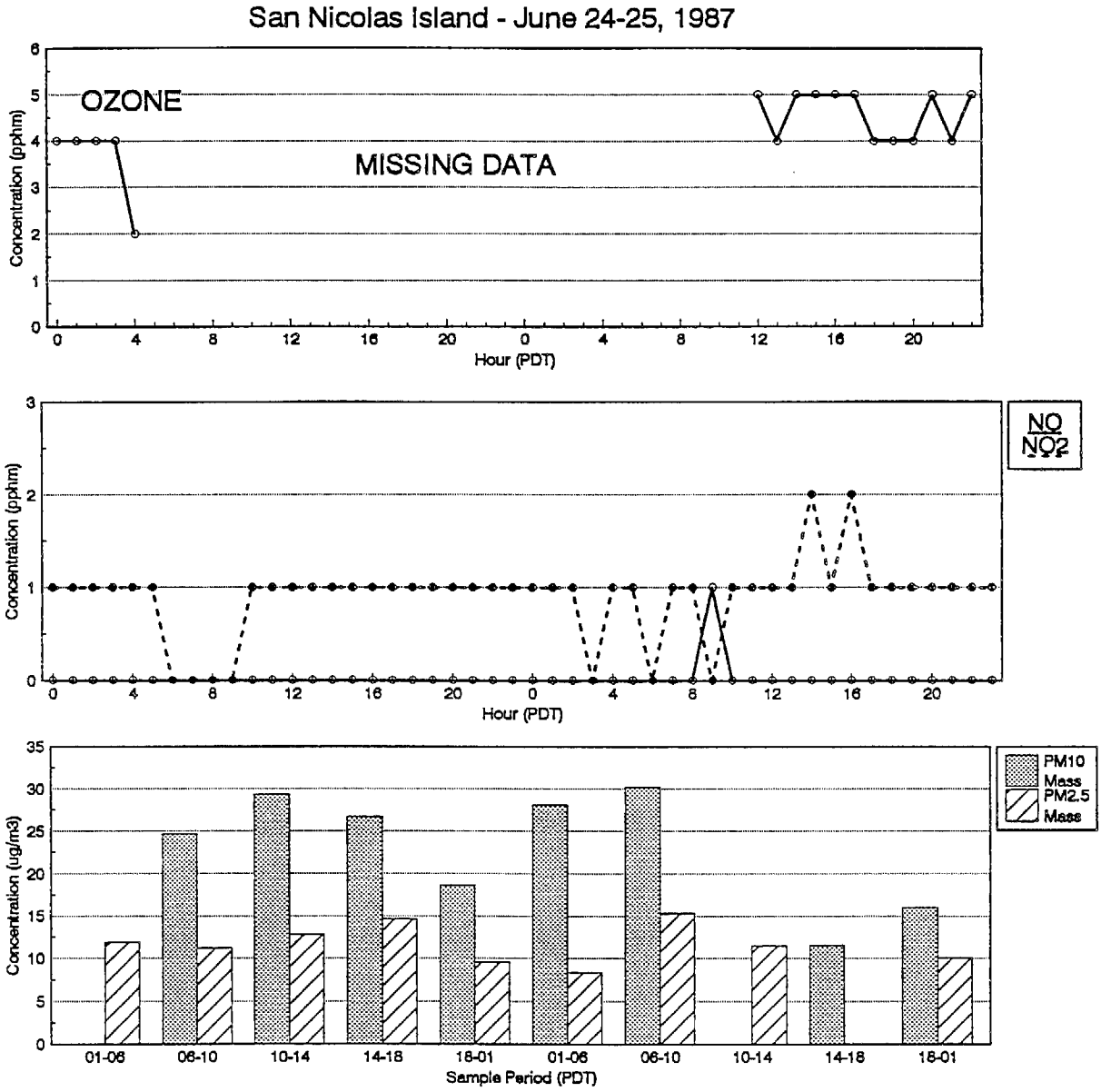

Figure 3-69. Ozone, NO, NO_2, and PM_{10} and $PM_{2.5}$ Mass Concentrations at San Nicolas Island on June 24-25, 1987.

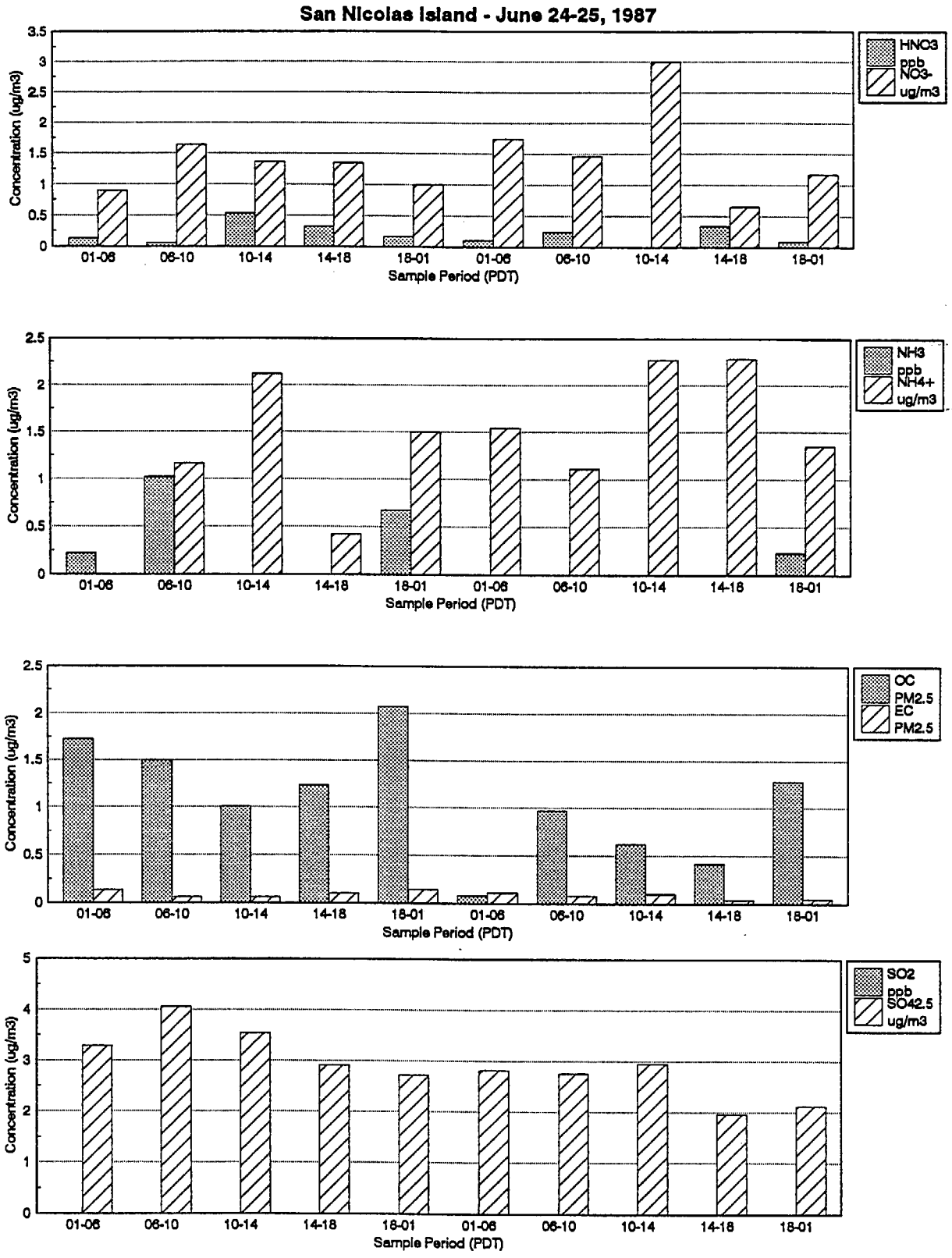

Figure 3-70. Nitric Acid, Ammonia, SO_2 and $PM_{2.5}$ Nitrate Ion, Ammonium Ion, Organic Carbon, Elemental Carbon, and Sulfate Ion Concentrations at San Nicolas Island on June 24-25, 1987.

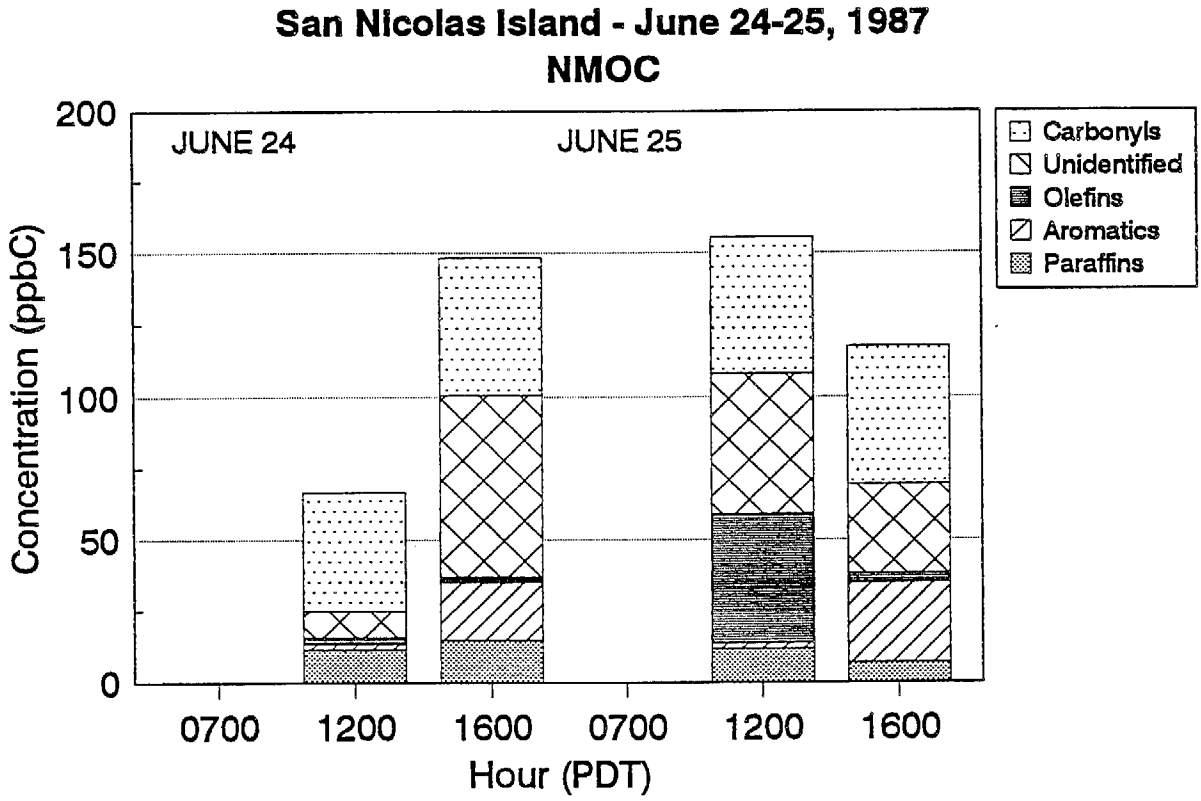

Figure 3-71. NMOC Concentrations at San Nicolas Island on June 24-25, 1987. Morning samples were missing.

4. CASE STUDY: JULY 13-15, 1987

Ozone concentrations exceeded the state standard at 21, 19, and 15 sites on July 13, 14, and 15, 1987, respectively; high PM_{10} concentrations were also measured at many sites. This episode has not been widely studied because of the development of the Catalina eddy on July 15. However, this episode is attractive for two principal reasons: 1) the surface and aloft data are quite complete for this episode and 2) aloft ozone concentrations on the morning of July 13 were relatively low and increased throughout the episode. This section is similar to Section 3 beginning with a summary description of the meteorology during the July 13-15 episode and continuing with a summary description of pollutant concentrations at both surface monitoring sites and aloft; including spatial and temporal concentration patterns, vertical profiles of pollutants aloft, and comparisons of pollutant concentrations at the surface and aloft.

4.1 EPISODE METEOROLOGY

The meteorology during the SCAQS has been well-described elsewhere (e.g. Surface winds - Zeldin et al., 1989; Aloft winds - Douglas et al., 1991 and SCAQMD, 1990). The following paragraphs summarize the meteorology during July 13-15, 1987 episode.

4.1.1 Synoptic Meteorology

A thermal low was centered near the Salton Sea with a weaker low extending into the San Joaquin Valley on July 13. A 5 to 7 mb pressure gradient between the coastal stations and the southern deserts maintained moderate onshore flow on July 13 and 14. On July 15, pressures fell over Nevada and the center of the thermal low moved northward. These changes were conducive to development of the Catalina eddy. The Catalina eddy is characterized by more southerly flow and widespread stratus clouds which limit the photochemical production of ozone.

4.1.2 Summary of Daily Meteorology

Figures 4-1 to 4-3 show surface streamline analyses prepared by Zeldin et al. (1989) for July 13-15, 1987. Plots are shown for 0700, 1200, and 1700 PDT to illustrate the morning stagnation or drainage wind conditions, early stages of the sea breeze, and the well-developed sea breeze. Surface streamlines were similar on July 13 and 14 midday; streamlines were different on each day of the episode in the morning and the afternoon. The surface winds are described in the following paragraphs.

July 13. In the morning, surface winds were light across the basin. North of Palos Verdes winds were onshore. South of Palos Verdes, winds were primarily northerly. Winds in the eastern basin were northerly and easterly through the passes. A weak cyclonic eddy existed over the Santa Monica Bay. Aloft, winds were light to moderate and predominately westerly. The sea breeze developed rapidly on this day. Westerly winds were observed in the Banning Pass by 0900 PDT.

By 1300 PDT, surface winds across much of the basin were westerly. Strong upslope flow was observed along the foothills and strong outflow at Cajon Pass was observed. By 1700 PDT, surface streamlines were nearly a straight line from west to east. Aloft, westerly flow dominated at 1000 m agl with southerly to south-easterly flow over the Coachella Valley.

July 14. In the morning, surface flow was weak and disorganized and no eddy was observed in the Santa Monica Bay. Flow was more southerly onshore in the southern basin than on the previous day. Most of the eastern basin showed westerly flow except at the far eastern basin and Cajon Pass, where flow was northerly. The western basin already showed a weak sea breeze, however a fully developed sea breeze occurred two hours later than on July 13. Overlying flow was weak and southerly to south-easterly at 300 m agl, but westerly to north-westerly at 1000 m agl.

Most of the surface streamlines were westerly at midday and in the afternoon. Southerly upslope flow at Glendora was weaker than the previous day. The 300 and 1000 m agl winds were westerly to south-westerly over the western two-thirds of the basin. Flow was south-easterly over the Coachella Valley.

July 15. In the morning, surface winds were still weak but had a more southerly component than on previous days. Winds were westerly in the eastern basin. Overlying flow was easterly to south-easterly.

By 1100 PDT, southerly flow over the central basin and foothills occurred. Flow was south-easterly in the Coachella Valley and easterly through the Banning Pass from the surface to over 1000 m agl. In the afternoon, winds were more westerly than at midday, but still contained a large southerly component. A weak sea breeze penetrated inland. Winds at the Banning Pass were north-westerly by 1700 PDT. South-easterly flow was observed in the Coachella Valley. Aloft, winds were south-easterly to westerly in the central basin, south-easterly over Burbank and Coachella Valley at 300 m agl. At 1000 m agl, winds were southerly to south-easterly.

A tracer release from Vernon on the morning of July 15 showed the tracer swept north and west into the San Fernando Valley. Particle trajectories using surface wind measurements lagged behind measured tracer transport. However, particle trajectories using upper level winds were in good agreement with the measured transport (Horrell et al., 1989, 1991). Tracers-of-opportunity measurements, also performed on July 15, indicated a basin residence time of about 6 hours on this day (Bastable et al., 1990).

4.1.3 Mixing Heights

Figures 4-4 and 4-5 show the mixing heights as determined from surface-based soundings and aircraft spirals for July 13-15 by T.B. Smith (T.B. Smith and Associates). Mixing heights across the basin varied each day. The coastal and some mid-basin stations had the lowest mixing heights, only up to about 600 m msl, on July 13. The maximum mixing heights at the other locations were similar all three days, but the diurnal shapes varied. The mixing heights ranged from about 800 to 1100 m msl in the afternoon and fell to about 300 to 400 m msl at night. The mixing heights determined from

aircraft spirals matched the nearby surface-based soundings very well, except at PADDR (offshore). The PADDR spirals were flown over the ocean and thus were dominated by the marine environment.

4.2 DIURNAL POLLUTANT PROFILES AT THE SURFACE

4.2.1 Ozone, NO, and NO_2

On July 13, the basin maximum ozone concentrations occurred at Glendora, Claremont, Fontana, San Bernardino, and Crestline (21 to 23 pphm). On July 14, the maximum surface ozone concentrations occurred at Fontana, Redlands, San Bernardino, Upland, and Crestline (23 to 25 pphm). On July 15, the maximum surface ozone concentrations occurred at the basin passes, Crestline and Banning (21-23 pphm).

Figures 4-6 and 4-7 show the diurnal profiles of ozone at the eight summer SCAQS surface B-sites. Ozone concentrations at Hawthorne and Long Beach were the lowest, while ozone concentrations at Claremont, Azusa, and Rubidoux were the highest. At night, ozone concentrations dropped to nearly zero at most sites except Hawthorne and Long Beach. Ozone concentrations at the surface increased abruptly for an hour early in the morning at Azusa on July 14. Wind data provided evidence of downslope flow.

The diurnal profiles of NO and NO_2 are shown in Figures 4-8 and 4-9 for the same sites. NO concentrations typically peaked in the early morning when traffic emissions were high and mixing heights were low. The highest NO concentrations were observed at Los Angeles and Rubidoux. A large NO peak was observed at Claremont overnight between July 13 and July 14. This peak corresponded to a large CO peak, indicating increased fresh emissions in the vicinity during that time period. NO and NO_2 concentrations were much lower on July 15 at Azusa and Anaheim than on the previous days. NO_2 concentrations were typically highest after the NO peak (oxidation of fresh NO). NO_2 concentrations remained relatively high, 4 to 10 pphm, July 13-14 at Azusa, Burbank, and Los Angeles. NO_2 concentrations at the western-basin sites were typically less than half these levels. The relatively high NO_2 concentrations observed in the afternoon were probably due to both transported pollutants and the oxidation of fresh (local) emissions.

4.2.2 Particulate and Gaseous Species

Figures 4-10 to 4-23 show the diurnal profiles of the gaseous and particulate pollutants measured at the eight surface sites during the July episode. The plots show PM_{10} and $PM_{2.5}$ mass and species concentrations for the most abundant $PM_{2.5}$ species; and formic, acetic, and nitric acids. One-hour averages for PAN and NMOC are also provided. Observations from these figures include the following:

- PAN concentrations (Figures 4-10 and 4-11) peaked at about the same time as ozone. Peak concentrations were 15, 16, and 10 ppb on July 13, 14, and 15, respectively at Claremont.

- Midday and afternoon peaks in PM_{10} and $PM_{2.5}$ mass (Figures 4-12, 4-13) were observed. PM_{10} mass concentrations were highest at Azusa and Rubidoux. The lowest concentrations were observed at Long Beach, Hawthorne, and Anaheim, where the diurnal variation in particulate mass concentration was small compared to other locations. $PM_{2.5}$ mass concentrations were highest at Burbank, Los Angeles, and Rubidoux. $PM_{2.5}$ mass concentrations peaked in the morning at Los Angeles, midday at Azusa and Burbank, and in the afternoon at Claremont and Rubidoux.

- Nitric acid concentrations (Figures 4-14, 4-15) were highest at Azusa and Claremont. Sites east of Los Angeles had peak concentrations in the afternoon, while Los Angeles and sites to the west had peak concentrations midday. Peak concentrations at Long Beach, Anaheim, and Rubidoux were low, below 5 ppb.

- $PM_{2.5}$ nitrate ion concentrations (Figure 4-14, 4-15) were highest at Rubidoux with relatively high concentrations also observed at Hawthorne. At Rubidoux, peak nitrate ion concentrations occurred during the night. At the other sites, the timing of peak nitrate ion concentrations varied.

- Ammonia concentrations (Figures 4-16, 4-17) were generally below 10 ppb at all sites except Rubidoux, where peak concentrations were up to 65 ppb. Peak ammonia concentrations occurred during the day.

- Ammonium ion concentrations (Figures 4-16, 4-17) were highest at Rubidoux. The Long Beach and Anaheim ammonium ion concentrations were lowest, with little temporal change (similar to PM_{10}). Ammonium ion concentrations at Azusa, Claremont, Los Angeles, and Burbank were mostly similar and peak concentrations typically occurred midday. Hawthorne had low concentrations of ammonium ion.

- The highest organic carbon (OC) concentrations (Figures 4-18, 4-19) were measured at Azusa, Burbank, and Claremont. Rubidoux and Los Angeles OC concentrations were also relatively high. OC concentrations at Long Beach, Hawthorne, and Anaheim were low and varied little during the episode. At the central- and eastern-basin sites, OC concentrations peaked in the midday or afternoon, corresponding to the peak ozone, PAN, and nitric acid concentration peaks.

- Elemental carbon (EC) concentrations (Figures 4-18, 4-19) were about one-fourth the OC concentrations. Concentrations were about the same at the central- and eastern-basin sites and showed little diurnal variation.

- SO_2 concentrations (Figures 4-20, 4-21) were highest at Hawthorne and Long Beach during the daytime. SO_2 concentrations were below 5 ppb at the other sites.

- Sulfate ion concentrations (Figures 4-20, 4-21) were highest at Hawthorne, Burbank, and Los Angeles with high concentrations occurring in the morning and midday. The lowest concentrations were on July 13.

Sulfate ions were present mostly in the fine aerosol, which is consistent with emissions and formation mechanisms.

- Formic and acetic acids (Figure 4-22) were significantly more abundant at Claremont than at Long Beach. Concentrations of both species peaked midday at Claremont.

- NMOC concentrations (Figure 4-23) were similar on July 13 and 14, and lowest on July 15. Concentrations were typically highest at Los Angeles and Burbank and lowest at coastal sites and Rubidoux. NMOC concentrations varied with time of day. On July 13, morning and midday NMOC concentrations were similar. On July 14, the midday concentrations were the highest at many sites, while on July 15, NMOC concentrations showed little diurnal variation.

4.3 VERTICAL POLLUTANT PROFILES

The air quality aircraft flew three flights daily during the summer: early morning, midday, and afternoon. On July 15, only the morning flight was made. Measurements were described in Section 2 and spiral and orbit locations are shown in Figure 2-10.

Vertical profiles of ozone, b_{scat}, NO, and NO_x by site, date, and time of day are shown in Figures 4-24 to 4-44. In these plots, the continuous data, which were collected every second (about every 3 meters) during each spiral, were averaged into 30 meter vertical bins. Data are plotted versus altitude in meters above mean sea level (m msl). Observations from these figures include the following:

Morning:

- Relatively high b_{scat} levels and NO, NO_x concentrations were observed in the surface layer on all three days (see Figures 4-29 and 4-30, for example). Ozone concentrations were low at these altitudes, probably because of titration by fresh NO emissions.

- On July 13, above the mixed layer, ozone concentrations were relatively low, below 120 ppb. A pollutant layer was observed at about 900 to 1200 m msl over the eastern basin. At Cable, elevated levels of both ozone and b_{scat} were present. A similar layer was present over Burbank but at a higher altitude. At El Monte, the layer contained elevated levels of ozone but not b_{scat}. Remnants of the ozone and b_{scat} layer were observed at Riverside two hours later. An ozone and b_{scat} layer was observed at PADDR, Fullerton, and Hawthorne just below 800 m msl.

- Also on July 13, a layer with relatively high concentrations of SO_2 was observed over the coastal sampling locations of Fullerton, Hawthorne, and PADDR. The layer contained higher levels of SO_2, NO_x, b_{scat}, and lower concentrations of ozone than the layers above and below. The layer was observed between 200 and 400 meters msl at all three spiral locations.

- On July 14, two layers of ozone and b_{scat} were apparent at El Monte, Riverside, and Cable (between about 800 and 1200 m msl). These layers may have been carried over from the previous day. Ozone concentrations were quite high in these layers, up to 200 ppb. High concentrations of SO_2 aloft were not observed.

- On July 15, two layers of pollutants were observed at Riverside and Cable (msl). At about the same altitude as the lower layer, a single layer was observed at El Monte. The top layer showed high concentrations of ozone (>150 ppb) and moderate levels of b_{scat} (200 Mm^{-1}), while the lower layer showed moderate concentrations of ozone (120 to 150 ppb), and high levels of b_{scat} (400 to 600 Mm^{-1}).

Midday and afternoon:

- On July 13 and 14 at midday, below about 750 m msl, ozone concentrations and b_{scat} levels were higher than in the morning. Above this layer, midday pollutant levels were similar to or higher than morning levels.

- On the afternoon of July 13, below about 750 m msl (slightly lower at the coastal sites), ozone concentrations and b_{scat} levels were reduced by the sea breeze influence at all onshore sites except Cable. At all spiral locations, above 750 m msl, ozone concentrations and b_{scat} levels were generally higher than earlier in the day. Above the surface layer, two pollutant layers (with elevated levels of both b_{scat} and ozone) were observed over El Monte, Burbank, Cable, and Riverside. The top layer had similar b_{scat} and ozone levels to the layer below it and may be due to slope flow. In the mixed layer, SO_2 concentrations were higher than on other days, possibly as a result of the entrainment of the thin SO_2 layer observed in the morning.

- At midday on July 14, traces of the two layers of ozone and b_{scat} observed earlier in the day were present at Cable, Riverside, and El Monte. At Burbank, two layers of ozone were observed above the mixed layer. By the afternoon, there were still traces of these two layers at El Monte, Cable, and Riverside however, the concentrations in the topmost layer were depleted compared to earlier in the day. At Burbank, concentrations in these aloft layers were higher than earlier in the day. The top layer may have been from upslope flow.

- On the afternoon of July 14, ozone concentrations and b_{scat} levels were significantly different from midday, again showing the sea breeze influence at all onshore sites except Cable and Riverside. Above the mixed layer, ozone concentrations and b_{scat} levels were typically lower than earlier in the day.

4.4 CHARACTERISTICS OF ALOFT INTEGRATED SAMPLES TAKEN DURING ORBITS

Integrated aerosol and gaseous samples were made during constant-altitude orbits using a modified version of the SCAQS sampler. These samples were later analyzed for nitric acid, SO_2, PAN, carbonyls, and particulate sulfur and nitrogen species similar to the surface samples. Orbit locations

are shown in Figure 2-10. Samples were collected by both the UW and STI aircraft during the SCAQS as described in section 2.2.2. The spatial distribution of these species aloft has not been investigated in much detail in past studies.

We computed the mean values of air quality parameters measured during the orbits and combined these parameters with the results of the integrated samples. Figures 4-45 to 4-53 show the orbit-averages of nitric acid, PAN, ozone, ammonia, SO_2, NO_x, NMOC, and $PM_{2.5}$ mass, organic and elemental carbon, nitrate ion, sulfate ion by date, time of day (morning and afternoon), and orbit location. All morning samples were collected above the mixing height. In the afternoon, the AMTRA and Long Beach samples were collected above the mixing height, while the Pomona and Riverside samples were collected within the mixed layer. Note that samples were collected offshore at DOYLE and PADDR only in the morning and inland at Pomona and Riverside only in the afternoon. No afternoon samples were collected on July 13. All $PM_{2.5}$ mass samples were invalid. Observations from these figures include the following:

- Ozone, nitric acid, and PAN concentrations were significantly higher in the afternoon than in the morning.
- Ozone, nitric acid, and PAN concentrations went up and down together.
- Elemental carbon, nitrate ion, ammonia, ammonium ion, and SO_2 concentrations were low, particularly in the morning samples. Nitrate ion concentrations were highest in the afternoon. Ammonium ion and ammonia concentrations in the afternoon at Riverside were relatively high compared to the other samples.
- $PM_{2.5}$ sulfate ion concentrations were generally higher in the afternoon. The highest sulfate ion concentrations were measured at Rubidoux on July 14.
- NMOC and OC concentrations were highest at AMTRA. The afternoon NMOC and OC concentrations were higher than the morning.
- Carbonyl compounds comprised a significant fraction of the NMOC aloft (typically more than 30% of the carbon).
- Over the episode, the morning pollutant concentrations were lowest on July 14. The afternoon samples collected on July 14 and 15 were similar.

4.5 COMPARISON OF SURFACE AND ALOFT POLLUTANTS

Air quality data at the surface are abundant both spatially and temporally in the basin. In contrast, aloft measurements of air quality are rarely available. In this section, we compare the aloft measurements of ozone, NMOC, and $PM_{2.5}$ mass and species made during July 13-15 with surface measurements.

4.5.1 Comparison of Aloft and Surface Ozone

We investigated how well the aloft ozone concentrations at the spiral locations compared to the measurements made at nearby surface sites. Figures 4-54 to 4-56 show the surface and aloft measurements made during the July 13-15, 1987 episode. Two ozone values are shown in the figures for the aircraft, the mixed-layer-average (MLA) and the 45-m average. The MLA was computed by averaging the ozone concentrations over the mixing height (determined by T.B. Smith and Associates) in the midday and afternoon. The 45-m average is the average ozone concentration in the lowest 45 m of the aircraft spiral. Most of the spirals during the summer SCAQS reached altitudes below 30 m agl.

At all sampling locations, the aircraft measurements were slightly higher than the surface in midday and afternoon. The Burbank and Cable aircraft data differed the most from the corresponding surface data, with the largest differences occurring in the afternoon. Over all SCAQS intensive days, MLA and 45-m average ozone concentrations were about 25 ppb higher than nearby surface concentrations (Roberts and Main, 1992).

4.5.2 Comparison of Aloft and Surface Particulate and Gaseous Species

Four of the aloft hydrocarbon and carbonyl samples were collected within about one hour of surface samples at nearby sites. The composition of the 25 most abundant species in the matched samples correlated poorly, r^2 = 0.0 to 0.38. NMHC concentrations at the surface were greater than aloft in all four matched pairs. Carbonyl compound concentrations aloft, on the other hand, were greater than concentrations at the surface in three of the four samples. Details are provided by Lurmann and Main (1992).

We matched aloft samples, collected during 30-minute orbits, with the nearest surface site data, collected during four-to six-hour periods. $PM_{2.5}$ elemental carbon and ammonium and nitrate ion concentrations aloft were almost always less than the matched surface concentrations. However, $PM_{2.5}$ organic carbon concentrations aloft were generally higher than at the surface. Nitric acid, ammonia and sulfate ion concentrations were sometimes higher and sometimes lower than matched concentrations at the surface.

4.6 THE PRESENCE AND STRUCTURE OF POLLUTED LAYERS ALOFT

4.6.1 Ozone and b_{scat} From West to East

In order to illustrate the structure of ozone concentrations aloft, we have constructed a 2-dimensional (2-D) plane from the surface to about 1500 m msl along a line from the coast to the eastern-basin (see map in Figure 3-44). This line passes near the Hawthorne, El Monte, Cable, and Riverside aircraft spiral locations. The PADDR, Burbank, and Fullerton spiral locations do not lie along this line, so we did not use these data in this analysis. We next interpolated and contoured data from spirals along the line to a 2-D plane which illustrates the pollutant structure aloft over the basin: Figures 4-57 and 4-58 show ozone and b_{scat} on July 13, 1987.

In the figures, the darkened area along the bottom of the figure shows the approximate ground level in the basin. Note that the ground level at Cable Airport is significantly higher than at either El Monte or Riverside; this is because Cable is part-way up the San Gabriel Mountains, as opposed to lower down along a straight line from El Monte to Riverside.

Figure 4-57 shows the 2-D ozone concentration plots for the morning, midday, and afternoon of July 13. On this morning, ozone concentrations were low across the basin, less than 120 ppb. Concentrations were highest over Cable. By afternoon, there was a 400 m-thick layer at about 500 to 900 m msl with ozone concentrations over 250 ppb covering most of the central and eastern basin. Peak surface ozone concentrations on this day reached 220 ppb at Claremont. The ozone and b_{scat} levels were lower to the west and showed a steep gradient inland. The b_{scat} levels were highest toward the ground and in the central and eastern basin. The sea breeze intrusion on the basin can be seen in Figure 4-58c; lower b_{scat} levels are seen near the surface from the coast to about El Monte.

On the morning of July 14, ozone concentrations near the ground were close to 0 ppb; probably titrated by fresh NO emissions. Aloft, there was a layer about 400 m thick with ozone concentrations over 100 ppb (from about 800 to 1200 m msl), with peak concentrations over 150 ppb. The b_{scat} levels were also high in this layer (Figure 4-60). This layer containing relatively high ozone concentrations was still present midday. By afternoon, ozone concentrations were high, over 250 ppb, in a layer between 500 and 800 m msl over most of the basin.

On the morning of July 15 (Figure 4-61), a layer with ozone concentrations over 100 ppb extended across most of the basin between 800 and 1200 m msl. This layer was similar to the layer observed on July 14 in location and extent; however, ozone concentrations were lower.

Figure 4-62 shows aerosol lidar results for the morning of July 13, 1987 along a 2-D plane from Ontario to San Bernardino; ground level is indicated along the bottom of the plot. The darker areas in the plot above the ground indicate higher particle backscatter and thus higher particle concentrations. Note that there is a layer of high particle backscatter between about 900 to 1100 m msl across the whole distance of the lidar image; this layer corresponds to the same ozone layer shown in Figure 4-57a over Cable. This layer was evident on numerous other lidar images covering a much wider area.

4.6.2 Ozone and b_{scat} From North to South

To investigate the layer structure from the north to the south, we prepared 2-D contours of ozone and b_{scat} along a plane from Burbank through El Monte to Fullerton (see map in Figure 3-45). Ozone and b_{scat} data were interpolated and contoured as described in Section 4.6.1. Figures 4-63 to 4-65 show these ozone and b_{scat} 2-D contours.

On July 13, morning pollutant concentrations aloft were low. In the afternoon, a layer with high ozone concentrations (peak values above 300 ppb) was observed from Burbank to Fullerton between about 700 and 1200 m msl. This layer was also observed in the central and eastern basin (Figure 4-47),

indicating this layer extended to the north and south as well. The b_{scat} levels aloft were higher at Burbank than at Fullerton.

On the morning of July 14, a layer containing ozone concentrations greater than 100 ppb was only observed at El Monte. Ozone and b_{scat} levels were about the same in altitude and magnitude below about 700 m msl from the north to the south. In the afternoon, the ozone layer observed in the central and eastern basin (Figure 4-59) at about 500 to 800 m msl (above 250 ppb) did not appear to extend north to Burbank or south to Fullerton.

On the morning of July 15, a layer containing ozone above 100 ppb extended over the central, eastern and northern basin at about 700 to 1100 m msl (see Figures 4-61). The b_{scat} levels were about the same from north to south.

4.7 ALOFT LAYER FORMATION

Aloft layers of pollutants can be formed by a number of mechanisms (Edinger, 1963; Blumenthal et al., 1974; Smith et al., 1976), including the following: Undercutting of the afternoon mixed layer by the sea breeze, isolation of polluted material aloft by the nocturnal boundary layer, upslope flow in the afternoon, injection of pollutants aloft by stationary source emissions, transport of buoyant air parcels from the mixed layer into the inversion layer (convective debris; Edinger, 1963), and injection aloft at a convergence zone formed in the eastern basin when the sea breeze meets a weak easterly flow.

Undercutting of the afternoon mixed layer by the sea breeze occurred regularly during the summer SCAQS. On most summer days, a shallow sea breeze penetrates the basin and undercuts the afternoon mixed layer, pushing a shallow polluted layer in front of it and leaving the top portion of the mixed layer aloft. The sea breeze is composed of relatively clean, cool air which does not mix significantly with the more-polluted mixed layer. Figure 4-66 shows pollutant profiles at Cable and El Monte on the afternoon of July 13, 1987. The sea breeze was not evident in the Cable pollutant profile; however, the sea breeze had undercut the mixed layer and cleaned out the lower 600 m at El Monte. The elevated polluted layer above 600 m msl at El Monte was formed at a relatively low altitude and thus, may be incorporated into the mixed layer the following day depending upon transport of this layer during the night. This type of undercutting of the mixed layer by the sea breeze was common during the SCAQS at locations from the coast inland to El Monte; the sea breeze seldom reached Cable or Riverside. The lidar gray-scale plot in Figure 4-67 shows that clean air due to the sea breeze (surface to about 500 m msl) has penetrated to about El Monte and isolated a polluted layer aloft on the same afternoon.

Another way in which pollutants may be transported aloft is upslope flow. Past research efforts have shown that the heating of the slopes and inland valleys provide a major mechanism for ventilation of the basin. Flow up the mountain slopes due to heating may carry pollutants aloft to form layers above the surface mixing layer. Dispersion of this aloft layer would be dependent on the aloft winds. Figure 4-68 shows a lidar gray-scale plot

for a flight from Mt. Gleason to South Pasadena on the afternoon of July 14, 1987. In the figure, higher particle backscatter is denoted by a darker signal. The mixed layer is shown rising up the mountainside and being injected aloft, some material is even being injected above the top of the mountain. Figure 4-66 shows a layer of b_{scat}, ozone, and NO_x at Cable and El Monte on the afternoon of July 13 from about 1100 to 1300 m msl which may be from upslope flow. This layer may or may not affect surface concentrations the next day, depending upon transport and mixing depth. Similar evidence of upslope flow was found in past studies (Wakimoto and McElroy, 1986).

Fresh emissions of SO_2, particles, and NO in narrow layers aloft were observed at offshore, coastal, and central basin locations on July 13 at fairly low altitudes (200 to 400 m msl). Concentrations were relatively low (SO_2 less than about 25 ppb). These layers may indicate the presence of power plant or other stationary source emissions and will probably be dispersed into the mixed layer because of their low altitudes. However, because of low SO_2 concentrations, these layers will likely have little impact on SO_2 or sulfate ion concentrations at the surface. Figure 4-69 shows the b_{scat}, ozone, NO, NO_2, and SO_2 concentration profiles at Hawthorne and Fullerton on the morning of July 13, 1987. The narrow layer between 200 and 400 m msl was typical of other days and locations when SO_2-containing layers were observed.

Figure 4-66 also shows evidence of polluted material above the afternoon mixed layer which might be Edinger's "convective debris". The ozone peak at about 900 m msl at El Monte is possibly the result of buoyant air parcels transported above the mixed layer. This mechanism may account for layers aloft all across the basin.

4.8 ISENTROPIC ANALYSIS OF ALOFT STRUCTURE FOR JULY 13-14, 1987

To further our investigations of the formation, structure, and fate of aloft layers of ozone, we performed isentropic analyses using upper air data collected on July 13-14, 1987. Isentropic analysis involves identifying levels of constant potential temperature in the atmosphere and examining their vertical, horizontal, and temporal structure and their relationship to other meteorological features, especially transport regimes. The potential temperature of an air parcel is the temperature the parcel would have if it was expanded or compressed adiabatically (that is, without addition or loss of heat) from its initial state to a reference pressure of 1000 mb. The equation for calculating potential temperature (θ) is as follows:

$$\frac{T}{\theta} = \left[\frac{p}{1000}\right]^k \qquad (1)$$

where:

p	=	pressure (mb)
T	=	temperature (K)
k	=	0.286

As an air parcel moves vertically during an adiabatic process, its temperature changes in response to the increase or decrease in pressure, but its potential temperature remains constant. Thus, potential temperature is a conserved property and air parcels will tend to remain confined to levels of constant potential temperature, referred to as isentropes, until such time as diabatic forces (e.g. convective mixing following sunrise) alter the parcel's heat content and thus its potential temperature. The potential temperature of an air parcel can be used as a tracer of opportunity to tag aloft layers that may contain high ozone concentrations and to monitor their evolution and fate.

Figure 4-70 shows an example of an isentropic analysis prepared from upper air data collected at 2200 PDT on July 13, 1987. The figure shows contours of potential temperature (isentropes) labeled in K or °K along a longitudinal-vertical cross-section (x-z plane) extending from the coast near Santa Monica eastward to Riverside. Ground level is indicated along the bottom of the plot by the thick dark band. The identification of the upper air stations from which data were taken to prepare the analysis are shown along the bottom of the cross-section. The vertical scale is plotted in m msl and the horizontal scale is plotted in kilometers inland from the origin of the cross-section, which very nearly corresponds to distance inland from the shoreline.

The large vertical gradient of potential temperature indicates the presence of a strong inversion. The base of the inversion began at approximately 300 m msl. This analysis indicates that the depth of the inversion extended to nearly 1500 m msl. The lower levels of the inversion were produced by a combination of the sea breeze that transported cool marine air inland and radiational cooling of the surface after sunset. The upper levels of the inversion were caused by synoptic-scale subsidence associated with the Pacific ridge. The combination of these processes produced an inversion of such strength and depth that vertical mixing was severely limited. If an aloft layer(s) of air containing high ozone concentrations existed at the time of this analysis at the 304 K level, for example, then this layer was effectively isolated from surface-based processes; it will either remain aloft over the basin at the 304 K level until daytime heating destroys the inversion and fumigates the layer into the daytime convective boundary layer (CBL); or it will be transported out of the region. The following steps were performed to prepare this analysis and the analyses to be presented below:

- An east-west oriented, longitudinal cross-section was defined as shown in Figure 4-71. The origin of the cross-section was placed at 34 00'00" north latitude and 118 30'00" west longitude, which is a point near the coast just west of the Santa Monica airport. The cross-section extends due eastward to Riverside.

- Upper air data collected at the following stations on July 13-14, 1987 were used in the analyses: Loyola Marymount University (LMUA), El Monte (EMUA), Yorba Linda County Park (YLUA), Ontario International Airport (ONT), and Riverside Municipal Airport (RAL). The location of these stations along the cross-section was calculated based on projecting each station's UTM Easting coordinate onto the cross-section.

- Potential temperatures as a function of altitude were computed for each upper air sounding using the measured pressure and temperature data. The potential temperatures were then interpolated to a uniform x-z grid along the cross-section shown in Figure 4-70. The vertical and horizontal extents of the grid were 3000 m and 100 km, respectively. The grid was divided into nodes of 100 m vertically by 4 km horizontally. Contours of potential temperature were generated from the gridded fields and plotted at 2 K intervals.

Figure 4-72 shows the isentropic analyses for three periods on July 13, 1987: 0500 PDT, 1100 PDT, and 1400 PDT. These three periods are presented because they correspond to the times that the aircraft was sampling. Figure 4-73 shows the isentropic analyses for the same periods on July 14, 1987.

The analysis of the July 13 data shows a strong inversion (nearly 15 K/km in the first 1000 m agl) over the entire basin in the early morning. In the 0500 PDT analysis, the base of the inversion over the western half of the basin was indicated by the 290 K isentrope, which was located at approximately 300 m msl. It is likely that this level corresponded to the base of the marine layer. Over the eastern half of the basin, the base of the inversion was indicated by the 296 K isentrope, which was located at approximately 500 m msl. The fact that the isentropes are nearly horizontal indicates that the inversion was not being strongly influenced by the terrain that rises from sea level to nearly 300 m as one follows the cross-section's path eastward across the basin. It appears that the influence of the marine air only extended inland to a point between El Monte and Yorba Linda, where the isentropic analysis indicated that a front-like structure separated the marine air from the continental air mass over the eastern basin. The ozone profiles did not show very high concentrations aloft (less than 110 ppb), but they did indicate that the previous day's ozone had been carried-over beginning at the base of the inversion, which is indicated by the 296 K isentrope.

The July 13 1100 PDT analysis shows destruction of the nocturnal inversion by inland heating, growth of the CBL over the central and eastern basin, and warming of the air over the basin and a decrease in the strength of the inversion (from 15 K/km in the early morning to approximately 8 K/km in the first 1000 m agl). Cool marine air was pushing into the western end of the basin as the sea breeze developed. Air at the 296 K level, which contained roughly 100 ppb ozone according to the early morning aircraft profiles, had been fumigated into the CBL over the central and eastern basin. Aloft ozone concentrations were comparable to their early morning values.

By early afternoon, the isentropic analysis shows that the sea breeze had penetrated farther inland and the base of the inversion over the western half of the basin was located at roughly 400 m msl. Ozone concentrations in the marine layer at El Monte were only 100 ppb, but aloft, ozone concentrations were as high as 350 ppb at the 304 K (900 m msl) and 308 K (1300 m msl) levels. A pronounced layered structure was also evident in the ozone profile at El Monte. Given the stability in these layers, the source of these high ozone concentrations is not immediately clear from this analysis. Vertical mixing near El Monte should be suppressed by the stability indicated

in the cross-section. The high ozone concentrations may be the result of transport of polluted air from other areas rather than vertical mixing of ozone produced in the vicinity of El Monte. At Riverside, the 304 K level marked the base of the inversion. In the CBL below the 304 K level, ozone concentrations ranged from 175 ppb to 225 ppb. Above the inversion base, ozone concentrations were lower, comparable to their morning values.

The isentropic analyses of the data collected on July 14 (Figure 4-73) revealed patterns that were similar to those depicted in the analyses of the July 13 data. A strong inversion was present over the entire basin at 0500 PDT on July 14. The marine layer over the western basin was deeper than on July 13, but the base of the inversion was still quite low (approximately 500 m msl), using the 292 K to 296 K isentropes for guidance. The top of the inversion, based on the location of the 312 K level, was located near 1500 m msl. Once again, the fact that the isentropes are nearly horizontal indicates little influence of the underlying terrain on the vertical structure of aloft layers.

The most significant difference between the July 13 and July 14 analyses is the presence of aloft layers on the 14th that contained relatively high concentrations of ozone. As discussed above, these aloft layers were the result of carry-over of ozone produced on the 13th. Ozone profiles showed concentrations as high as 150 ppb at 302 K (roughly 900 m msl) at El Monte. At Riverside, a layer with 150 ppb ozone was seen at about 298 K (700 m msl); a second layer containing 200 ppb of ozone was present near the 304 K level (approximately 1000 m msl). Figure 4-74 shows the ozone concentration contours lined up with the potential temperature contours for the morning of July 14.

The fate of these aloft layers containing high ozone concentrations can be monitored by observing the evolution of the 296 K, 304 K, and 312 K isentropes from 0500 PDT until 1400 PDT, as shown in Figure 4-73.

By 1100 PDT, one can no longer identify the 296 K layer over the eastern half of the basin (the 296 K level still marks the base of the inversion over the western half of the basin). Vertical mixing and growth of the convective boundary layer has entrained air originally at the 296 K to 300 K levels (approximately 500-800 m msl) over the eastern basin into the new daytime boundary layer. Ozone concentrations in these layers, based on the early morning aircraft spirals, were only 50-100 ppb at El Monte but 100-150 ppb at Riverside. Ozone concentrations in the CBL at 1100 PDT were 50 ppb at El Monte and 150 ppb at Riverside, comparable to the concentrations in the aloft layers that were fumigated by 1100 PDT. The 304 K level over Riverside and the 302 K level over El Monte still contained the 200 ppb and the 150 ppb of ozone observed during the early morning aircraft spirals, respectively.

By 1400 PDT, air at the 304 K to 306 K levels (approximately 800-1000 m msl) has been entrained into the CBL over the eastern basin. The 1100 PDT aircraft spiral at Riverside showed aloft ozone concentrations of 200 ppb at levels corresponding to 304 K (approximately 900 msl). By 1400 PDT, the Riverside profile showed ozone concentrations in the CBL of 200-225 ppb, again comparable to concentrations observed aloft before those

layers were mixed downwards. Over the central basin (El Monte), ozone concentrations in the CBL were 150 ppb, with a maximum concentration of 300 ppb near the base of the inversion at 302 K. Recall that ozone concentrations at the 302 K level at 0500 PDT and 1100 PDT were 150 ppb, so that the 300 ppb concentration may be a combination of the carry-over of this aloft layer plus production of new ozone on the 14th. Farther westward, the 296 K isentrope marks the top of the shallow marine layer as the sea breeze continues to transport cool marine air inland.

In summary, isentropic analyses of the July 13-14, 1987 episode were successful at providing evidence of the entrainment of aloft layers containing high ozone values into the convective boundary layer over the basin. The analyses of the spatial and temporal distributions of potential temperature helped to define the locations of these aloft layers, their vertical extent, and those regions where aloft air had been mixed into lower levels.

4.9 ALOFT TRANSPORT ANALYSIS FOR JULY 13-14, 1987

The isentropic analyses summarized in Section 4.8 do not explicitly address the issue of aloft transport regimes and how they may affect the distribution of the aloft layers of ozone identified in our analyses. Following the procedures of Whiteman et al. (1991), we investigated aloft daytime transport conditions during the July 13-14, 1987 episode by calculating integral quantities that represented the cumulative scalar wind run (Sw), vector-averaged transport distance (L), and vector-averaged wind direction (D) as a function of altitude. We also calculated a recirculation factor (R), defined as the ratio of the vector-averaged transport distance to the cumulative wind run (L/Sw). These quantities were computed over the same longitudinal domain used for the isentropic analyses (Figure 4-71). The equations used to calculate these quantities were as follows:

$$Sw = \int_{t}^{t+T} |\bar{V}| dt \qquad (2)$$

$$X = \int_{t}^{t+T} u \, dt \qquad (3)$$

$$Y = Sv \, dt \qquad (4)$$

$$L = \sqrt{X^2 + Y^2} \qquad (5)$$

$$D = \sin^{-1}\left(\frac{Y}{L}\right) \qquad (6)$$

$$R = \frac{L}{SW} \qquad (7)$$

The wind vectors (V) were resolved into their individual east-west (u) and north-south (v) components before X and Y were calculated. The integration period (T) was from 0500 PDT through 1700 PDT each day with the differential *dt* equal to the interval between soundings (approximately three hours). The wind run (Sw) and vector transport distances (X, Y, L) were calculated as meters and converted to kilometers. The vector-averaged wind direction was calculated as degrees from true north. The recirculation factor, R, was used as an indicator of local circulations or stagnations. R varied from a maximum of 1, implying straight-line transport, to a minimum of 0, signifying that zero net transport occurred over the integration period.

The quantities defined by equations (2) through (7) were calculated using the upper air data collected at Loyola Marymount, El Monte, Yorba Linda, Ontario, and Riverside at 0500 PDT, 0800 PDT, 1100 PDT, and 1400 PDT on July 13 and July 14, 1987. The upper air wind data in each sounding were first averaged over 100 m layers from the surface to 3000 m msl before the integrations were performed. The integrated data were then interpolated to the same x-z cross-section grid used for the isentropic analyses and contoured. Figures 4-75 and 4-76 show the results of this procedure for the days of July 13 and July 14, respectively. The top panel in each figure shows the contours of the recirculation factor, R. The middle and bottom panels of the figures show the contours of the cumulative wind run (Sw) and the vector-averaged wind direction (D) for the 0500-1700 period.

The results for both days were generally comparable. At the altitudes where aloft ozone layers were present before being mixed into the growing CBL (800-1200 m msl), R varied from 0.4 to 0.8, implying moderate straight-line transport and minimal local recirculation. Integrated transport distances ranged from 50-100 km, and the resultant transport direction indicated westerly transport of air across the basin. Above the subsidence inversion, relatively steady transport occurred; the mean transport wind was south-easterly and transport distances exceeded 200 km. The one exception to this pattern occurred at Ontario, where a local circulation is evident on both days near 1500 m msl. On both days, the winds near 1500 m msl at Ontario were westerly in the early morning, became easterly by mid- to late-morning, and then westerly to south-westerly again by the afternoon. We do not yet have an explanation for this pattern. The fact that it occurred above the altitudes where high ozone concentrations were observed indicates that it probably did not affect ozone distributions over the eastern basin.

In summary, analyses of transport regimes during the daytime on July 13 and 14, 1987 revealed light to moderate transport of air during the daytime from the western to the eastern basin both in the CBL and aloft in layers where carry-over ozone concentrations existed. However, because we did not

have aloft wind measurements between 2200 and 0500 PDT, we were not able to extend the transport analyses to evaluate carryover and recirculation overnight.

4.10 POLLUTANT CONCENTRATIONS AT SAN NICOLAS ISLAND

Figure 4-77 shows ozone, NO, NO_2, and PM_{10} and $PM_{2.5}$ mass concentrations for July 13-15, 1987 at San Nicolas Island. Ozone concentrations ranged from 2 to 4 pphm, near background levels. NO and NO_2 concentrations were low, ranging from 0 to 1 pphm. PAN concentrations were below 1 ppb during this episode.

Particulate mass concentrations at San Nicolas Island were a factor of two to ten lower than onshore basin PM_{10} and $PM_{2.5}$ mass concentrations. All pollutant concentrations were low, in fact, nitric acid, ammonia, $PM_{2.5}$ elemental carbon, and SO_2 were near or below the detection limits (Figures 4-77 and 4-78). Sulfate ion and organic carbon comprised the largest portion of the PM_{10} mass. Chloride and sodium ions also were significant contributors to the PM_{10} mass. In addition to sulfate ion and organic carbon, nitrate and ammonium ions were a significant portion of the $PM_{2.5}$ mass. The composition of the particulate mass is consistent with its location and land cover. The composition reflected contributions from crustal, marine, and traces of urban sources.

NMOC concentrations (Figure 4-79) were significantly lower than NMOC concentrations measured onshore. The carbonyl fraction of the NMOC during this episode was similar to onshore surface samples. The unidentified fraction of the NMOC was significantly higher than onshore samples. Detailed summaries of the average hydrocarbon and carbonyl compounds at San Nicolas Island are provided by Main et al., 1990.

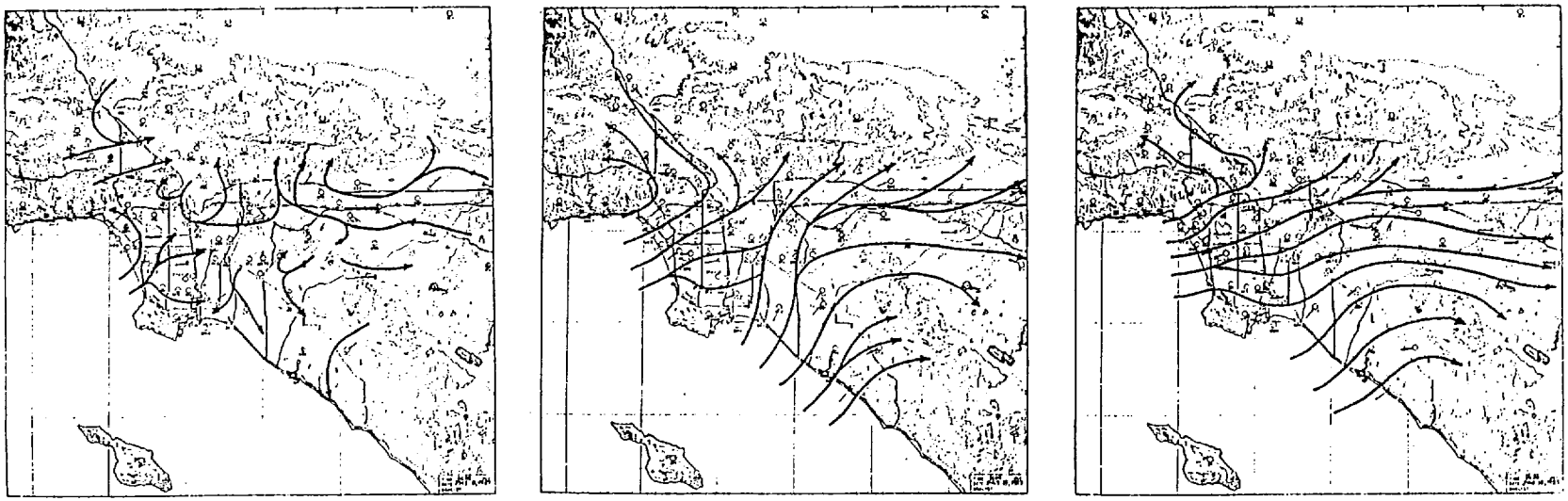

Figure 4-1. Surface Wind Streamline Analyses for July 13, 1987 at (a) 0700 PDT, (b) 1200 PDT, and (c) 1700 PDT (From Zeldin et al., 1989).

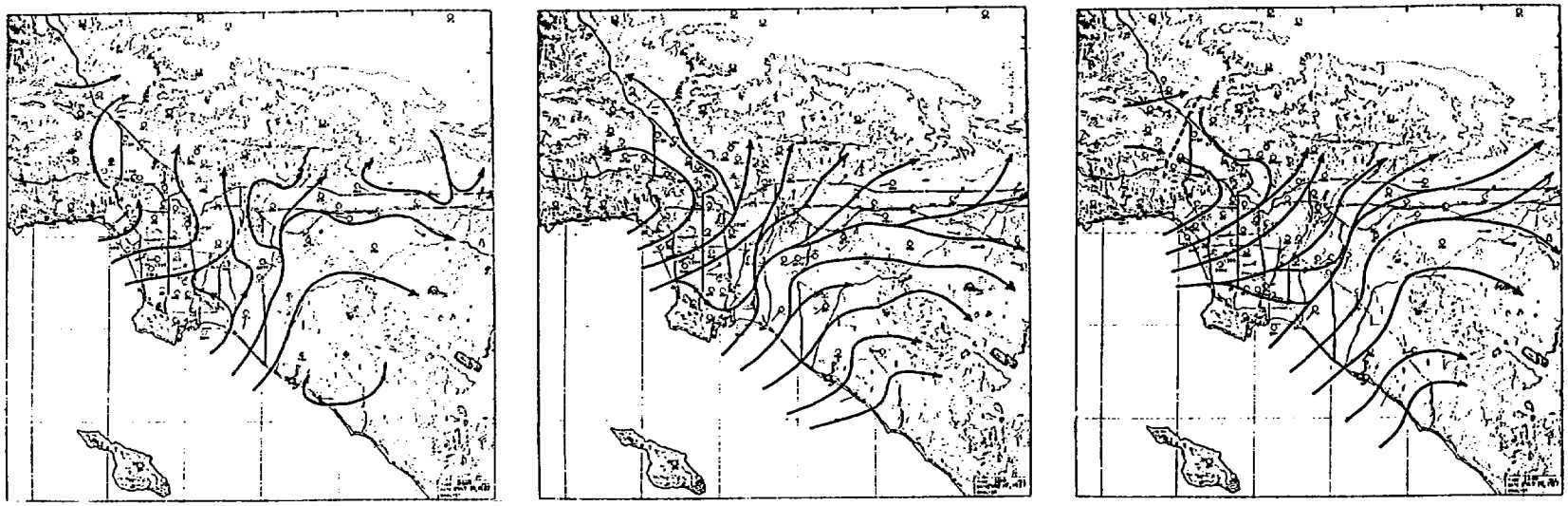

Figure 4-2. Surface Wind Streamline Analyses for July 14, 1987 at (a) 0700 PDT, (b) 1200 PDT, and (c) 1700 PDT (From Zeldin et al., 1989).

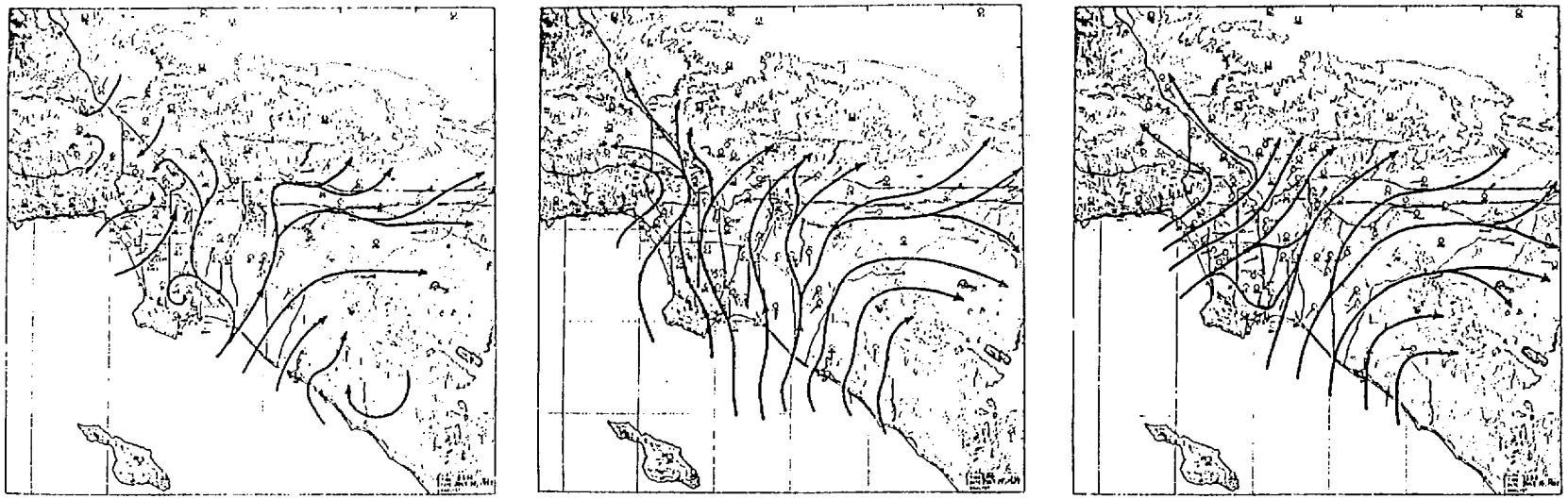

Figure 4-3. Surface Wind Streamline Analyses for July 15, 1987 at (a) 0700 PDT, (b) 1200 PDT, and (c) 1700 PDT (From Zeldin et al., 1989).

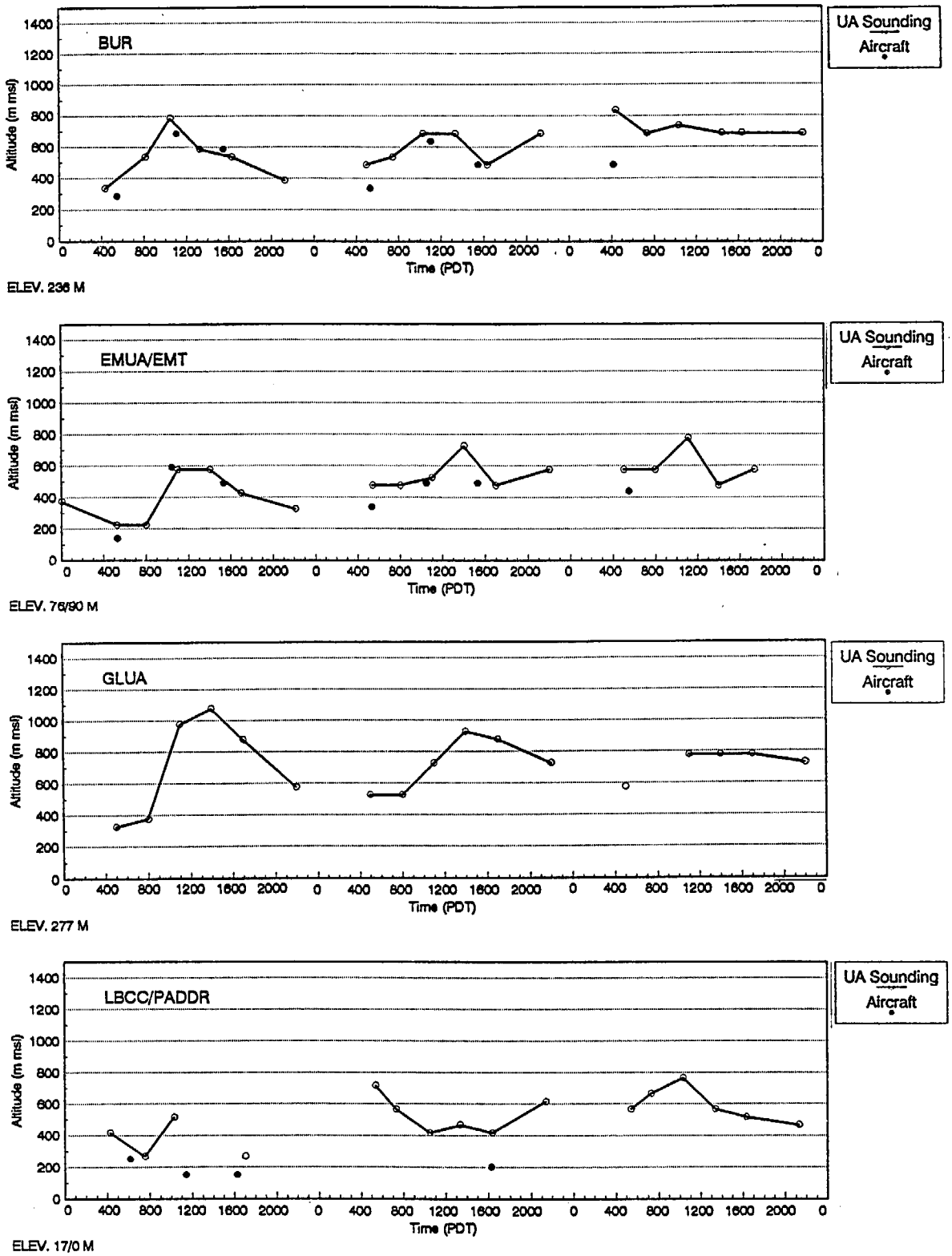

Figure 4-4. Estimated Mixing Heights on July 13-15, 1987 at Burbank, El Monte, Glendora, and Long Beach Using Rawinsonde Temperature Data and Nearby Aircraft Temperature and Air Quality Data. Elevations are given for the upper air and aircraft measurement locations.

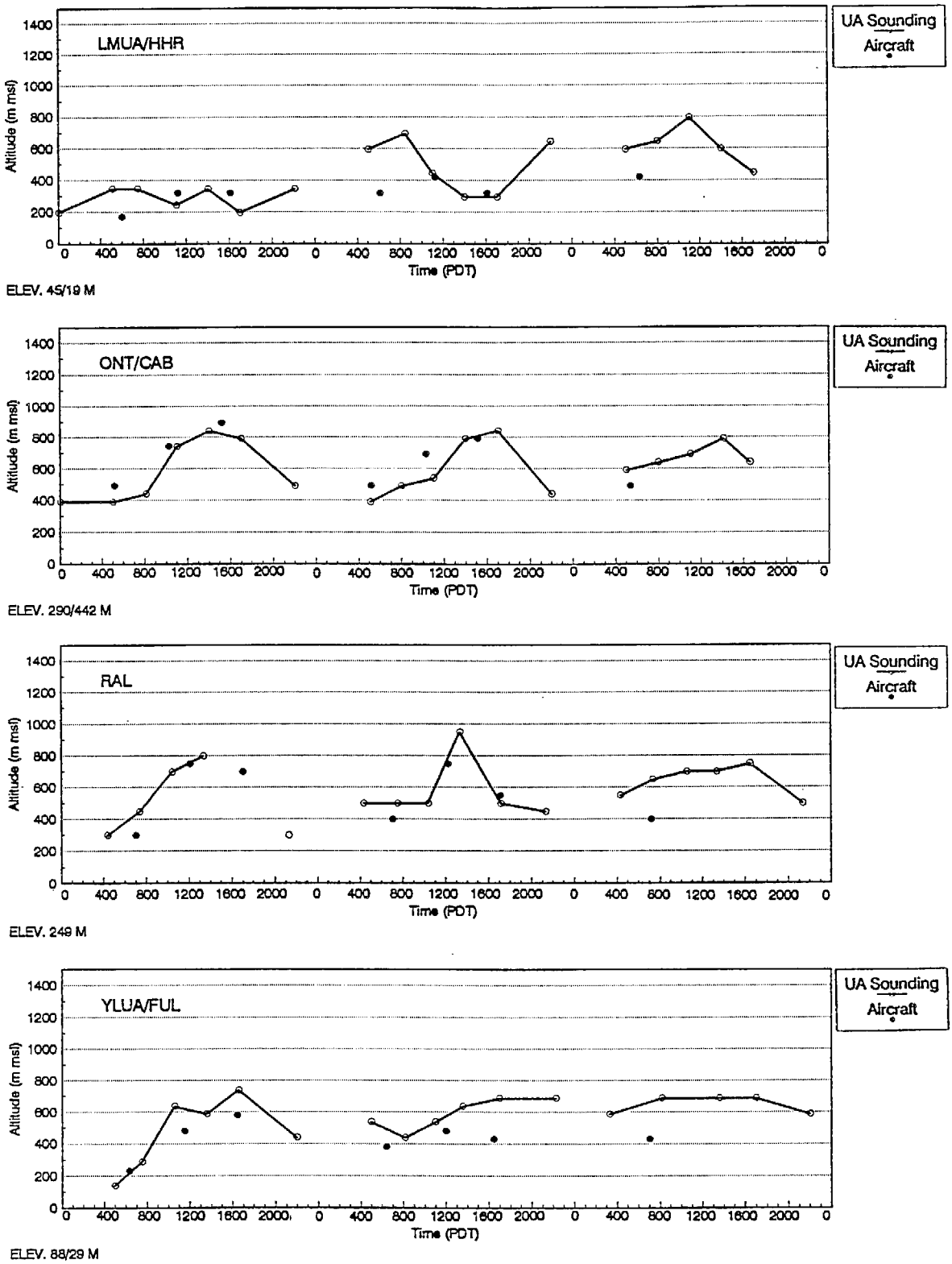

Figure 4-5. Estimated Mixing Heights on July 13-15, 1987 at Loyola-Marymount University, Ontario, Riverside, and Yorba Linda Using Rawinsonde Temperature Data and Nearby Aircraft Temperature and Air Quality Data. Elevations are given for the upper air and aircraft measurement locations.

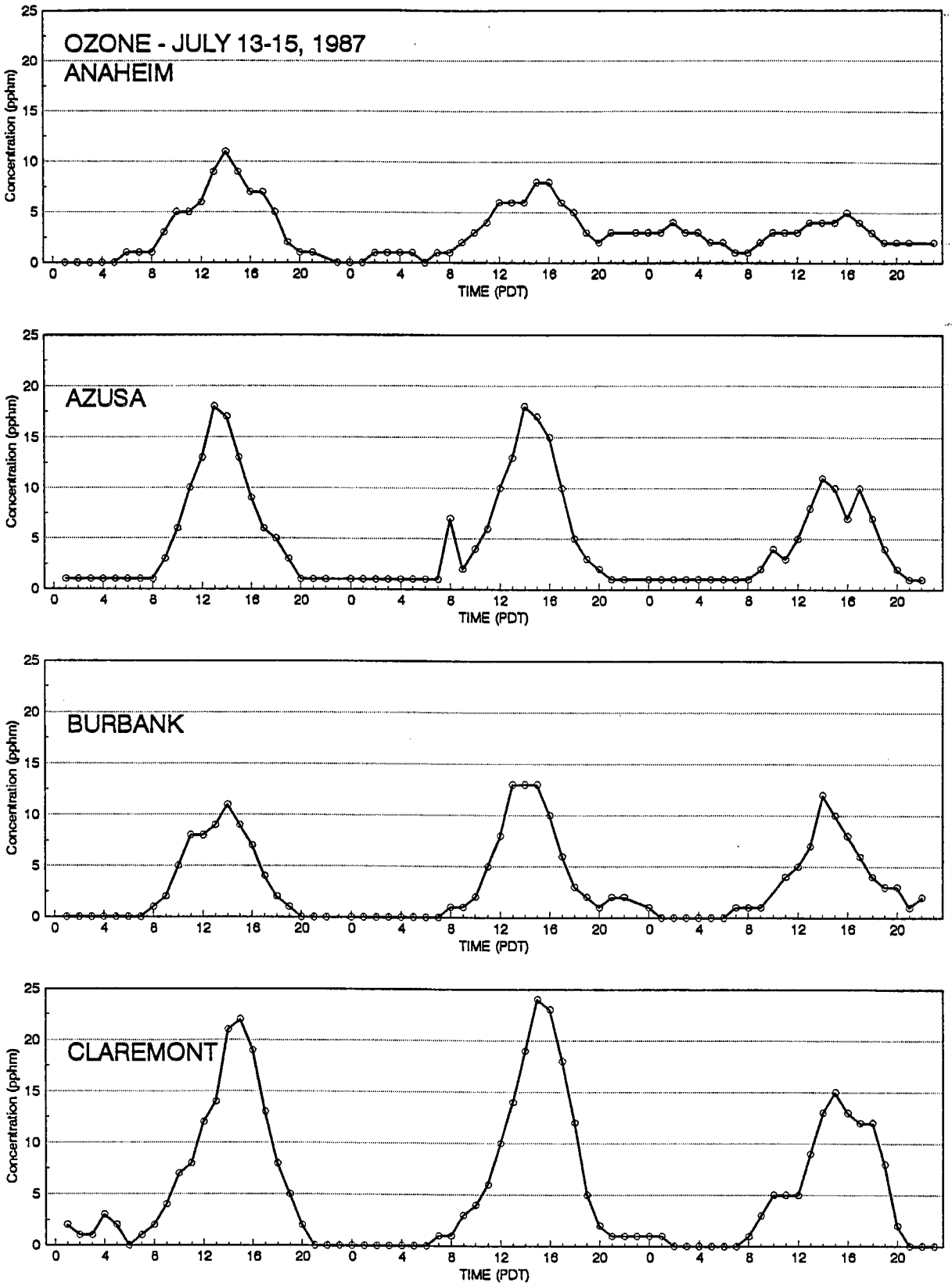

Figure 4-6. Diurnal Ozone Concentrations on July 13-15, 1987 at Anaheim, Azusa, Burbank, and Claremont.

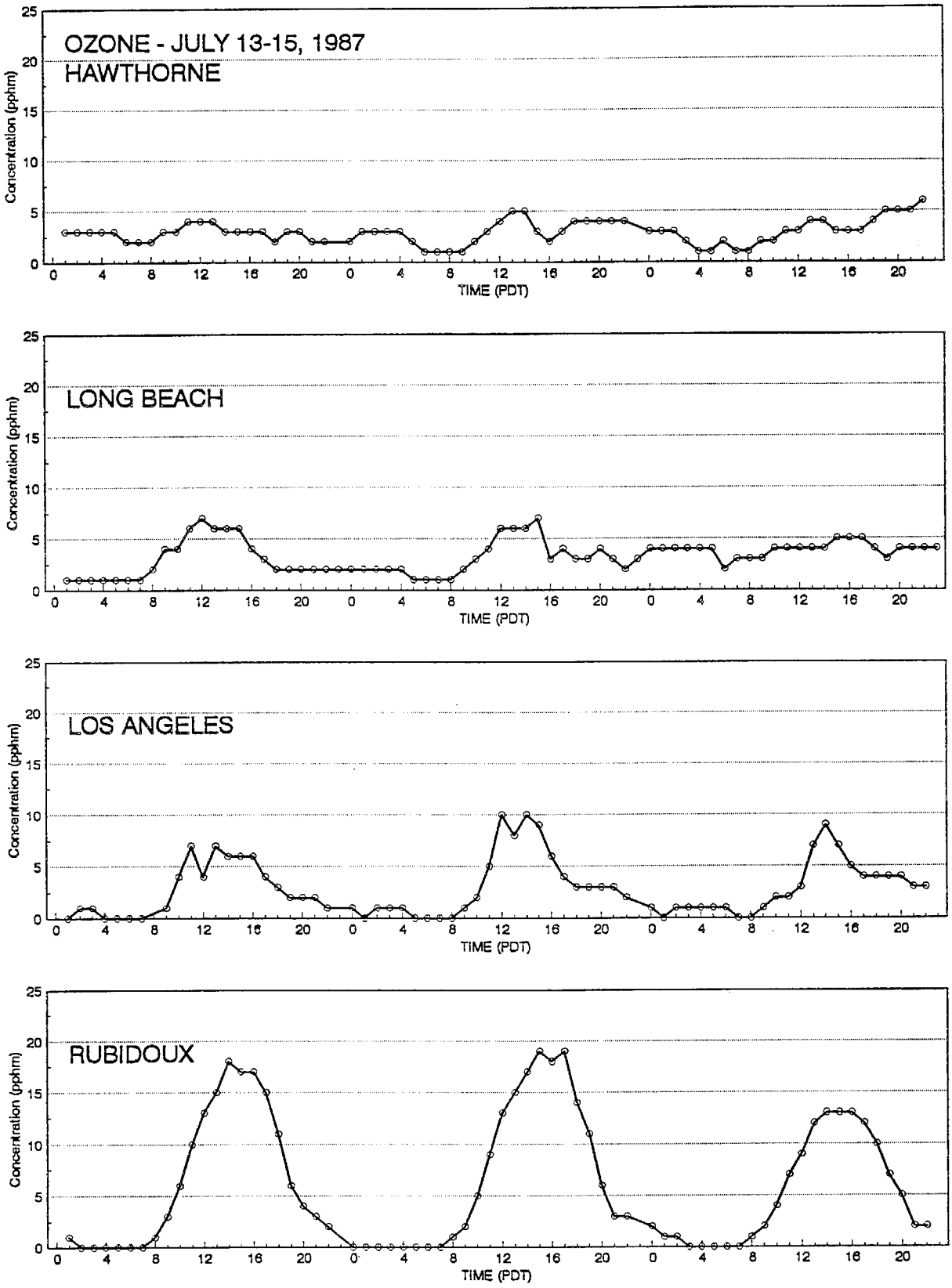

Figure 4-7. Diurnal Ozone Concentrations on July 13-15, 1987 at Hawthorne, Long Beach, Los Angeles, and Rubidoux.

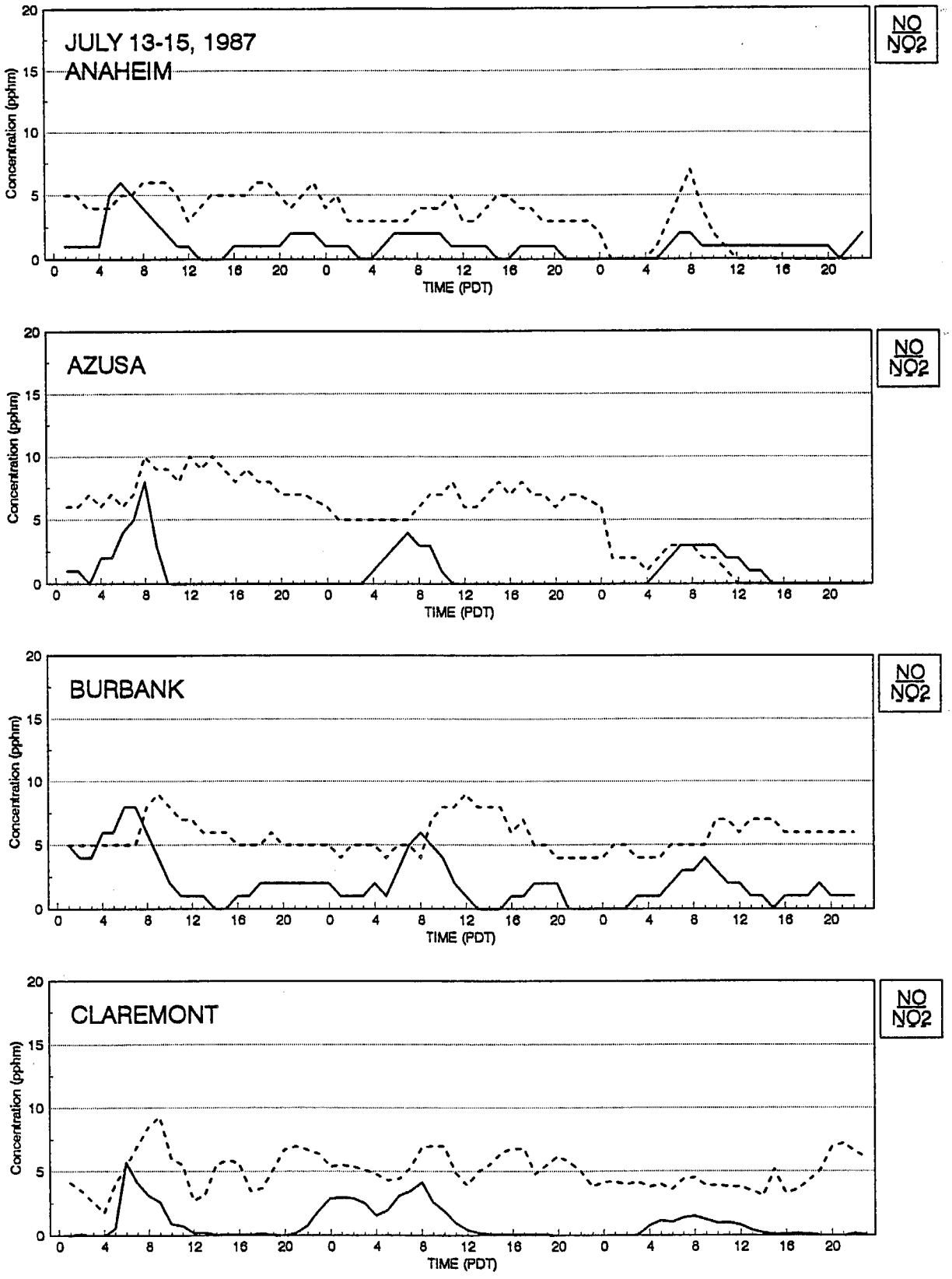

Figure 4-8. Diurnal NO and NO_2 Concentrations on July 13-15, 1987 at Anaheim, Azusa, Burbank, and Claremont.

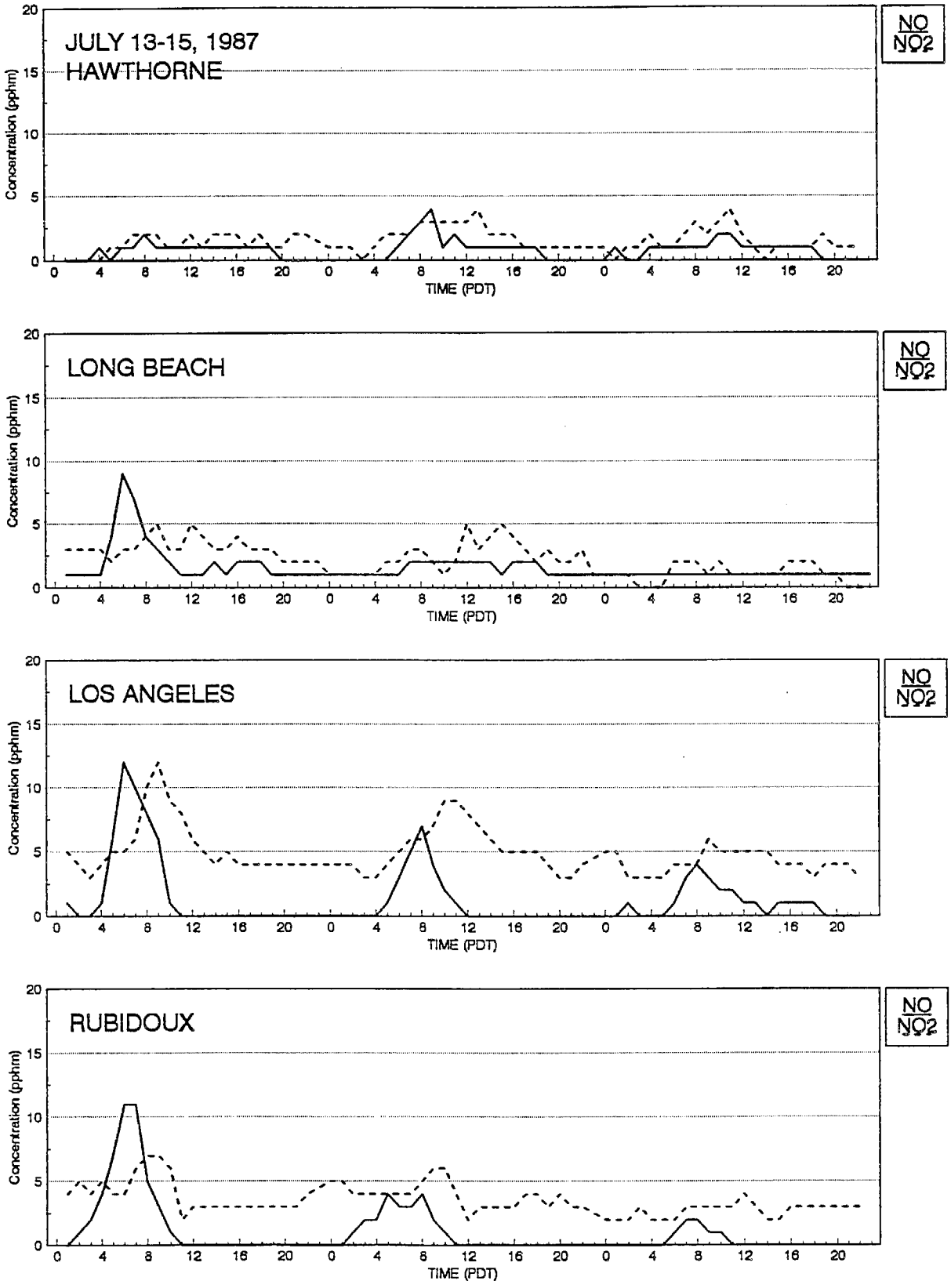

Figure 4-9. Diurnal NO and NO_2 Concentrations on July 13-15, 1987 at Hawthorne, Long Beach, Los Angeles, and Rubidoux.

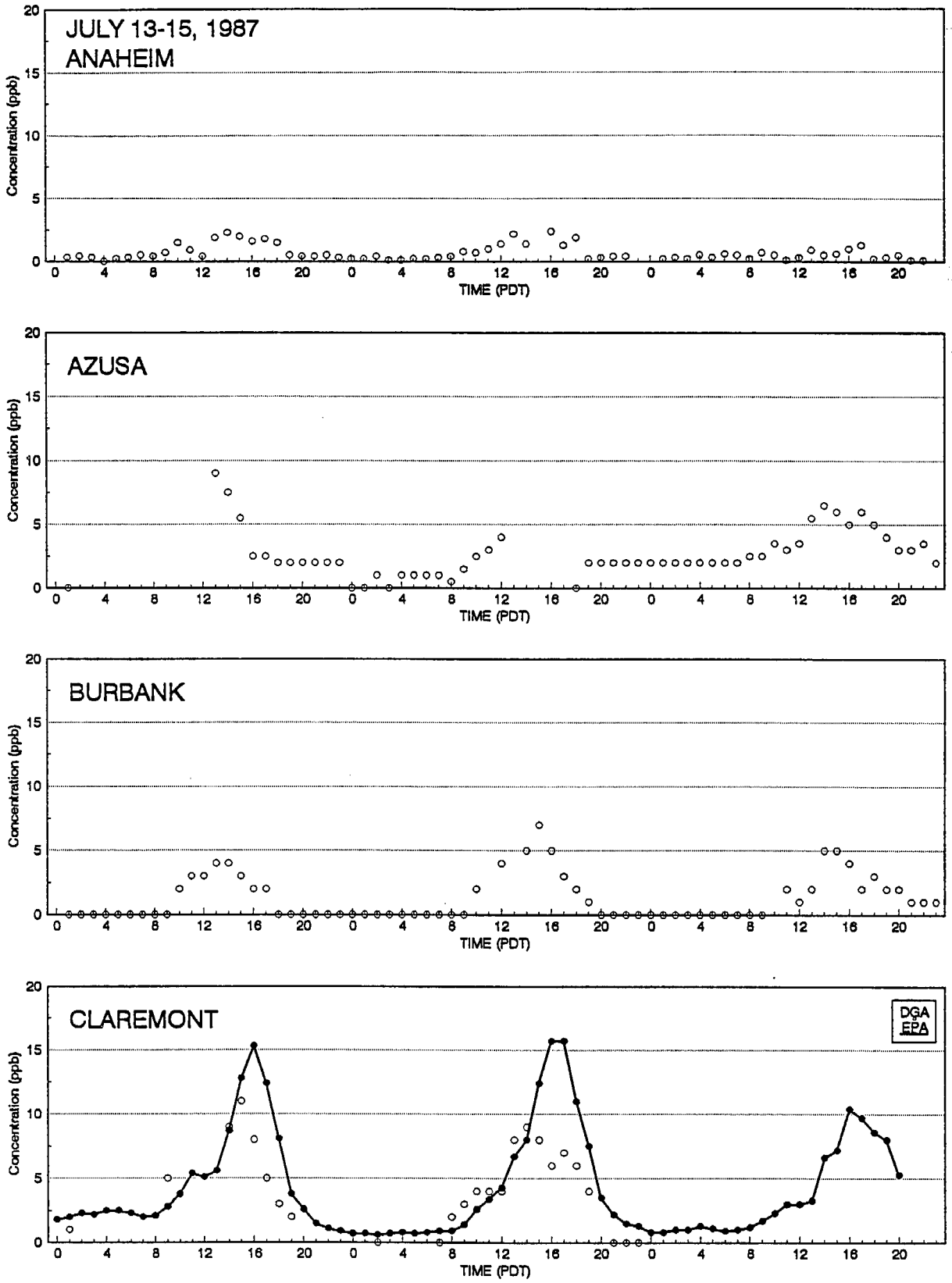

Figure 4-10. Diurnal PAN Concentrations by DGA on July 13-15, 1987 at Anaheim, Azusa, Burbank and Claremont. EPA only sampled PAN at Claremont.

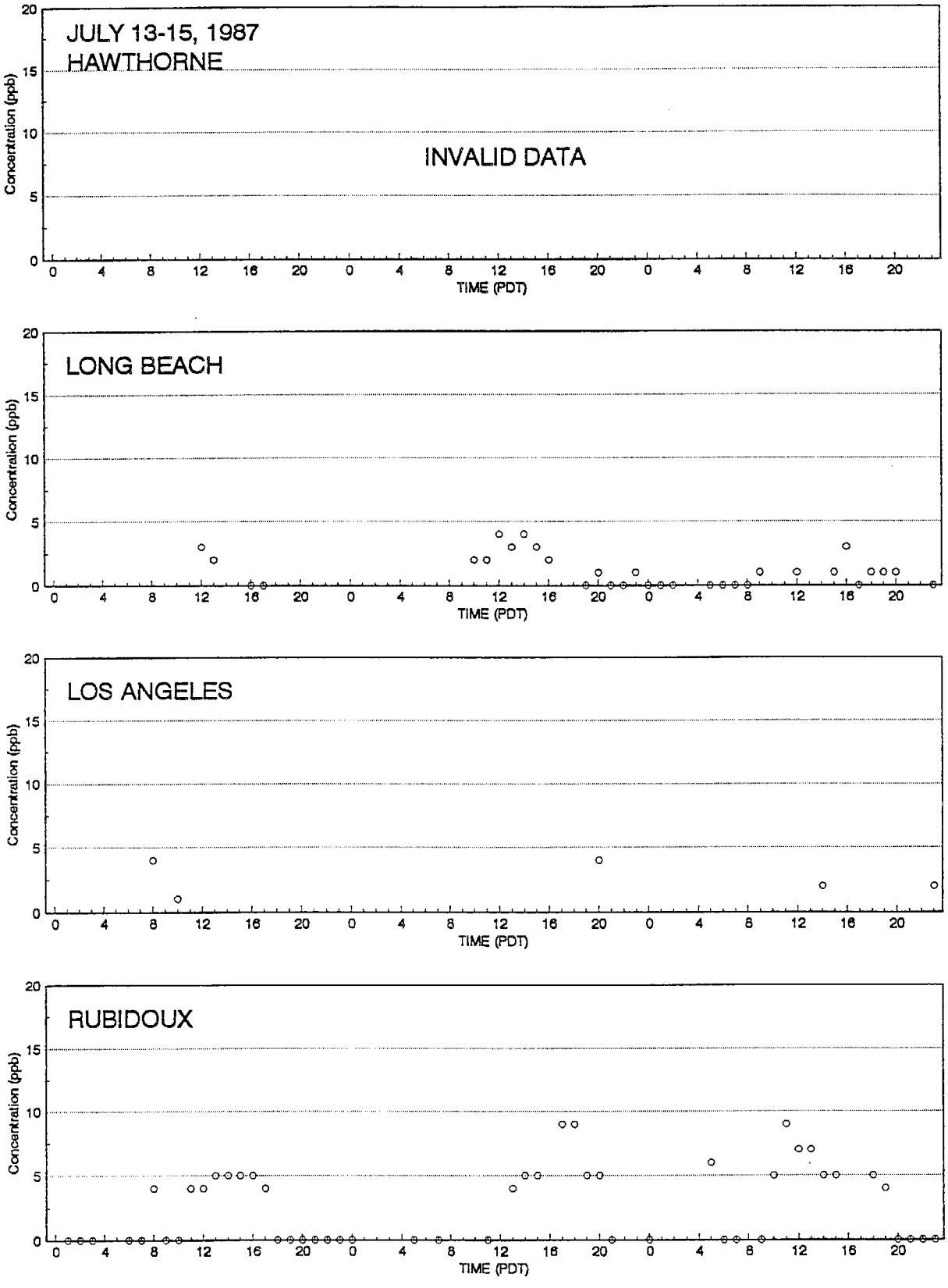

Figure 4-11. Diurnal PAN Concentrations by DGA on July 13-15, 1987 at Hawthorne, Long Beach, Los Angeles, and Rubidoux. Several hours of PAN data were invalid.

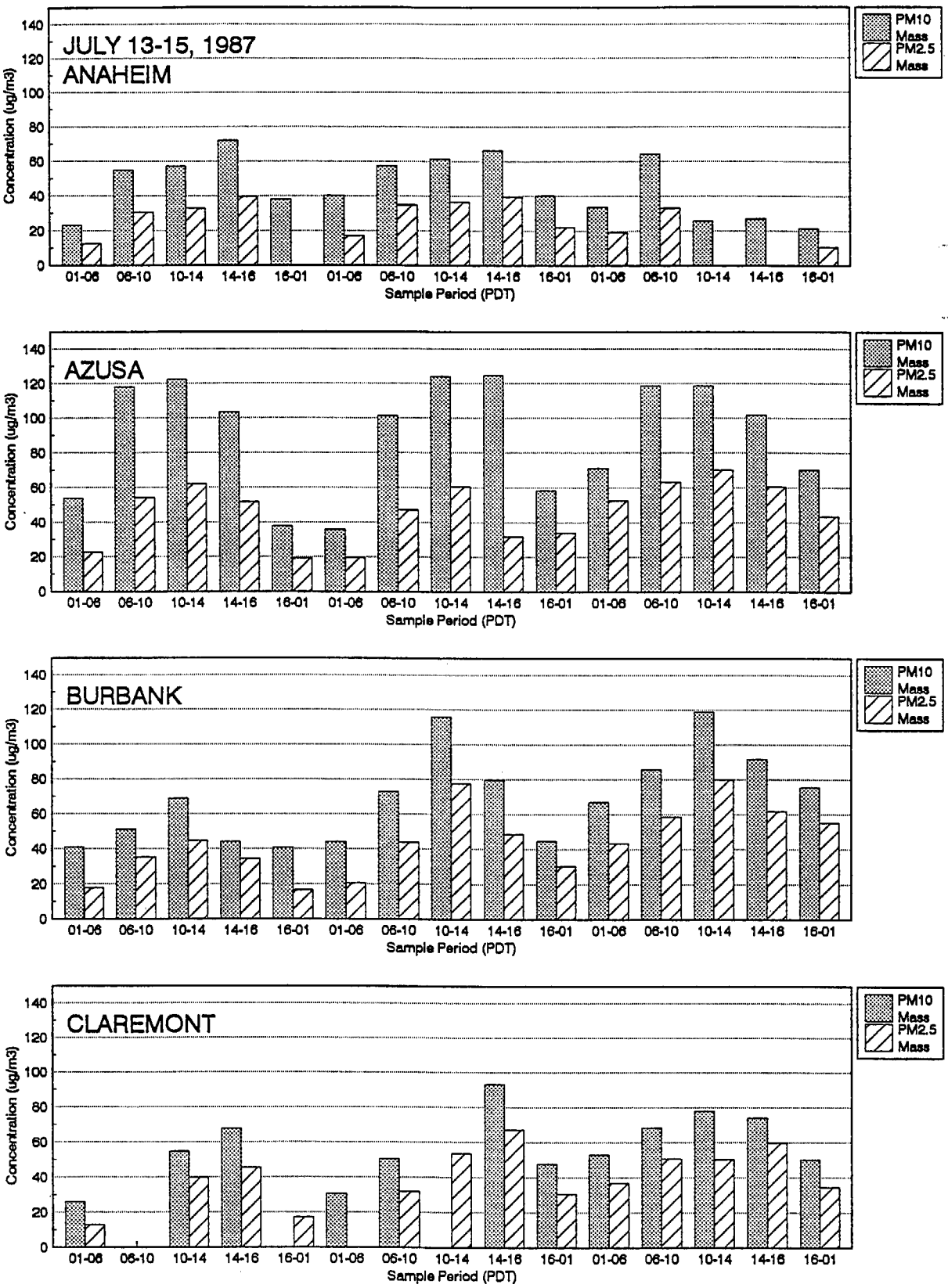

Figure 4-12. PM_{10} and $PM_{2.5}$ Mass Concentrations on July 13-15, 1987 at Anaheim, Azusa, Burbank, and Claremont.

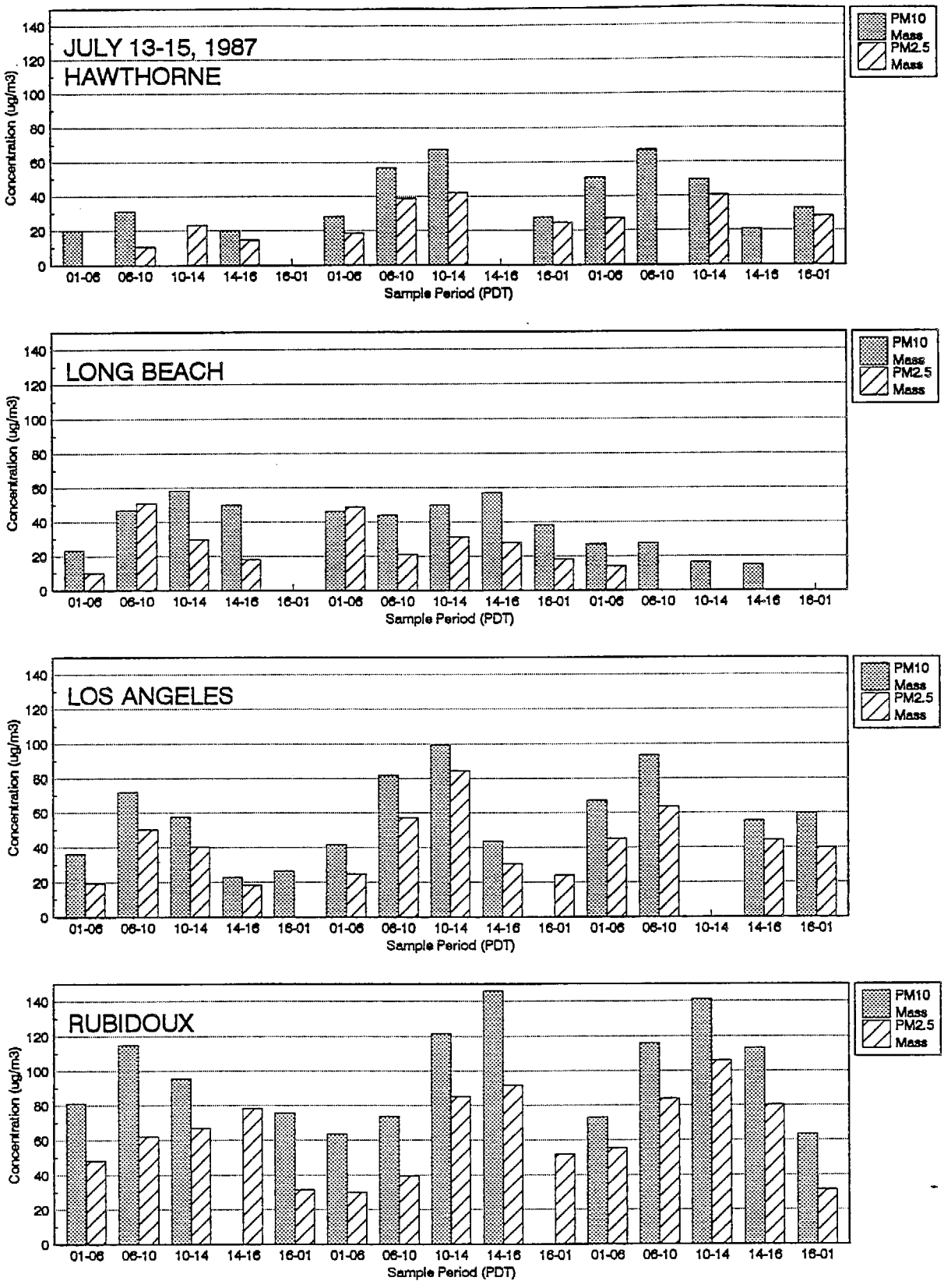

Figure 4-13. PM_{10} and $PM_{2.5}$ Mass Concentrations on July 13-15, 1987 at Hawthorne, Long Beach, Los Angeles, and Rubidoux.

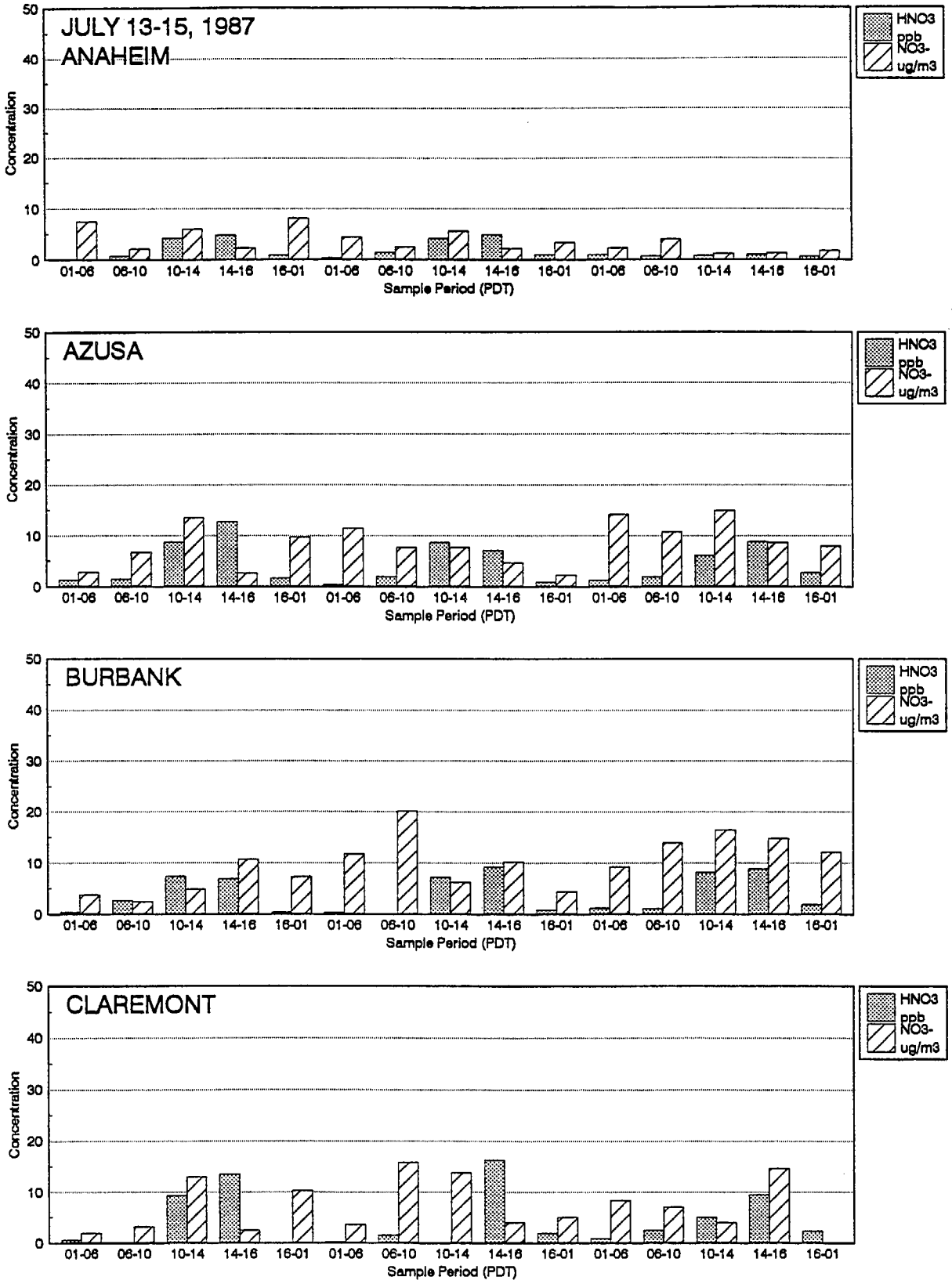

Figure 4-14. Nitric Acid and $PM_{2.5}$ Nitrate Ion Concentrations on July 13-15, 1987 at Anaheim, Azusa, Burbank, and Claremont.

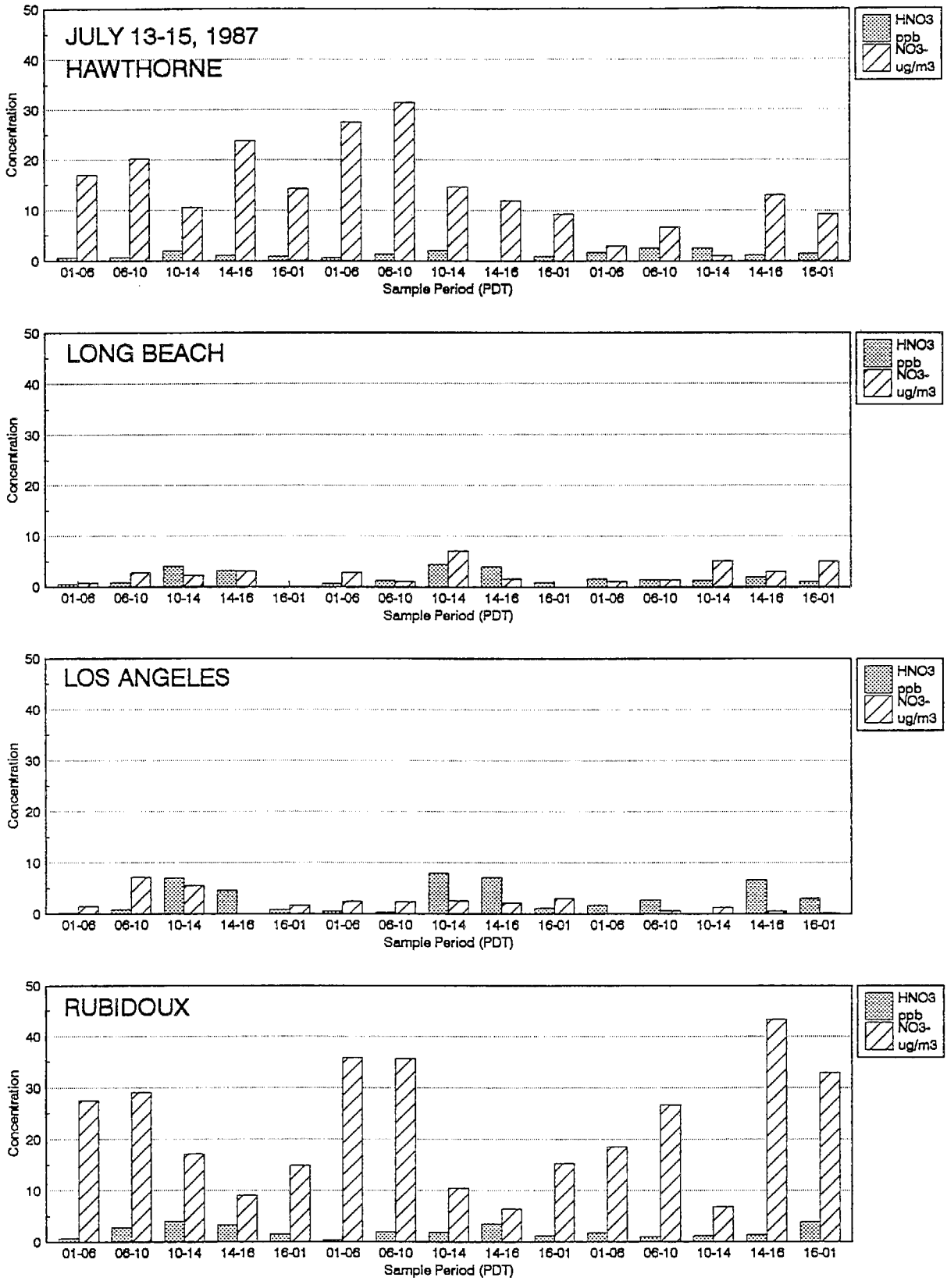

Figure 4-15. Nitric Acid and $PM_{2.5}$ Nitrate Ion Concentrations on July 13-15, 1987 at Hawthorne, Long Beach, Los Angeles, and Rubidoux.

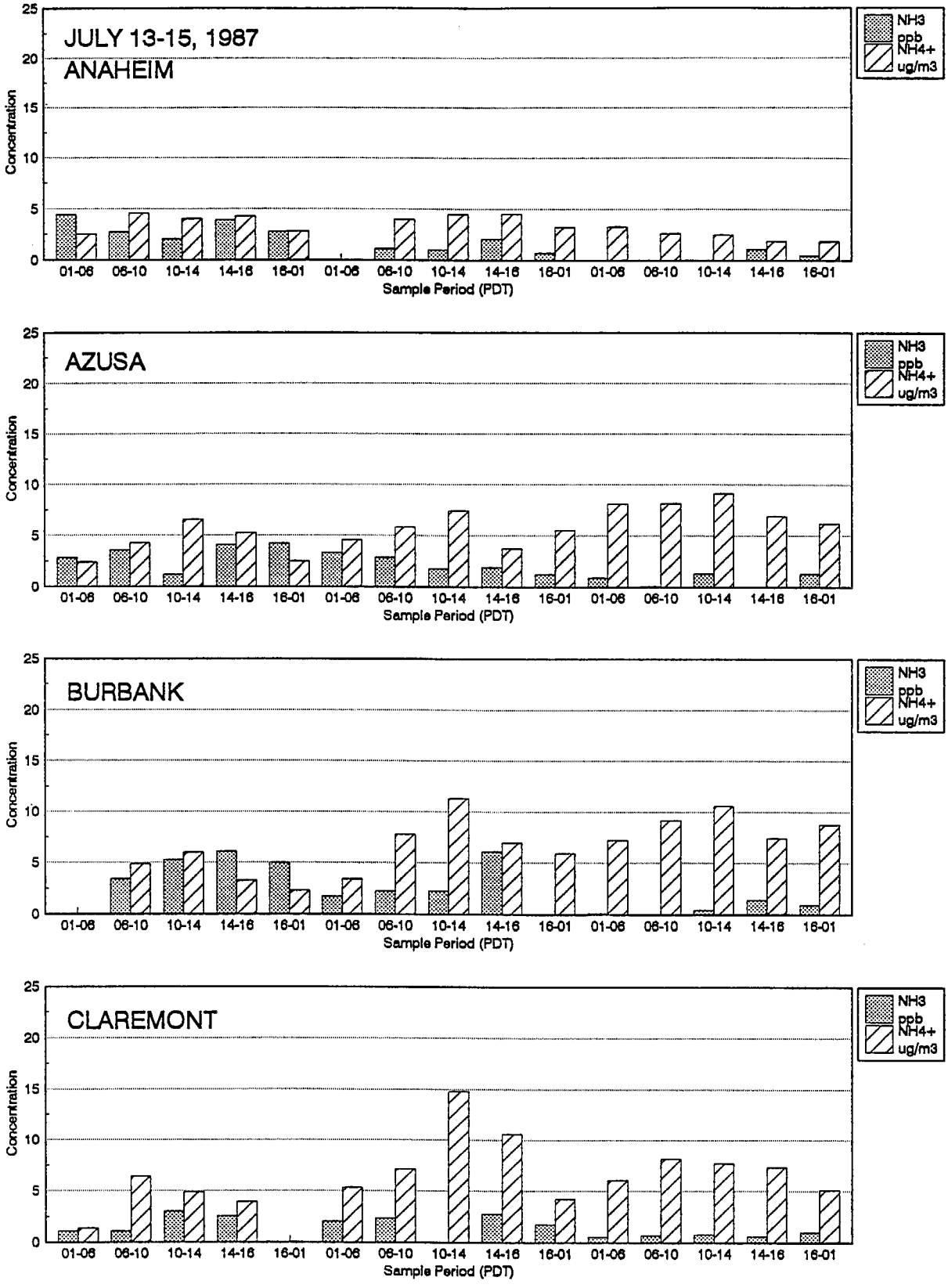

Figure 4-16. Ammonia and $PM_{2.5}$ Ammonium Ion Concentrations on July 13-15, 1987 at Anaheim, Azusa, Burbank, and Claremont.

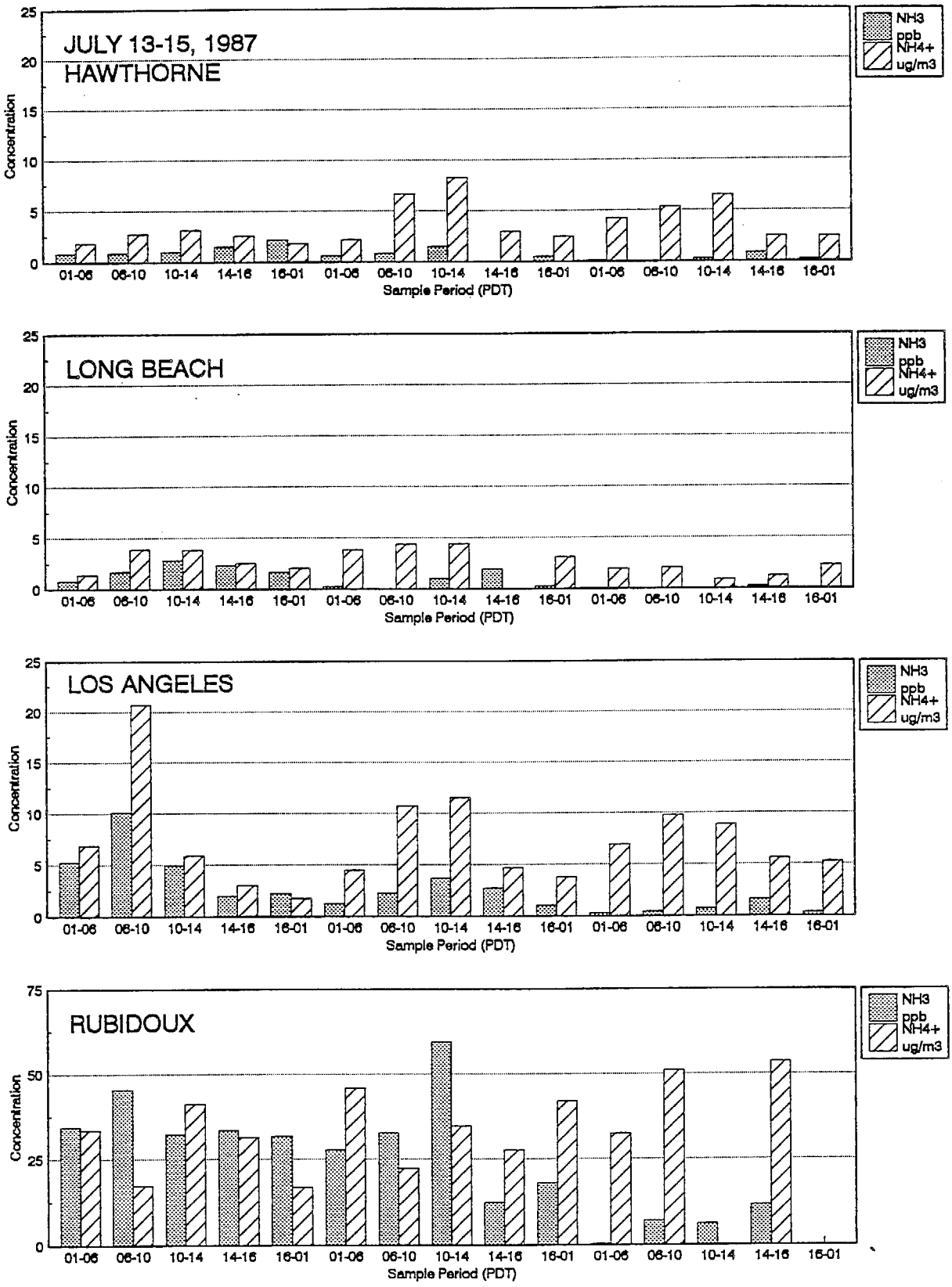

Figure 4-17. Ammonia and $PM_{2.5}$ Ammonium Ion Concentrations on July 13-15, 1987 at Hawthorne, Long Beach, Los Angeles, and Rubidoux. Note that the scale for ammonia and NH_4^+ at Rubidoux is three times higher than the scale for the other sites in Figures 4-16 and 4-17.

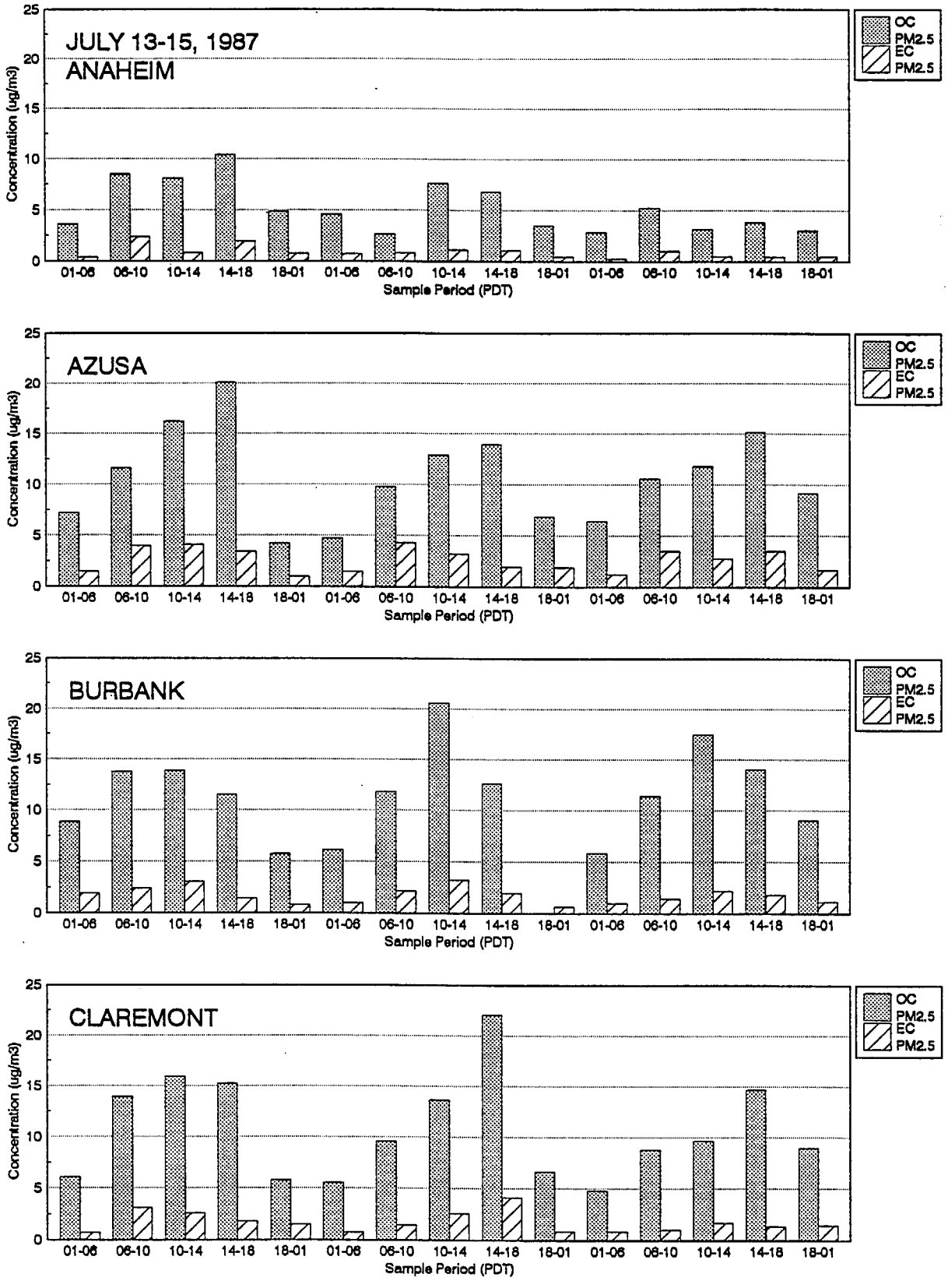

Figure 4-18. $PM_{2.5}$ Organic and Elemental Carbon Concentrations on July 13-15, 1987 at Anaheim, Azusa, Burbank, and Claremont.

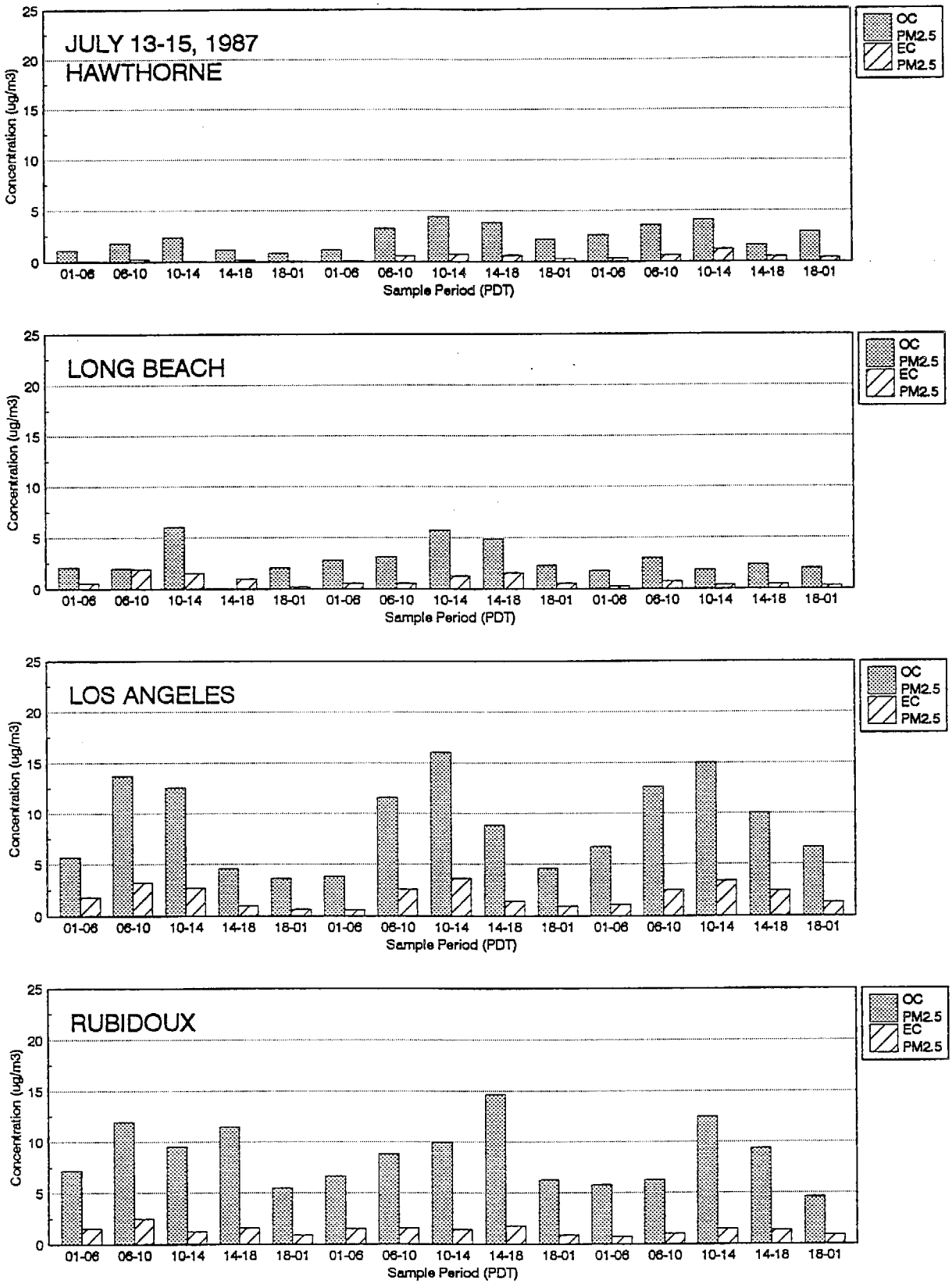

Figure 4-19. $PM_{2.5}$ Organic and Elemental Carbon Concentrations on July 13-15, 1987 at Hawthorne, Long Beach, Los Angeles, and Rubidoux.

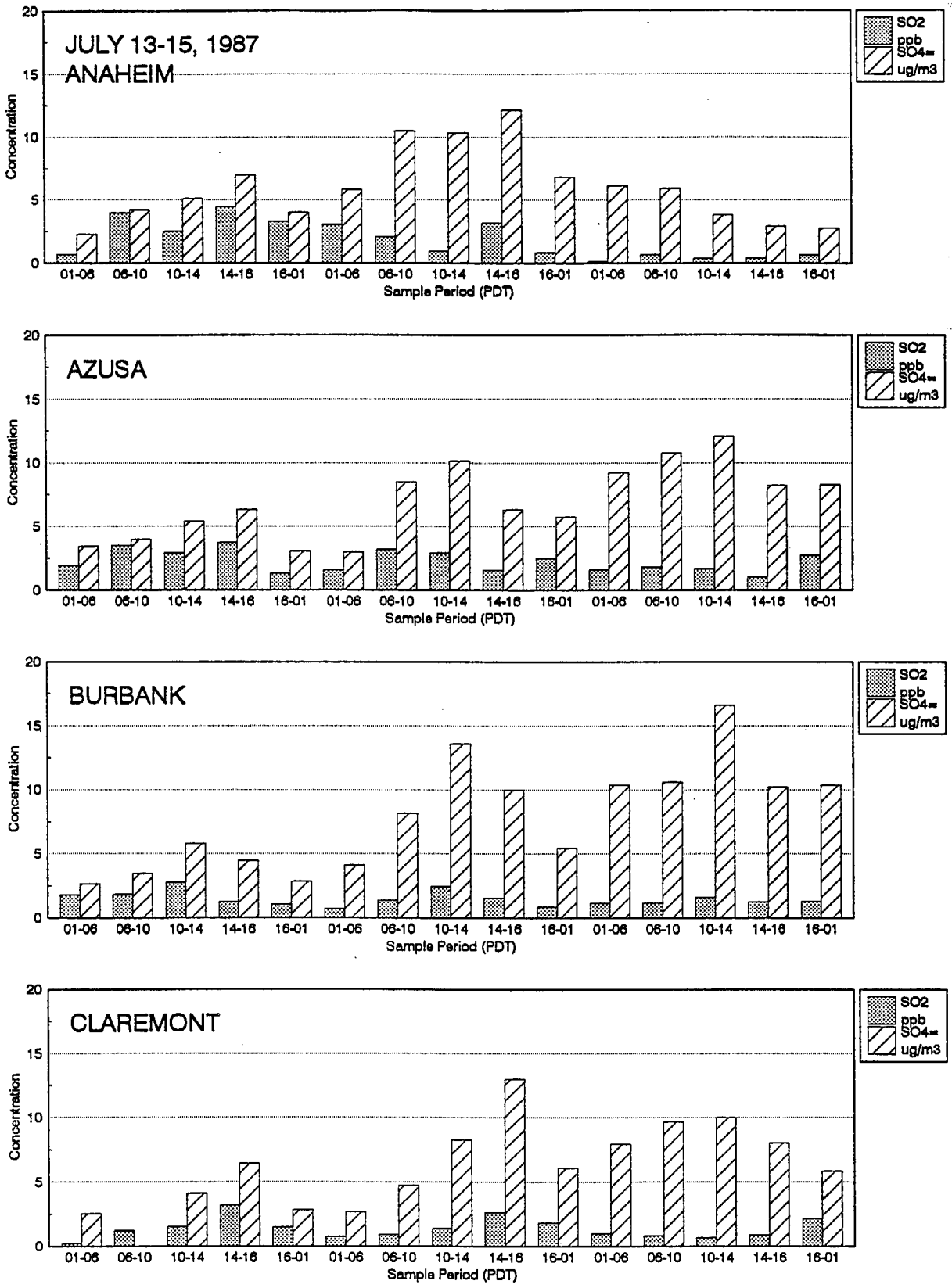

Figure 4-20. SO_2 and $PM_{2.5}$ Sulfate Ion Concentrations on July 13-15, 1987 at Anaheim, Azusa, Burbank, and Claremont.

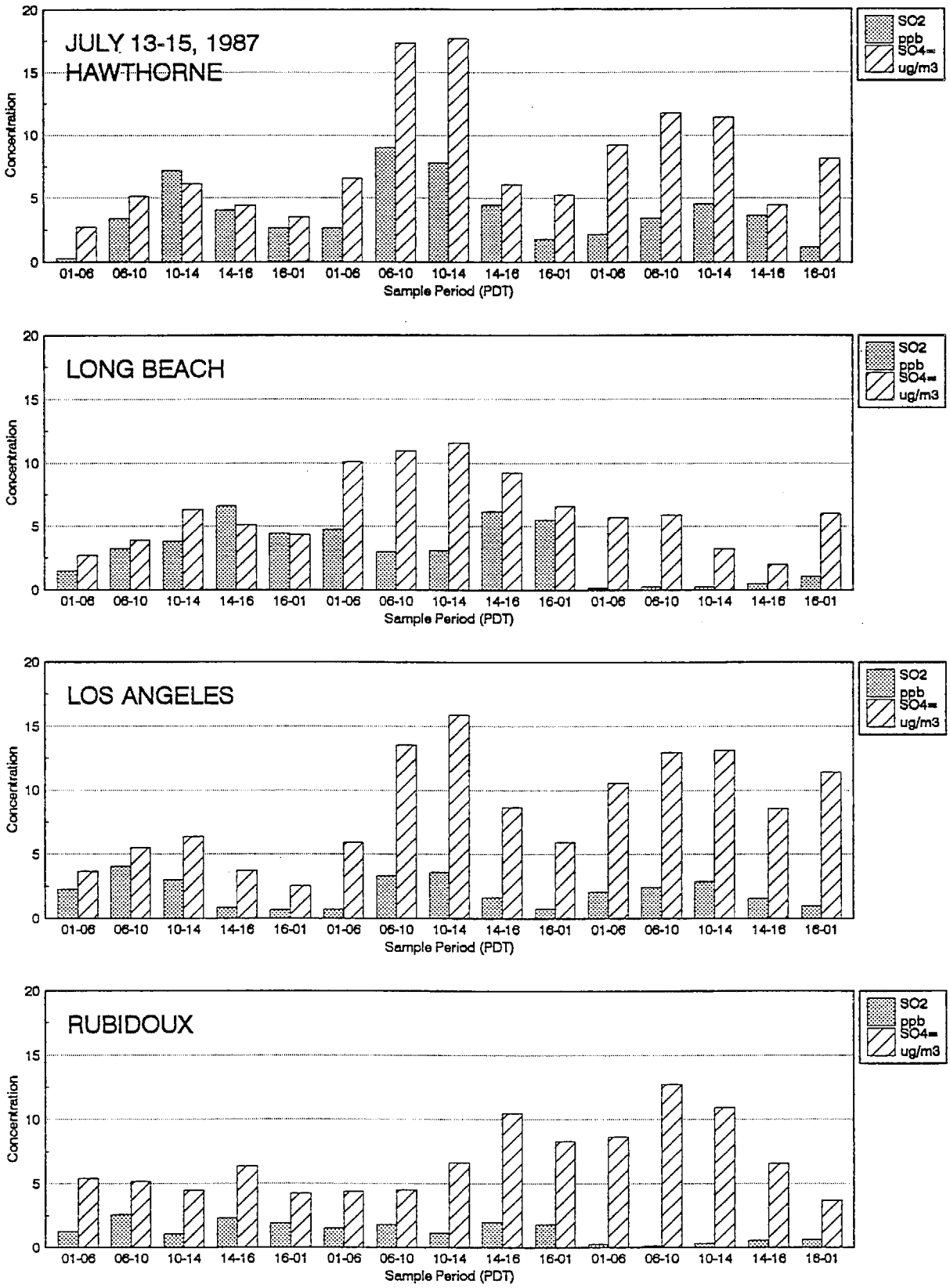

Figure 4-21. SO_2 and $PM_{2.5}$ Sulfate Ion Concentrations on July 13-15, 1987 at Hawthorne, Long Beach, Los Angeles, and Rubidoux.

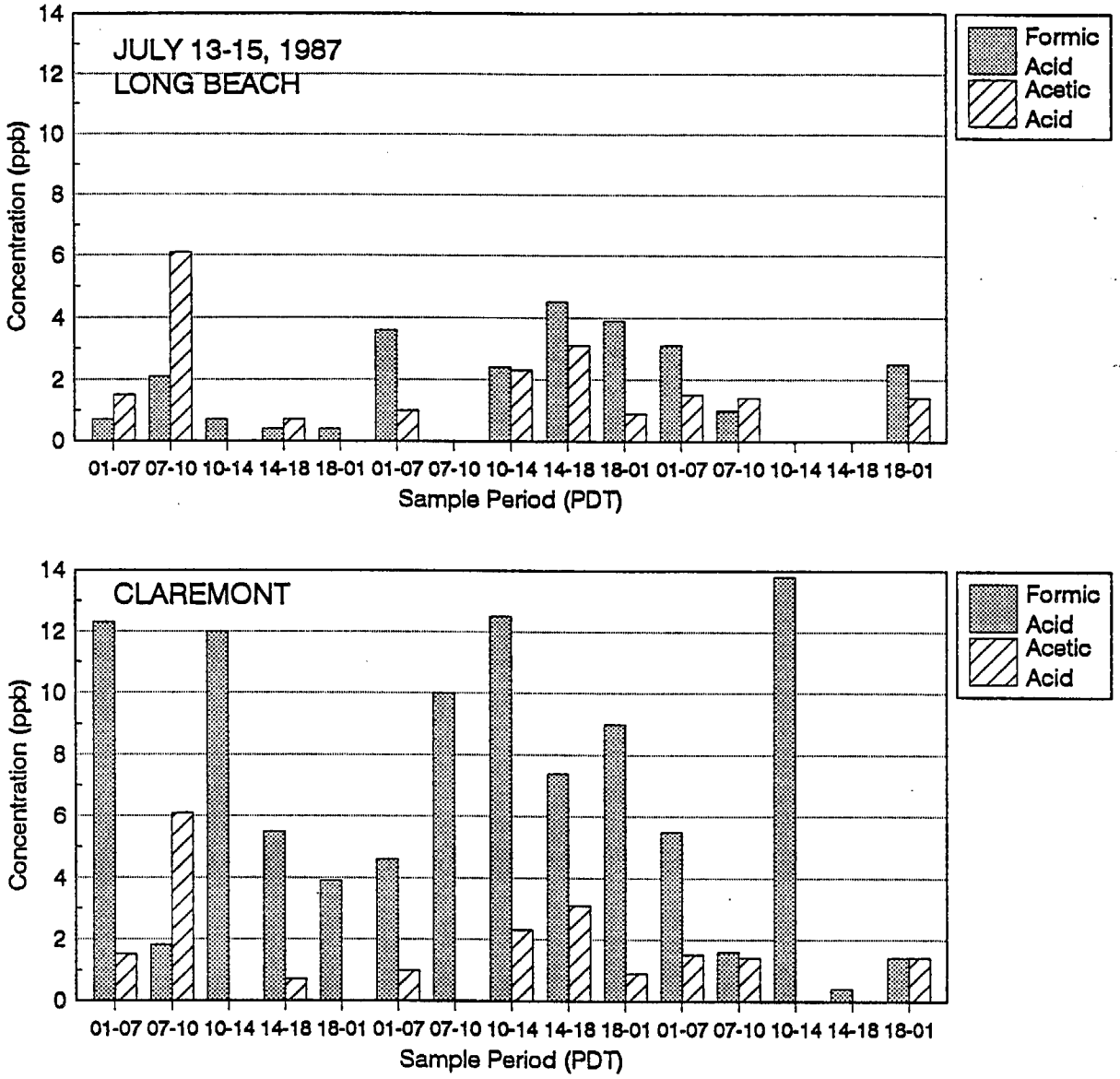

Figure 4-22. Formic and Acetic Acid Concentrations on July 13-15, 1987 at Long Beach and Claremont.

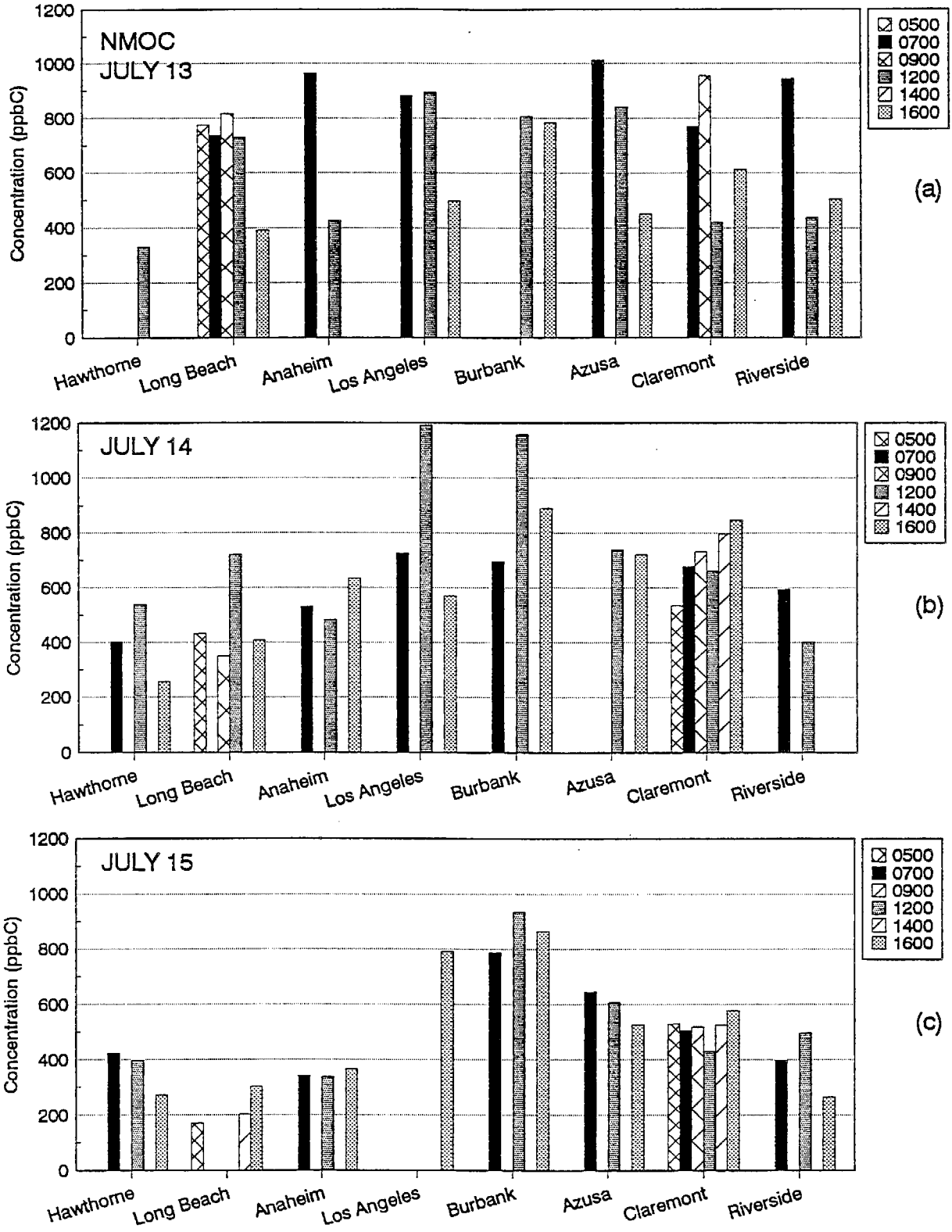

Figure 4-23. NMOC Concentrations on at Each Sampling Location by Time of Day on a) July 13, b) July 14, and c) July 15, 1987. Samples were not taken at all times at all sites and numerous samples were invlaid (see Section 2.1.3).

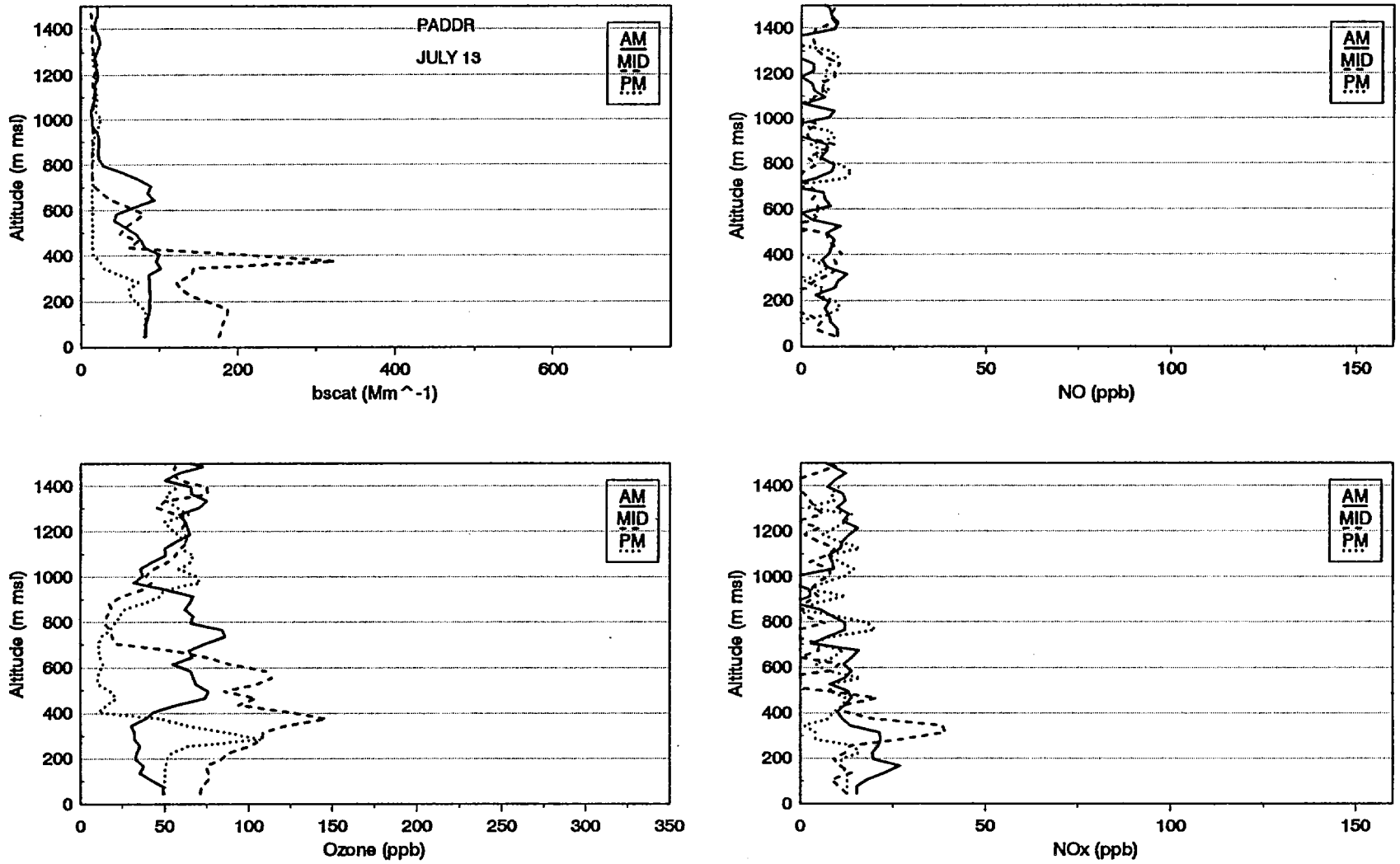

Figure 4-24. Light Scattering (b_{scat}), and Ozone, NO, and NO_x Concentrations for Morning, Midday, and Afternoon Aircraft Spirals on July 13, 1987 at PADDR.

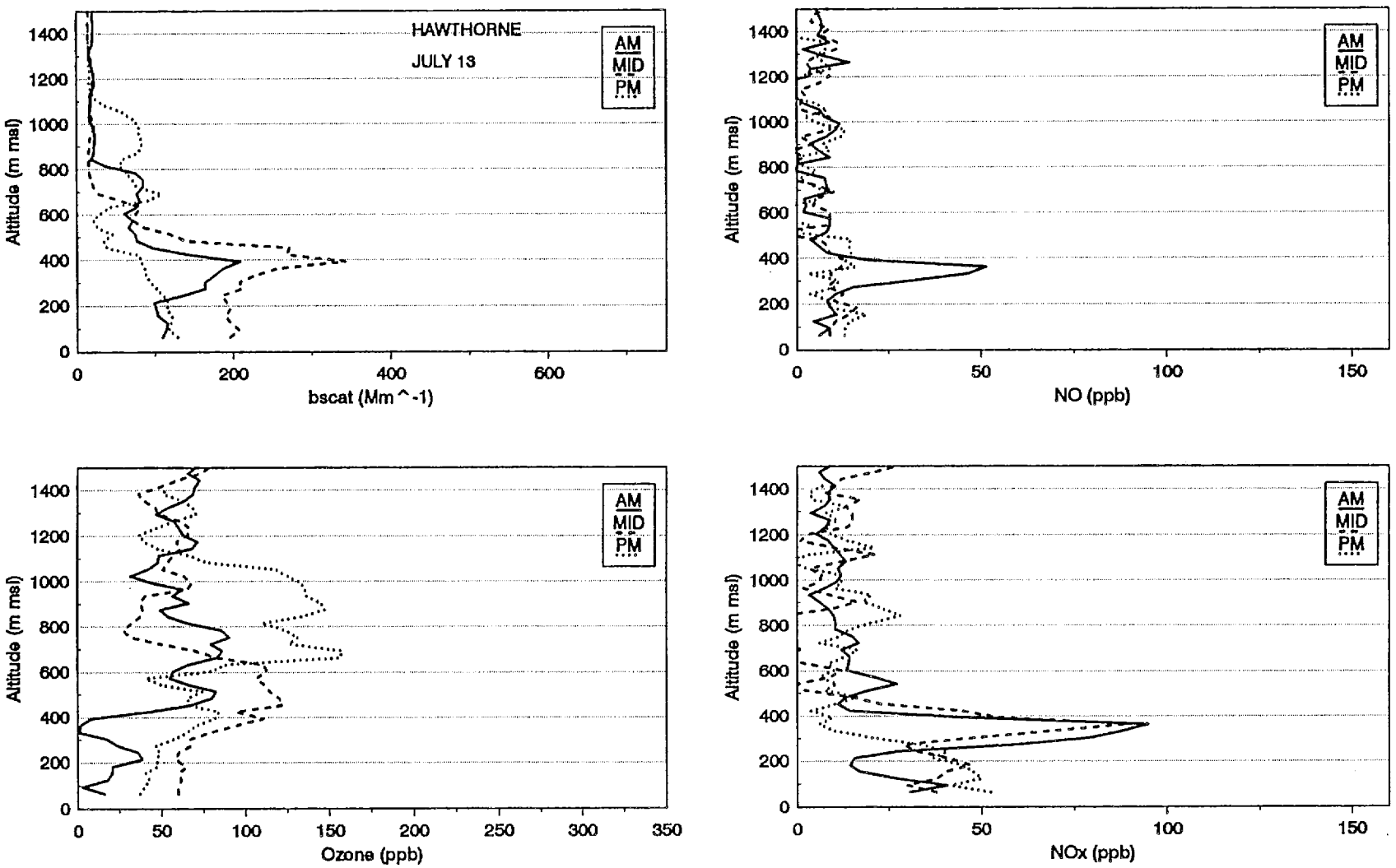

Figure 4-25. Light Scattering (b_{scat}), and Ozone, NO, and NO_x Concentrations for Morning, Midday, and Afternoon Aircraft Spirals on July 13, 1987 at Hawthorne.

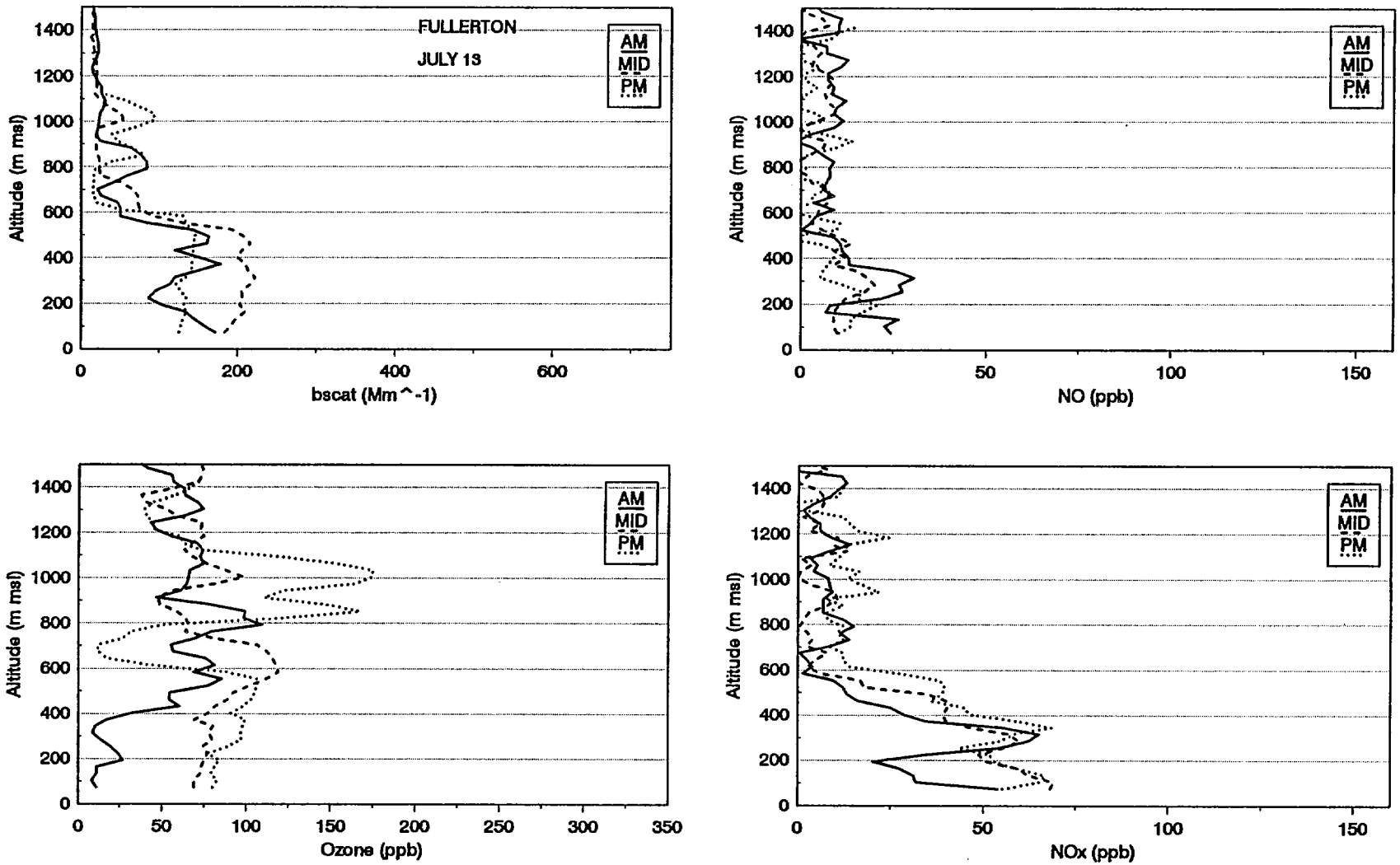

Figure 4-26. Light Scattering (b_{scat}), and Ozone, NO, and NO_x Concentrations for Morning, Midday, and Afternoon Aircraft Spirals on July 13, 1987 at Fullerton.

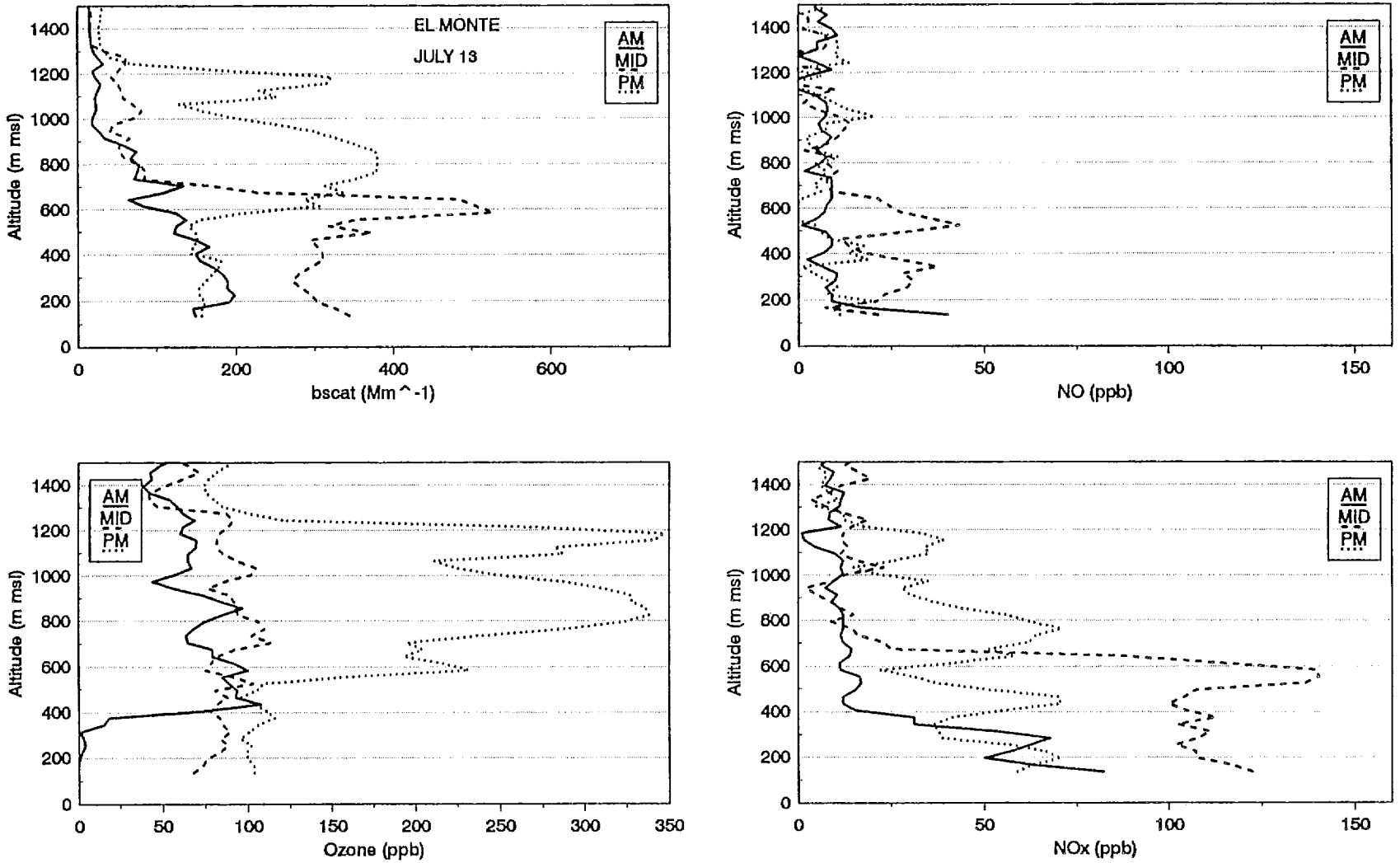

Figure 4-27. Light Scattering (b_{scat}), and Ozone, NO, and NO_x Concentrations for Morning, Midday, and Afternoon Aircraft Spirals on July 13, 1987 at El Monte.

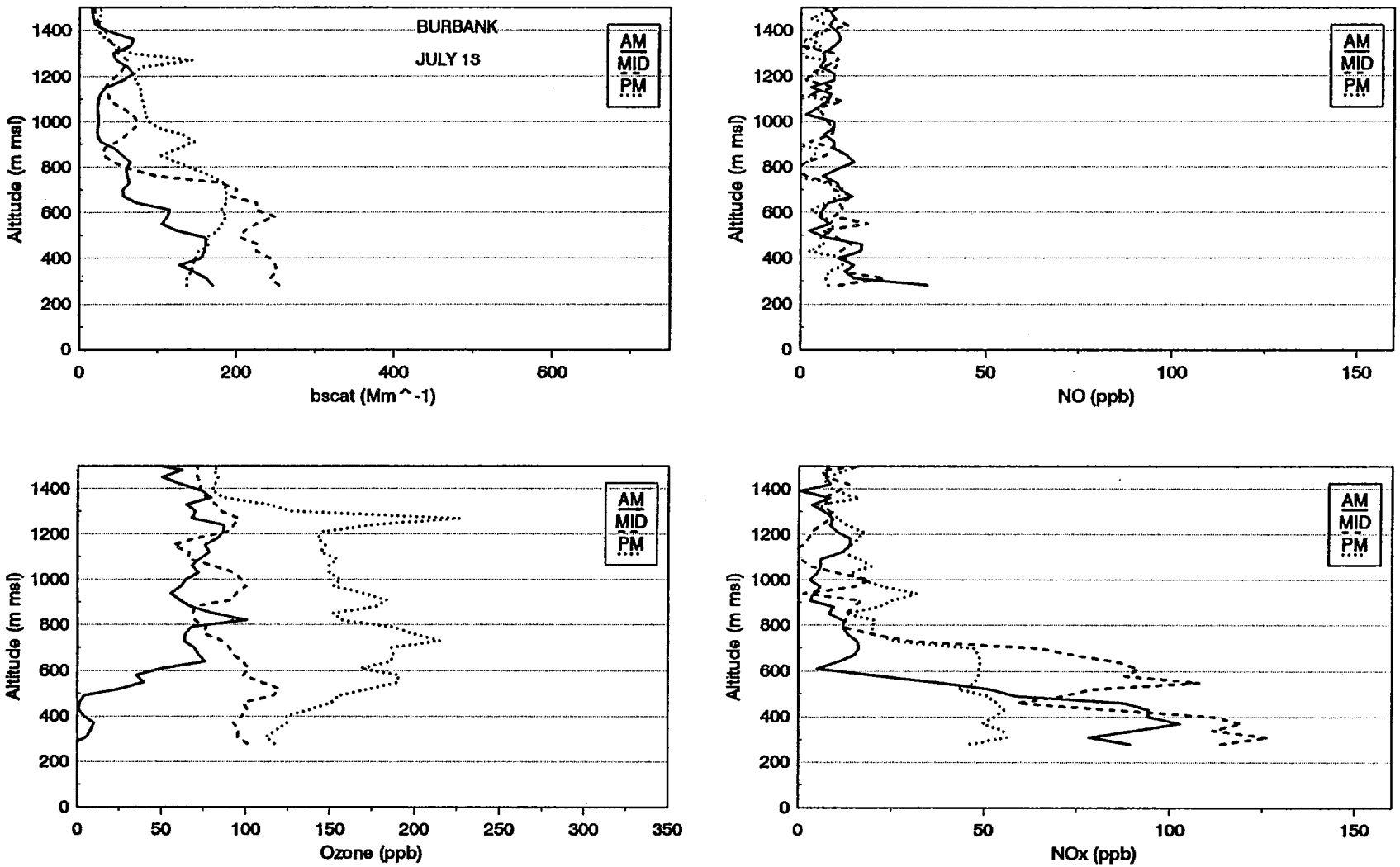

Figure 4-28. Light Scattering (b_{scat}), and Ozone, NO, and NO_x Concentrations for Morning, Midday, and Afternoon Aircraft Spirals on July 13, 1987 at Burbank.

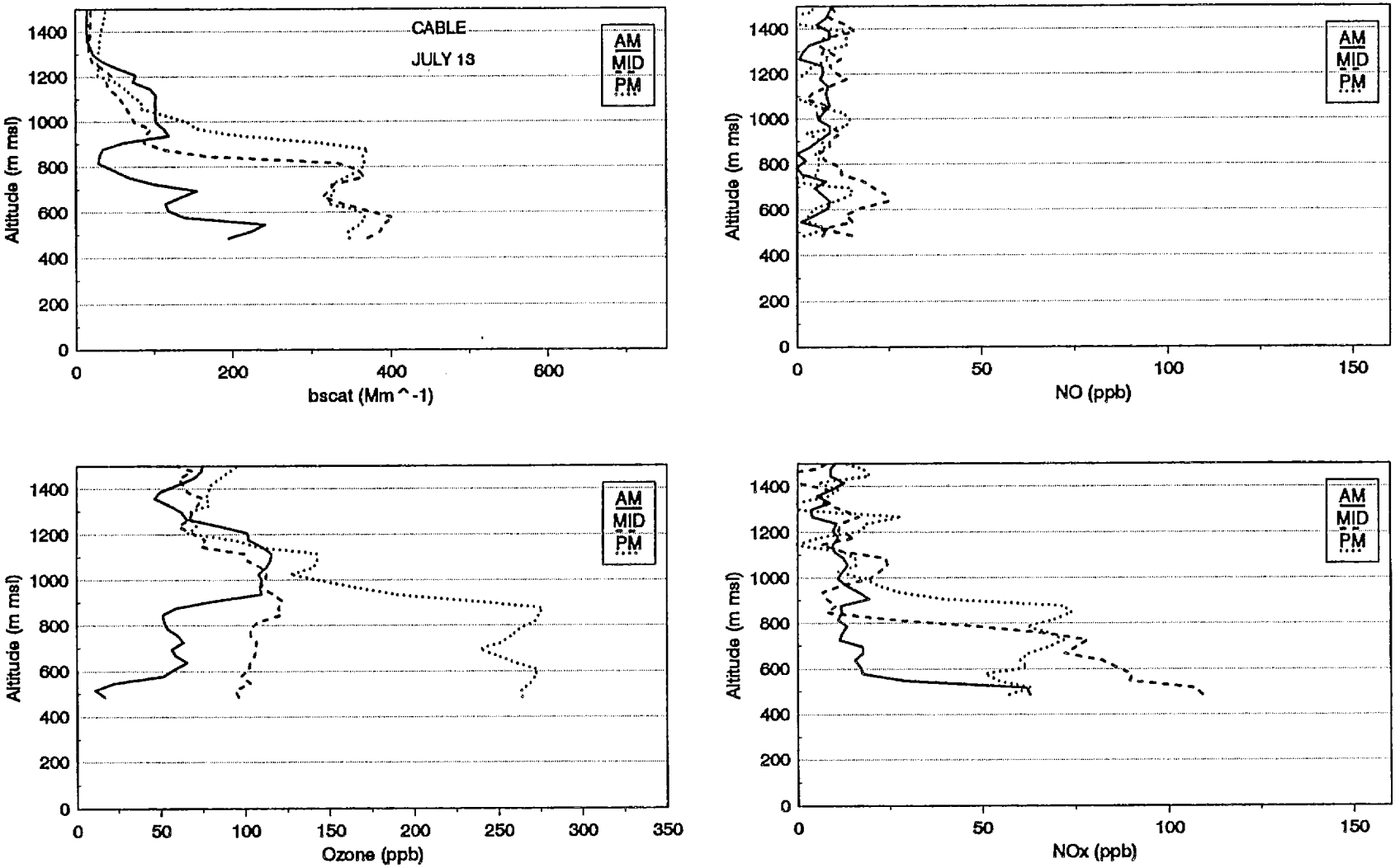

Figure 4-29. Light Scattering (b_{scat}), and Ozone, NO, and NO_x Concentrations for Morning, Midday, and Afternoon Aircraft Spirals on July 13, 1987 at Cable.

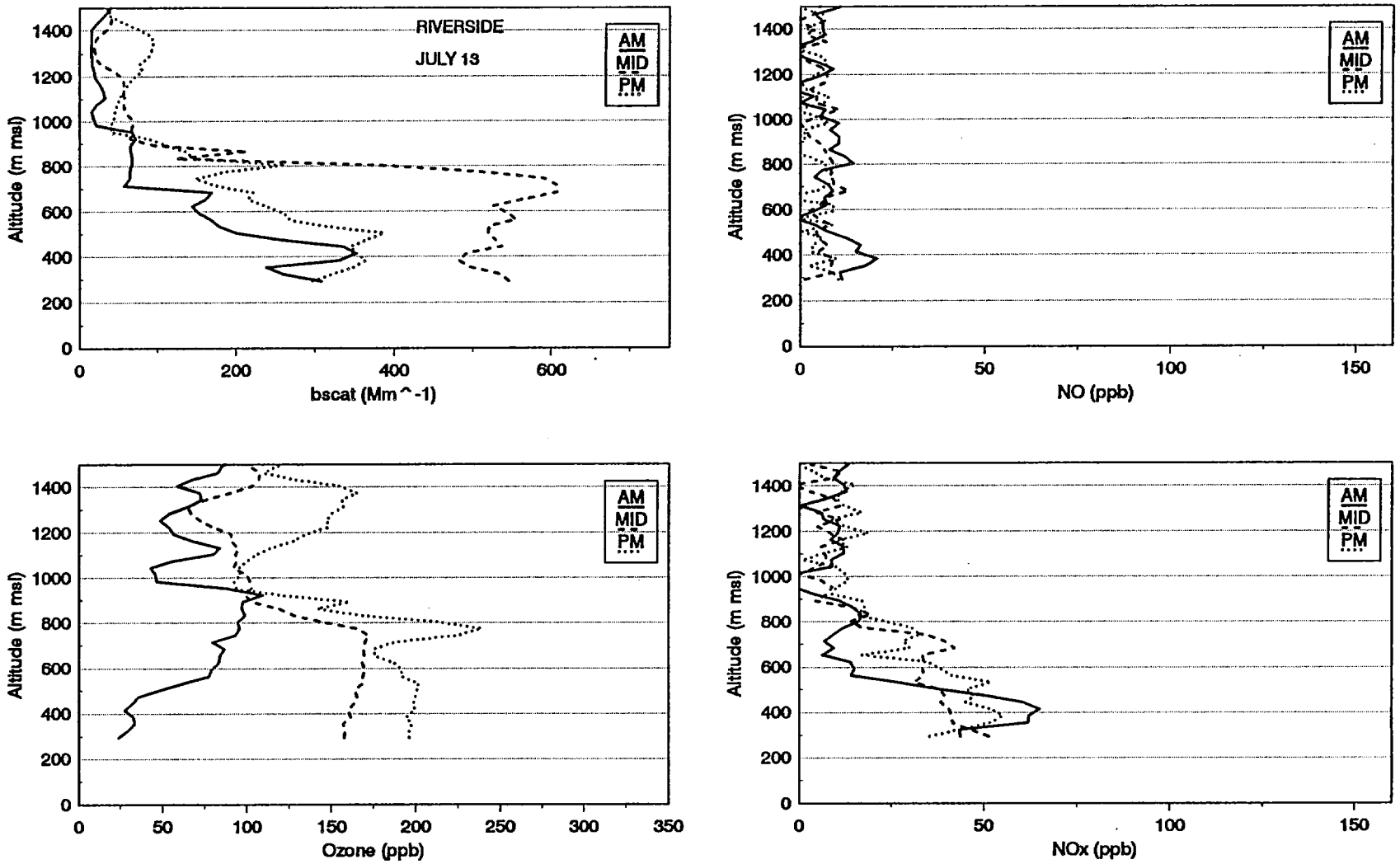

Figure 4-30. Light Scattering (b_{scat}), and Ozone, NO, and NO_x Concentrations for Morning, Midday, and Afternoon Aircraft Spirals on July 13, 1987 at Riverside.

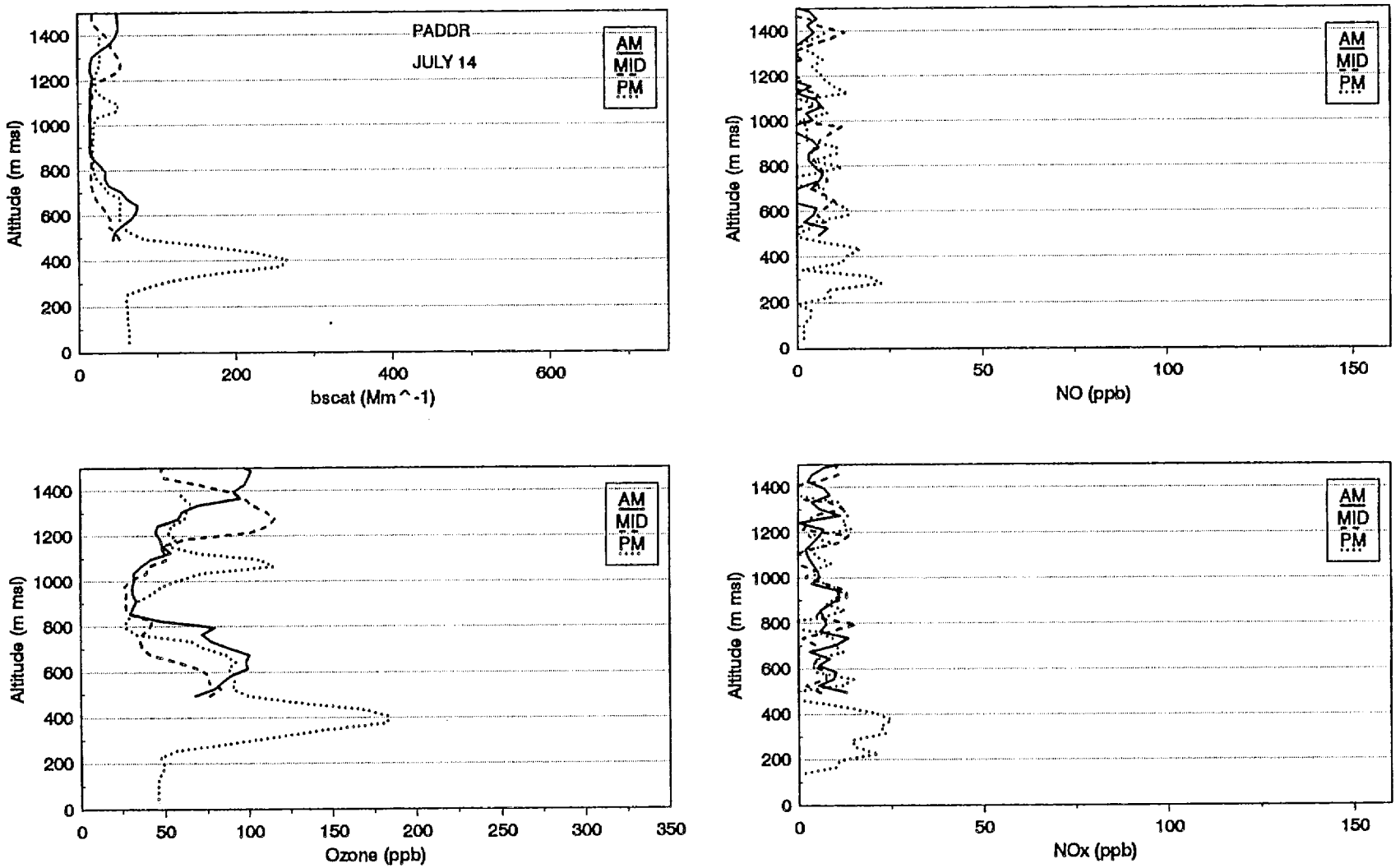

Figure 4-31. Light Scattering (b_{scat}), and Ozone, NO, and NO_x Concentrations for Morning, Midday, and Afternoon Aircraft Spirals on July 14, 1987 at PADDR. Morning data were not collected below about 500 m msl because of reduced visibility due to clouds.

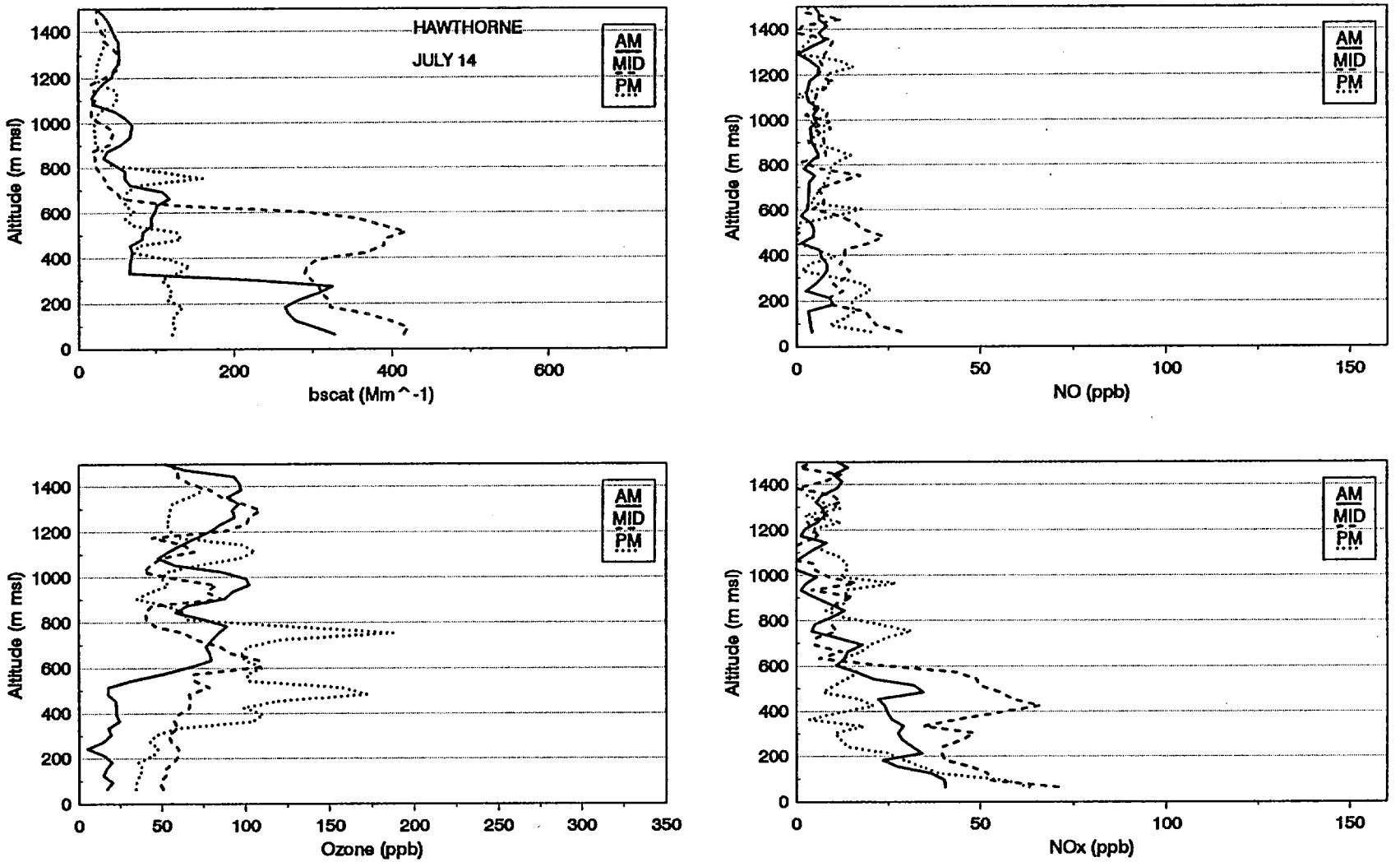

Figure 4-32. Light Scattering (b_{scat}), and Ozone, NO, and NO_x Concentrations for Morning, Midday, and Afternoon Aircraft Spirals on July 14, 1987 at Hawthorne.

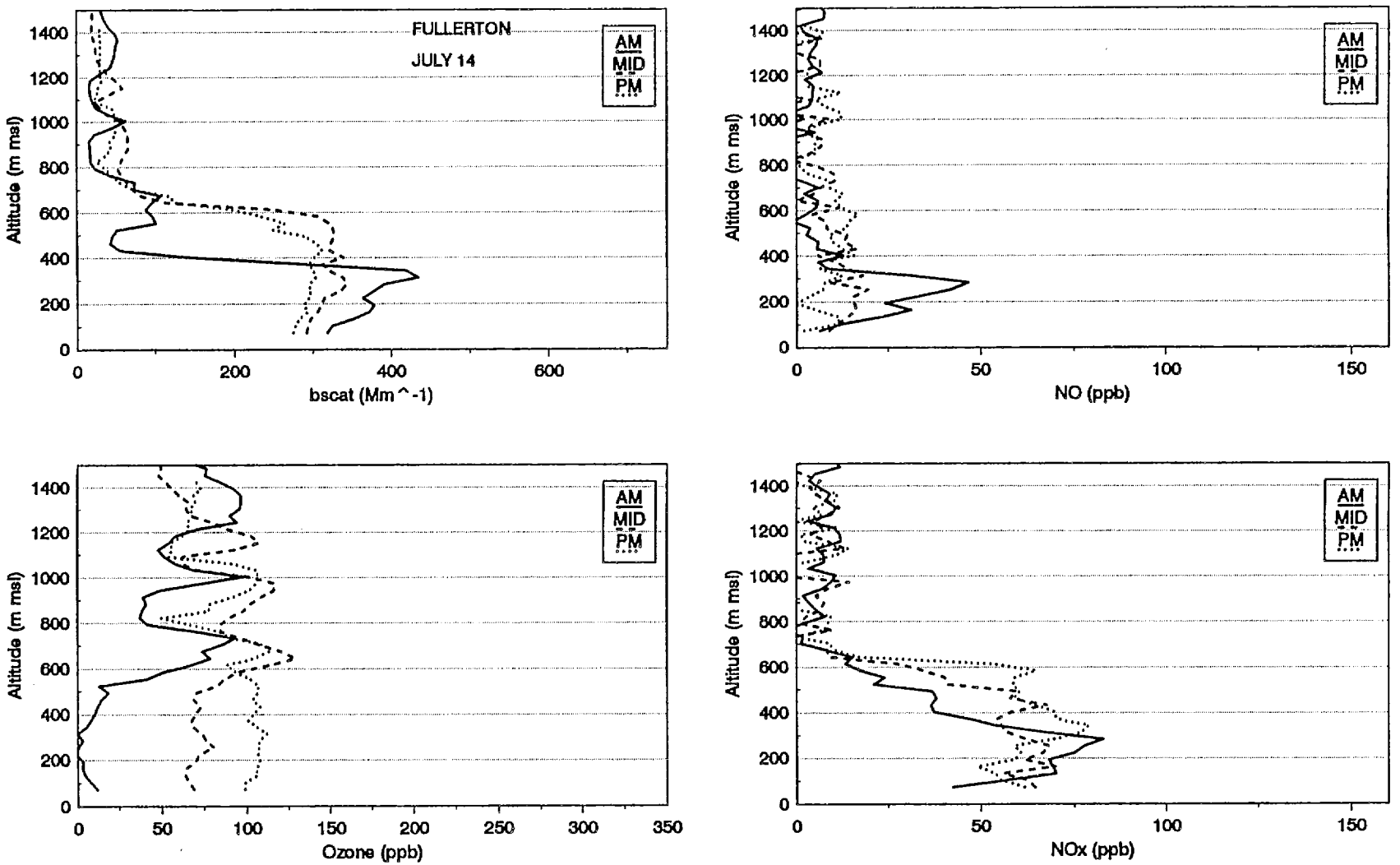

Figure 4-33. Light Scattering (b_{scat}), and Ozone, NO, and NO_x Concentrations for Morning, Midday, and Afternoon Aircraft Spirals on July 14, 1987 at Fullerton.

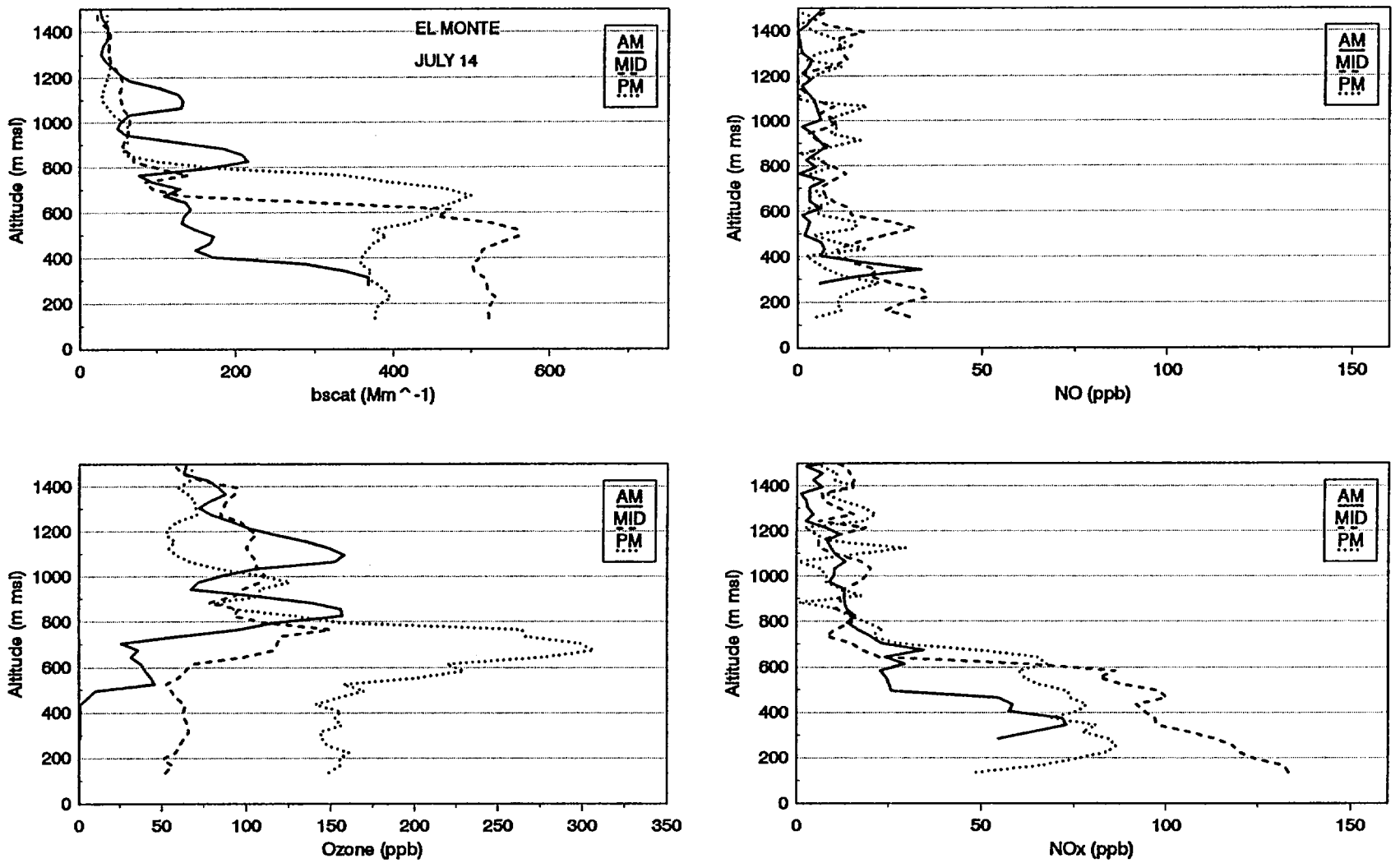

Figure 4-34. Light Scattering (b_{scat}), and Ozone, NO, and NO_x Concentrations for Morning, Midday, and Afternoon Aircraft Spirals on July 14, 1987 at El Monte. Morning data were not collected below about 300 m msl because of reduced visibility due to clouds.

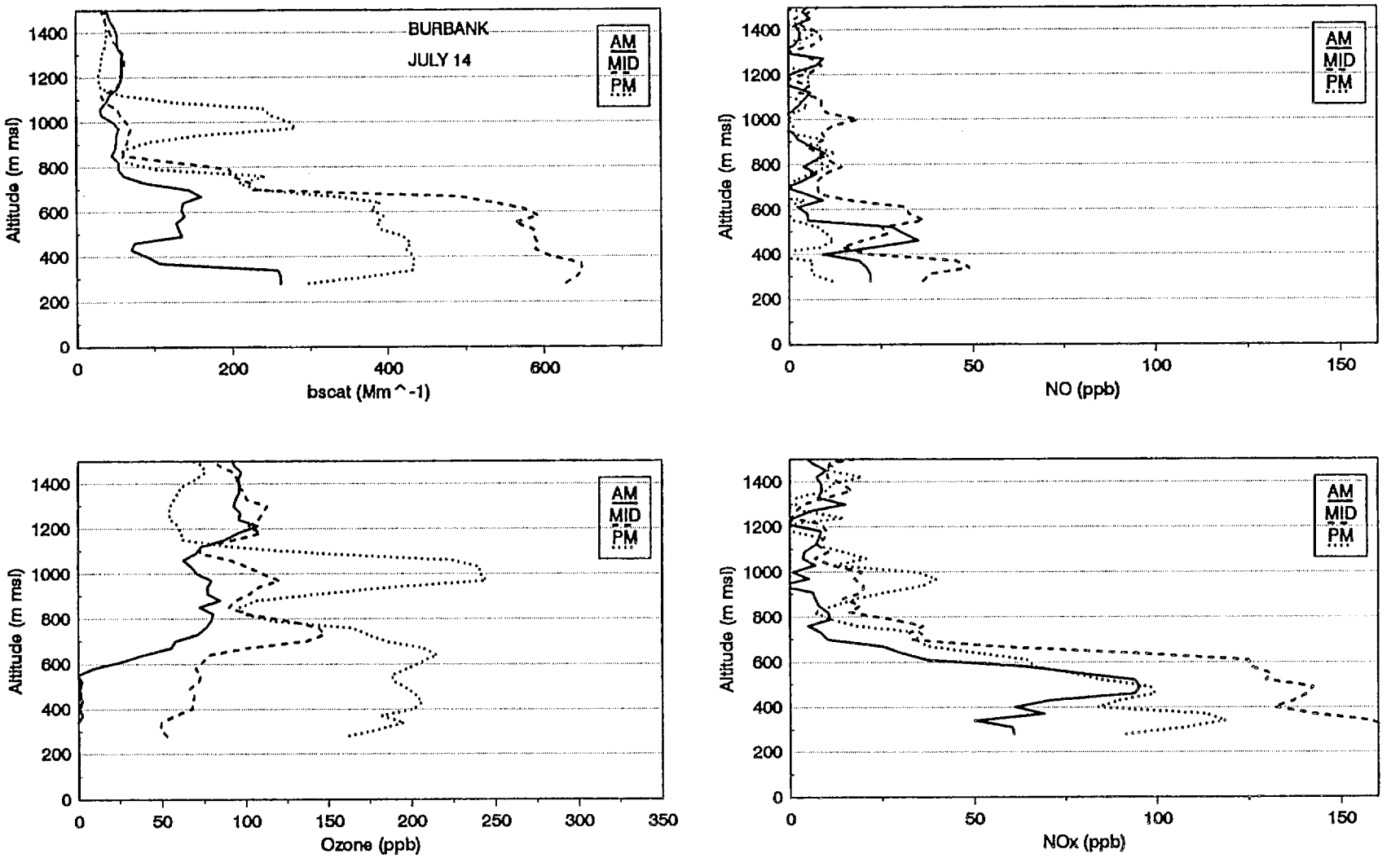

Figure 4-35. Light Scattering (b_{scat}), and Ozone, NO, and NO_x Concentrations for Morning, Midday, and Afternoon Aircraft Spirals on July 14, 1987 at Burbank.

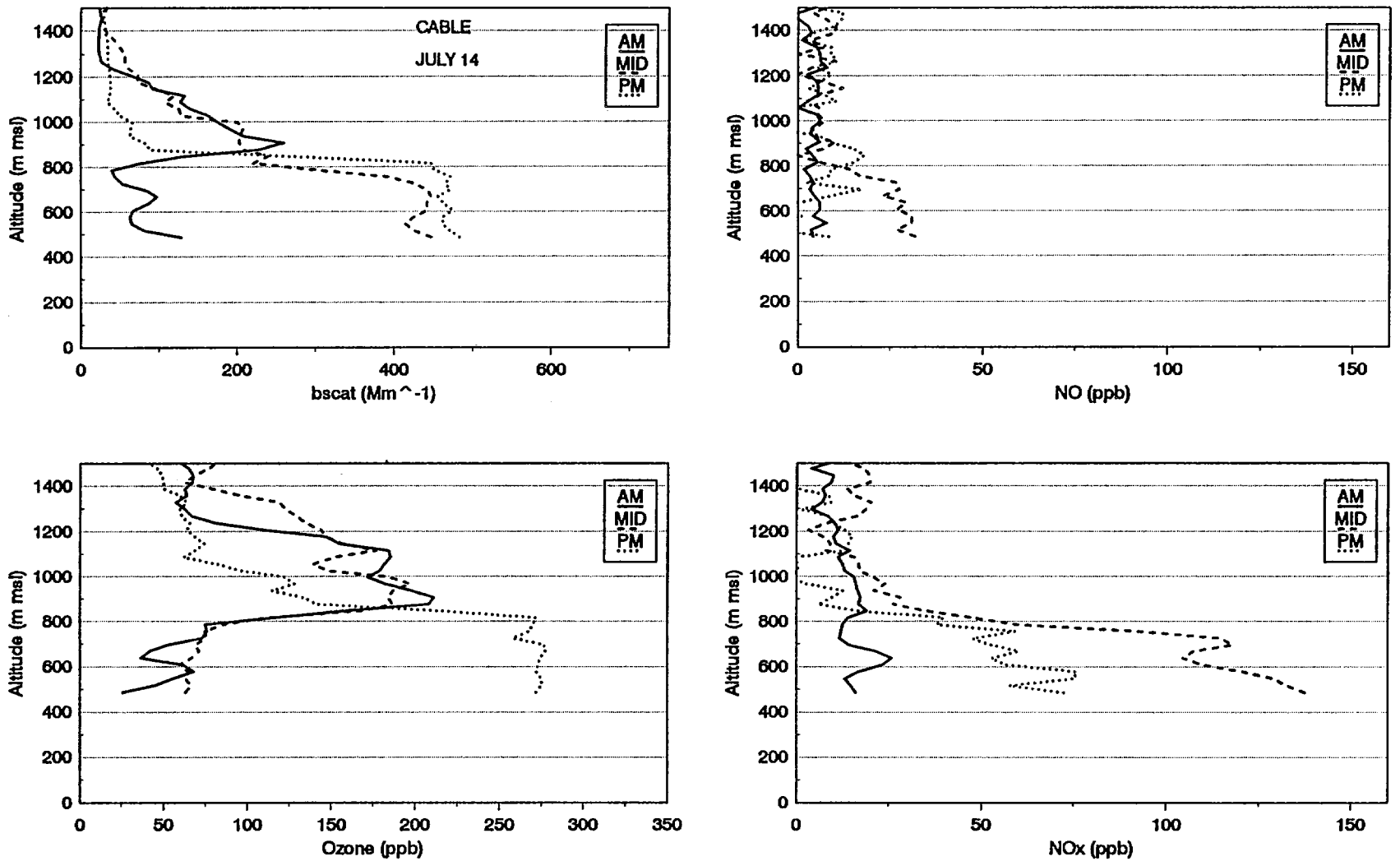

Figure 4-36. Light Scattering (b_{scat}), and Ozone, NO, and NO_x Concentrations for Morning, Midday, and Afternoon Aircraft Spirals on July 14, 1987 at Cable.

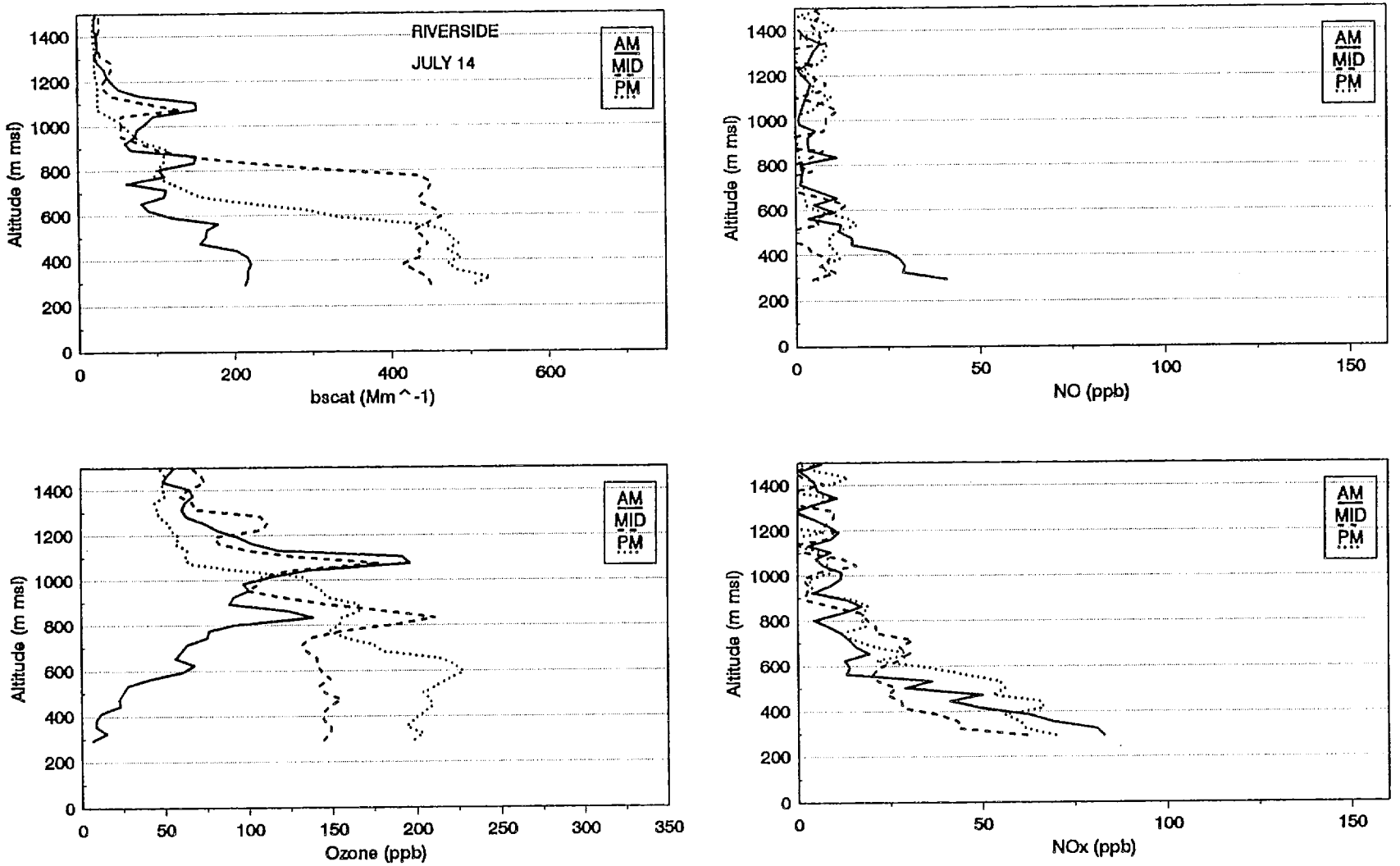

Figure 4-37. Light Scattering (b_{scat}), and Ozone, NO, and NO_x Concentrations for Morning, Midday, and Afternoon Aircraft Spirals on July 14, 1987 at Riverside.

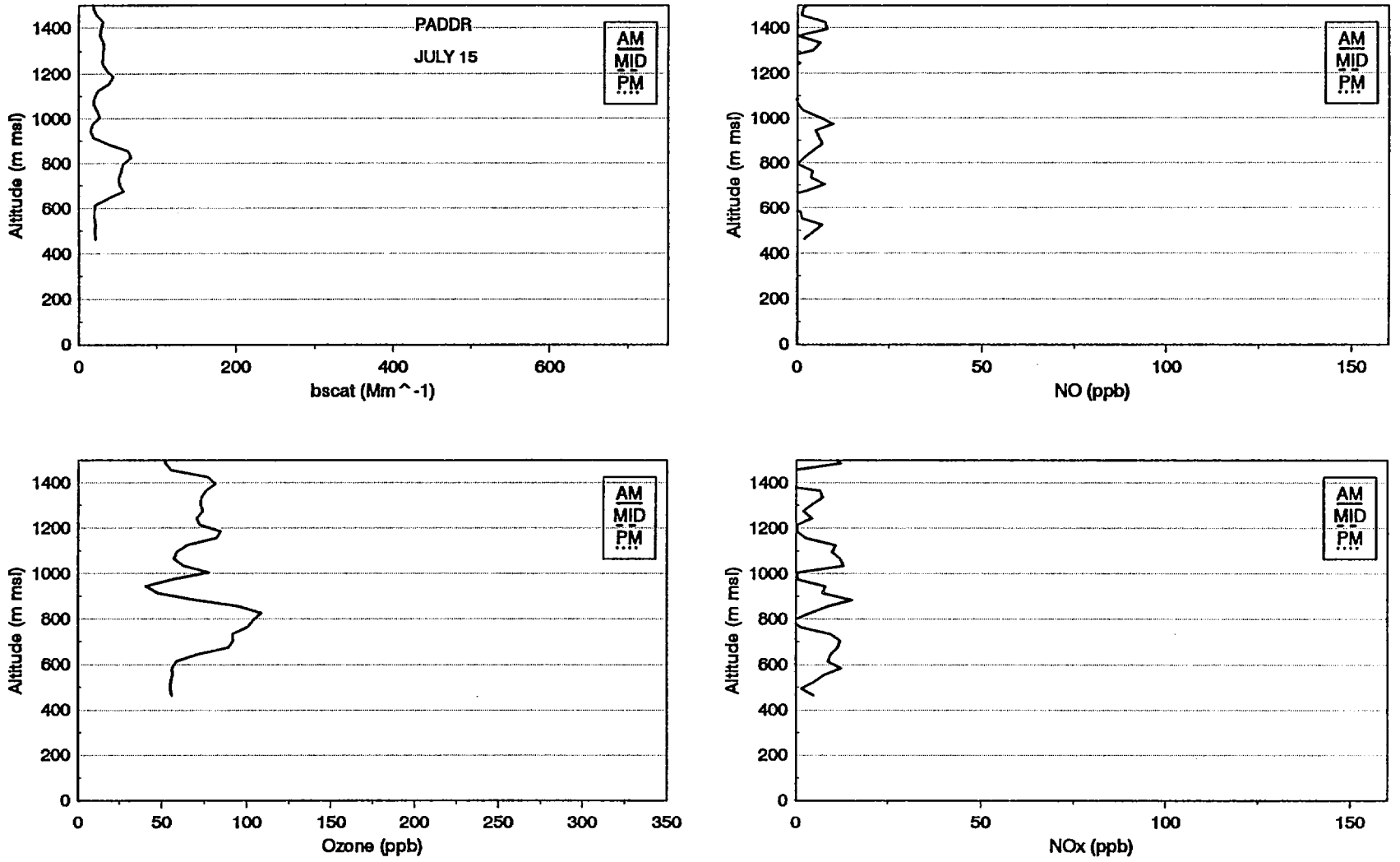

Figure 4-38. Light Scattering (b_{scat}), and Ozone, NO, and NO_x Concentrations for the Morning Aircraft Spiral on July 15, 1987 at PADDR. Midday and afternoon aircraft flights were not made. Morning data were not collected below about 450 m msl because of reduced visibility due to clouds.

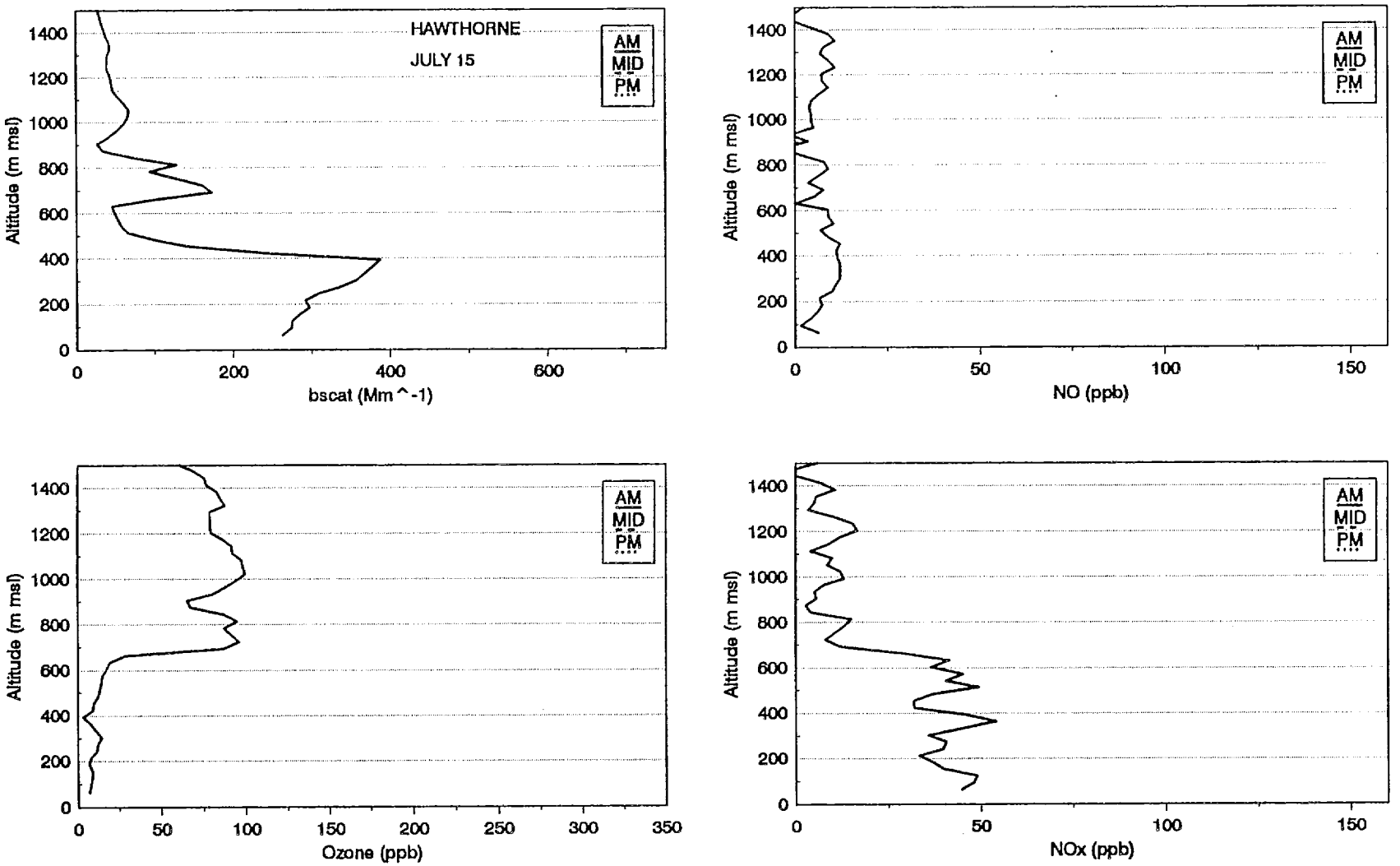

Figure 4-39. Light Scattering (b_{scat}), and Ozone, NO, and NO_x Concentrations for the Morning Aircraft Spiral on July 15, 1987 at Hawthorne. Midday and afternoon aircraft flights were not made.

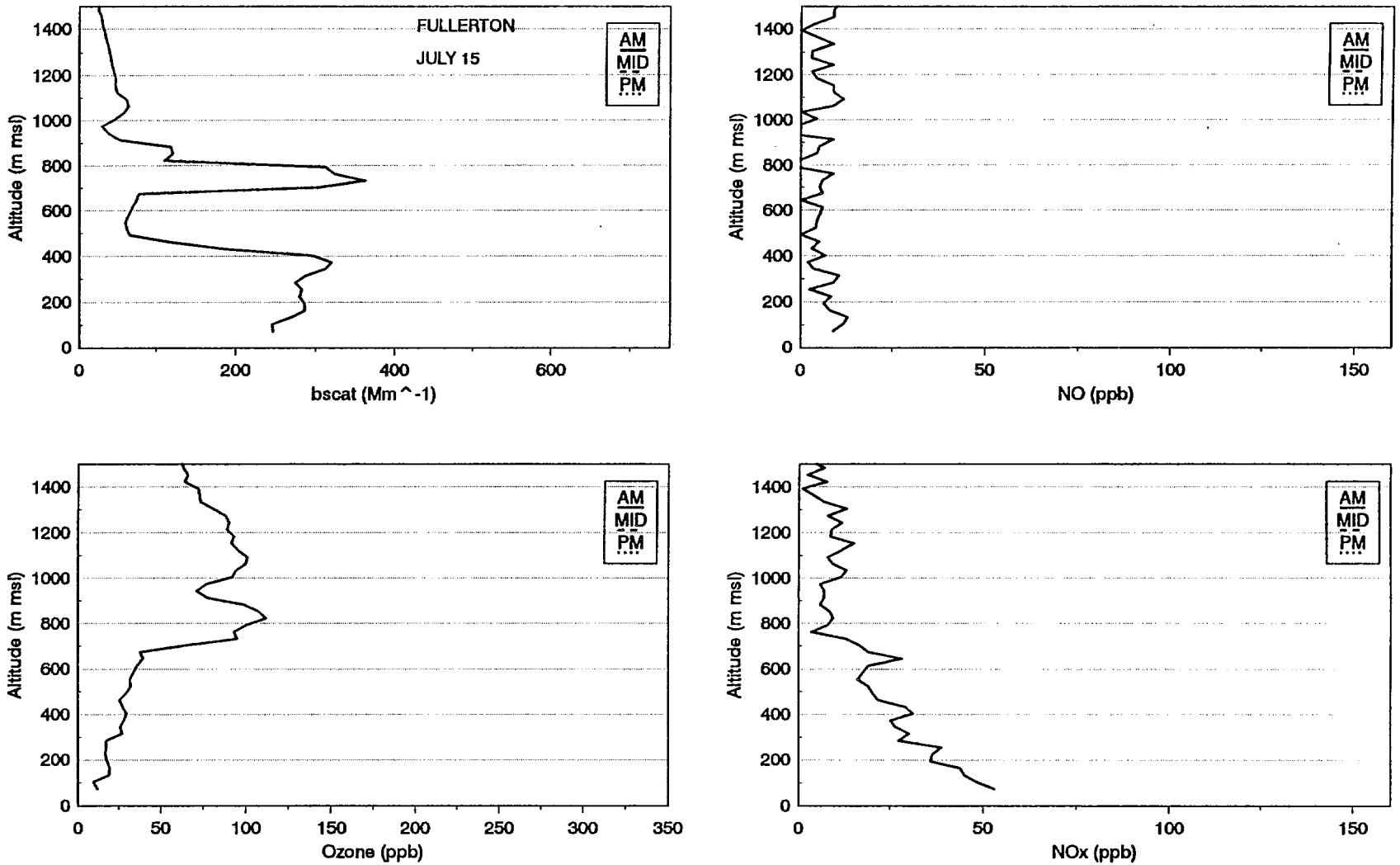

Figure 4-40. Light Scattering (b_{scat}), and Ozone, NO, and NO_x Concentrations for the Morning Aircraft Spiral on July 15, 1987 at Fullerton. Midday and afternoon aircraft flights were not made.

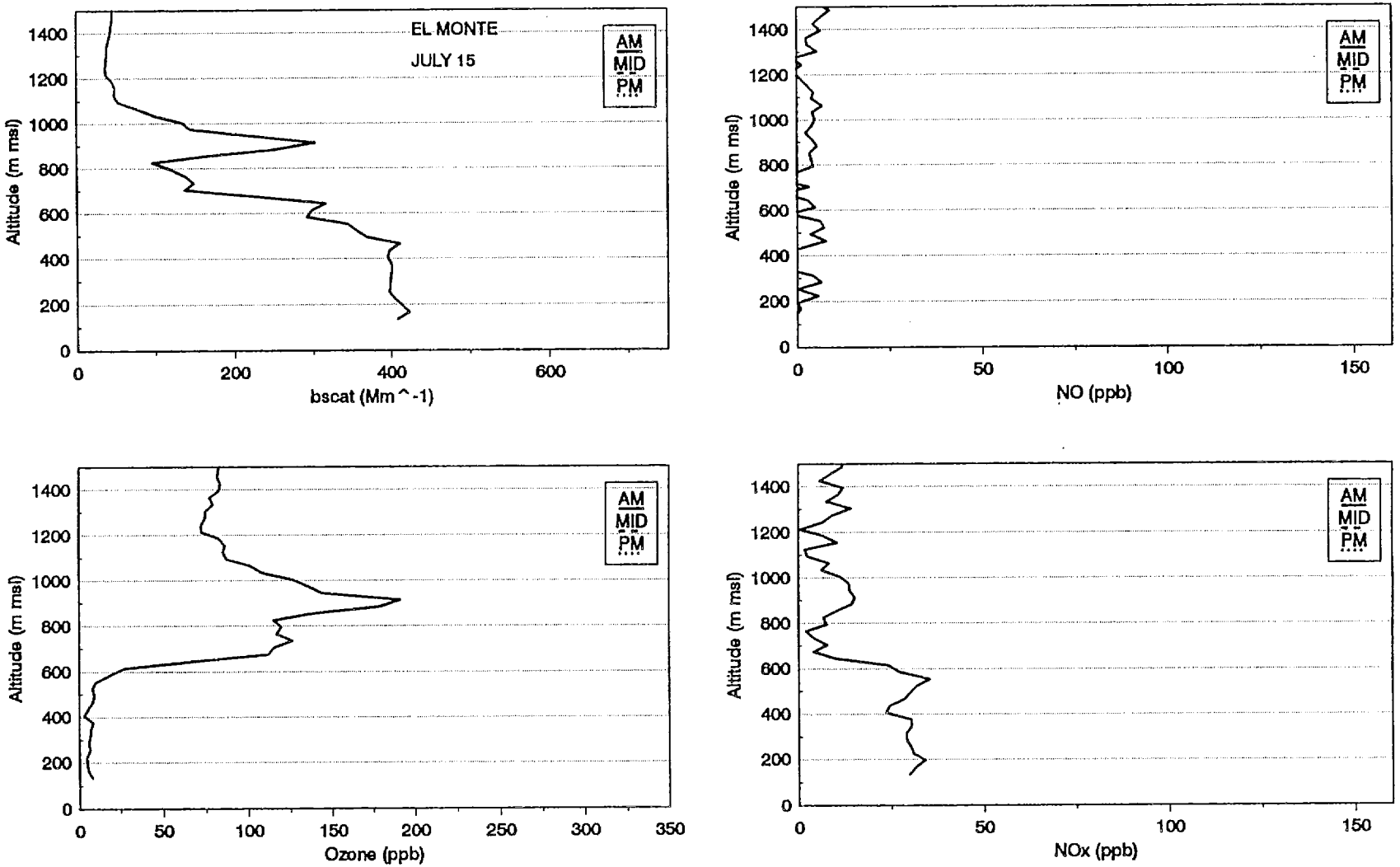

Figure 4-41. Light Scattering (b_{scat}), and Ozone, NO, and NO_x Concentrations for the Morning Aircraft Spiral on July 15, 1987 at El Monte. Midday and afternoon aircraft flights were not made.

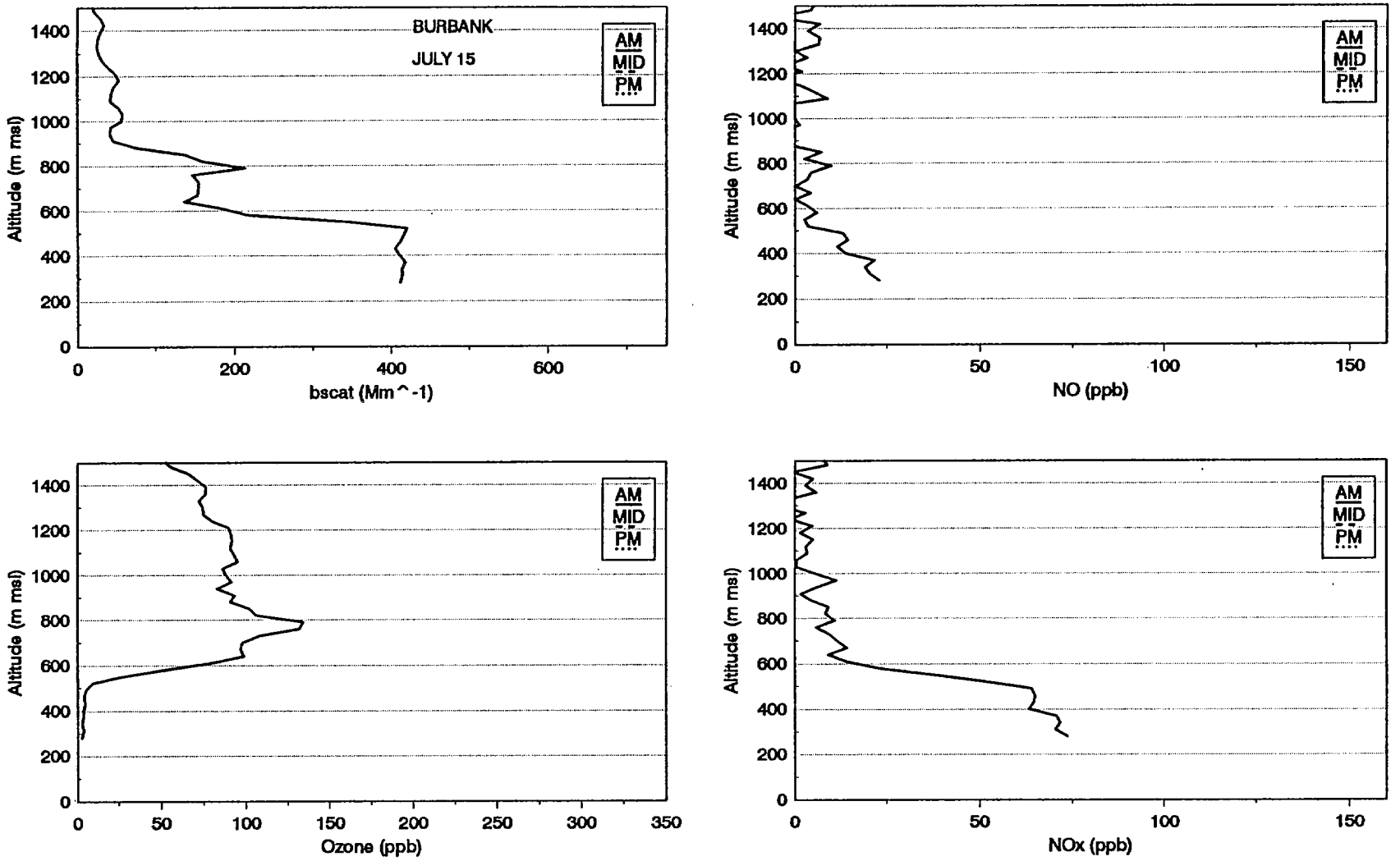

Figure 4-42. Light Scattering (b_{scat}), and Ozone, NO, and NO_x Concentrations for the Morning Aircraft Spiral on July 15, 1987 at Burbank. Midday and afternoon aircraft flights were not made.

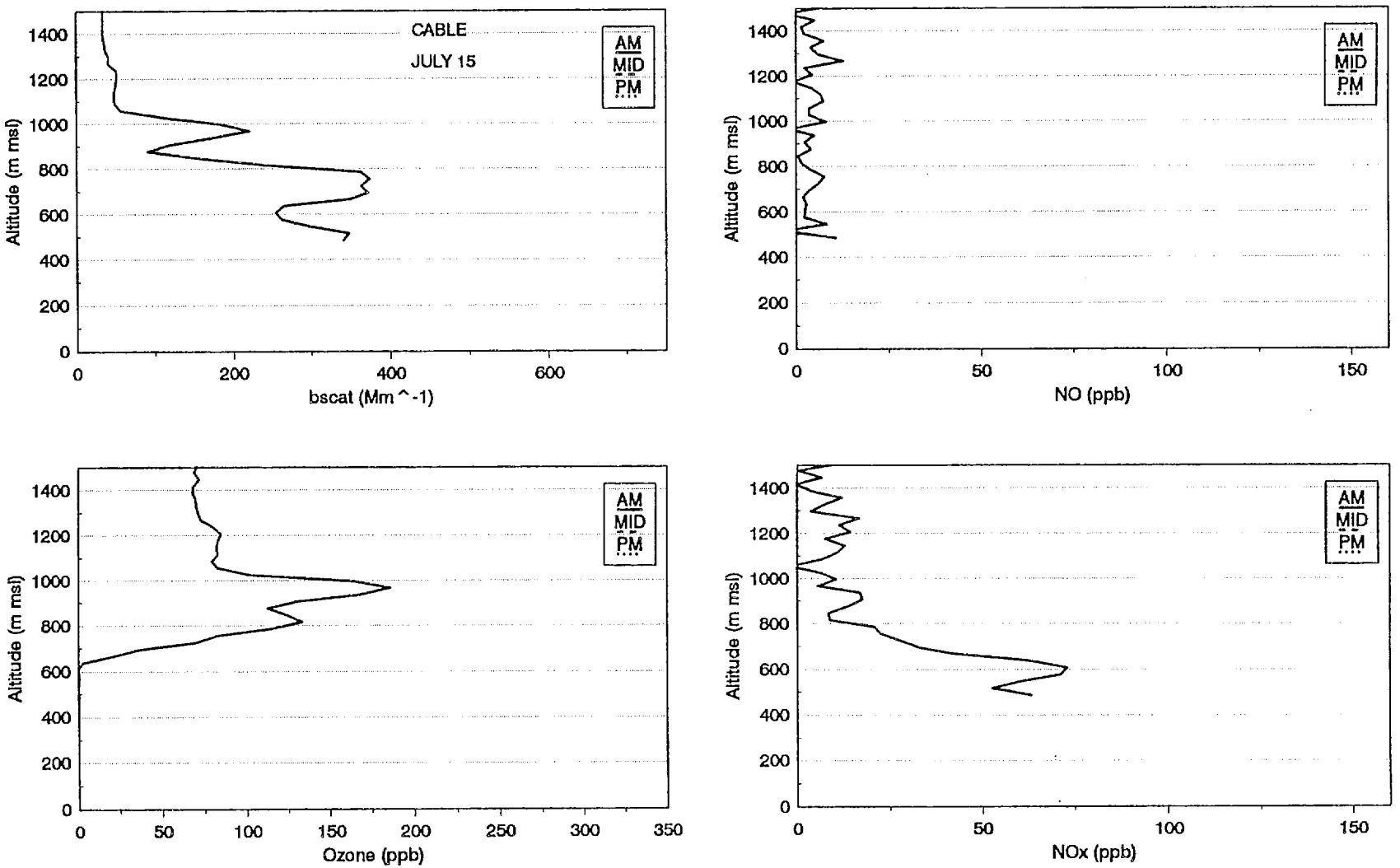

Figure 4-43. Light Scattering (b_{scat}), and Ozone, NO, and NO_x Concentrations for the Morning Aircraft Spiral on July 15, 1987 at Cable. Midday and afternoon aircraft flights were not made.

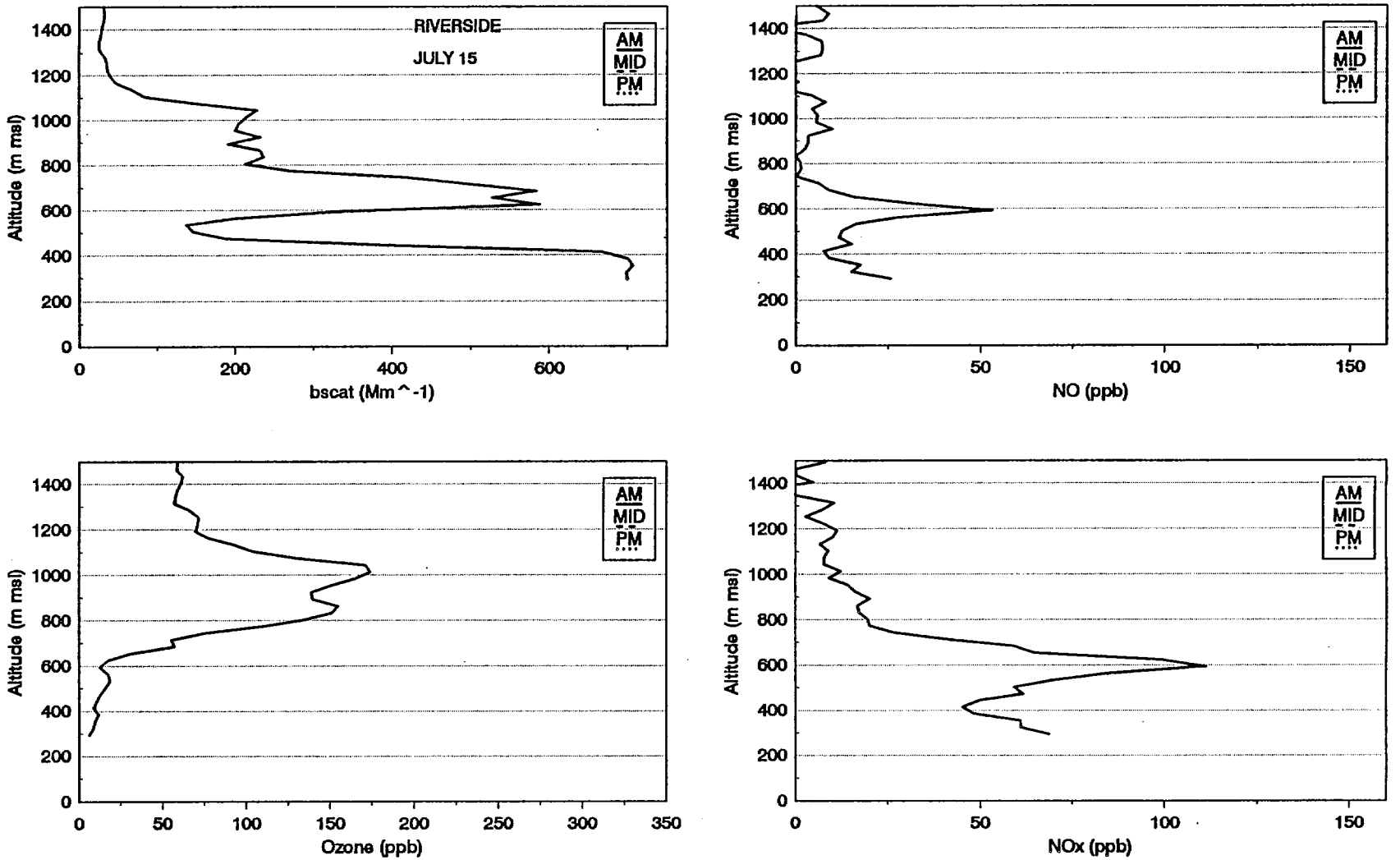

Figure 4-44. Light Scattering (b_{scat}), and Ozone, NO, and NO_x Concentrations for the Morning Aircraft Spiral on July 15, 1987 at Riverside. Midday and afternoon aircraft flights were not made.

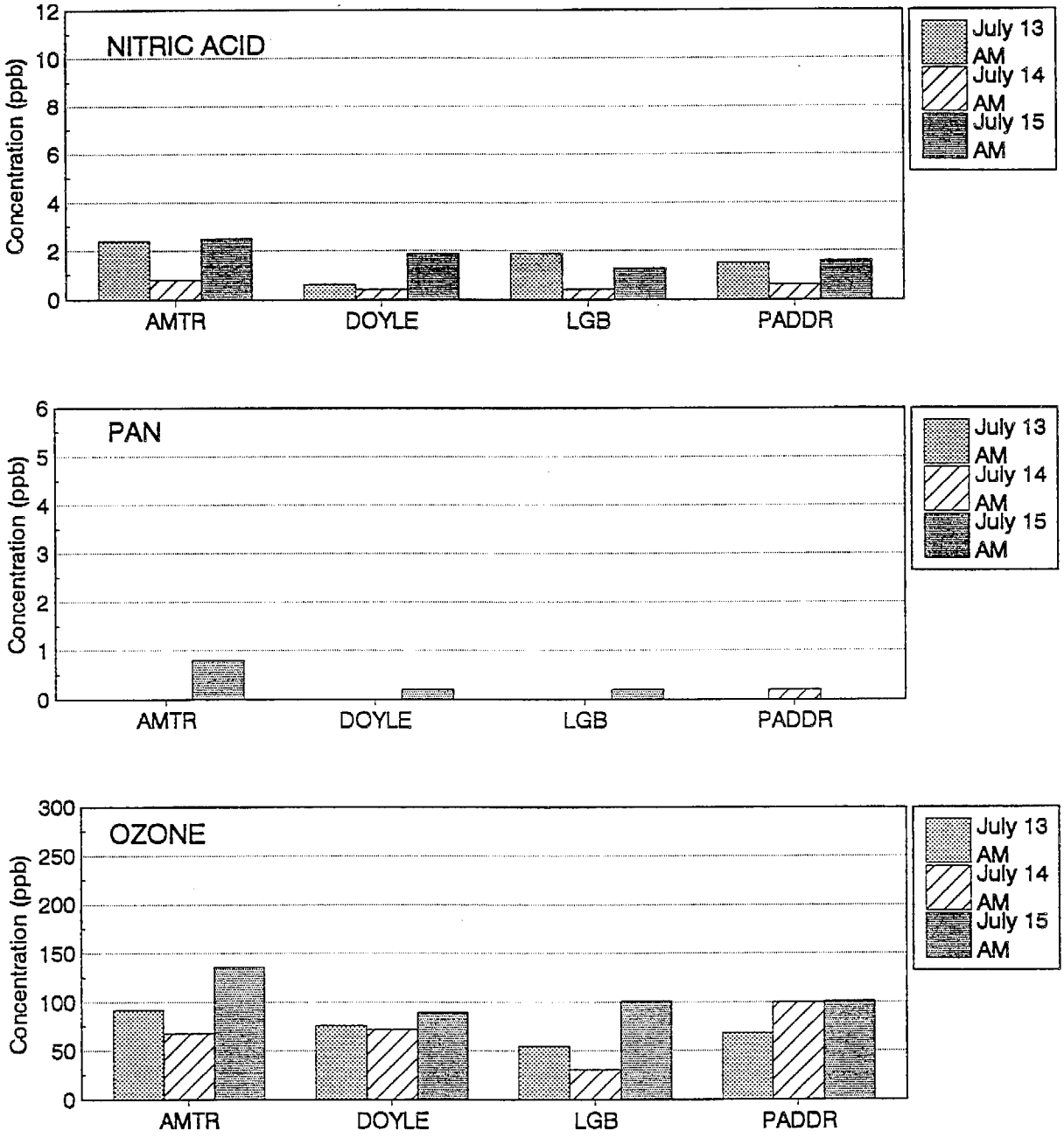

Figure 4-45. Orbit-Averages of Nitric Acid, PAN, and Ozone Measured Aloft on the Mornings of July 13-15 for Each Orbit Location. All samples were collected above the mixed layer.

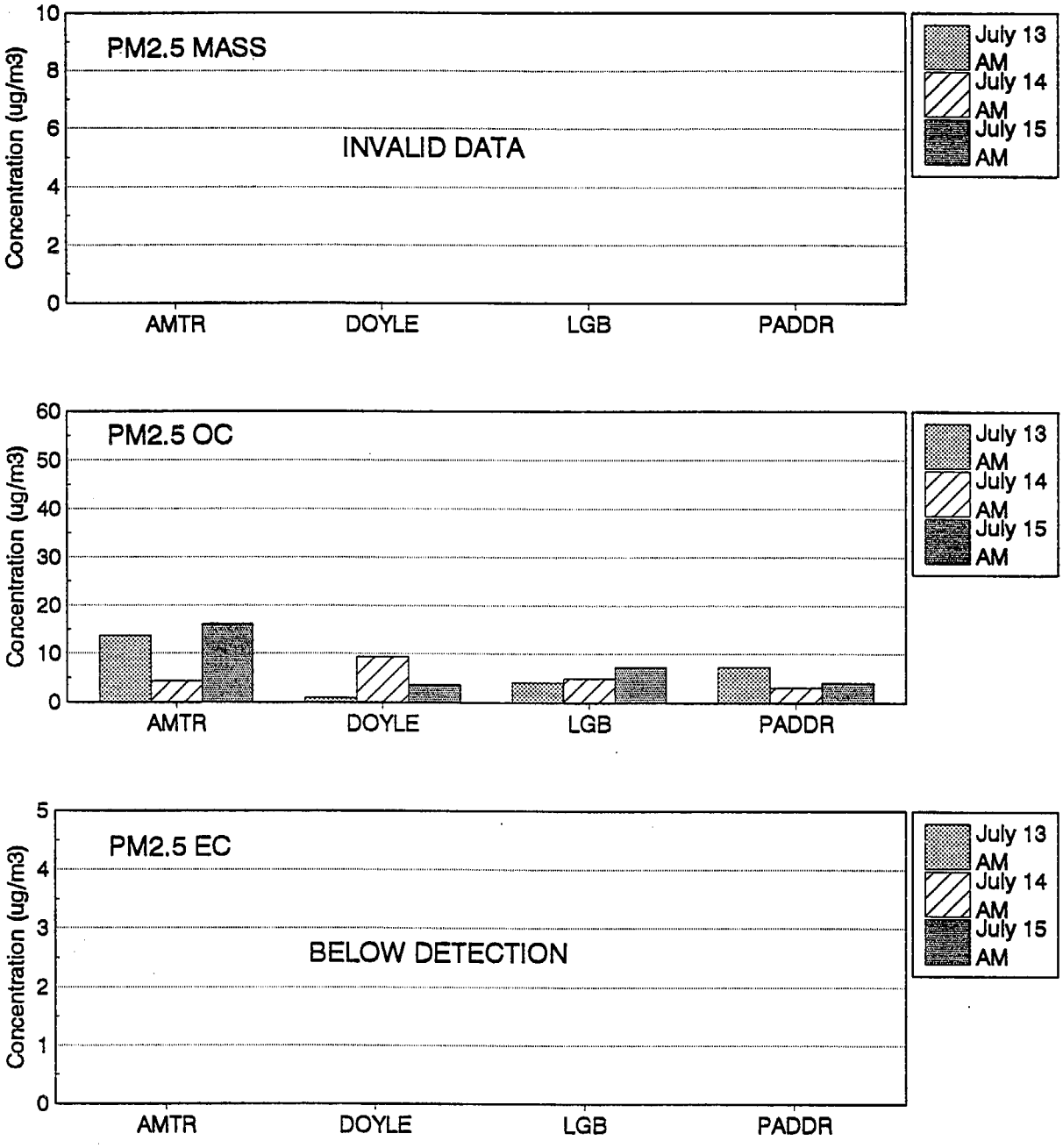

Figure 4-46. Orbit-Averages of $PM_{2.5}$ Mass, Organic Carbon, and Elemental Carbon Measured Aloft on the Mornings of July 13-15 for Each Orbit Location. All samples were collected above the mixed layer.

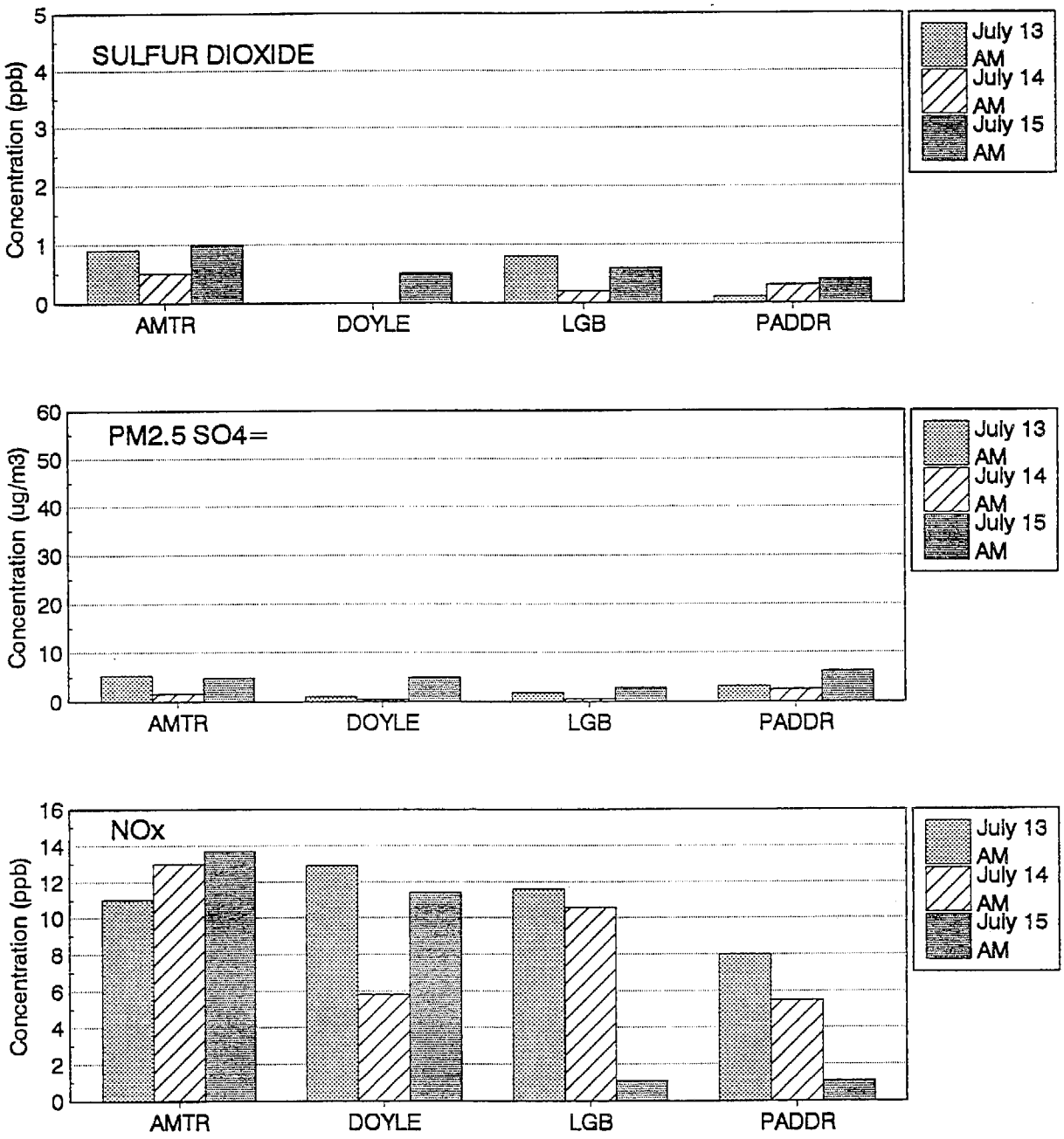

ALL SAMPLES COLLECTED ABOVE THE MIXED LAYER

Figure 4-47. Orbit-Averages of SO_2, $PM_{2.5}$ Sulfate Ion, and NO_x Measured Aloft on the Mornings of July 13-15 for Each Orbit Location. All samples were collected above the mixed layer.

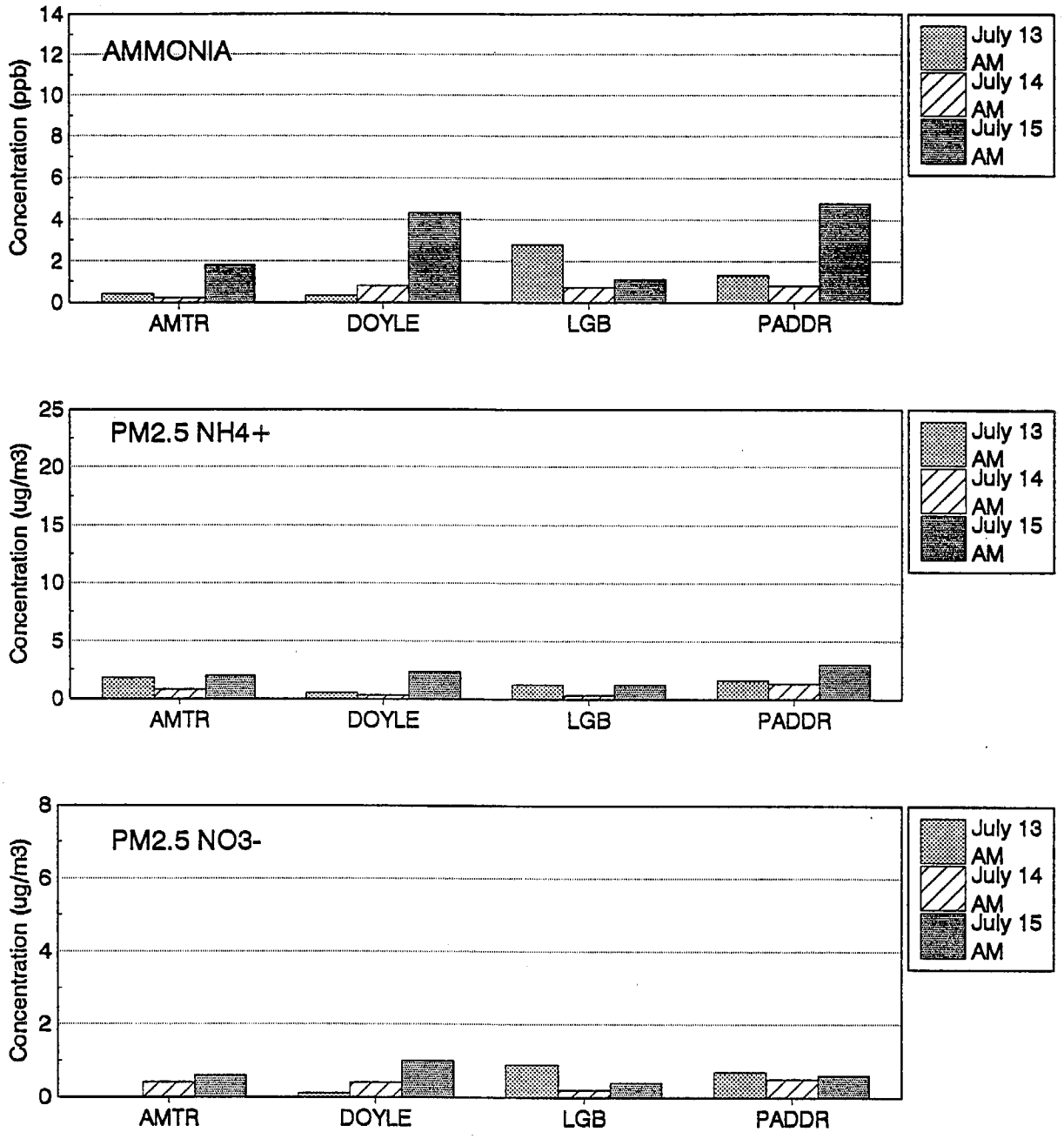

ALL SAMPLES COLLECTED ABOVE THE MIXED LAYER

Figure 4-48. Orbit-Averages of Ammonia and $PM_{2.5}$ Ammonium and Nitrate Ions Measured Aloft on the Mornings of July 13-15 for Each Orbit Location. All samples were collected above the mixed layer.

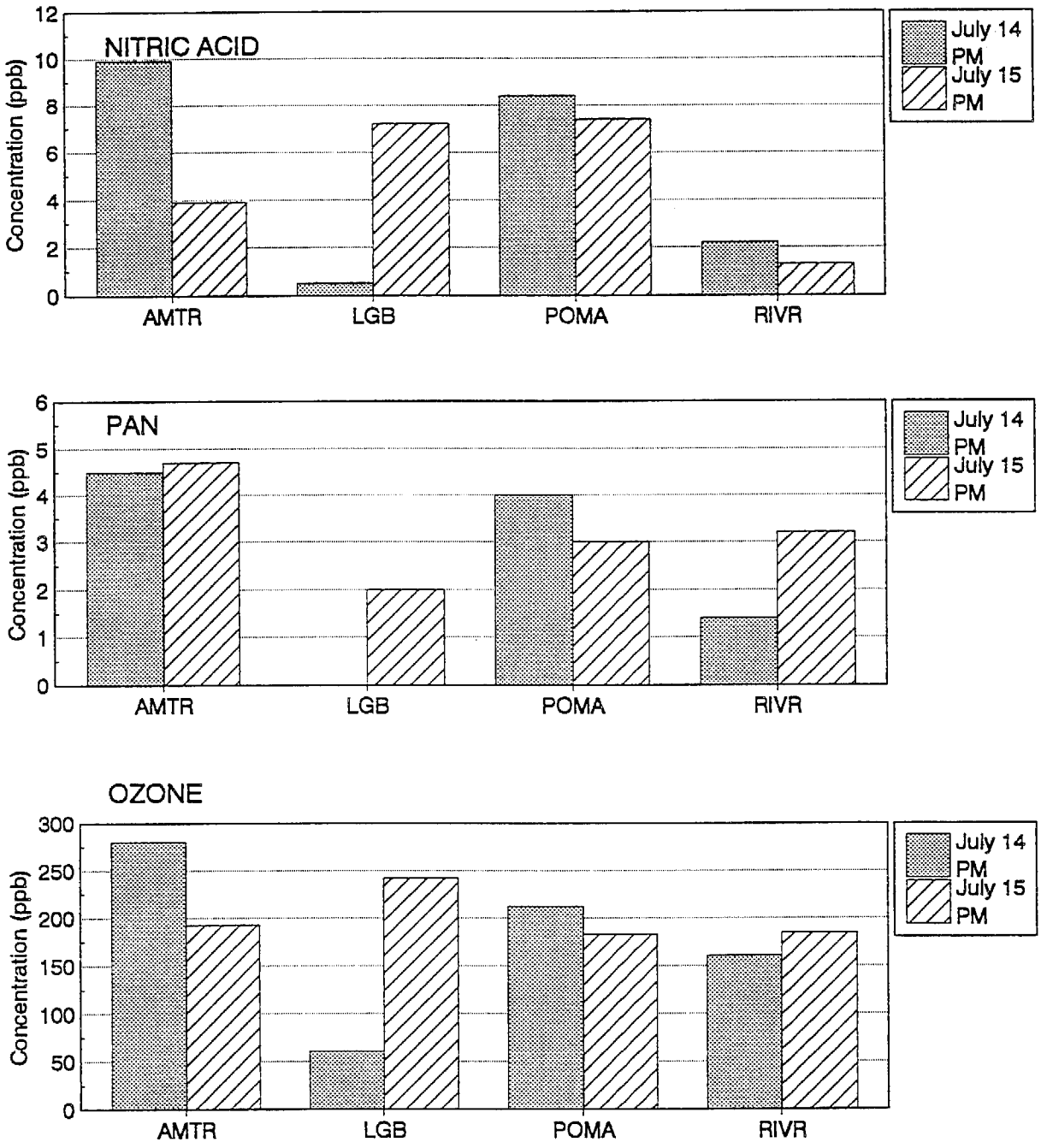

Figure 4-49. Orbit-Averages of Nitric Acid, PAN, and Ozone Measured Aloft on the Afternoons of July 14-15 for Each Orbit Location. AMTRA and Long Beach samples were collected above the mixed layer; Pomona and Riverside samples were collected within the mixed layer.

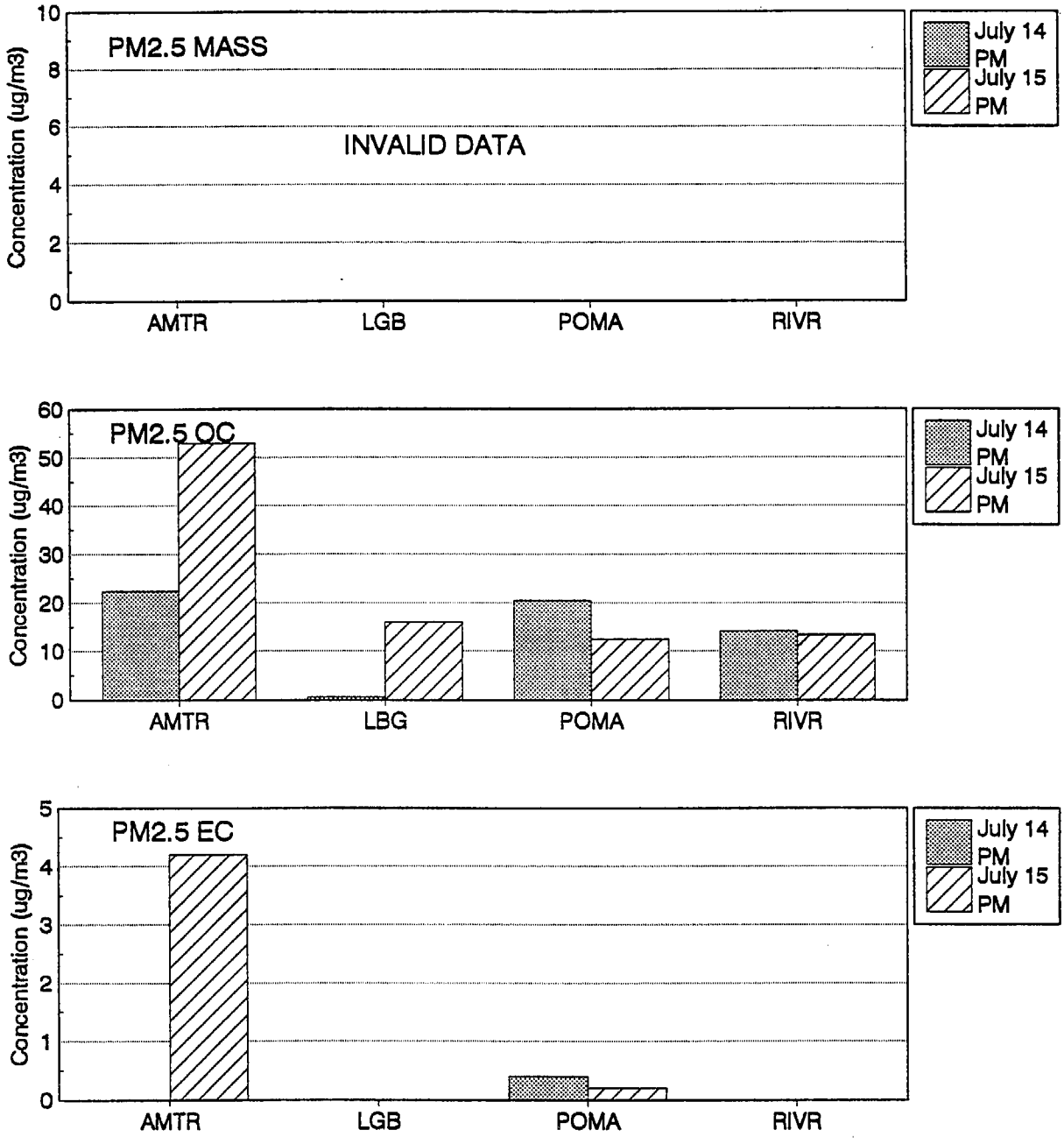

Figure 4-50. Orbit-Averages of $PM_{2.5}$ Mass, Organic Carbon, and Elemental Carbon Measured Aloft on the Afternoons of July 14-15 for Each Orbit Location. AMTRA and Long Beach samples were collected above the mixed layer; Pomona and Riverside samples were collected within the mixed layer.

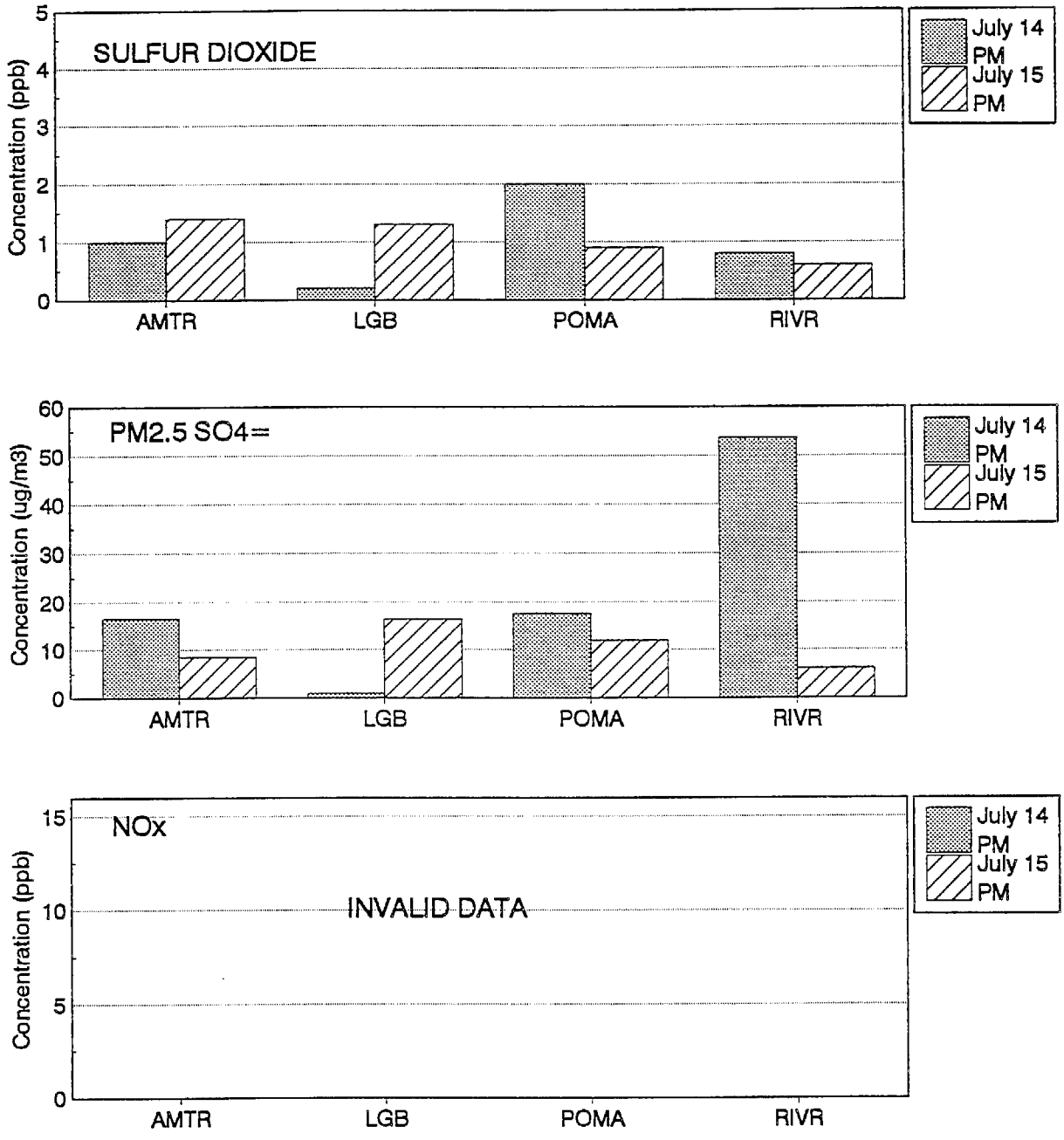

Figure 4-51. Orbit-Averages of SO_2, $PM_{2.5}$ Sulfate Ion, and NO_x Measured Aloft on the Afternoons of July 14-15 for Each Orbit Location. AMTRA and Long Beach samples were collected above the mixed layer; Pomona and Riverside samples were collected within the mixed layer.

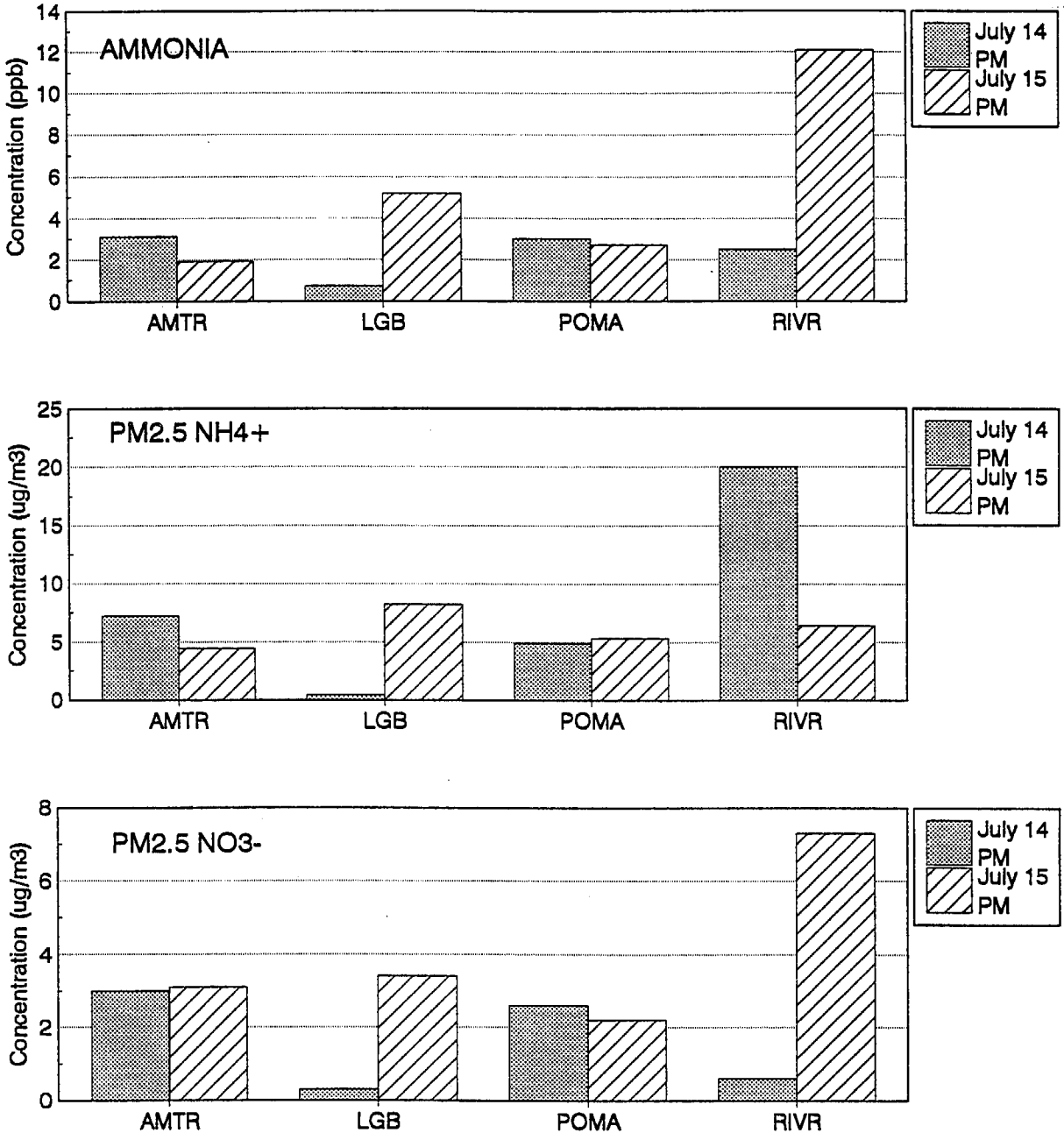

Figure 4-52. Orbit-Averages of Ammonia and $PM_{2.5}$ Ammonium and Nitrate Ions Measured Aloft on the Afternoons of July 14-15 for Each Orbit Location. AMTRA and Long Beach samples were collected above the mixed layer; Pomona and Riverside samples were collected within the mixed layer.

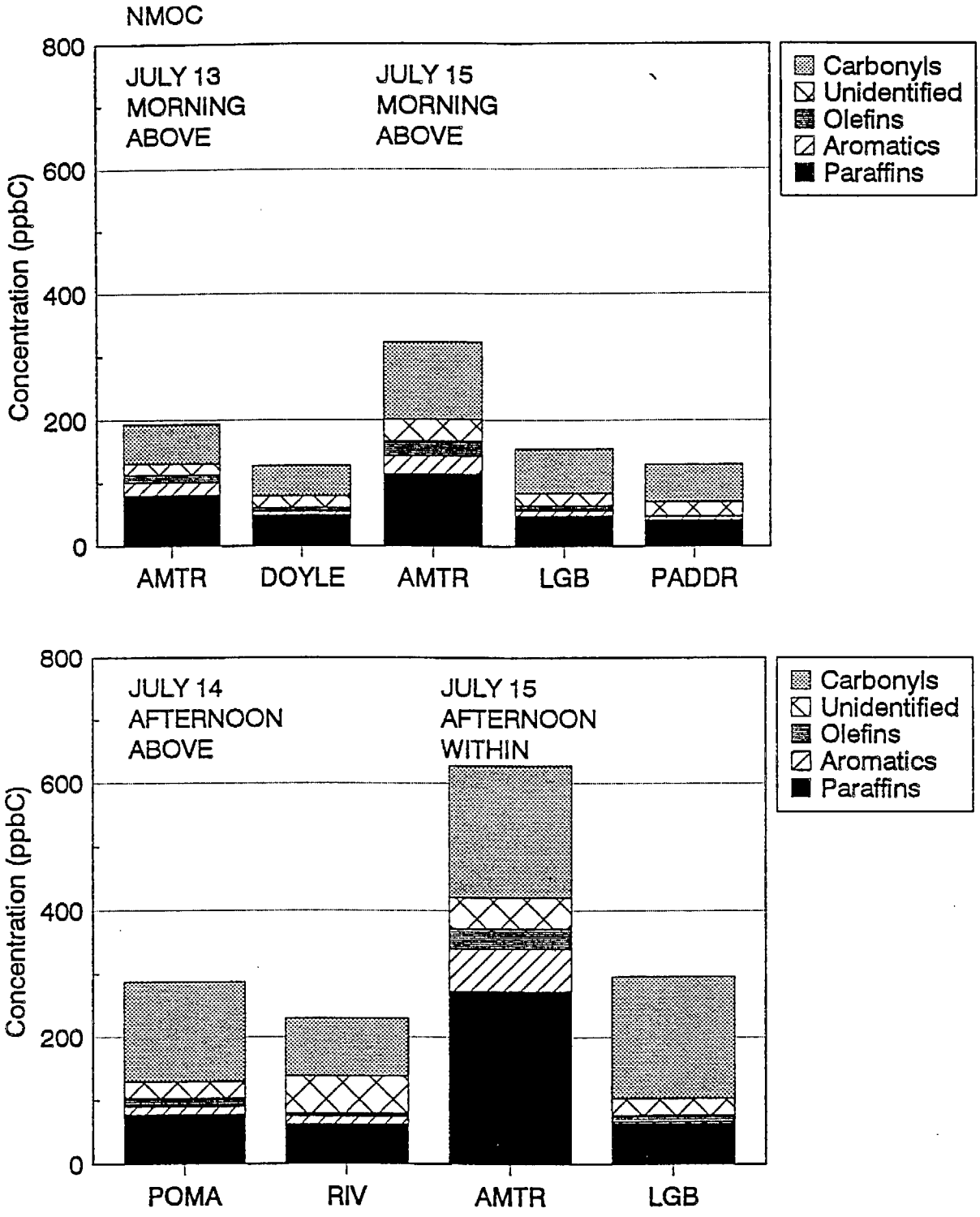

Figure 4-53. Orbit-Averages of NMOC Measured Aloft on (a) Morning of July 13 and 14 and (b) Afternoon of July 14 and 15 for Each Orbit Location.

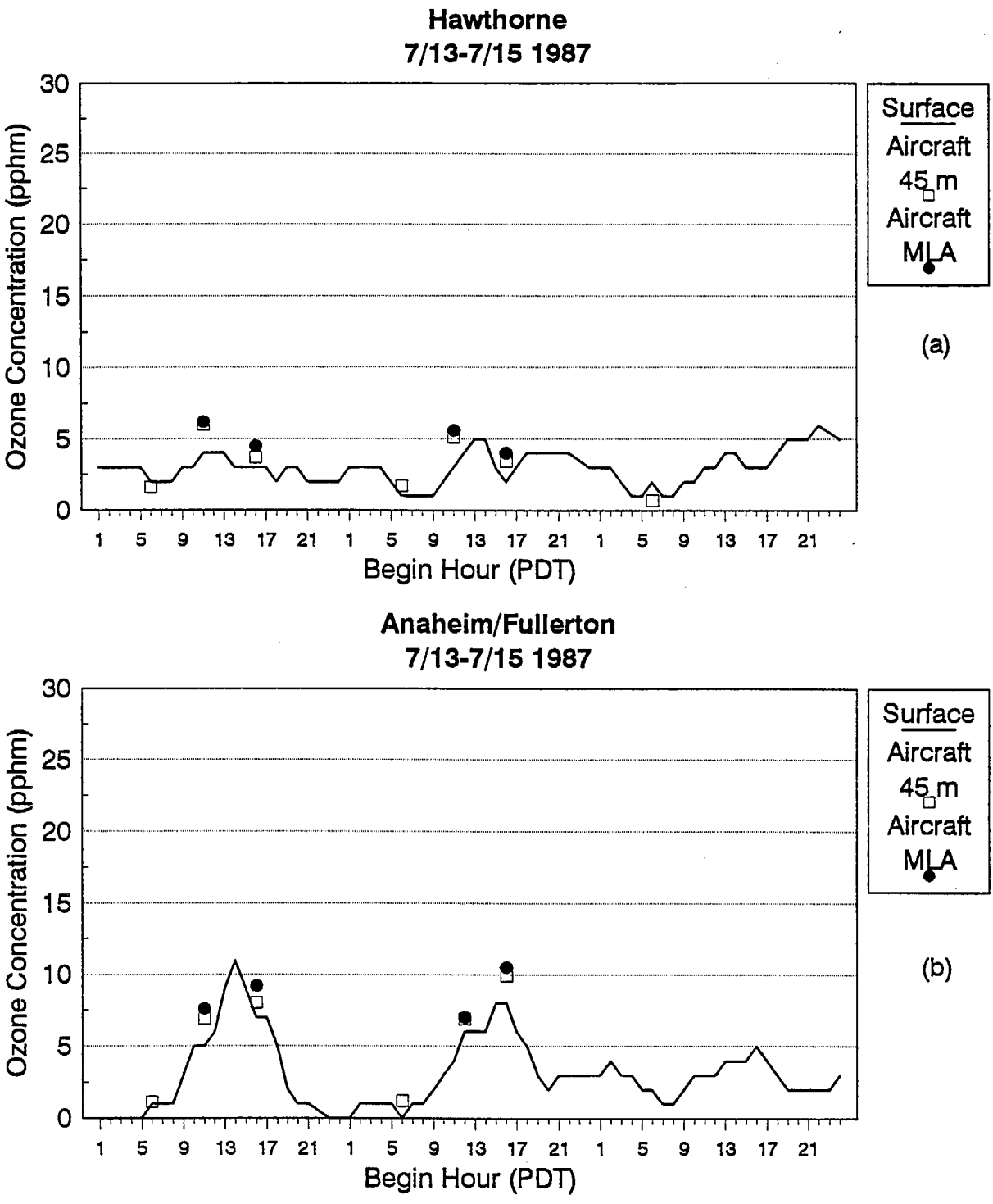

Figure 4-54. Comparison of Surface Ozone Concentrations With Mixed-Layer-Average (MLA) and the Lowest 45-Meter Average (45 m) Ozone at (a) Hawthorne and (b) Fullerton on July 13-15, 1987. The data compared to the Fullerton spiral are from the Anaheim surface monitor.

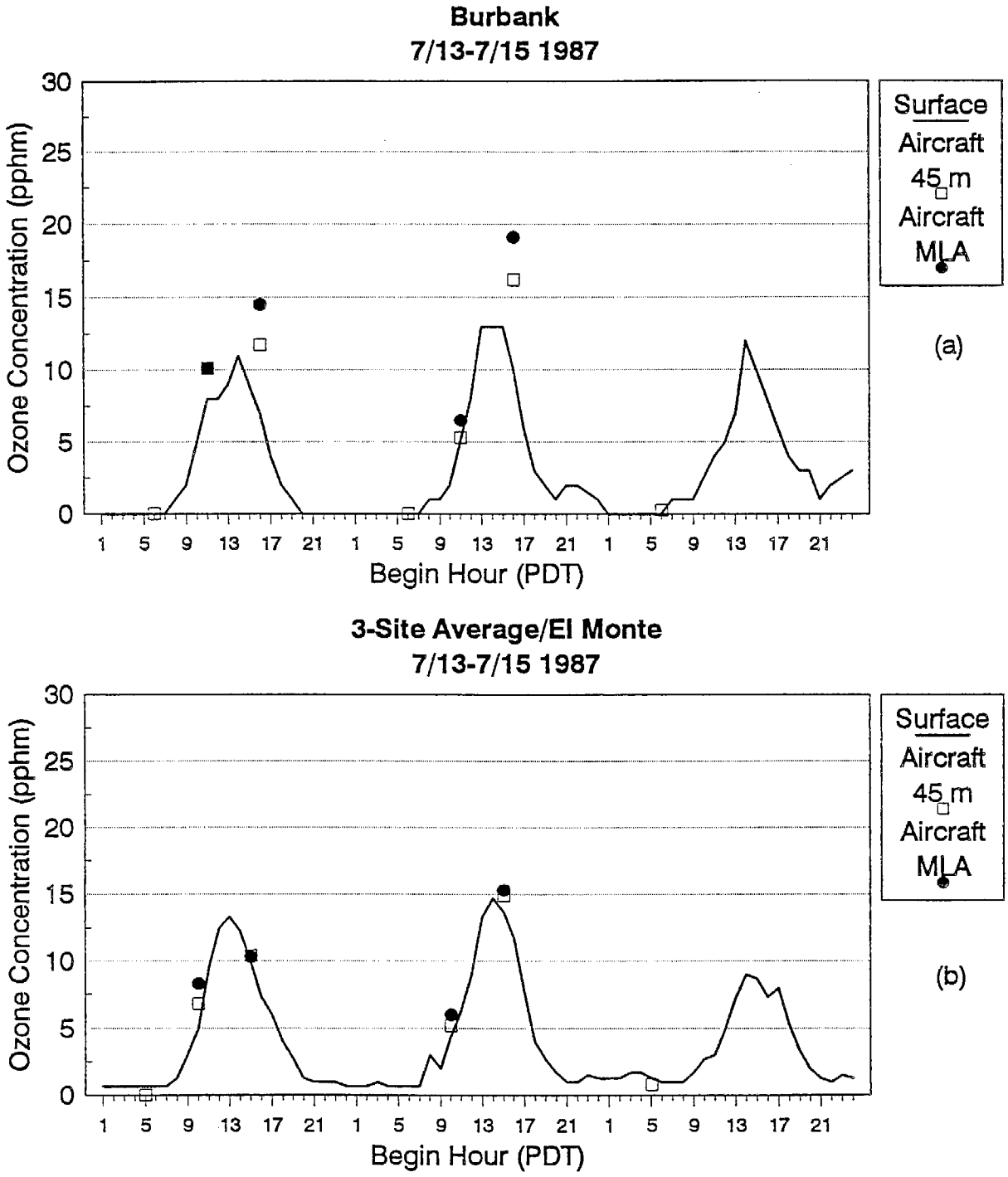

Figure 4-55. Comparison of Surface Ozone Concentrations With Mixed-Layer-Average (MLA) and the Lowest 45-Meter Average (45 m) Ozone at (a) Burbank and (b) El Monte on July 13-15, 1987. The data compared to the El Monte spiral are from the average of the Pico Rivera, Pasadena and Azusa surface monitors.

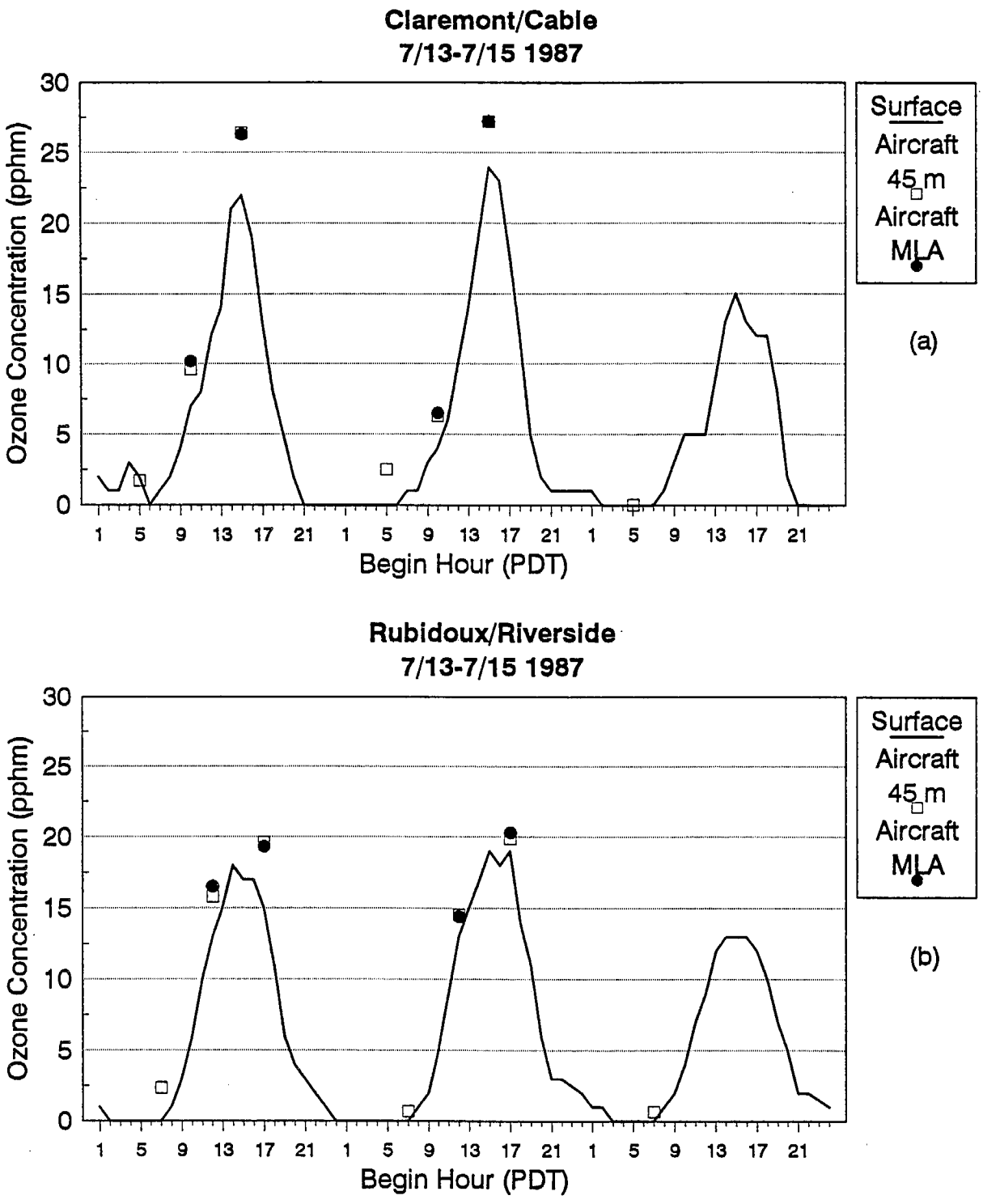

Figure 4-56. Comparison of Surface Ozone Concentrations With Mixed-Layer-Average (MLA) and the Lowest 45-Meter Average (45 m) Ozone at (a) Cable and (b) Riverside on July 13-15, 1987. The data compared to the Cable and Riverside spirals are from the Claremont and Rubidoux surface monitors, respectively.

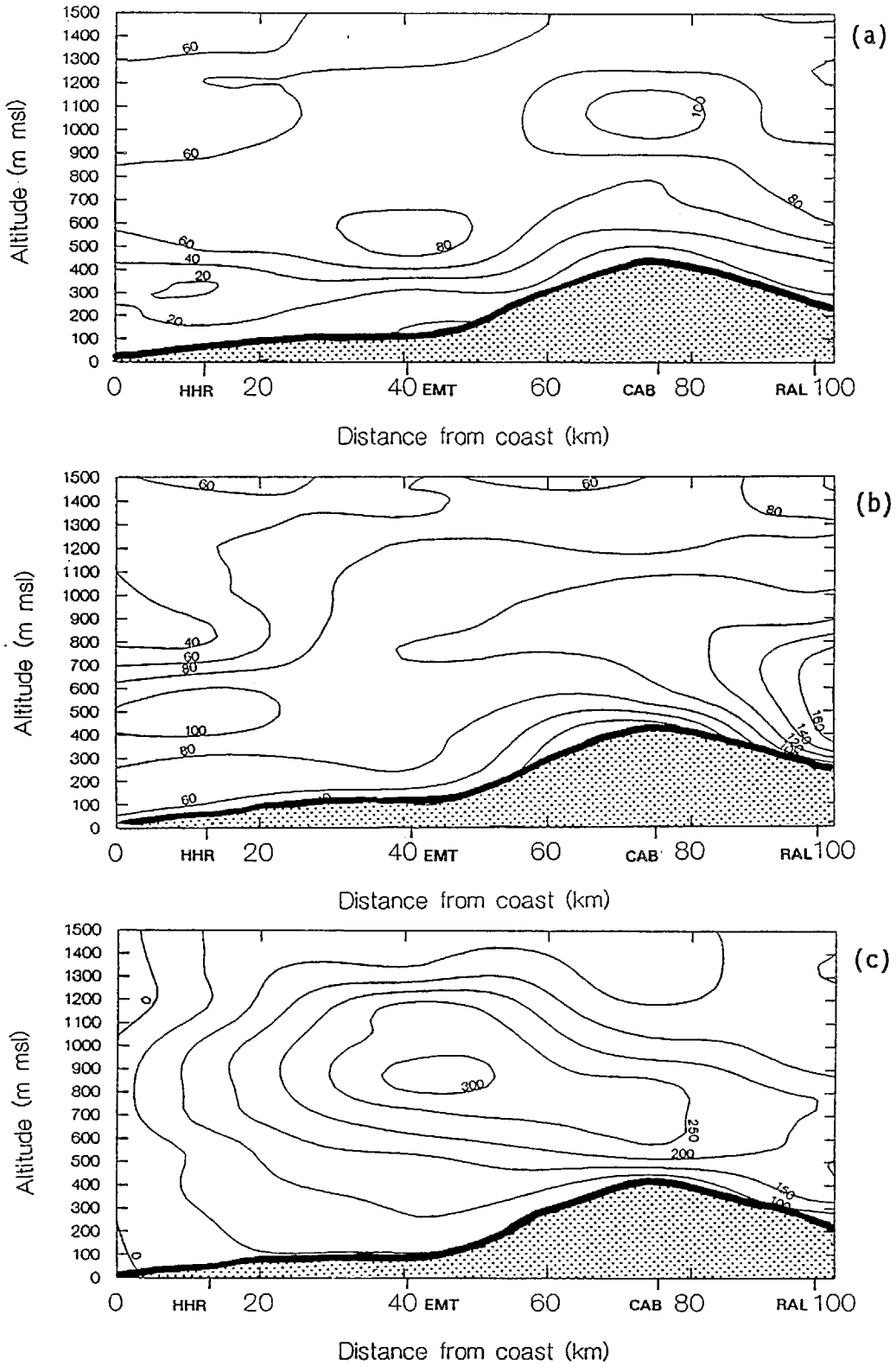

Figure 4-57. Ozone Concentrations (ppb) Aloft During the (a) Morning, (b) Midday, and (c) Afternoon of July 13, 1987. Ozone contours were generated along a west-to-east plane from the coast near Hawthorne to Riverside using data from aircraft spirals. The shaded area approximately represents the ground.

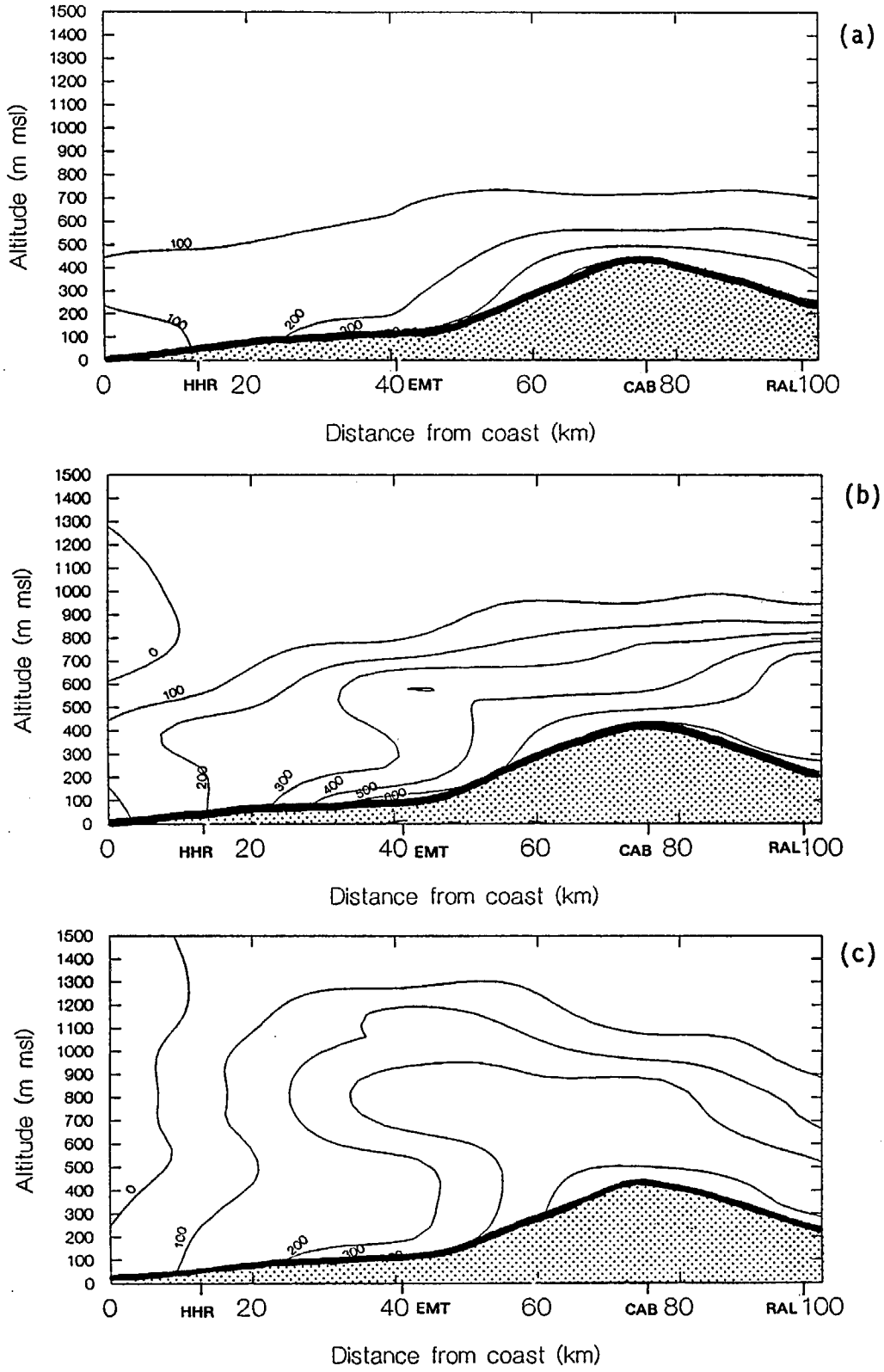

Figure 4-58. Light Scattering (b_{scat} - Mm^{-1}) Aloft During the (a) Morning, (b) Midday, and (c) Afternoon of July 13, 1987. Contours were generated along a west-to-east plane from the coast near Hawthorne to Riverside using data from aircraft spirals. The shaded area approximately represents the ground.

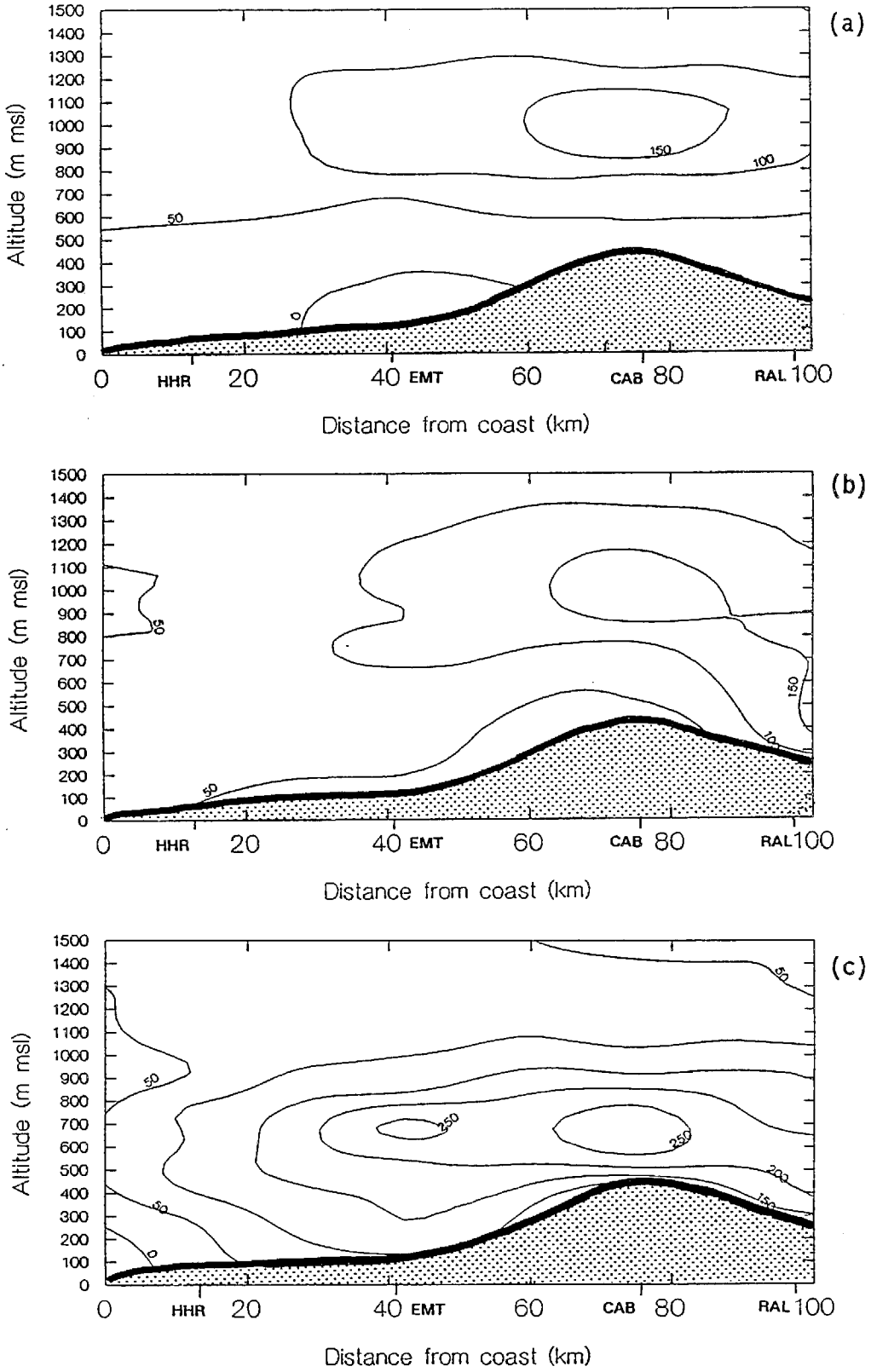

Figure 4-59. Ozone Concentrations (ppb) Aloft During the (a) Morning, (b) Midday, and (c) Afternoon of July 14, 1987. Ozone contours were generated along a west-to-east plane from the coast near Hawthorne to Riverside using data from aircraft spirals. The shaded area approximately represents the ground.

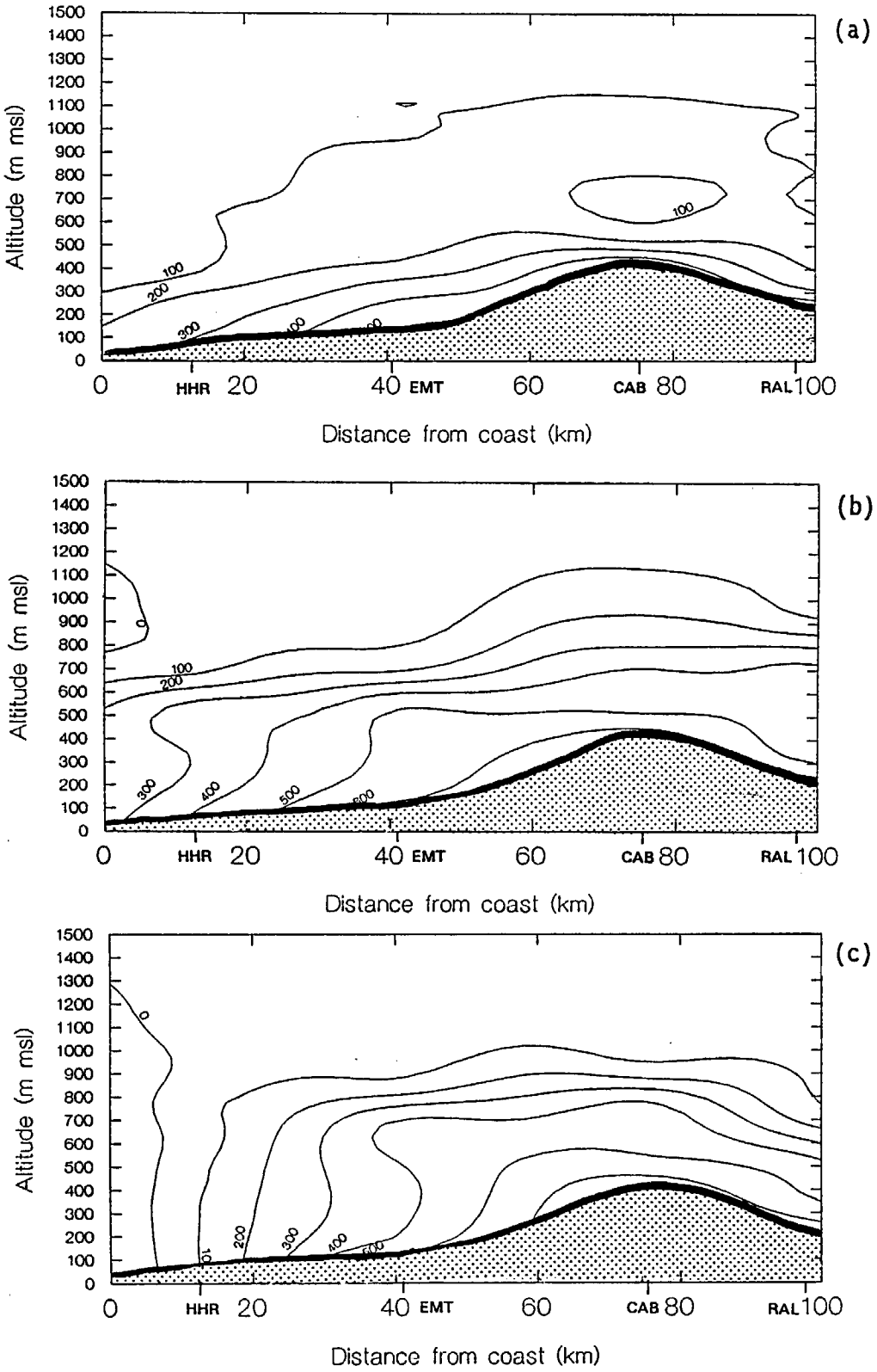

Figure 4-60. Light Scattering (b_{scat} - Mm^{-1}) Aloft During the (a) Morning, (b) Midday, and (c) Afternoon of July 14, 1987. Contours were generated along a west-to-east plane from the coast near Hawthorne to Riverside using data from aircraft spirals. The shaded area approximately represents the ground.

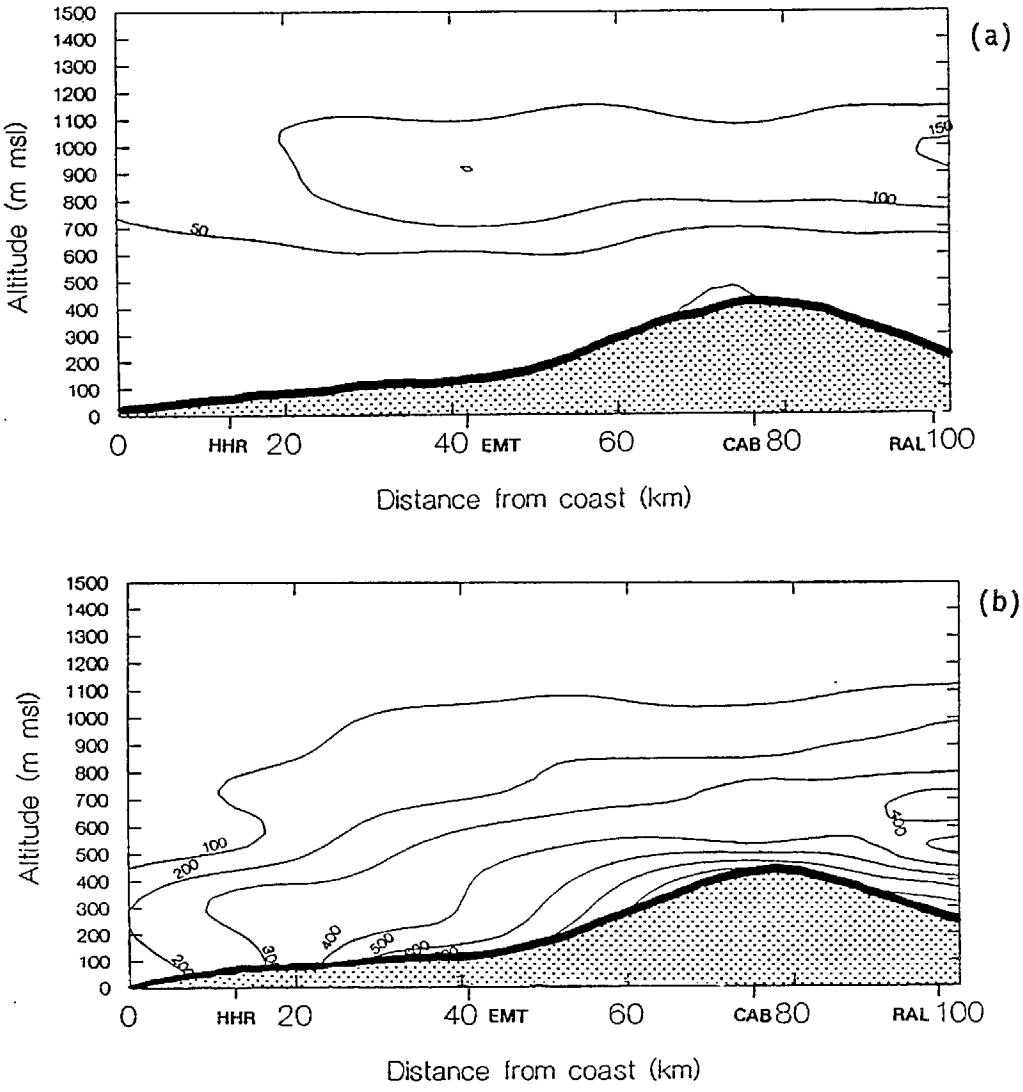

Figure 4-61. Contours of a) Ozone Concentrations (ppb) and b) b_{scat} (Mm^{-1}) Aloft During the Morning of July 15, 1987. Contours were generated along a west-to-east plane from the coast near Hawthorne to Riverside using data from aircraft spirals. The shaded area approximately represents the ground.

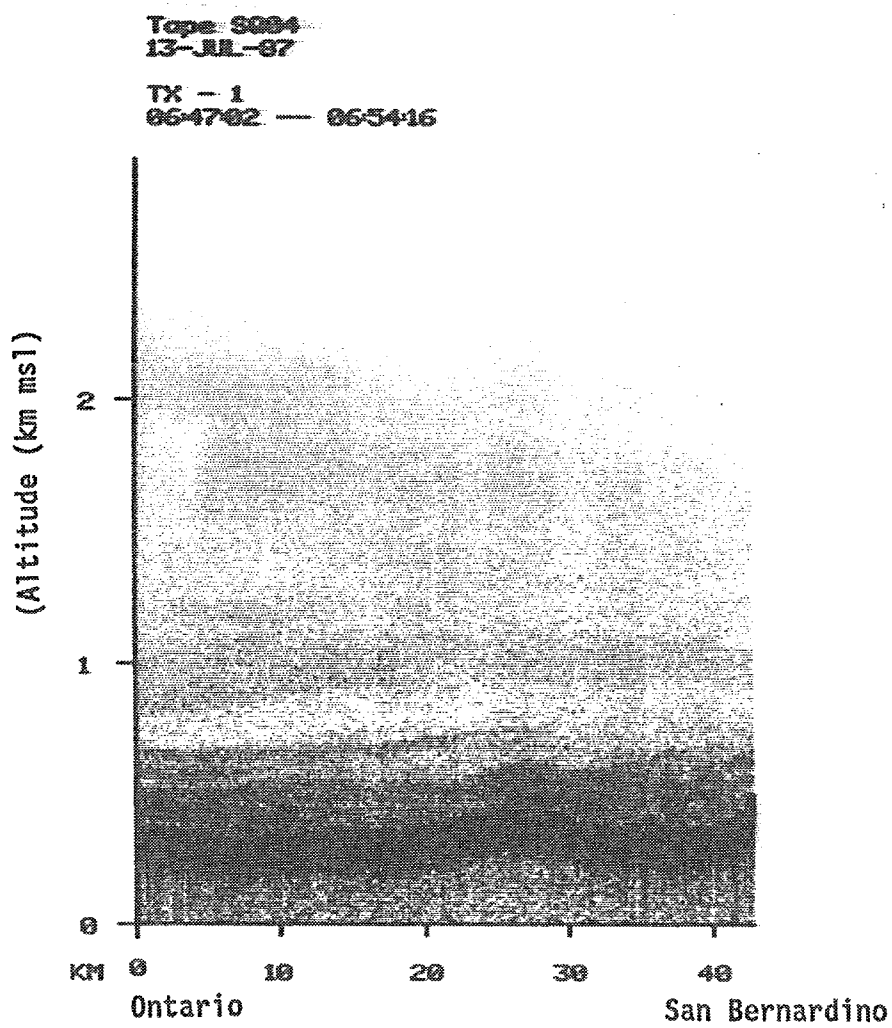

Figure 4-62. Aircraft Lidar Gray-Scale Plot of Particle Backscatter on the Morning of July 13, 1987 From Ontario to San Bernardino, Looking From the South. The layer of high particle backscatter between about 900-1100 m msl across the whole distance of the lidar image corresponds to the same ozone layer shown in Figure 4-57a.

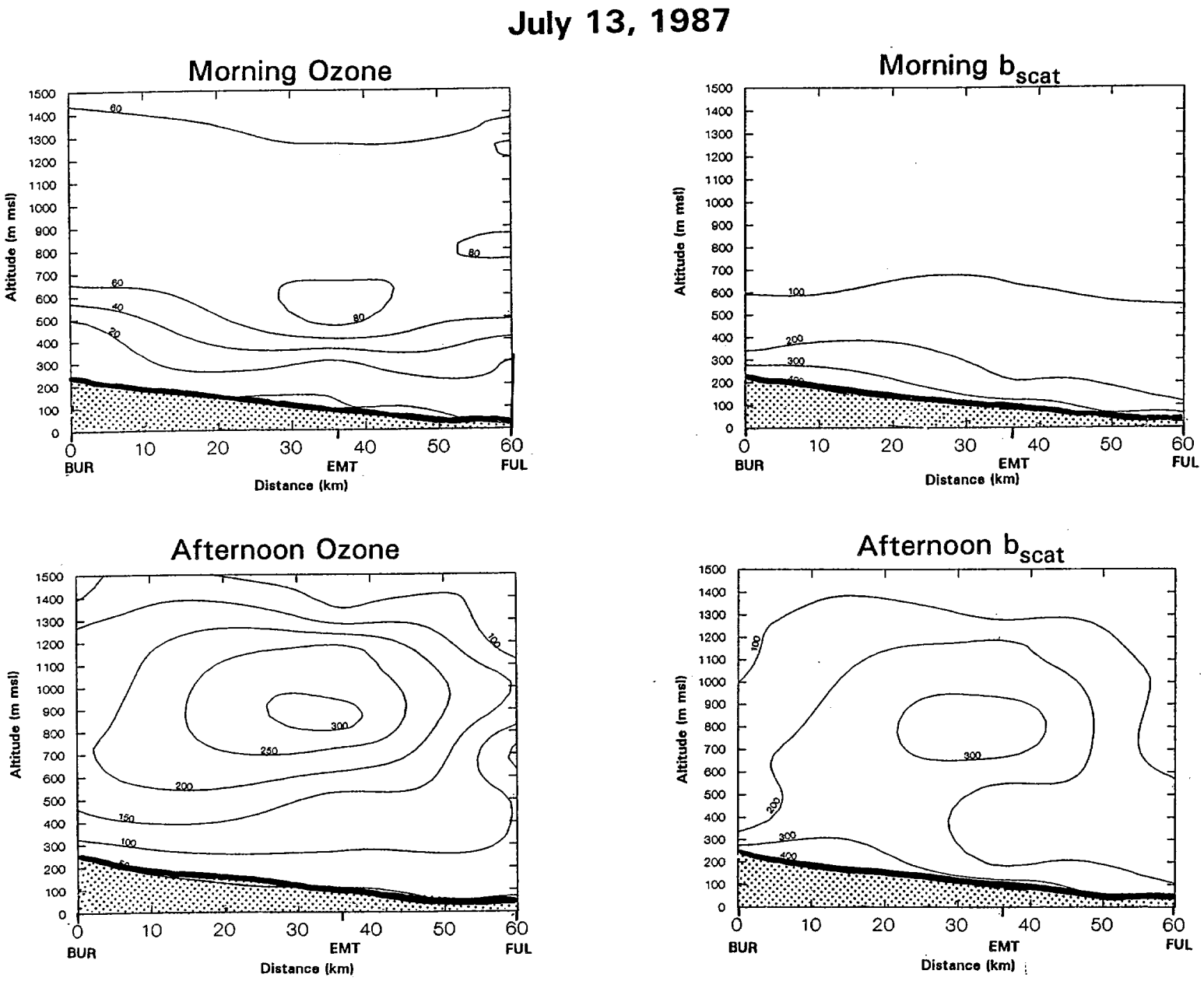

Figure 4-63. Ozone Concentrations (ppb) and Light Scattering (b_{scat} - Mm^{-1}) Aloft on the Morning and Afternoon of July 13, 1987 Along a North-to-South Plane From Burbank to Fullerton Using Data From Aircraft Spirals. The shaded area approximately represents the ground.

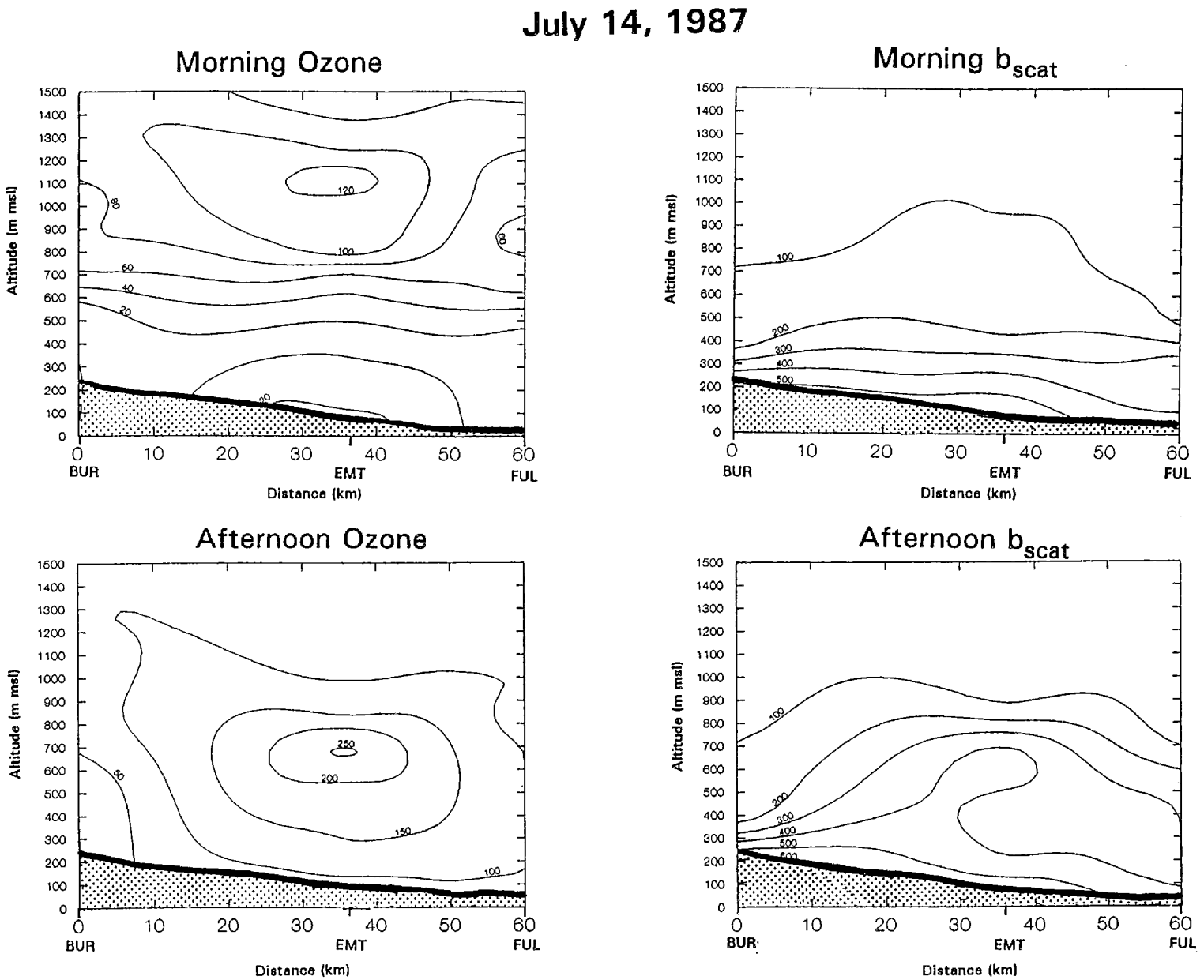

Figure 4-64. Ozone Concentrations (ppb) and Light Scattering (b_{scat} - Mm^{-1}) Aloft on the Morning and Afternoon July 14, 1987 Along a North-to-South Plane From Burbank to Fullerton Using Data From Aircraft Spirals. The shaded area approximately represents the ground.

July 15, 1987

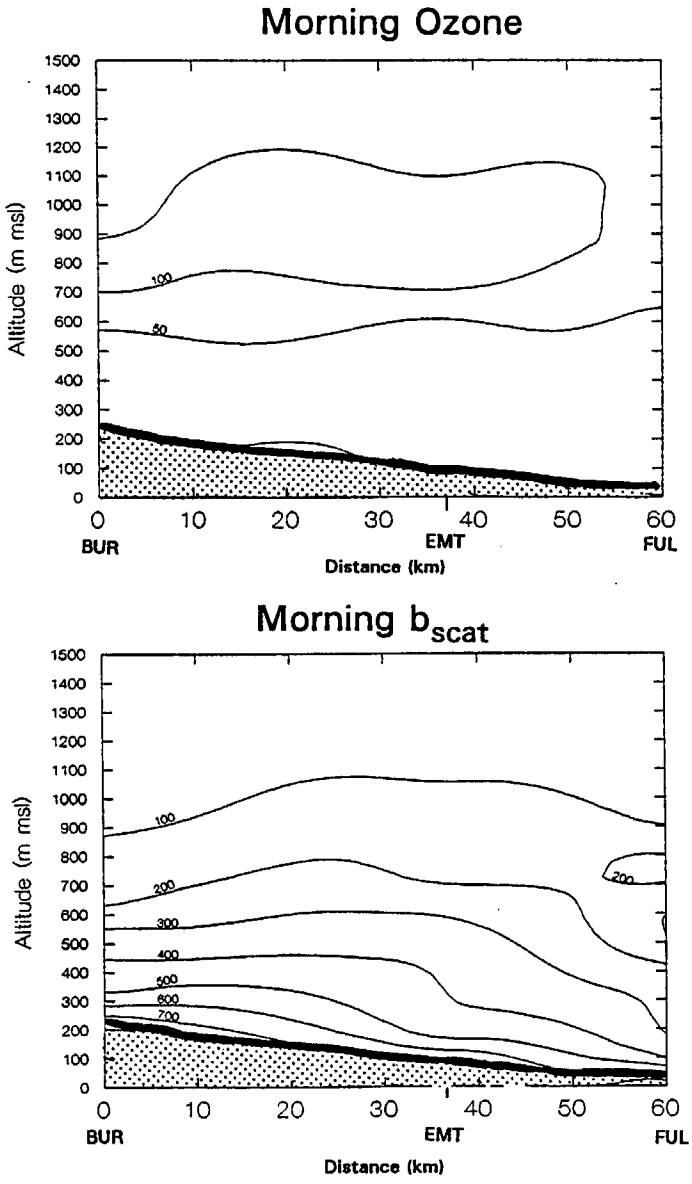

Figure 4-65. Ozone Concentrations (ppb) and Light Scattering (b_{scat} - Mm^{-1}) Aloft on the Morning of July 15, 1987 Along a North-to-South Plane From Burbank to Fullerton Using Data From Aircraft Spirals. The shaded area approximately represents the ground.

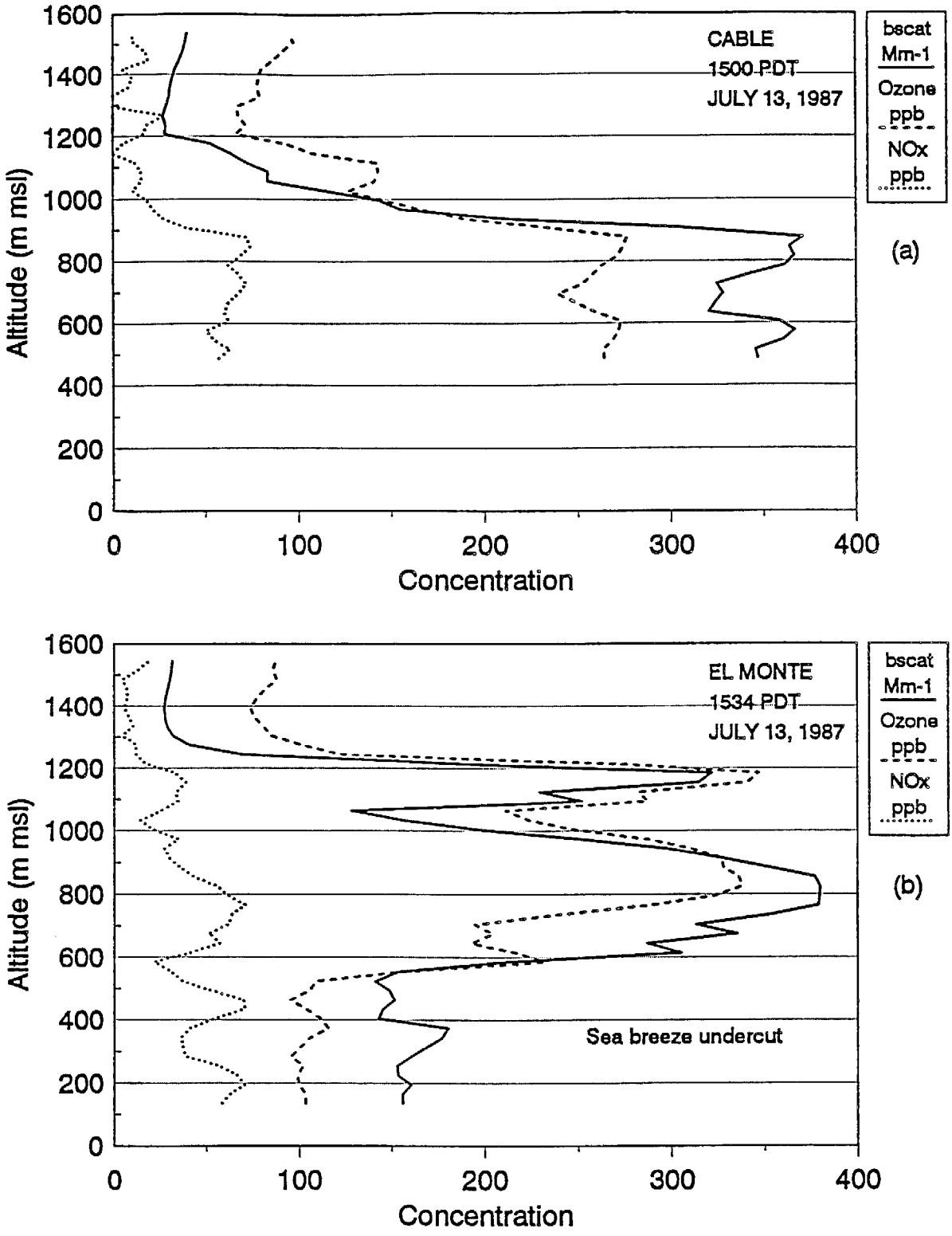

Figure 4-66. NO_x, b_{scat}, and Ozone Profiles at (a) Cable and (b) El Monte on the Afternoon of July 13, 1987 (b_{scat} Units are Mm^{-1}). The sea breeze has "cleaned out" the lower 600 m at El Monte. The layer of NO_x, b_{scat}, and ozone just above 1100 m msl at both locations may be due to upslope flow. The ozone peak at about 900 m msl at El Monte may represent Edinger's "convective debris".

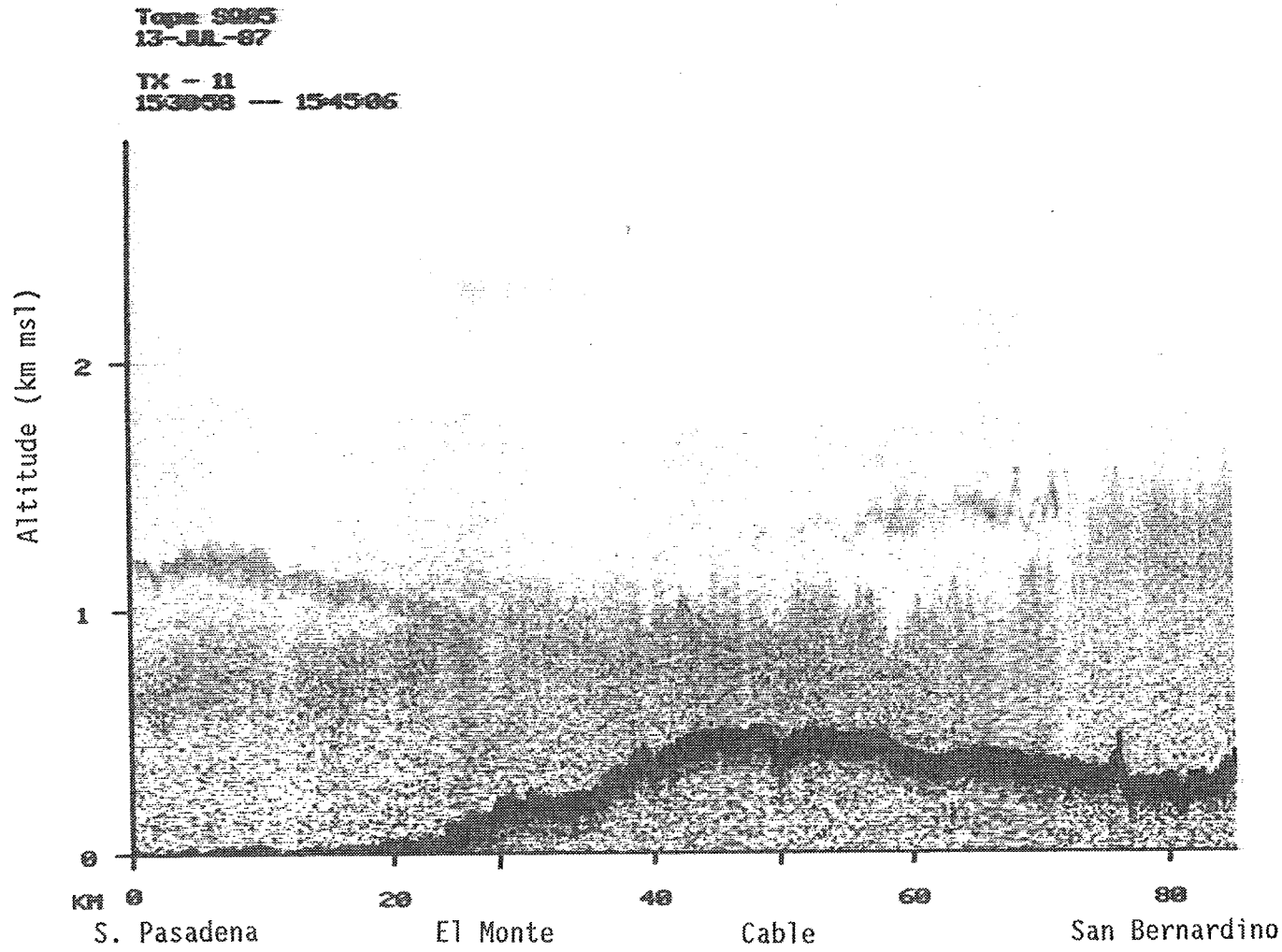

Figure 4-67. Aircraft Lidar Gray-Scale Plot of Particle Backscatter on the Afternoon of July 13, 1987 From South Pasadena to San Bernardino, Looking From the South. The cleaner air below about 500 m msl and west of El Monte is a result of the sea breeze. The thin layer of particle backscatter above Cable shows evidence of the injection of pollutants above the mixed layer.

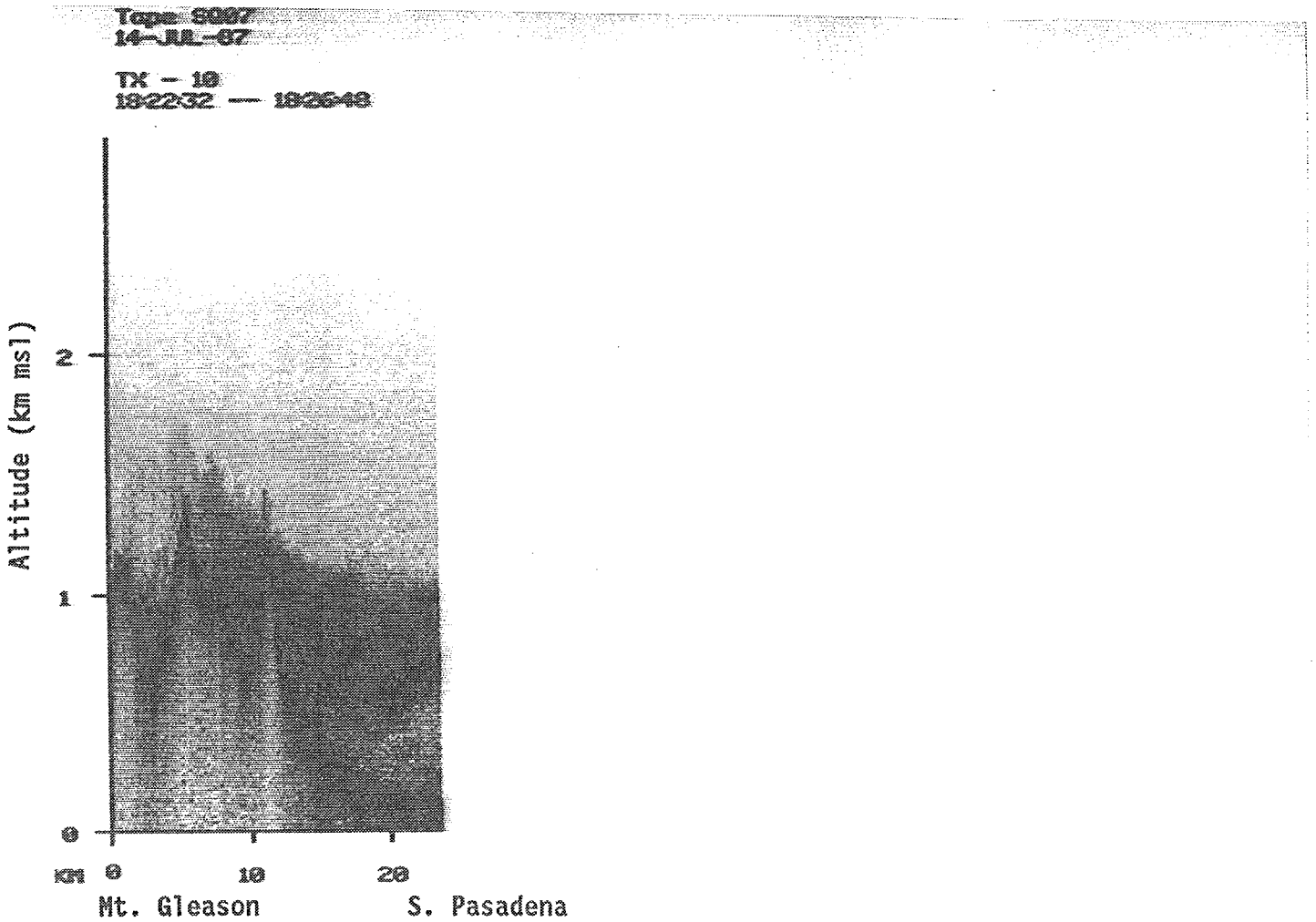

Figure 4-68. Aircraft Lidar Gray-Scale Plot of Particle Backscatter on the Afternoon of July 14, 1987 From Mt. Gleason to South Pasadena, Looking From the West. The upslope flow of the mixed layer is clearly seen in this plot.

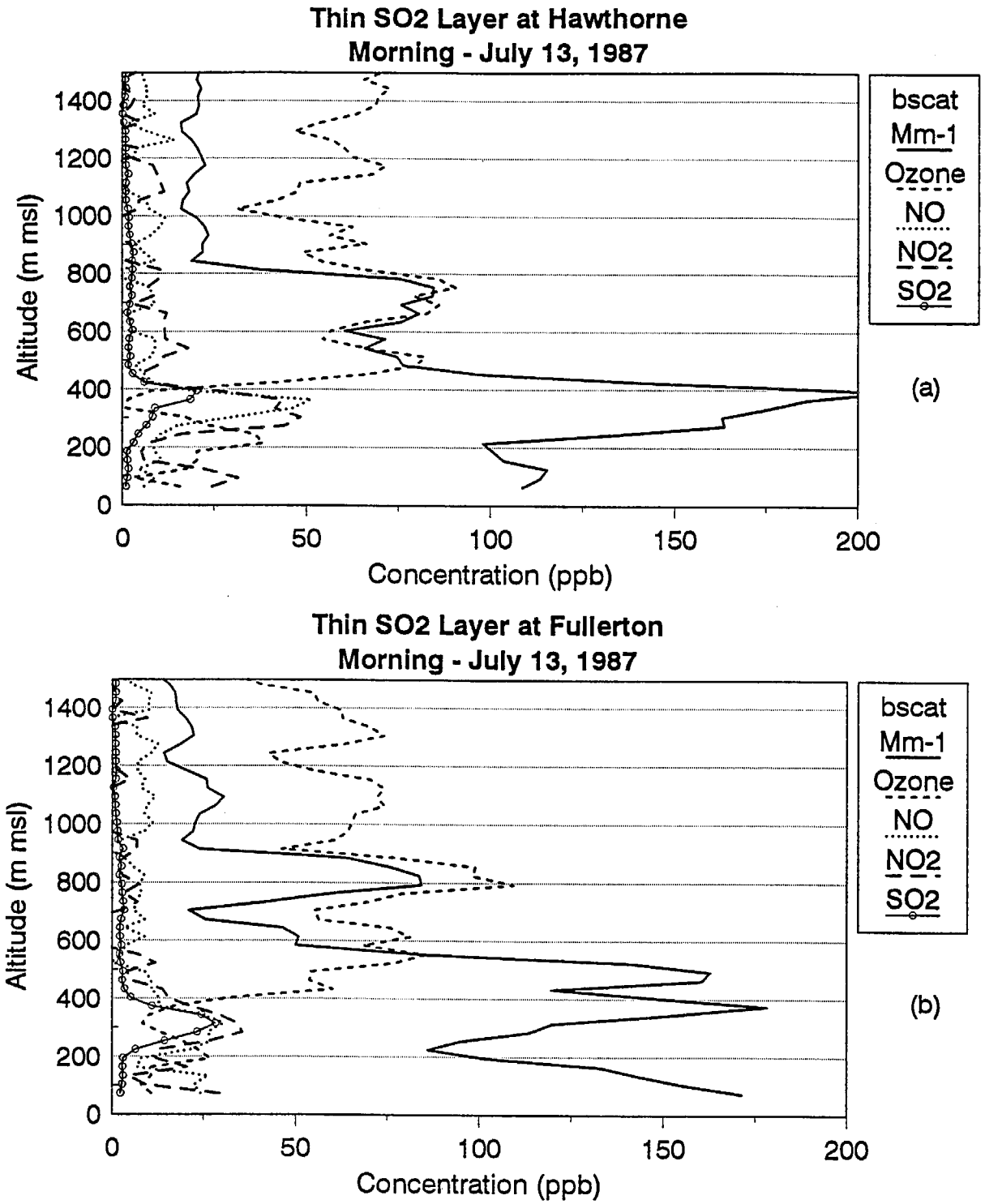

Figure 4-69. Ozone, NO, NO_2, SO_2, and b_{scat} Profiles at (a) Hawthorne and (b) Fullerton on the Morning of July 13, 1987. The layer of NO, NO_2, SO_2, and b_{scat} centered at about 300 to 350 m msl may be due to buoyant point source emissions.

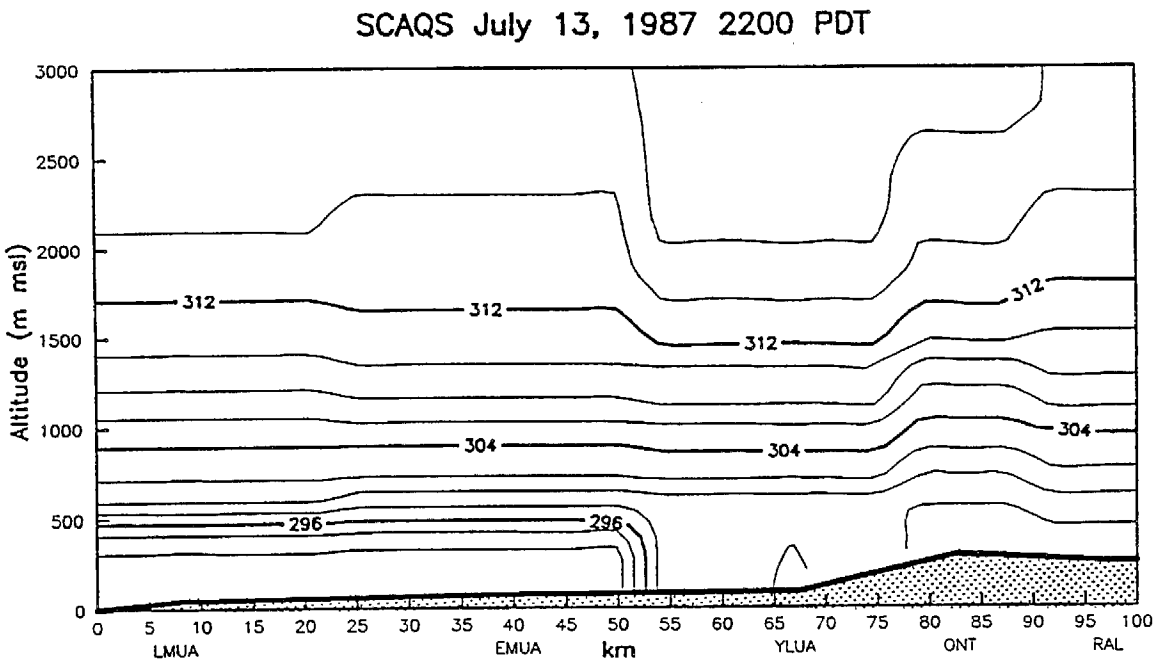

Figure 4-70. Isentropic Analysis Showing Aloft Potential Temperature (K) on the Evening of July 13, 1987. Contours were generated along a west-to-east plane from the coast near Santa Monica to Riverside using data from upper air meteorological soundings.

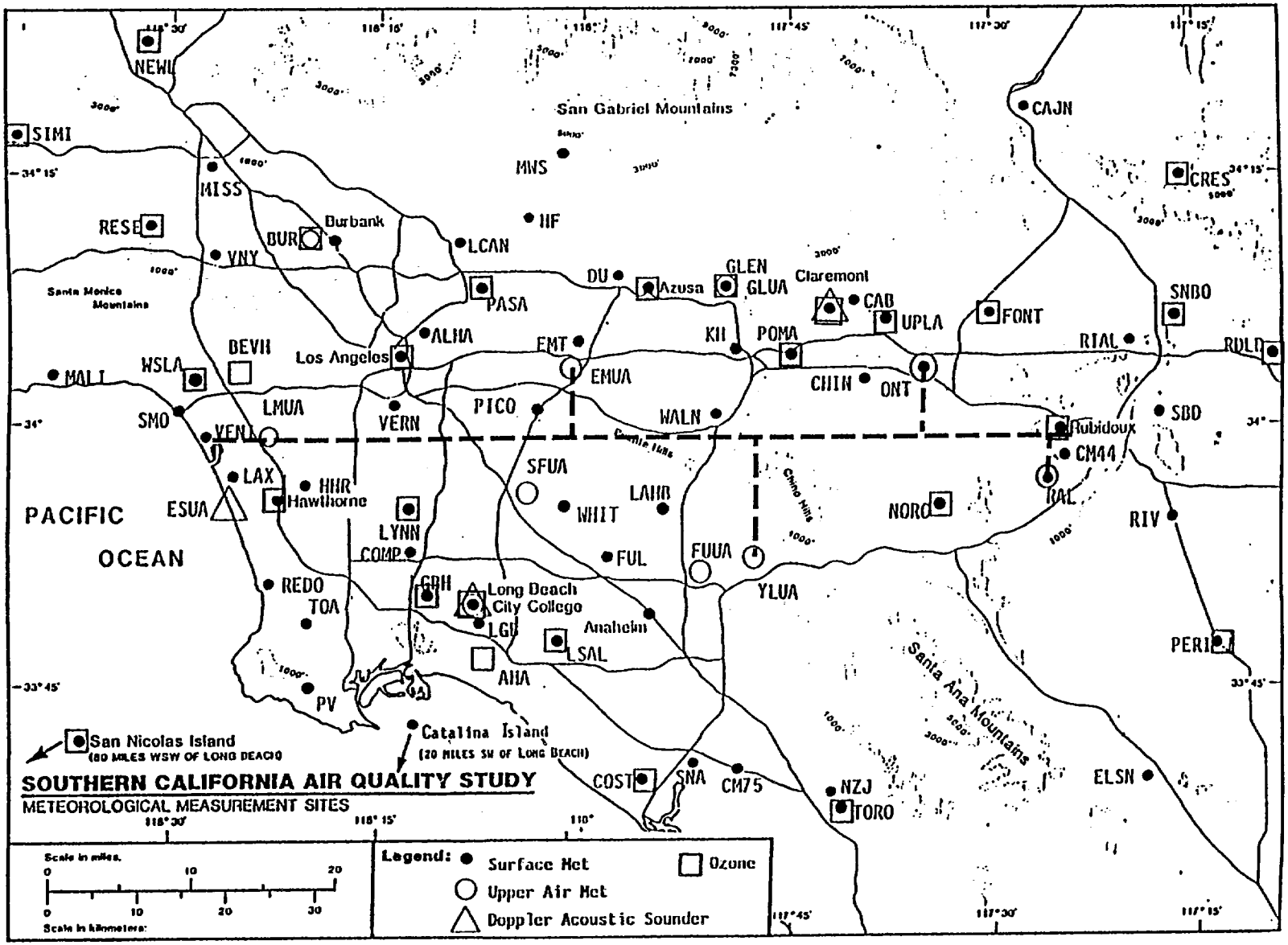

Figure 4-71. Location of Upper Air Meteorological Measurement Sites on West-East Line Used in Isentropic Analysis Plots. All sites are listed in Appendix A. (Base map from Hering and Blumenthal, 1989.)

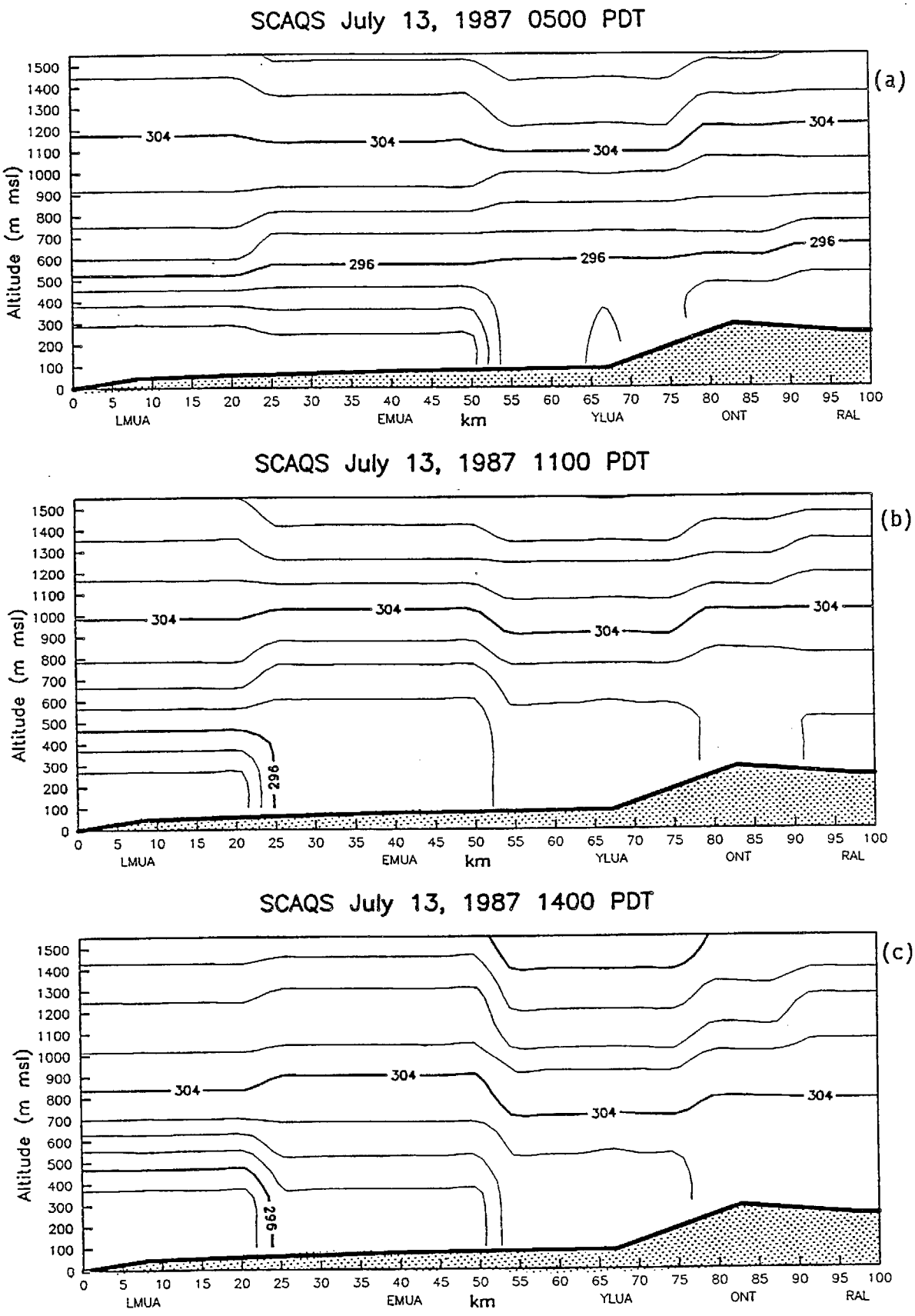

Figure 4-72. Isentropic Analysis Showing Aloft Potential Temperature (K) During the (a) Morning, (b) Midday, and (c) Afternoon of July 13, 1987.

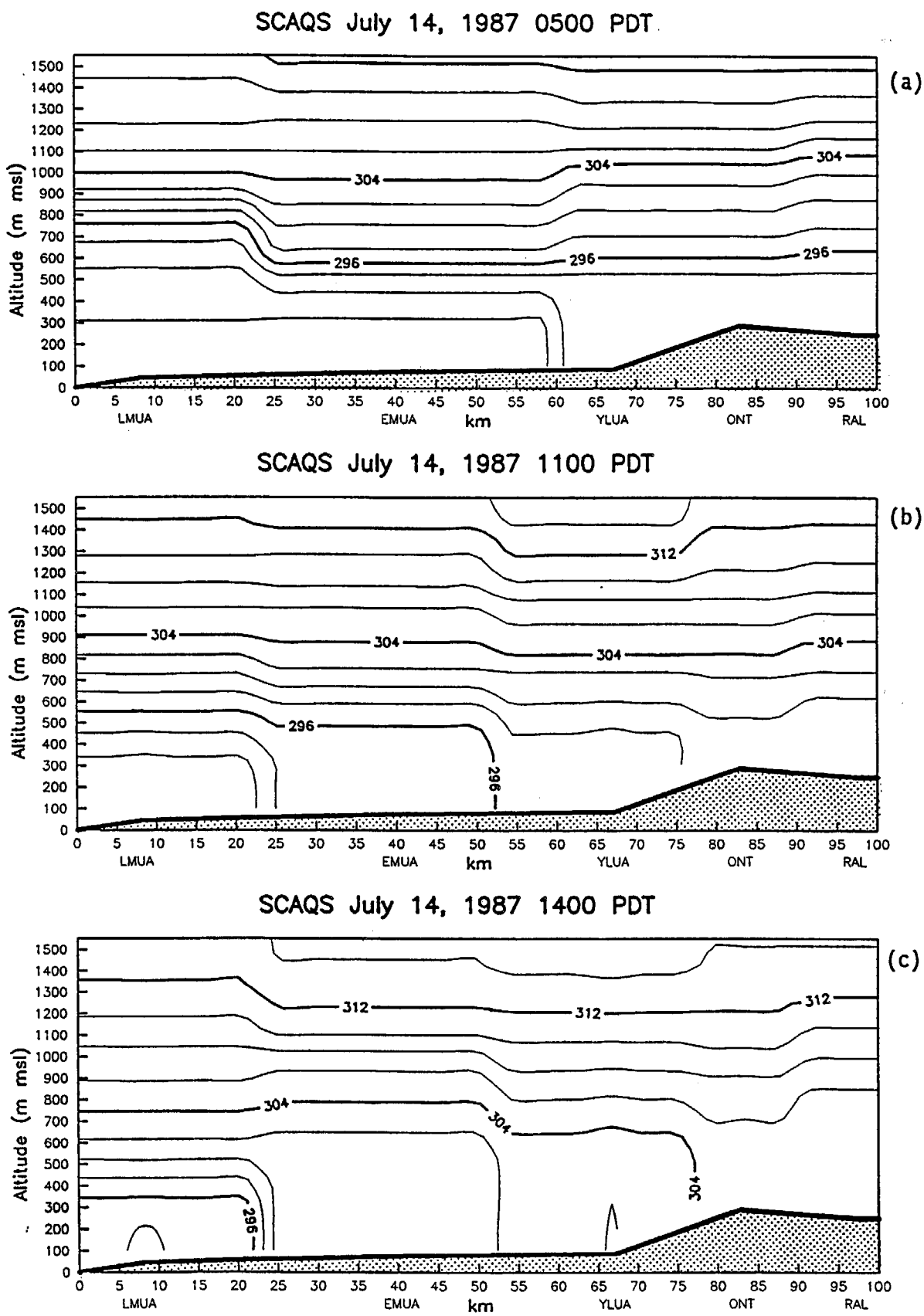

Figure 4-73. Isentropic Analysis Showing Aloft Potential Temperature (K) During the (a) Morning, (b) Midday, and (c) Afternoon of July 14, 1987.

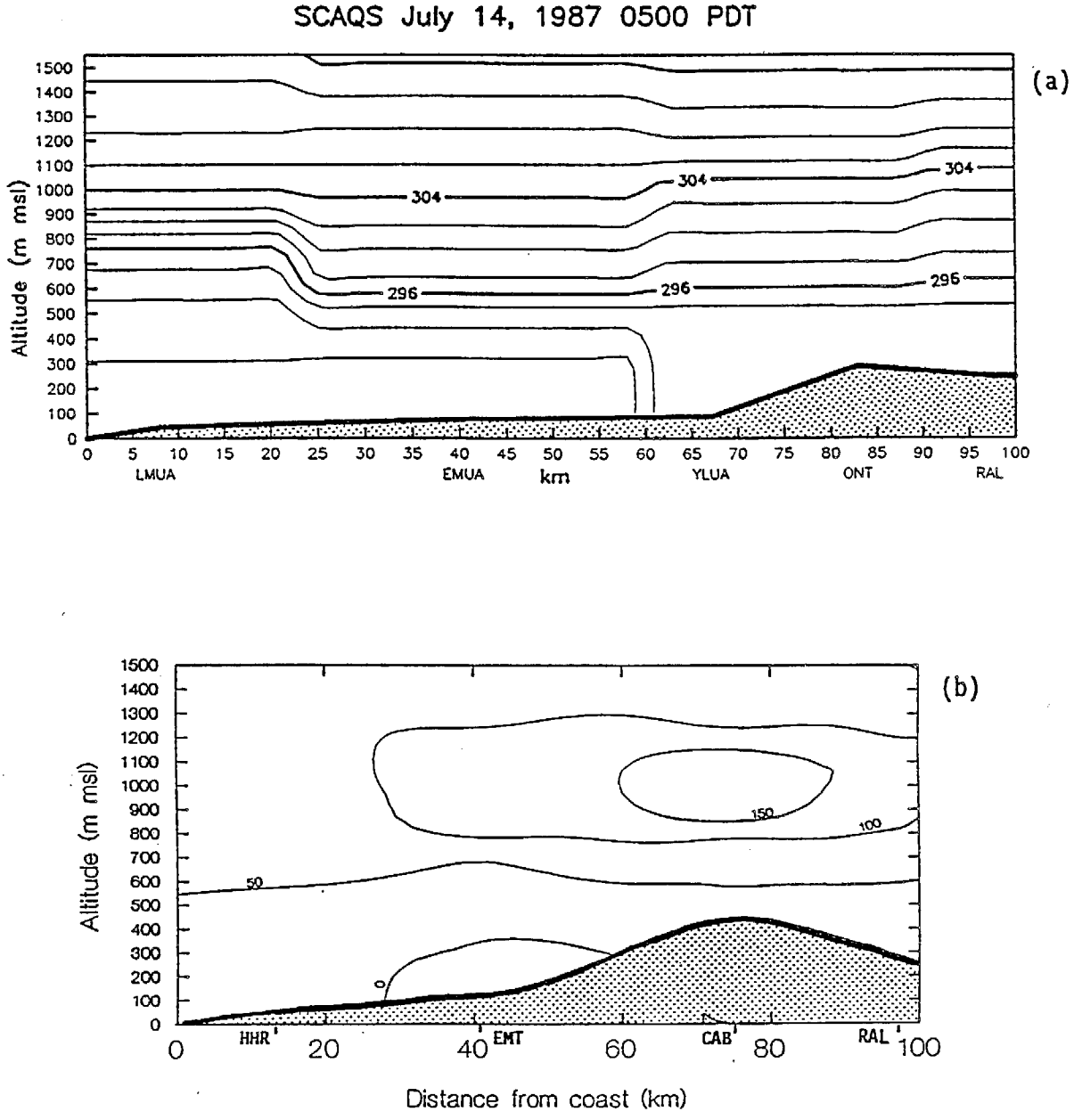

Figure 4-74. (a) Isentropic Analysis Showing Potential Temperature (K) and (b) Ozone Concentrations (ppb) Aloft on the Morning of July 14, 1987.

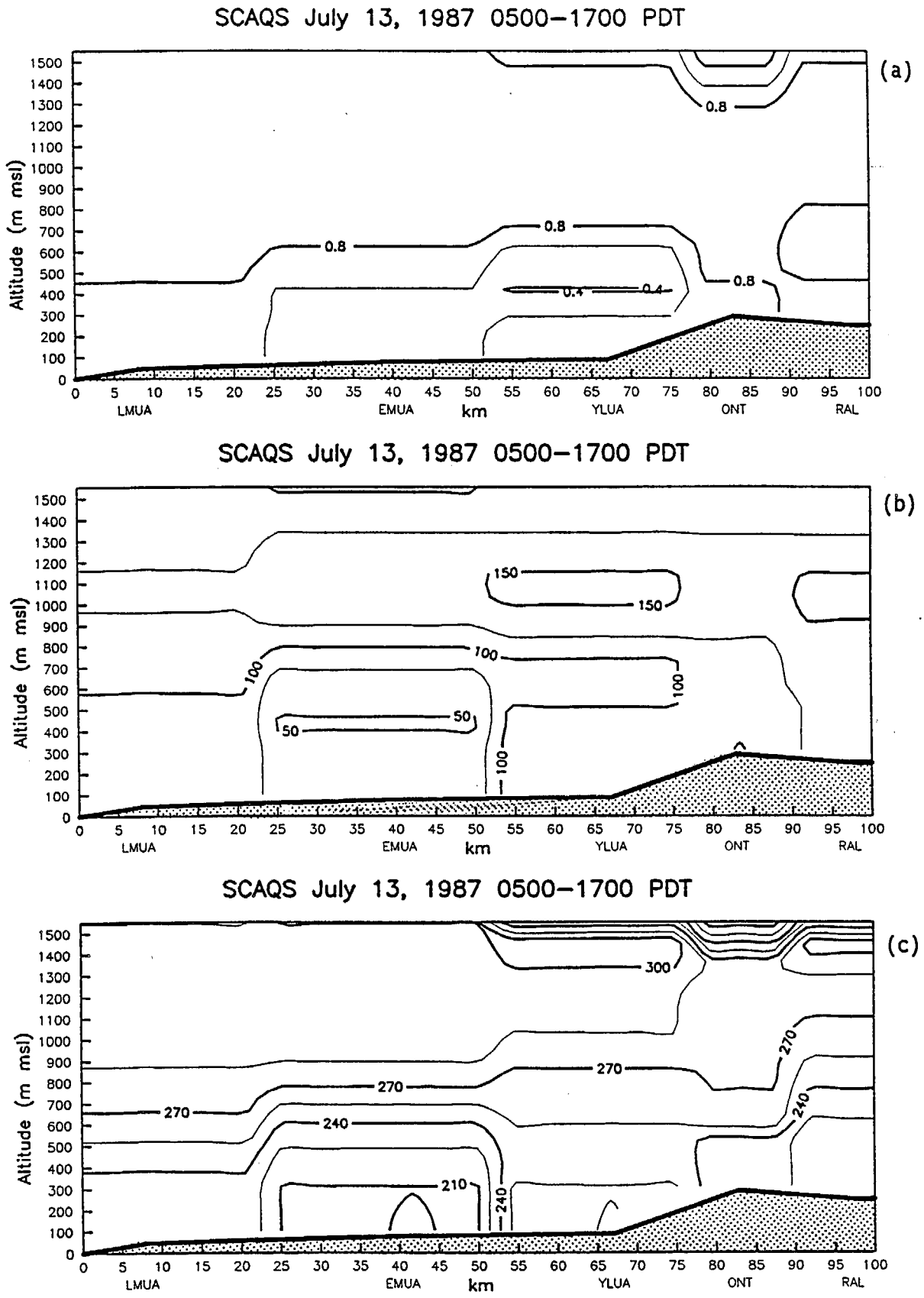

Figure 4-75. Recirculation Analysis Results Showing Aloft Contours of (a) Recirculation Factor, (b) Cumulative Wind Run, and (c) Vector-Averaged Wind Direction During July 13, 1987.

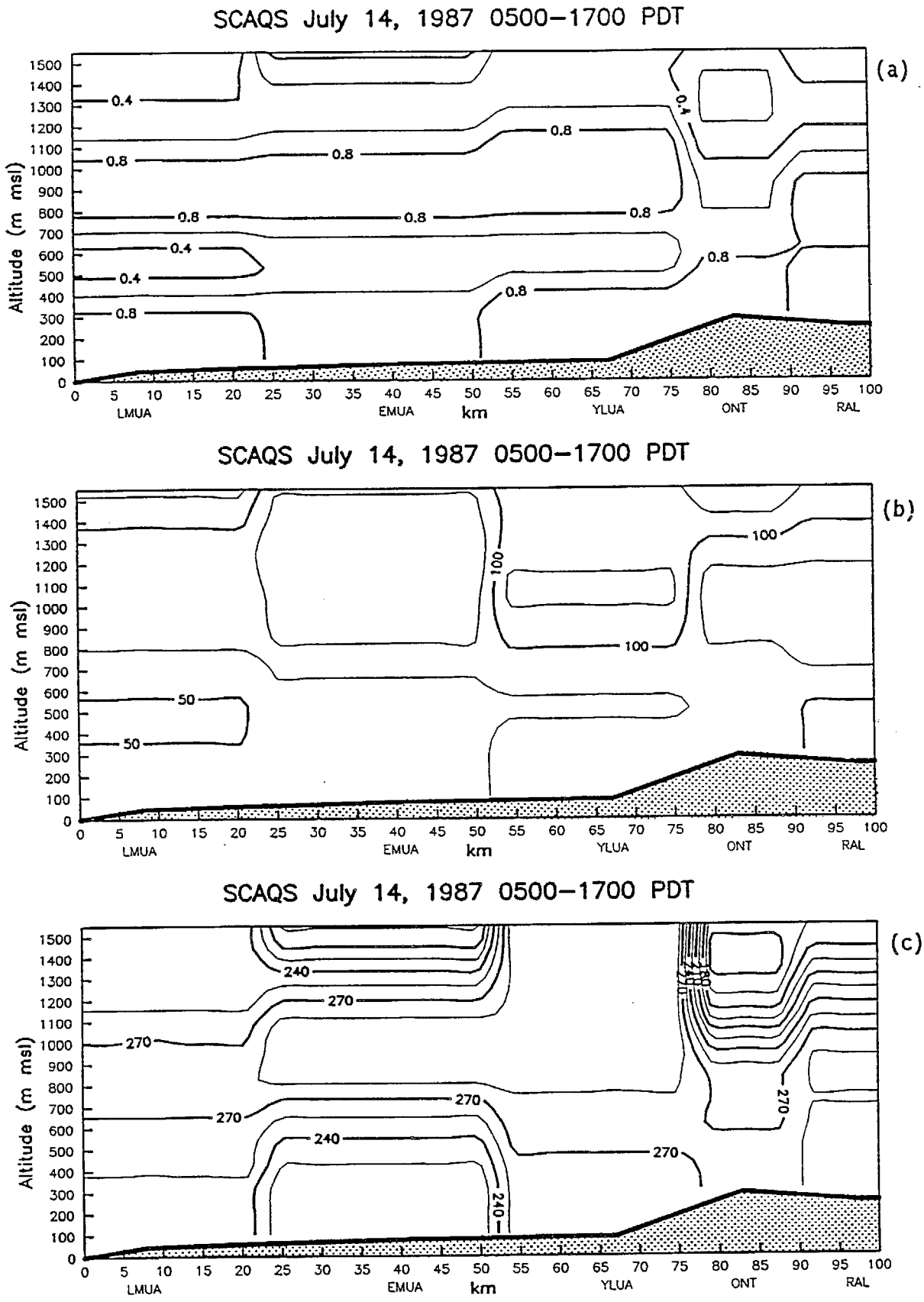

Figure 4-76. Recirculation Analysis Results Showing Aloft Contours of (a) Recirculation Factor, (b) Cumulative Wind Run, and (c) Vector-Averaged Wind Direction During July 14, 1987.

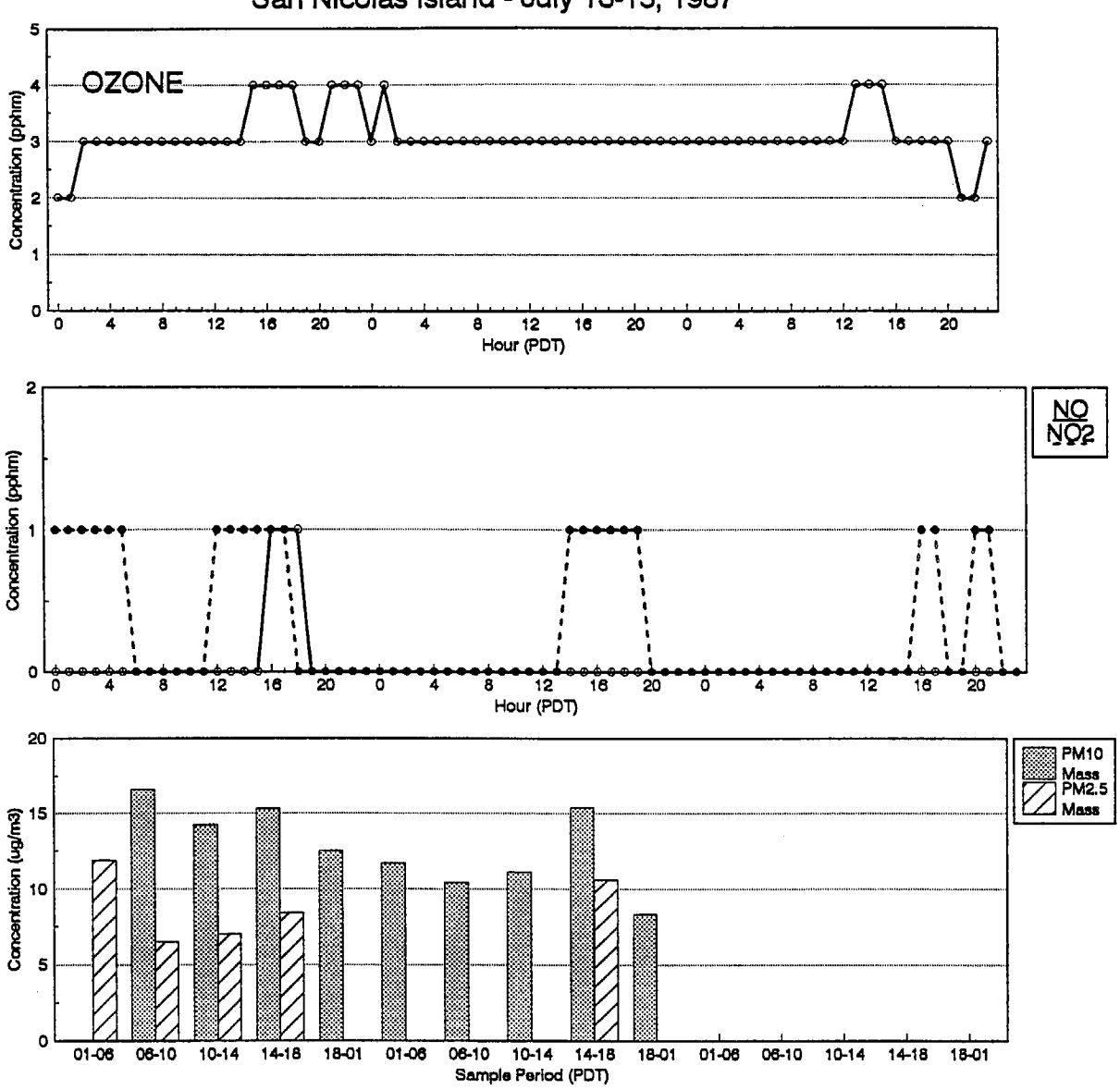

Figure 4-77. Ozone, NO, NO_2, and PM_{10} and $PM_{2.5}$ Mass Concentrations at San Nicolas Island on July 13-15, 1987. Mass data on July 15 are invalid.

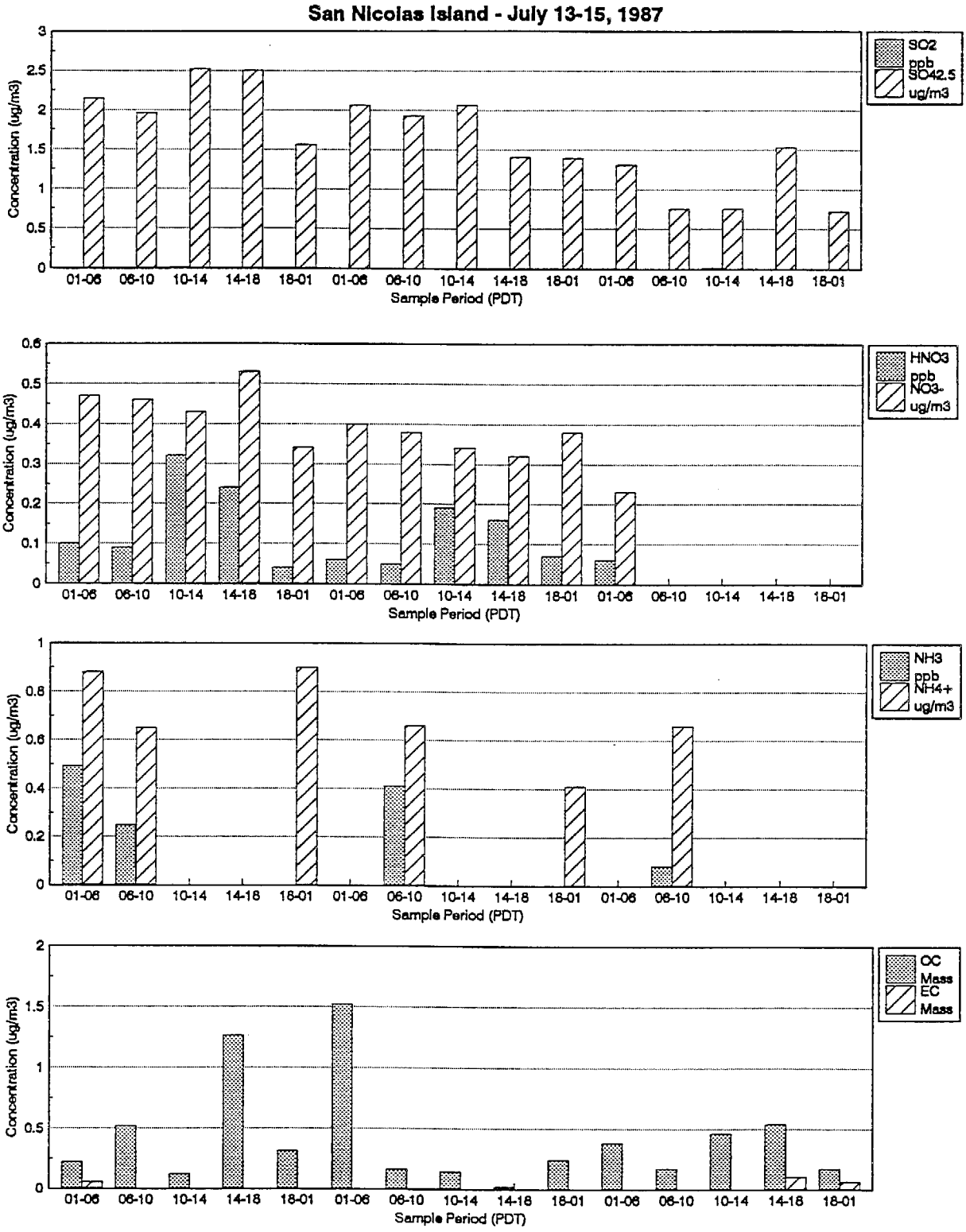

Figure 4-78. Nitric Acid, Ammonia, SO_2 and $PM_{2.5}$ Nitrate Ion, Ammonium Ion, Organic Carbon, Elemental Carbon, and Sulfate Ion Concentrations at San Nicolas Island on June 13-15, 1987.

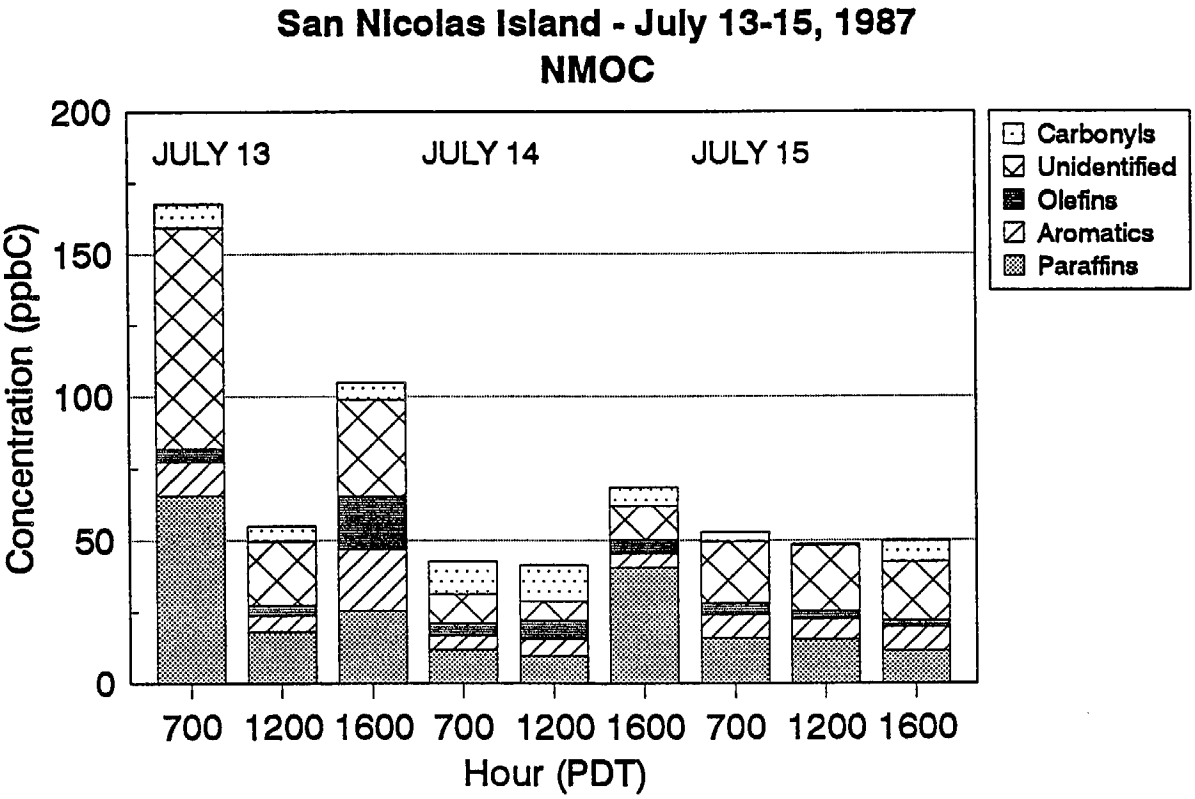

Figure 4-79. NMOC Concentrations at San Nicolas Island on July 13-15, 1987.